universität wien

DISSERTATION / DOCTORAL THESIS

Titel der Dissertation /Title of the Doctoral Thesis

„Investigations on Base Metal-assisted Synthesis of Amines"

verfasst von / submitted by

Leonard Homberg, BSc MSc

angestrebter akademischer Grad / in partial fulfilment of the requirements for the degree of

Doktor der Naturwissenschaften (Dr. rer. nat.)

Wien, 2020 / Vienna 2020

Gutachter

Univ.-Prof. Dr. Marko Hapke

Ao. Univ.-Prof. Dipl.-Ing. Dr. Karl Kirchner

So eine Arbeit wird eigentlich nie fertig, man muß sie für fertig erklären,

wenn man nach Zeit und Umständen das Möglichste getan hat.

„Johann Wolfgang von Goethe"

Statutory Declaration

The work presented in this doctoral thesis was conducted from December 2014 till April 2019 at the University of Vienna (Austria) under the supervision of Univ.-Prof. Dr. Kai Carsten Hultzsch.

I hereby solemnly declare that I wrote the report in hand by myself without outside help, that I clearly marked all the passages I adopted, and that I did not use any other sources than the ones I quoted.

Parts of this thesis have also been published in a journal article:

L. Homberg; A. Roller; K. C. Hultzsch. A Highly Active PN^3 Manganese Pincer Complex Performing N-Alkylation of Amines under Mild Conditions. *Org. Lett.* **2019**, *21*, 3142–3147.

_____

Widmung

Für meine Eltern Christiane und Ulrich.

Widmung

Danksagung

Zunächst möchte ich mich bei meinem Betreuer Herrn Univ.-Prof. Dr. Kai Hultzsch für die beiden interessanten Themen meiner Doktorarbeit sowie den anregenden Ideenaustausch während Seminaren und Kurzbesprechung bedanken.

Meinen Gutachtern Herrn Ao. Univ.-Prof. Dipl.-Ing. Dr. Karl Kirchner und Herrn Univ.-Prof. Dr. Marko Hapke möchte ich dafür danken, dass sie zuvorkommend und unkompliziert die vorliegende Arbeit bewerten. Zudem möchte ich Rudi und Natalie für das Korrekturlesen meiner Arbeit danken.

Hans-Peter, Susanne und Ricarda möchte ich vielmals für die Messung von NMRs und Hilfe bei verschiedenen Fragestellungen bedanken.

Alexander und Natalie möchte ich für ihre Arbeit mit der X-Ray Analyse meiner nicht immer schönen Kristalle danken.

Viele Ideen und Experimente wären ohne meine Kollegen gar nicht zustande gekommen, weshalb ich der gesamten Gruppe der Chemischen Katalyse für das freundliche und produktive Klima danken möchte. Besonders Mirjana – dem Herzstück der Gruppe – sowie meine ehemaligen Kollegen John, Rudi, Natalie, Lisa und Felicity, sowie die Masterstudenten Josip, Tom und Qi haben die Zeit der Dissertation zu einem einzigartigen Erlebnis gemacht. Viele meiner Ergebnisse wären ohne den unermüdlichen Einsatz meiner Studenten Ammon, David, Erwin, Farouk, Josip, Kim, Klara, Mario, Maximilian, Nazi, Pao und Selin nicht zustande gekommen.

Zwar habe ich John schon erwähnt, aber ich möchte mich nochmal herzlichst für die Freundschaft, kollegiale Zusammenarbeit, abstrusen Laborhumor und Ideen seit unserem ersten Treffen in den USA im Jahr 2013 bedanken.

Auch wenn die Chemie mal nicht stimmte hat mich meine Familie stets unterstützt und auch Verständnis für meinen weiteren Lebens- und Arbeitsweg fernab der Heimat gezeigt. Und auch wenn ich meine liebste Karin erst während der letzten Phase meiner Doktorarbeit kennengelernt habe, so hat sie wohl das gesamte Spektrum meiner Launen mitbekommen und ertragen müssen. Auch als es nicht so gut lief hat sie mich immer unterstützt, wieder aufgebaut aber auch in den Hintern getreten, so dass ich es soweit geschafft habe nun diese Danksagung schreiben zu können.

Abstract

The formation of carbon-heteroatomic bonds is a basic principle of synthetic chemistry and is usually achieved by the reaction of highly active substrates. However, with additives and catalysts also less active substrates can be employed as reagents. In this thesis iron and manganese complexes were investigated with an emphasis on application in synthetic strategies.

In the first part, iron olefin piano stool complexes were prepared and structurally investigated with NMR spectroscopy. Then, the addition of heteroatomic nucleophiles to the coordinated olefin was examined. Different amines and phosphines were used as nucleophiles and the formation of carbon-heteroatomic bonds was observed. The obtained iron-alkyl complexes were tested for the release of a desired higher amine or phosphine under different reaction conditions. As a proof of concept, ethyl diphenyl phosphine was prepared in a one-pot NMR experiment by nucleophilic addition of diphenylphosphine to an iron-ethylene complex followed by electrophilic cleavage with trifluormethanesulfonic acid. Moreover, investigation on the catalytic hydrophosphination of styrene was conducted.

In the second part, manganese pincer complexes were prepared and their catalytic activity for borrowing hydrogen mediated N-alkylation of amines with alcohols was investigated. Guided by prior research in metal-ligand cooperated catalyst systems, a suitable non-C_2-symmetric PN^3 pincer ligand (bpy-^{6}NH-P) was identified and its preparation successfully optimized. With the ligand in hand, we were able to develop a manganese based pincer catalyst that performed N-alkylation of anilines and other amines at 60 °C with primary alcohols using substoichiometric amounts of base additive. The high reactivity under mild reaction conditions prompted us to employ more challenging substrates. Therefore, secondary alcohols, benzylic and aliphatic amines were successfully utilized as substrates in N-alkylation reactions. Other dehydrogenation/hydrogenation reactions like aldol condensation and transfer hydrogenation were briefly investigated, as well as the employment of urea and other amides as substrates for both C-N and C-C bond formation. Aside from the development of our most active catalyst system, a modular synthetic approach of other PN^3 pincer ligands and their application in catalysis was pursued.

Zusammenfassung

Die Knüpfung von Kohlenstoff-Heteroatom-Bindungen ist eines der grundlegenden Prinzipien der chemischen Synthese und wird meistens erst durch die Reaktion hochreaktiver Substrate ermöglicht. Jedoch ist es durch den Einsatz verschiedener Additive und Katalysatoren möglich weniger reaktive Reagenzien zu verwenden. In dieser Dissertation wurden verschiedene Eisen- und Mangankomplexe untersucht, wobei der Schwerpunkt auf deren möglichen Einsatz als Katalysatoren in der chemischen Synthese lag.

Die Arbeit ist in zwei Abschnitte aufgeteilt. Im ersten Abschnitt wurden verschiedene Eisen-Olefin Halbsandwich-Komplexe synthetisiert und Strukturaufklärung mittels NMR Spektroskopie durchgeführt. In der Folge wurde die Addition unterschiedlicher Nukleophile an das am Eisen koordinierte Olefin untersucht. Dabei wurde durch den Einsatz von Aminen und Phosphinen die Bildung neuer Kohlenstoff-Heteroatom-Bindungen beobachtet. Die Freisetzung der gewünschten höher substituierten Amine und Phosphine, ausgehend von den erhaltenen Eisen-Alkyl-Komplexen, wurde unter verschiedenen experimentellen Bedingungen getestet. Exemplarisch wurde die schrittweise Addition von Diphenylphosphin an einen Eisen-Ethylen-Komplex und die anschließende Freisetzung von Ethyldiphenylphosphin in einem NMR Experiment gezeigt. Des Weiteren wurden Untersuchungen der katalytischen Hydrophosphinierung von Styrol durchgeführt.

Im zweiten Abschnitt wurden mehrere Mangan-Pincer-Komplexe synthetisiert und deren katalytische Aktivität für die N-Alkylierung von Aminen mit Alkoholen entsprechend der „borrowing hydrogen" Methodologie untersucht. Auf Literaturdaten basierend wurde ein passender nicht-C_2-symmetrischer PN^3-Pincer Ligand (bpy-^{6}NH-P) identifiziert und erfolgreich synthetisiert. Mit diesem Liganden wurde ein Mangan-Pincer-Komplex gebildet, welcher durch Optimierung mehrerer Parameter als Katalysator für die N-Alkylierung von verschiedenen Anilinen und anderen primären Aminen mit Alkoholen etabliert werden konnte. Reaktionstemperaturen von 60 °C konnten in Kombination mit dem Einsatz eines Basen-Additivs im Unterschuss realisiert werden. Die hohe Reaktivität des entwickelten katalytischen Systems bei milden Reaktionsbedingungen ermöglichte es uns anspruchsvollere Substrate wie sekundäre Alkohole, Benzylamin und aliphatische Amine erfolgreich umzusetzen. Darüber hinaus wurde die Aktivität für andere Reaktionstypen wie Transfer-Hydrierung, Aldol-Kondensationen sowie kombinatorische Ansätze untersucht. Abschließend wurde die Modularität des gewählten PN^3 Systems durch die exemplarische Erweiterung durch strukturelle Modifikation und deren Einfluss auf die katalytische Aktivität untersucht.

Table of Contents

List of Charts

List of Figures

List of Schemes

List of Schemes

List of Tables

List of Abbreviations

AB	azobenzene
Ac	acetyl
ADC	acceptorless dehydrogenative coupling
AOB	azoxybenzene
APT	attached proton test
ATR	attenuated total reflectance
bpy	2,2'-bipyridin
BH	borrowing hydrogen
BINOL	1,1'-bi-2-naphthol
*n*Bu	*n*-butyl
*s*Bu	*sec*-butyl
*t*Bu	*tert*-butyl
Cp	η_5-cyclopentadienyl
Cp*	η_5-1,2,3,4,5-pentamethyl cyclopentadienyl
CPME	cyclopentyl methyl ether
DFT	discrete Fourier transform
dipp	2,6-di-*iso*-propylphenyl
DME	1,2-dimethoxyethane
DMF	*N,N*-dimethylformamide
DSMO	dimethylsulfoxide
dppe	1,2-bis(diphenylphosphino)ethane
e.g.	exempli gratia
equiv	equivalent
Et	ethyl
Fp	cyclopentandienyliron dicarbonyl
Fp*	1,2,3,4,5-pentamethylcylclopentadienyliron dicarbonyl
GC-FID	gas chromatography-flame ionization detector
GC-MS	gas chromatography- mass spectrometry
HOMO	highest occupied molecular orbital

HRMS	high resolution mass spectrometry
IR	infrared
LUMO	lowest unoccupied molecular orbital
MACHO	ligand type based on $HN(C_2H_4PR_2)_2$
Me	methyl
MLC	metal-ligand cooperation
m.p.	melting point
MS	molecular sieves
MTBE	*tert*-butyl methyl ether
NMR	nuclear magnetic resonance
Nu	nucleophile
ox	2-oxazoline
Ph	phenyl
phen	1,10-phenanthroline
py	pyridyl
*i*Pr	*iso*-propyl
Tf	trifluoromethanesulfonyl
TFA	trifluoroacetic acid
THF	tetrahydrofuran
TLC	thin-layer chromatography
TMS	tetramethyl silane
TPP	triphenylphosphine
TPOP	triphenylphosphite
*p*Ts	*para*-toluenesulfonyl

1 General Introduction

1.1 Amines

Nitrogen containing compounds are of significant importance in many fields of chemistry. Applications range from multi-ton-scale agrochemicals to pharmaceuticals and fine chemicals.[1] Atom-efficient processes utilizing benign starting materials are being sought to meet the insatiable demand while ensuring sustainability.[2]

Cinacalcet
Hyperparathyroidism

Atomoxetin
Attention Deficit Hyperactivity Disorder

Fentanyl
Opioid

Metoprolol
β_1-blocker
sold as racemate

Tamsulosin
α_1-blocker
Benign prostatic hyperplasia

(S)-Metolachlor
Herbicide
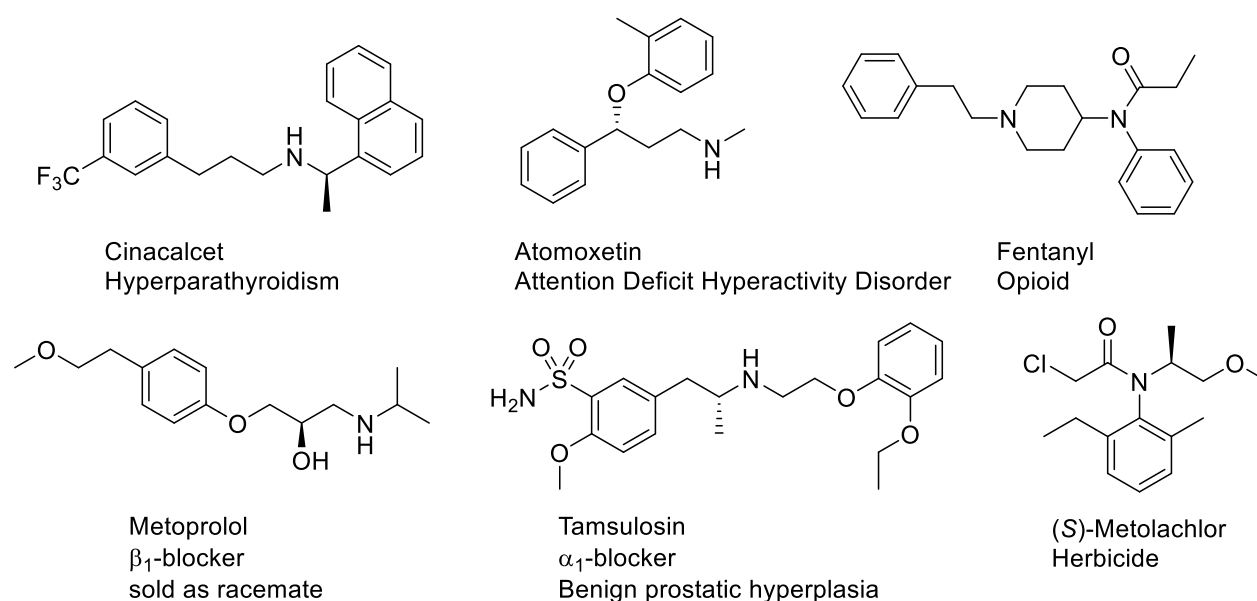
Chart 1. Prominent examples for different secondary and tertiary amines that are used as pharmaceuticals and herbicides.

C_1-C_6 alkyl amines are robust and can be prepared by few steps at harsh conditions in gas phase reactions with little to no side reactions. For large scale reactions ammonia is reacted with a corresponding alcohol undergoing N-alkylation catalyzed by solid acids (Scheme 1).[3]

$$ROH \ + \ NH_3 \xrightarrow[\text{gas phase alyklation}]{\text{solid acid catalyst}} RNH_2 \ + \ R_2NH \ + \ R_3N$$
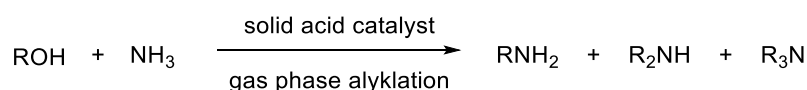
Scheme 1. Schematic depiction of the gas phase alkylation of ammonia to obtain higher amines.

More complex amines require multiple selective steps in their synthesis to ensure incorporation of different heteroatoms, as well as structural features (Chart 1). A selection of

reactions including C-N coupling, reduction of nitrogen containing functional groups and rearrangements is presented in chapter 1.2. In the field of "green chemistry" synthetic reactions are categorized by their efficiency by introduction of the environmental (E) factor (Table 1). This factor takes the amount of employed reagents, additives, catalysts, by-products and waste, and puts it in relation to the amount of desired product. The E factor is lower when more atoms are being utilized in a product in relation to the used materials and waste production. While the production of simple intermediates in a multi-ton scale requires low E factors to prevent large quantities of waste, smaller scale reactions tolerate higher E factors due to a higher price of the product.[4] However, industrial processes like oil refining contain only limited steps which are constantly optimized so all obtained products can be used for further applications. In contrast, pharmaceutical compounds are usually complex molecules (Chart 1) that require multiple preparation steps which are challenging to optimize.

Table 1. Different E factors in the chemical industry.[4]

$$E\ factor = \frac{total\ waste}{product}$$

Industry segment	Annual production [t]	E factor	Waste produced [t]
Oil refining	10^6–10^8	ca 0.1	10^5–10^7
Bulk chemicals	10^4–10^6	<1 to 5	10^4–5×10^6
Fine chemical industry	10^2–10^4	5 to >50	5×10^2–5×10^5
Pharmaceutical industry	10–10^3	25 to >100	2.5×10^5

In pharmaceutical research the preparation of lead structures and desired amines usually aims for a pure product at a small scale in disregard of sustainability. Once compounds are identified as biologically active agents, their preparation has to be scaled up to enable further testing. Thus, catalytic reactions that provide functional group tolerance while suppressing the production of side-products and waste are highly desirable and being sought for.[5]

1.2 Strategies for Amine Synthesis

Amines can be prepared by employing different synthetic strategies. Commonly used methods are stoichiometric reactions that rely on a non-efficient transformation with high amounts of side products and excessive use of reagents. However, these reactions are robust and represent a "dirty but efficient way" which is often being used to justify the

downsides. One of most important industrial processes for the preparation of primary aromatic amines is the reduction of nitroarenes to provide respective amines (Scheme 2).[6]
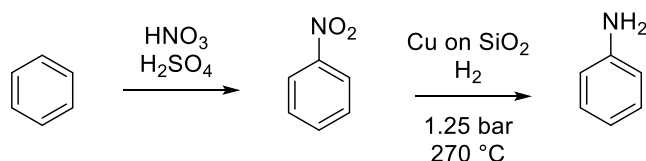
Scheme 2. Two-step preparation of aniline by nitration and reduction.[6]

While nitration of aromatic compounds can be performed selectively under relatively mild conditions in a lab scale, the preparation of nitroalkanes is performed by gas phase reaction of nitrous acid with the corresponding alkane. The reaction follows a radical mechanism which provides a mixture of different nitroalkanes that are separated after the process (Scheme 3).[7]
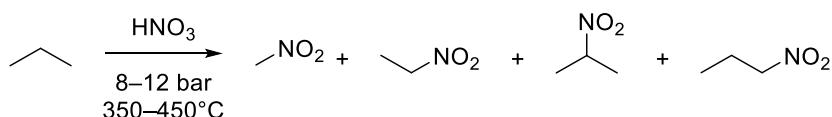
Scheme 3. Industrial process for the preparation of nitro alkanes by gas phase reaction of propane with nitric acid governed by a radical mechanism.[7]

Also other nitrogen containing groups like nitriles, amides, azides and hydroxylamine can be reduced to primary amines in a similar fashion. Amides can also be used in rearrangement reactions which are an elegant method for preparation of primary amines. Multiple "classic" name-reactions (e.g. Curtius-, Schmidt-, Lossen- and Hoffmann-rearrangement) have been established, all utilizing an *in-situ* formed isocyanate which is then hydrolyzed to an amine under CO_2 evolution (Scheme 4).[8-11]
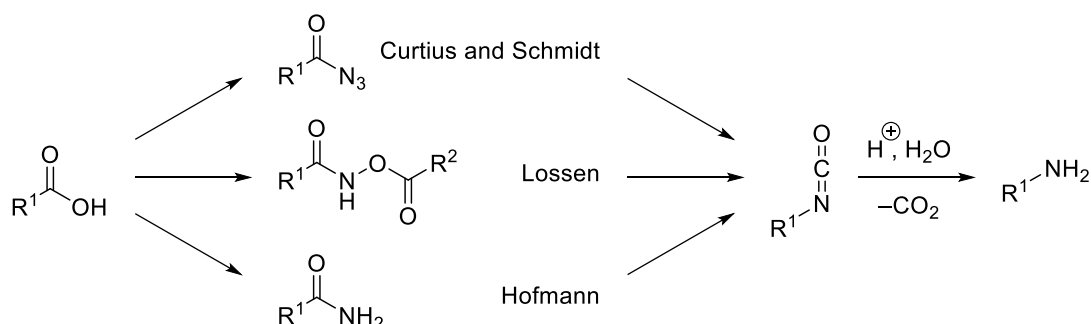
Scheme 4. Rearrangement name-reactions for the conversion of carboxylic acids into amines *via* isocyanate formation.[8-11]

One specific class of the preparation of secondary and tertiary amines is the nucleophilic substitution, which requires base additives and halogenated alkyls as substrates. Aside from the stoichiometric amount of waste being produced, this reaction does not provide mono-alkylated amines, but a mixture of multiple alkylated amines and even quaternary ammonium salts (Scheme 5).[12]
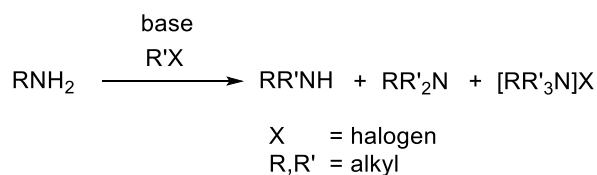
Scheme 5. Schematic reaction of primary alkylamines with alkyl halides under basic conditions providing a mixture of higher amines.[12]

The Gabriel synthesis is a special type of substitution reaction which exclusively provides primary amines by utilizing potassium pthalamide as ammonia surrogate (Scheme 6).[13-14]
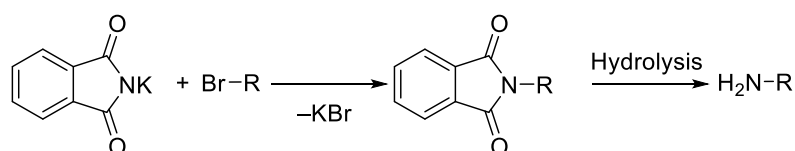
Scheme 6. Gabriel synthesis for the selective preparation of primary amines *via* nucleophilic substitution.[13-14]

Transition metal catalysts can be employed as well, not only suppress the generation of side-products but also to address more challenging substrates in terms of halogenated alkyls and also amine nucleophiles. A famous transformation is the Buchwald-Hartwig amination which allows the amination of aryl halides with a Pd catalyst (Scheme 7).[15-20]
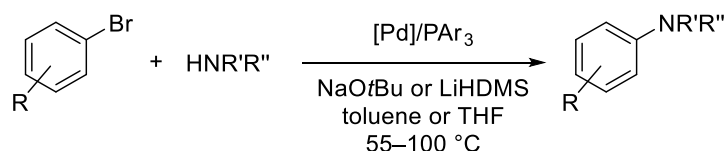
Scheme 7. First generation Buchwald-Hartwig amination reaction.[15-20]

Also reductive amination of electrophilic carbonyl compounds with amines can be used as viable strategy to selectively prepare secondary or tertiary amines. The stepwise preparation of an aldimine or ketimine and subsequent reduction is limited to secondary amines. In the Leuckart reaction both condensation and reduction are performed in a one-pot reaction with formic acid with the role of both coupling and reducing agent. In this, even primary amines can be obtained when ammonium formate is applied in a closed vessel (Scheme 8).[21] The Eschweiler-Clarke reaction is a variation which utilizes formaldehyde and formic acid providing bis-methylated amines in a selective manner (Scheme 8).[22] Also hydrogen can be applied as reductant in transition metal catalyzed reactions (Scheme 8).[23-25]
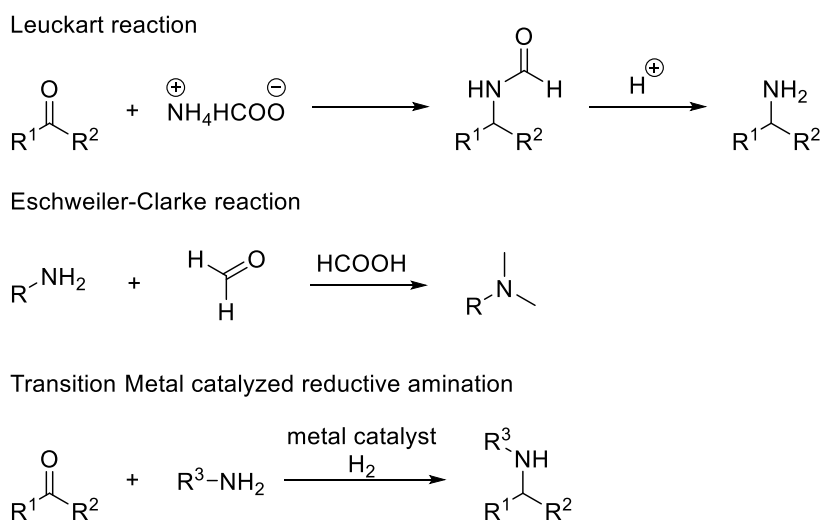
Scheme 8. Preparation of primary, secondary and tertiary amines by reductive amination.[21-25]

A further approach is using alcohols as substrates which provides non-toxic water as side product and prevents the formation of ammonium salts. A wide variety of catalysts was developed for that purpose ranging from noble metal homogeneous approaches (Rh, Ir, Ru, Pt) to heterogeneous approaches (Ni, Co, Fe, Cu, Fe, Al, Ti, Au) for industrial applications (Scheme 9).[12, 26]

$$3\ C_2H_5OH\ +\ NH_3\ \xrightarrow[\substack{0.5–25\ MPa \\ 100–250\ °C}]{\substack{Ni/Co/Cu/Fe \\ on\ ZrO_2/SiO_2/Al_2O_3 \\ H_2}}\ (C_2H_5)_3N\ +\ 3\ H_2O$$
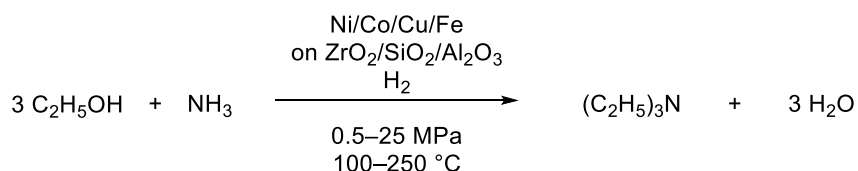
Scheme 9. Schematic depiction of the synthetic process of triethylamine from ammonia and ethanol under hydrogen.[12]

Heterogeneous applications remain challenging in terms of product selectivity since the required harsh reaction conditions hamper e.g. selective methylation of ammonia with methanol to produce methylamine. Noble metal catalysts however, were found to be very active and catalyze the reaction at relatively low loadings but under comparatively harsh conditions.[27] Recently, the interest not only in active but also in less toxic and more abundant resources for catalysts has been growing.[27] Thus, first row "base metals" became more interesting for replacing noble metals in catalytic applications. Compared to their noble siblings, base metals have been found to be less active catalysts and require higher catalyst and additives loadings.[28] But taking the natural abundance and the cost of metal precursors into account further research in that area is justified.[29] Since both, first row and noble metals exhibit toxic characteristics low catalyst loadings are highly desirable.[30-32] In N-alkylation reactions with alcohols some noble metal catalysts can also be used as simple carbonyl compounds, while their first row counterparts rely heavily on suitable ligands to enable catalytic activity. The metal-ligand cooperated (MLC) catalysis was already observed with Ru and Ir complexes and successfully applied in base metal-based systems (Scheme 10).[33-37]

Ar   Ar = 4-CF$_3$-C$_6$H$_4$ Ph

$(i$Pr)$_2$P—Ir—P(iPr)$_2$

$(i$Pr)$_2$P—Mn—P(iPr)$_2$

OH + OH + OH + $\underset{H_2N}{\overset{R'''}{\diagdown}}$NH $\xrightarrow[\text{KO}t\text{Bu}]{\text{[Ir] or [Mn]}}$
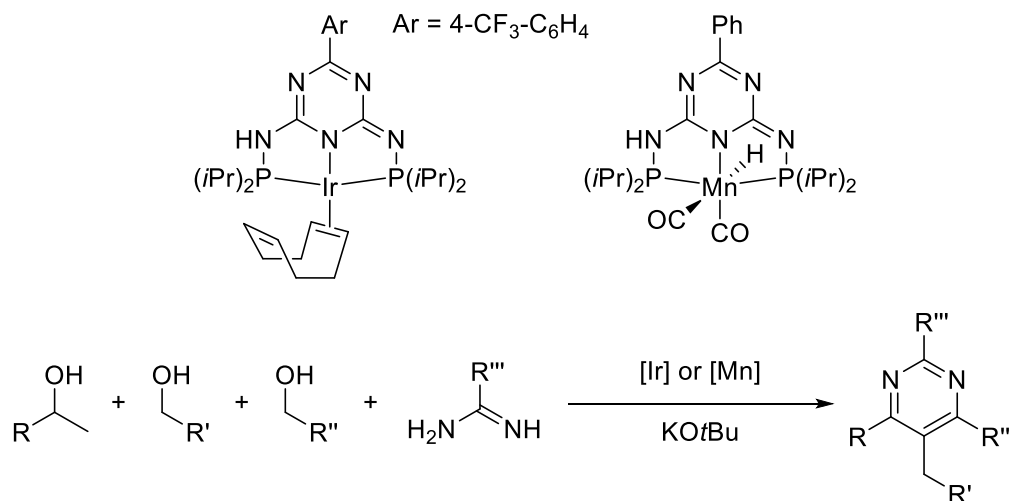
Scheme 10. Multicomponent synthesis of pyrimidines from alcohols and amidines catalyzed by both iridium and manganese pincer complexes.[33-35]

A further step to improve amine synthesis efficiency is the hydroamination reaction. It enables the direct addition of N-H across an unsaturated C-C bond, providing a clean way to prepare higher amines. This reaction resembles a nucleophilic addition to an unsaturated bond. However, this comes with a manifold of problems due to electronic repulsion and will be discussed in chapter 3.1.1.

2 Aim of this Work

Formation of carbon-heteroatom bonds is one of the main goals of chemical synthesis. Different approaches ranging from stoichiometric reactions to catalytic transformation of substrates can be chosen to reach this goal. While noble metal catalysts are widely employed for preparation of target molecules, base metals did not get as much attention in homogeneous catalysis. However, in terms of sustainable chemistry and employment of abundant resources, base metals provide a welcome alternative for catalytic approaches.[38]

This work is focusing on the investigation and development of well-defined iron- and manganese complexes as suitable catalysts for carbon-heteroatom bond formation. The approach is driven by the idea to implement or adapt catalytic systems for direct amination reactions.

3 Chapter I – Olefin Activation at Defined Cationic Iron Centers

3.1 Introduction

3.1.1 Hydroamination

Common multistep syntheses of amines are rather expensive and a wide range of reagents are used (see also chapter 1.2). Hydroamination is a good alternative, considering atom efficiency and count of synthetic steps. The hydroamination reaction involves the addition of an amine group to an unsaturated carbon-carbon bond. As a result, highly valuable compounds are obtained by the reaction of readily available amines and alkenes or alkynes.[39-48] Although this reaction is slightly exothermic, its hindrance, caused by electrostatic repulsion of the lone pair of nitrogen and the electrons in the HOMO orbital of the olefin, leads to a high activation barrier (Scheme 11).[49]

$$NH_3 \quad + \quad \diagup\!\!\!\diagup \quad \longrightarrow \quad \diagdown\!\!\!\diagup NH_2 \qquad \begin{aligned} \Delta H^\circ &= -52.7 \ \text{kJ/mol} \\ \Delta S^\circ &= -127.3 \ \text{kJ/mol} \\ \Delta G^\circ &= -14.7 \ \text{kJ/mol} \end{aligned}$$
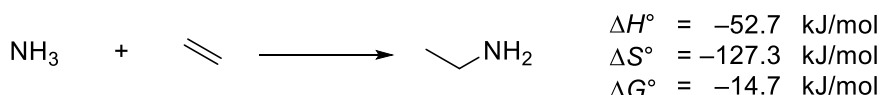
Scheme 11. Thermodynamic calculation for amine addition to an olefin.[49]

Aside from the Takasago-Menthol synthesis,[50] no suitable homogenous catalysts for industrial applications have been found yet. Catalysts either lack activity or its cost is out of proportion with its products. Implemented systems can be divided by the governed mechanisms in hydroamination. Complexes based on alkaline earth metals (calcium, magnesium, strontium, barium), rare earth metals (yttrium, lanthanum, lutetium, neodymium, samarium), actinides (thorium, uranium), and early transition metals (titanium, zirconium, niobium, tantalum) are found to employ an inner sphere mechanism including amine activation.[39-40, 42, 51-54] The accepted mechanism for those metals proposes the formation of a metal amide or imide followed by an olefin insertion into the metal nitrogen bond (Scheme 12).
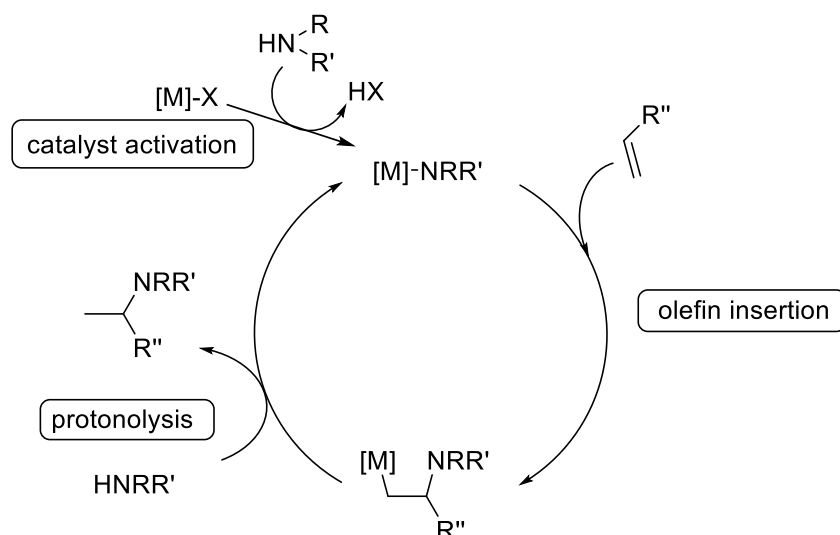
Scheme 12. Exemplary inner sphere mechanism for hydroamination of olefins.[55-59]

For late transition metals like ruthenium (Group 8), iridium, rhodium (Group 9), nickel, palladium, platinum (Group 10), copper, gold (Group 11) and zinc (Group 11) an outer sphere mechanism is proposed.[43, 55-59] This involves π-coordination of an olefin to the metal center, followed by a nucleophilic attack at the olefin (Scheme 13). Known base metal catalyzed systems have either a limited applicability or are less atom efficient.[43, 57, 60-65]
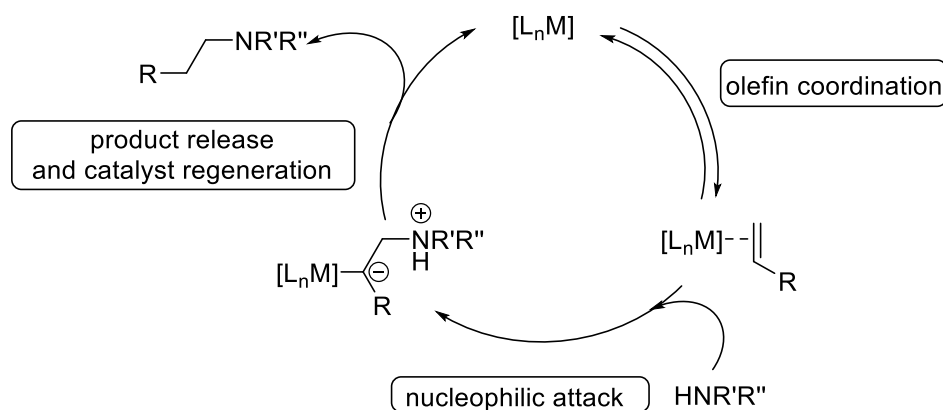
Scheme 13. Exemplary outer sphere mechanism for intermolecular hydroamination with late transition metal complexes.[58]

When primary amines are used as substrates, both mechanisms bear the possible side reaction of β-hydride elimination and the release of an imine as the reductive amination product (Scheme 14). To suppress the formation of a metal hydride species, complexes with only one open coordination site are preferred.
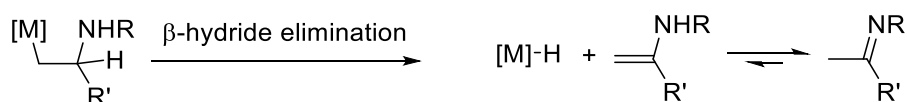
Scheme 14. Possible β-hydride elimination pathway and release of imine.

Controlling the outcome of the product is an important aspect since the linear anti-Markovnikov addition to the olefin is highly preferred.[66-67]

3.1.2 Nucleophilic Addition to Activated Olefins

Addition of nucleophiles across an unsaturated carbon-carbon bond is hindered by electrostatic repulsion which results in the need for an olefin activation. This activation can either be achieved by substrate alteration with electron withdrawing substituents or by an external activation by coordination to a metal center. A metal-π-complex is formed and electron density at the olefin is reduced by σ-donation. In that, the filled HOMO π-orbital of the olefin interacts with a LUMO metal orbital, transferring electron density to the metal. Further, electron rich metal centers exert π-backbonding in which the HOMO metal orbital is interacting with the LUMO p*-orbital of the coordinated olefin. Strong interactions even result in the formal formation of sp^3 carbon centers which are not desired for nucleophilic attacks (Figure 1).[68] Thus, an electron-deficient metal center is sought for activation of olefins for nucleophilic addition.

σ-donation π-backbonding
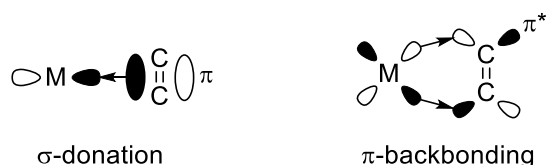
Figure 1. Dewar-Chatt-Duncanson model of electronic interactions of metal and olefin in π-complexes.[68]

Nucleophilic additions to cationic complexes were thoroughly investigated which led to the establishment of the empirical Green-Davis-Mingos rules for 18 valence electron metal-olefin complexes (Figure 2).[69-70] Nucleophilic addition to ethylene should be favored in systems with multiple different olefins coordinated to a metal center. However, the formation of adducts provides the formation of Markovnikov adducts which is thermodynamically controlled.[71]

1. Nucleophiles add preferarbly to polyenes with even hapticity
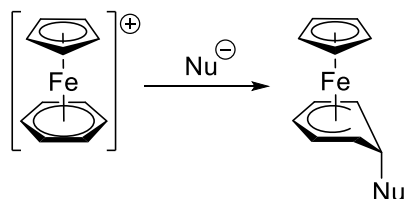
2. Nucleophiles add to acyclic polyenes rather than cyclic polyenes
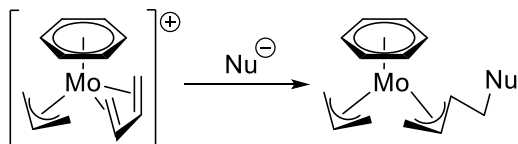
3. Nucleophiles add preferentially to the terminal site of polyenes
   Unless a polyene with uneven hapticity is coordinated to an electron rich metal

Figure 2. Chosen examples for Green-Davis-Mingos rules for the addition of nucleophiles to cationic metal olefin complexes.[69-70]

Rosenblum *et al.* investigated the addition of enolates and different hetero nucleophiles to cationic 18 valence electron iron-ethylene complexes. Various sets of adducts were isolated as iron-alkyl complexes. While lithium compounds were used for C-C bond formation, thiols were combined with potassium carbonate as basic additive. Hydrides were introduced with sodium cyanoborohydride. Amines, phosphines and phosphites readily reacted under the formation of quarternary compounds. When secondary amines are used, it is possible to enforce a double addition when excess of base is added.[72-75]
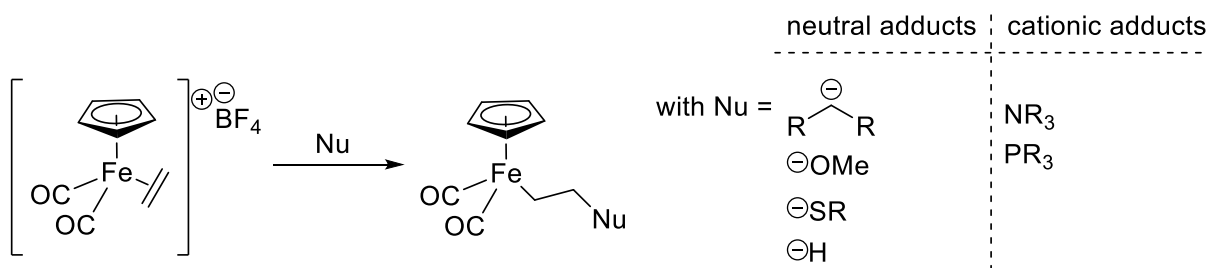
Scheme 15. Addition of nucleophiles to cationic iron ethylene complexes under formation of new carbon-nucleophile bonds.[72-75]

Initial attempts to cleave the iron-carbon bond resulted in complex degradation.[72] So different studies for controlled iron-carbon bond cleavage were performed including oxidative, electrophilic and thermal bond cleavage.[76-80] In all cases the iron piano stool

complex was found to degrade in stoichiometric reactions while the organic product was liberated. Thus, the use of dicarbonyl iron cyclopentadienyl as synthetic auxiliary was proposed.[71, 81-83]

3.1.3 Established 3d-metal Catalysts for Hydroamination *via* Olefin Activation

A well-defined aminotroponiminate zinc methyl catalyst was introduced by Roesky *et al.* for the intramolecular hydroamination of amino-olefins.[84] The system was adjusted by Mandal *et al.* by introduction of a ligand with a different aromatic backbone (Scheme 16).[85-86]

$R^1 = {}^iPr, Cy$
$R^2 = H, CH_2(hetero)aryl$
$R^3 = Ph, alkyl$
$R^4 = H, Me$
$n = 1, 2$

5 mol% [Zn]
5 mol% [PhNMe$_2$H][B(C$_6$F$_5$)$_4$]

C$_6$D$_6$
80–120 °C
0.5–110 h

91–99% NMR yield
(15 examples)
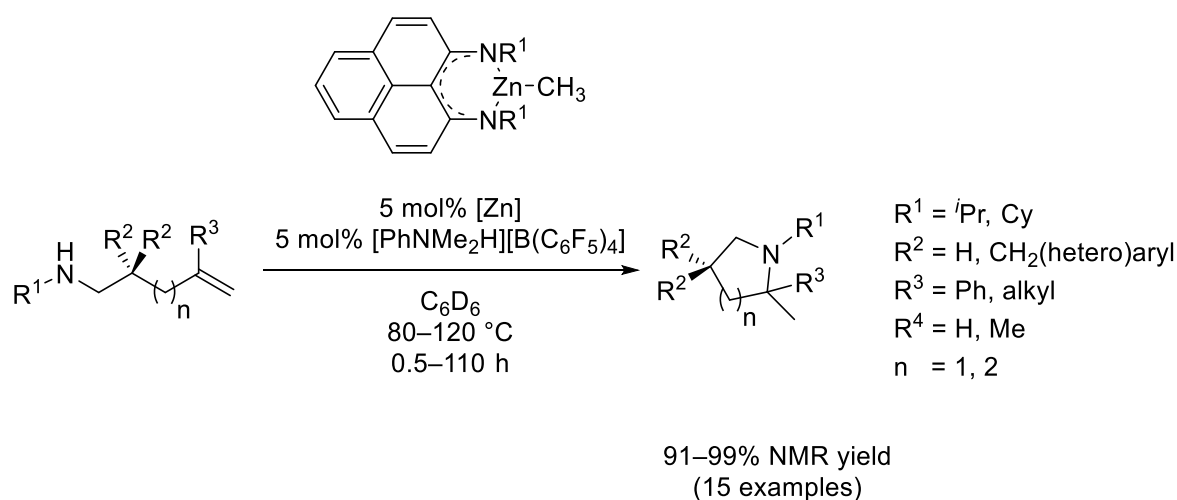
Scheme 16. Organozinc catalyst for intramolecular hydroamination of amino-olefins.[43, 85-86]

It was observed that the catalytic system can also perform with a dialkyl zinc precatalyst without any ligand.[87] However, it relies on an acidic additive for the catalyst activation by dealkylation. The scope of the well-defined catalysts is limited to gem-disubstituted substrates which facilitate cyclisation featuring the Thorpe-Ingold effect (Figure 3).[42, 88-91] The gem-substitution pattern causes the substrate to "fold" which reduces the spatial distance of the reactive terminal groups.

H H
Et⌣Et
115.3 °

Me Me
Et⌣Et
109.5 °

Ph Ph
Et⌣Et
<109.5 °
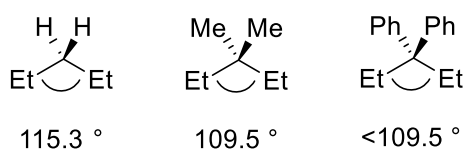
Figure 3. Exemplary depiction of the influence of gem-substitution on bond angles.[88, 92]

In 2016, the group of Monnier introduced a copper catalyst for intermolecular hydroamination of allenes.[93] It was proposed that during the catalytic cycle a cationic copper-amine complex is formed and that the allene is activated by π-coordination.[94]
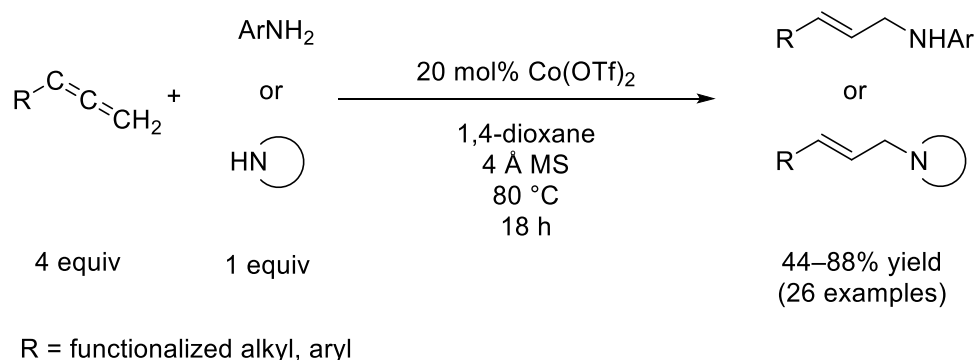
Scheme 17. Copper catalyzed intermolecular hydroamination of allenes.[43, 93-94]

In 2006 the groups of Takaki reported FeCl$_3$ as suitable catalyst for intramolecular hydroamination.[51] In the following years, the scope was extended to intermolecular hydroamination of styrenes, norbornenes and allenes.[95-97] As a strong Lewis acid, FeCl$_3$ is proposed to activate the olefin by π-coordination followed by nucleophilic addition of the amine (Scheme 13).[96] However, no well-defined Fe(III) system for π-coordination was reported in the literature which limits possibilities of catalyst design for tailor-made applications.

In conclusion, no suitable and well-defined catalytic system for intermolecular hydroamination of alkenes has been introduced so far. Even though, the Green-Davis-Mingos rules support the olefin activations at 3d metal centers.

3.1.4 Established Iron Catalysts for Hydroamination *without* Olefin Activation

A range of catalytic systems based on iron were described not following an olefin activation mechanism. A good example are well-defined systems based on Fe(III) for hydroamination that provide tandem hydrogenation of nitro-groups. A complex one-electron step mechanism with a hydride source is proposed for that system.[98] Initially started with an undefined precatalyst, further optimizations towards a well-defined catalyst were developed by the groups of Thomas and Shaver (Scheme 18).[99]
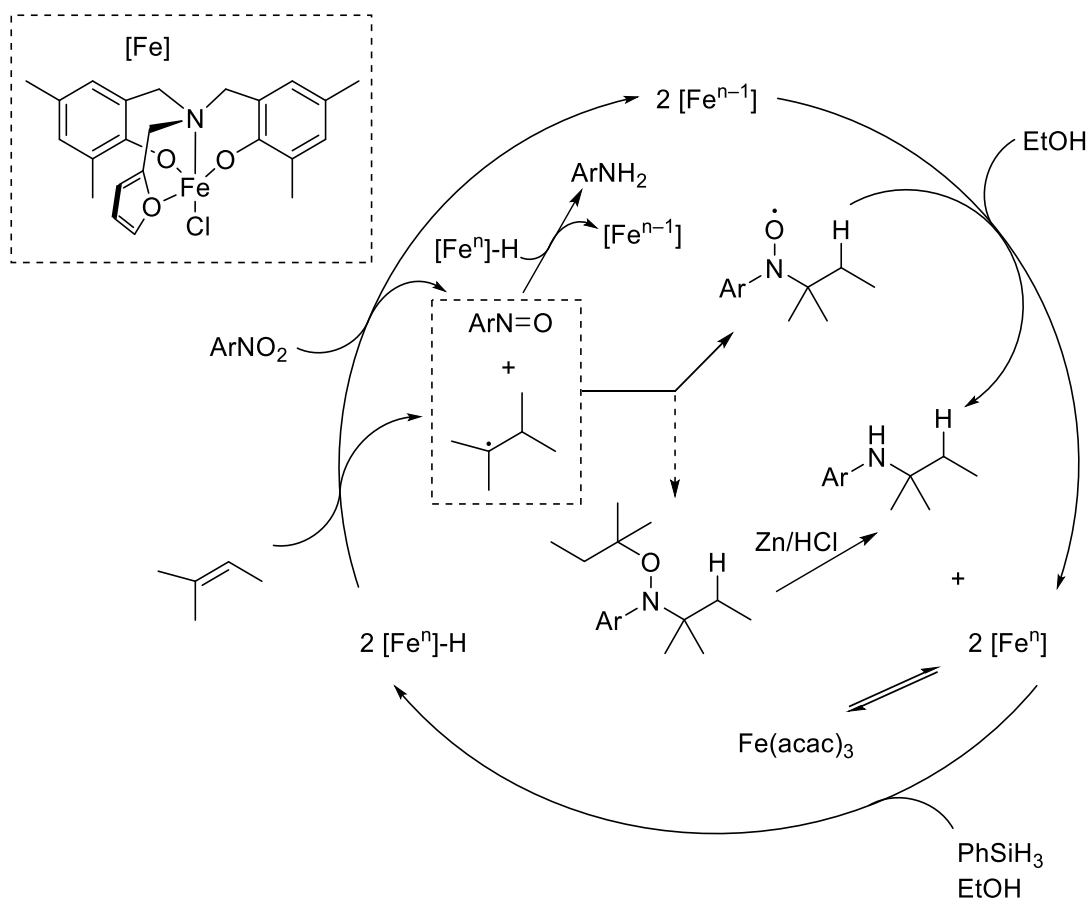
Scheme 18. Proposed mechanism for reduction-hydroamination of 2-methyl-2-butene with nitroarenes.[98-100]

In 2014, the groups of Hannedouche and Yang independently developed systems based on Fe(II) (Chart 2).[53-54] The system presented by the group of Hannedouche is a well-defined complex and can be employed for intramolecular hydroamination with a proposed mechanism comparable to early transition metals (Scheme 12). The substrate scope is limited to gem-disubstituted substrates since the Thorpe-Ingold effect seems necessary for the catalytic conversion (Figure 3).[53]
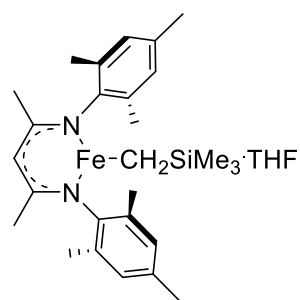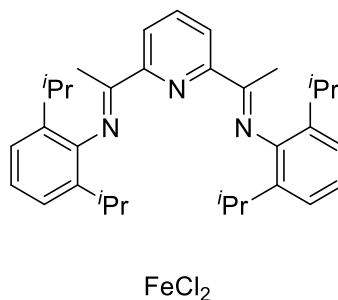
Hannedouche *et al.*   **Yang *et al.***

Chart 2. Fe(II)-based catalysts for hydroamination.[53-54]

The system presented by Yang can be applied for intermolecular hydroamination of styrenes with *O*-benzoyl-*N,N*-dialykl hydroxylamines and a Grignard-reagent as additive. The proposed catalyst is formed *in-situ* by combination of metal precursor and ligand (Scheme 19).[54]
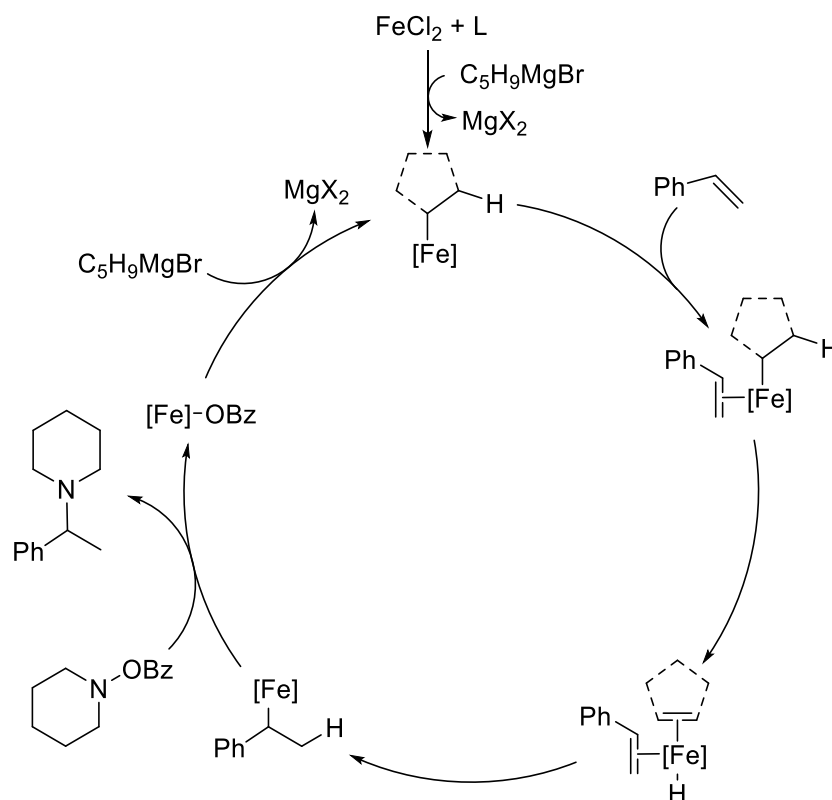
Scheme 19. Proposed mechanism for intermolecular formal hydroamination of styrene *via* an iron-hydride.[54]

In the proposed catalytic cycle the active iron-hydride species is formed by a salt metathesis. Styrene coordinates to the iron center and β-hydride elimination releases

cyclopentene. By migratory insertion an iron-alkyl complex is formed, which is then converted to an iron-benzoyl complex by nucleophilic substitution. The formed benzoate complex is then regenerated by the Grignard-reagent (Scheme 19).[54]

Fe(II)-based systems were also investigated for hydrophosphination including salen and piano stool complexes.[101-104] Interestingly, Nakazawas research focused on neutral alkyl piano stool complexes with the idea of empty coordination sites on the Fe(II) center. The proposed mechanism also involved activation of the nucleophilic moiety with subsequent alkyne coordination and migratory insertion (Scheme 20).[102]
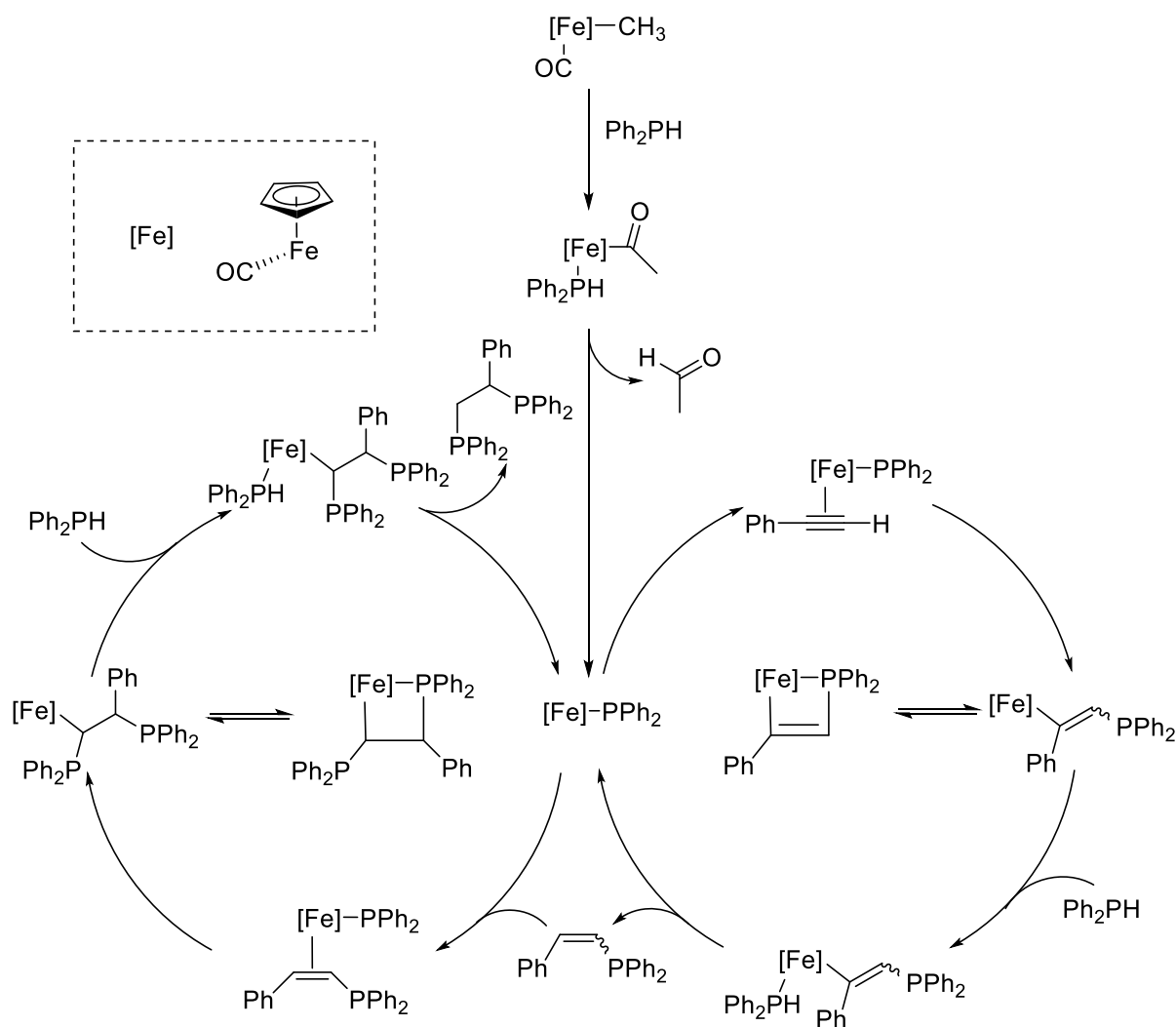
Scheme 20. Proposed mechanism for iron-catalyzed double-hydrophosphination of phenylacetylene.[102]

Although, there are some examples for iron catalyzed hydroamination and also hydrophosphination with piano stool complexes, there are no reports on hydroamination reactions catalyzed by piano-stool iron (II) complexes to the best of our knowledge. Also, the

published well-defined iron catalysts are either limited to intramolecular hydroamination or are highly depending on additives to perform catalytic reactions.

3.2 Motivation

Iron catalyzed hydroamination has been subject to limited development in comparison to other metals, but found interest in the recent years with the emphasis of developing well-defined catalytic systems.[39, 43, 105] While the well-defined catalytic iron systems are proposed to employ either amine activation or one-electron step pathways, the Lewis acid-catalyst $FeCl_3$ is proposed to follow an olefin activation pathway.[51, 53, 98] Based on the reports of Rosenblum, cationic iron(II) complexes can activate olefins for the addition of nucleophiles.[72-75, 106] However, the complexes have been used as synthetic auxiliaries and were never introduced as catalysts for hydrofunctionalization.[71, 77-78, 107]

The first chapter of this work focuses on investigations on the activation of olefins at well-defined cationic iron centers. The findings of Rosenblum for cationic iron piano stool complexes are revisited and structural alterations by ligand substitution are studied. Further, nucleophilic addition to coordinated olefins and development of a hydrofunctionalization reaction are researched.

Introduction of a well-defined catalytic iron system that employs an olefin-activation mechanism could provide a powerful tool to control selective synthesis of desired molecules. As a metal-complex, the system could provide a tunable catalytic approach to hydrofunctionalization reactions utilizing an abundant metal as resource.

3.3 Results and Discussion

3.3.1 Structural Investigation of Cationic Iron Olefin Complexes

3.3.1.1 General Route for Preparation of Cationic Iron Half-Sandwich Complexes
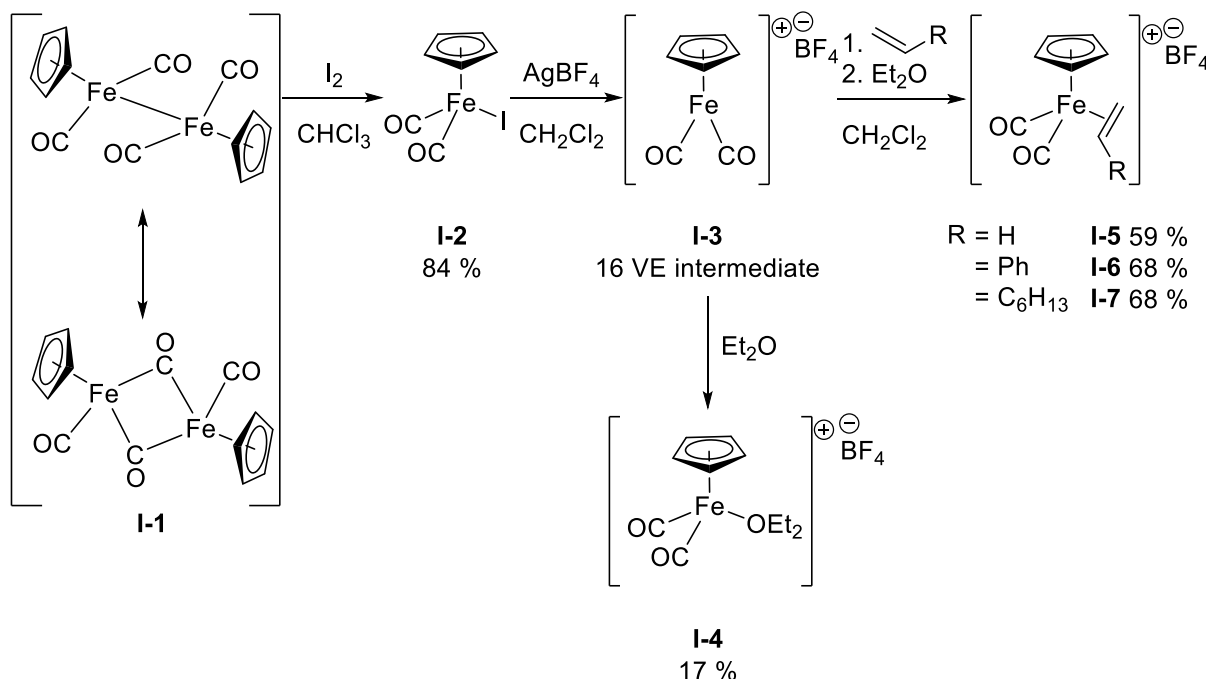
Chart 3. Preparation of different cationic cyclopentadienyl iron dicarbonyl (Fp) complexes.[108-109]

Half-sandwich or piano-stool complexes of iron are prepared in a straight forward manner in two steps. In the first step (not shown), reaction of iron pentacarbonyl with cyclopentadiene (CpH) forms the commercially available cyclopentadienyl dicarbonyl iron(I) dimer Fp_2 (**I-1**).[108] The second step involves oxidative cleavage of the iron-iron bond with a halogen. FpI (**I-2**) was obtained in a good yield by treating Fp_2 with iodine in chloroform and was readily purified by removing residual iodine under vacuum.[108] The neutral complex **I-2** was then treated with $AgBF_4$ in a salt metathesis reaction, creating the cationic 16 VE intermediate **I-3**.[109] Upon addition of electron donating substrates either the intense red diethylether complex **I-4** or different olefin complexes **I-5**–**I-7** were obtained in average to good yields, respectively.[109] The resulting cationic complexes were found to be stable indefinitely under argon at –35 °C and were characterized by ^{1}H NMR spectroscopy.

When **I-7** was dissolved in CD_2Cl_2 for NMR spectroscopic analysis, the formation of crystals was observed at room temperature overnight. The obtained crystals were suitable for X-ray analysis and the molecular structure showed the coordination of styrene to the cationic iron center (Figure 4). Especially the elongated C–C bond with 1.486 Å (compare C-

C single bond, 1.54 Å, and C=C double bond, 1.33 Å) indicates a strong interaction between styrene and iron. Also the carbonyl ligands show an increased Fe-C bond distance (1.815 Å vs. 1.769 Å) which supports that higher electron density leads to weaker interaction with CO ligands.[110]
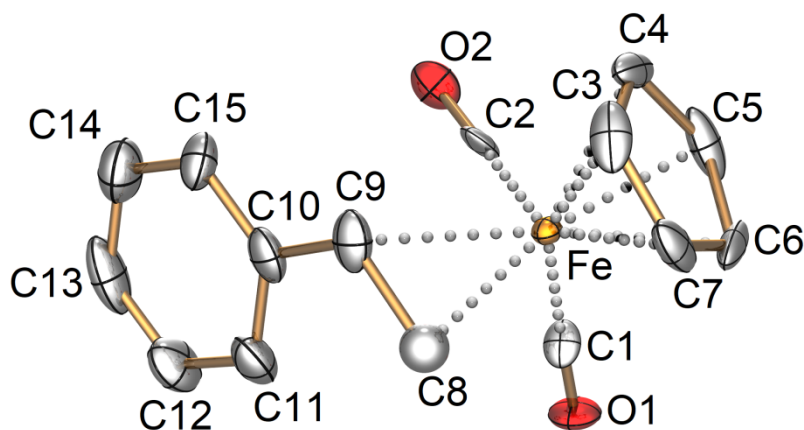
Figure 4. Molecular structure of cationic species [Fp(η_2-styrene)]BF$_4$ (**I-7**) with thermal ellipsoids set at 50% probability. The anion BF$_4^-$ and all hydrogen atoms are omitted for clarity. Selected bond lengths [Å]: Fe–C1 = 1.815, Fe–C2 = 1.815, Fe–C8 2.159, Fe–C9 = 2.261, C8–C9 = 1.486.

3.3.1.2 Replacement of CO with Phosphorus(III)-based Ligands

A set of phosphines and phosphites was chosen in order to investigate the potential structural tunability of iron piano-stool complexes. The selected ligands were supposed to cover the main aspects of low electronic density and different steric demand due to their cone angle. Also bidentate ligands were chosen to investigate potential influences on a proposedly slightly strained iron complex.

Table 2. Electronic parameters and cone angles for different mono- and bidentate phosphorus(III) ligands in $Ni(CO)_{4-n}L_n$ systems.

overall higher amount of electron density donating to metal center

$$PX_1X_2X_3: \nu = 2056.1 + \sum_{i=3}^{3} \chi_i \text{ [}\nu \text{ in cm}^{-1}\text{]}$$

With χ_i [ν in cm^{-1}]: Et 1.8, Me 2.0, Ph 4.3, OPh 9.7, CF$_3$ 19.7[111]

Entry	Phosphine ligand	ν(CO) [cm^{-1}]	^{31}P{^{1}H} NMR [ppm]	θ(XPX) [°]
1	P(CF$_3$)$_3$	2114.9[a]	–2[b]	137
2	(CF$_3$)$_2$PC$_2$H$_4$P(CF$_3$)$_2$ **I-8**	2097.3[a]	–2[112]	120[c,d]
3	P(C$_6$F$_5$)$_3$ **I-9**	2090.9	–77[b]	184
4	P(OCH$_2$)$_3$CEt **I-10**	2086.8	93	101
5	P(OPh)$_3$ **I-11**	2085.3[a]	129	128
6	(PhO)$_2$PC$_2$H$_4$P(OPh)$_2$ **I-12**	2077.3[a]	179	111[b,c]
7	PPh$_3$ **I-13**	2068.9	–8	145
8	Ph$_2$PC$_2$H$_4$PPh$_2$ **I-14**	2066.5[a]	–13[b]	125[b]

[a] calculated, ethylene bridge was accounted as Et; [b] calculated values;[111] [c] Value was given for half chelate assuming coordinated angle of M[R$_2$P(CH$_2$)$_2$PR$_2$] of 85°; [d] assumed from Et$_2$PCH$_2$CH$_2$PEt$_2$ (115°) vs. PEt$_3$ (132°) $\Delta\theta$ = 17.[111, 113]

As a starting point we chose seven different P-ligands (**I-8**–**I-14**) which were ranked by their electronic interaction with Ni in Ni(CO)$_3$L. The values were taken from the literature, which quantified π-back donation into CO π^*-orbitals by IR measurements of ν(CO) vibrations indicating the CO bond strength.[111, 113] Some values (Table 2, entries 1–2, 5–6 and 8) were calculated according to a semi empirical formula developed by Tolman *et al.* which predicts the vibrational band by summarizing incremental factors of the substituents on the

phosphorus ligand.[111, 113] The electron density of $R_2PC_2H_4PR_2$ is assumed to be similar to $PEtR_2$ in order to use Et for incremental calculations with the empirical formula. A combination of weak σ-donating and strong π-accepting P-ligands results in less electron density that can populate the CO π^*-orbitals providing relatively strong CO bond and thus lead to ν(CO) vibrations at higher frequency (Table 2, entry 1). More σ-donating effects and/or weaker π-acceptor strength lead to more electron density at the Ni center, which ultimately cause ν(CO) vibrations at lower frequency (Table 1, entry 8). The effect is not solely relying on electronic density, which is directly correlating with NMR spectroscopic shifts (Table 1, column 4), since no correlation between ν(CO) and NMR chemical shifts was observed. In addition to the electronic interaction we also took the cone angle of the P-ligand into account, which was thought to be important for substitution of multiple CO ligands as well as for sterically hindering multiple substrates from coordinating to the metal center. **I-9**, **I-10** and **I-11** represent a perfect set of ligands for comparable electronics but different bulkiness. Another pair is **I-13** and **I-14**, whilst **I-12** remains a good average alternative in terms of electronics and bulkiness. Compounds **I-8**, **I-10** and **I-12** were synthesized for our investigation on CO ligand substitution, whereas **I-9**, **I-11**, **I-13** and **I-14** are commercially available.

The preparation of monodentate **I-10** was achieved by transesterification of triethylphosphite and 1,1,1-trimethylol propane under basic conditions.[114] This continuous distillation reaction provided good yields in gram scale and the obtained product could be used for complexation without further purification (Scheme 21).
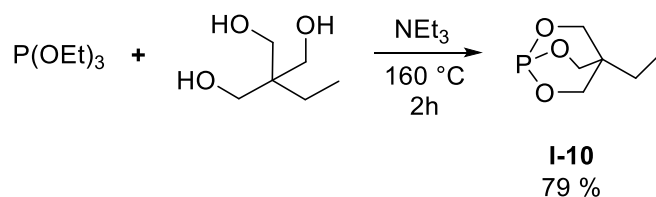
Scheme 21. Preparation of monodentate (L_1) phosphite ligand **I-10**.[114]

The bidentate ligands shared a synthetic route, with **I-12** being a precursor for the preparation of **I-8**. **I-12** could be prepared in good yield by alcoholysis of 1,2-bis dichlorophosphino ethane with phenol at low temperatures and under argon atmosphere. According to literature, treatment of **I-12** with excess of trimethylsilyl triflouromethane in the presence of cesium fluoride would provide **I-8**.[112] No product could be isolated and $^{19}F\{^1H\}/^{31}P\{^1H\}$ NMR spectroscopic investigations showed the formation of multiple products which could not be separated though. The literature procedure suggested crystallization at

–35 °C from Et$_2$O, but only oily residues containing a mixture of different phosphorus species were obtained (Scheme 22). The main side-product was believed to be partially oxidized **I-8** with some unreacted **I-12** present since ^{31}P{^{1}H} NMR spectroscopic investigations showed two different multiplets at –1.47 to –0.36 ppm (expected product)[112] and 1.76 to 2.73 ppm respectively.

PhOH + [PCl$_2$ / PCl$_2$] $\xrightarrow[\text{−78°C to rt} \\ \text{16h}]{\text{NEt}_3 \\ \text{Et}_2\text{O}}$ [P(OPh)$_2$ / P(OPh)$_2$] $\xrightarrow[\text{Et}_2\text{O} \\ \text{rt} \\ \text{24h}]{\text{CsF, TMSCF}_3}$ ✗ [P(CF$_3$)$_2$ / P(CF$_3$)$_2$]

I-12
80 %

I-8
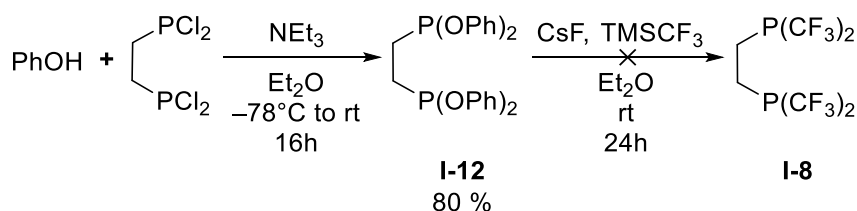
Scheme 22. Attempted stepwise preparation of bidentate (L$_2$) phosphorus(III) ligands **I-12** and **I-8**.[112]

To prepare different iron half-sandwich complexes, our strategy involved the introduction of P-ligands in FpI (**I-2**) to create bench stable precursors for further reactions. According to literature, CO can easily be substituted under reflux conditions in toluene (Table 3).[115-117] The substitution reaction is proposed to proceed stepwise through an external ligand coordinating to iron and pushing iodine out of the coordination sphere. The resulting cationic intermediate is only sparingly soluble in toluene and then iodine returns to the coordination sphere under loss of CO. The intermediate species was sometimes observed as undesired side product for bidentate ligands and could also be isolated. To convert it to the desired product prolonged reaction times were employed.

Table 3. Yields of schematic preparation of differently phosphorus coordinated Fp-type iodide complexes.[115-117]

#	P ligand	L_1	L_2	Product	Yield [%]
1	$P(C_6F_5)_3$ **I-9**	**I-9**	CO	-	-
2	$P(OCH_2)_3CEt$ **I-10**	**I-10**	**I-10**	**I-15**	79
3	$P(OPh)_3$ **I-11**	**I-11**	CO	**I-16**	92
4	$(PhO)_2PC_2H_4P(OPh)_2$ **I-12**	**I-12** [a]		**I-17**	27
5	PPh_3 **I-13**	**I-13**	CO	**I-18**	93
6	$Ph_2PC_2H_4PPh_2$ **I-14**	**I-14** [a]		**I-19**	95

[a] bidentate ligand.
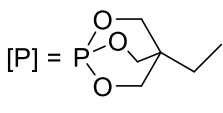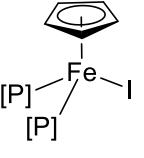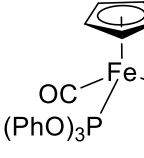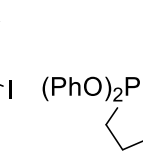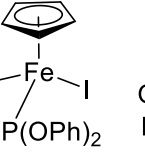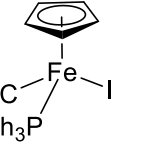
The attempt to introduce **I-9** as ligand by CO substitution was unsuccessful, with all starting materials being recovered even after prolonged reaction time, providing no observable product (Table 3, entry 1). When **I-10** was introduced, an inseparable mixture of the mono- and disubstituted product **I-15** was observed. Even using non-stochiometric amounts of **I-10** resulted in exchange of both CO ligands which may indicate that the second substitution step is occurring faster than the initial substitution. Since substitution of both CO was already anticipated for bidentate ligand, we decided to use 2.5 equivalents of **I-10** in the preparation and obtained **I-15** with a 78 % yield (Table 3, entry 2). Introduction of sterically more demanding **I-11** and **I-13** resulted only in mono substituted products **I-16** and **I-17** in excellent yield (Table 3, entries 3 and 5). Substitution of both CO ligands was not observed upon using excess of **I-11** or **I-13**, respectively (*vide supra*). Bidentate ligand **I-12** and **I-14** showed significantly lower activity in the substitution reaction to obtain neutral iodide complexes. The reason for this is the formation of relatively stable cationic κ_2-complex intermediates **I-15a–I-19a**. As mentioned before, the intermediates could also be isolated and were investigated in following experiments. Thus, complex **I-17** was obtained in a poor yield (Table 3, entry 4), while **I-19** provided improved yield after prolonged reaction time (Table 3, entry 6).[115-116] A potential alternative route for the preparation of piano stool iron complexes is starting from iron(II) halides which is addressed in chapter 3.3.1.4.

With the complexes **I-15**–**I-19** in hand the first investigation on the change of the electronic density at the iron central atom was conducted. The effects were identified by using Cp as ^{1}H NMR spectroscopic probe and comparing chemical shifts of **I-2** with **I-15**–**I-19** and ν(CO) bands of **I-2** with **I-16** and **I-18**, respectively.

The ^{1}H NMR spectroscopic data suggests that the electronic environment of the Cp ring is not only influenced by electron density at the iron center but is greatly affected by the substitution pattern on the ligands. In all cases the signal of Cp is shifted upfield which means more electron density is located at the protons resulting in a shielding effect. The same correlation can be observed for coordination of mono- and bidentate ligands of the same type (Table 4, entries 3–6). In contrast to the significant change in the ^{1}H NMR chemical shift of the Cp signal, the ATR-IR measurement showed that ν(CO) is only slightly reduced frequency for **I-16** compared to **I-2**, but the effect is stronger for **I-18**. This observation is in good agreement with our proposed approach, which suggests phosphites being electronically comparable to CO in terms of coordinative interaction (Table 2).

Table 4. Comparison of ^{1}H/^{31}P{^{1}H} NMR shifts in CDCl$_3$ and ν(CO) of prepared iron half-sandwich compounds.

| # | Compound | ^{31}P{^{1}H} NMR [ppm] | | ^{1}H NMR [ppm] (C$_5$$H_5$) | ν(CO) [cm^{-1}] |
		Free ligand	Complex		
1	**I-2**	-	-	5.05	1966.3
2	**I-15**	93	168	4.32	-
3	**I-16**	129	173	4.19	1963.6
4	**I-17**	179	248	3.93	-
5	**I-18**	–8	67	4.49	1932.9
6	**I-19**	–13	66	4.26	-

The modified iron complexes were then employed in the preparation of cationic iron complexes via salt metathesis with $AgBF_4$.[116] To investigate the simplest system, ethylene was used as a coordinating olefin (Table 5). Of the 5 modified iron iodide complexes only **I-16**, **I-17** and **I-18** were successfully converted into cationic ethylene complexes with average yields in the range of 62–72 %. Reactions of **I-15** and **I-19** did not result in suitable ethylene complexes, which might indicate that stabilized complexes like **I-3** (see Chart 3) form during the reaction.

Table 5. Preparation of different cationic iron ethylene complexes. ^{1}H NMR signals of cationic iron ethylene complexes.

#	Compound	Product	Yield [%]	^{1}H NMR [ppm] (C_5H_5)	^{1}H NMR [ppm] (C_2H_4)
1	**I-2**	**I-6**	59	5.92	3.88
2	**I-15**	-[a]	-	-	-
3	**I-16**	**I-20**	62	5.24[b]	3.78 m, 3.44 m
4	**I-17**	**I-21**	72	3.74	1.16 m, 4.48 m
5	**I-18**	**I-22**	63	5.29[b]	4.81 m[c], 4.54 m[c]
6	**I-19**	-[a]	-	-	-
7	**I-19a**	-[a]	-		-

Shifts in δ ppm against TMS in acetone-d_6; [a] no desired products could be obtained; [b] observed as doublets while substrates **I-16** and **I-18** provided singlets, respectively; [c] supposed signals in CD_2Cl_2 that vanished after addition of $HPPh_2$, although no nucleophilic addition was observed.[118]

The solubility of compounds **I-20–I-22** was found tolerable in acetone-d_6 (10–15 mg mL^{-1}) and very low in CD_2Cl_2 (<5 mg/mL). Once sterically demanding phosphines were introduced, the ethylene proton signals were observed separately in ^{1}H NMR spectroscopic investigations (Figure 5). Two possible explanations are that the effect is (**A**) caused by steric hindrance by the phosphite. In that case ethylene could not rotate freely and protons that face towards the iron center (H^a) and away (H^b) would be distinguishable. A different possible effect (**B**) would be electronic interaction of the phosphite and ethylene. While ethylene can

rotate freely along its carbon-carbon bond, protons (H^a) on one end face towards the phosphite and other side (H^b) towards CO.

Figure 5. Proposed effects **A** and **B** of sterically demanding phosphorus-based ligands on the ethylene ligand in **I-20**.

^{1}H NMR spectroscopic data showed that removal of the electron withdrawing iodine and introduction of ethylene as electron donating group results in a de-shielding effect on the Cp ligand (compare Table 4, entry 1, 3–5 with Table 5, entry 1, 3–5). The coordinated olefin in **I-6** and **I-20** is observed at similar chemical shifts, which is in agreement with the observation that the CO stretching frequency in their precursor complexes **I-2** and **I-16** (Table 4) is similar as well. Interestingly, the ^{1}H NMR spectroscopic data for **I-21** showed a significant high field chemical shift for the Cp ligand compared to the compounds **I-2**, **I-20** and **I-22**. In addition, the signals for the coordinated olefin were observed with a different chemical shift at 1.16 and 4.48 ppm. The difference in chemical shift might be explained by a strong interaction of ethylene with the iron center combined with electronic influence by the bidentate ligand. Low solubility of **I-22** resulted in difficulties identifying ethylene signals. Possible signals for ethylene were observed at low field chemical shift at 4.54 and 4.81 ppm based on the observation that the signals vanished upon addition of diphenyl phosphine (HPPh$_2$) (*vide infra*).

Since we observed the readily formation of **I-21** bearing a bidentate ligand, the preparation of a cationic compound bearing dppe (**I-14**) as ligand was attempted with a different approach (Scheme 23). The starting point was the observation and isolation of the cationic intermediate **I-19a**, which was formed when **I-19** was prepared (Table 3, entry 6).

I-19a

I-19b
75 %

I-19c

Scheme 23. Attempted preparation of cationic compound **I-19c** starting from the intermediate **I-19a**.

I-19a was treated with KBF$_4$ to exchange the iodide counter ion and to provide increased solubility in less polar solvents such as CH$_2$Cl$_2$. Insoluble potassium salts were removed by filtration and **I-19b** was obtained in a good yield (Scheme 23). The next step was the attempted removal of CO by oxidation to CO$_2$ with either trimethyl-*N*-oxide or *N*-methylmorpholine-*N*-oxide. Various attempts with and without donor ligands to create **I-19c** remained unsuccessful. ^{31}P{^{1}H} NMR spectra exhibited signals at 92.2 ppm that indicate that no reaction of the substrate **I-19b** had taken place.

In conclusion, substitution reactions of CO with phosphorus-based ligands in FpI complexes was successful to a certain extend. Substitution with monodentate ligands **I-9**–**I-11** and **I-13** was mostly influenced by their steric demand, ranging from no reaction (**I-9**), over single (**I-11** and **I-13**) to double substitution reaction (**I-10**). When bidentate ligands **I-12** and **I-14** were used, the formation of a significant amount of the cationic complexes (see Table 3, **I-17a** and **I-19a**) as undesired side-product was observed. The preparation of cationic olefin complexes was successful starting from **I-16**–**I-18**. For both **I-15** and **I-19**, introduction of an olefin after salt metathesis was not achieved. Also a different attempt from the cationic intermediate **I-19a** did not lead to the desired olefin complexes.

3.3.1.3 A cationic 1,2,3,4,5-Pentamethylcyclopentadienyl dicarbonyl iron ethylene complex

The investigations in the previous section showed the successful preparation of different cationic Fp olefin complexes with limited solubility in CD_2Cl_2. To address this issue, Cp was sought to be replaced with 1,2,3,4,5-pentamethylmethyl cylclopentadienide (Cp* **I-23**).[119] Iron pentacarbonyl was treated with **I-23** in xylenes under reflux, providing the permethylated Fp₂ analogue $Fp*_2$ (**I-24**) in a moderate yield of 55 %.[120-121] Finally, Fp*I (**I-25**) was obtained by oxidizing **I-24** with iodine in CH_2Cl_2 in an excellent yield. The obtained Fp*I was treated with $AgBF_4$ to produce a cationic iron complex that was used for olefin complexation. The reactivity towards $AgBF_4$ was found comparable to the analogue **I-6** (59 %) providing **I-26** as a grey powder in an average yield (Scheme 24). Complexes of 1-octene and styrene were observed in NMR experiments, but could not be isolated. A significant enhancement in solubility was observed since even ^{13}C NMR spectras were successfully recorded in CD_2Cl_2 with a reasonable number of scans.

Scheme 24. Preparation of $Fp*_2$ (**I-24**) and cationic Fp* ethylene complex **I-26**.[120-121]

3.3.1.4 A different attempt for the preparation of piano stool complexes

As discussed in 3.3.1.2, the preparation of different piano stool complexes was successfully achieved starting from **I-1** and substitution of CO with phosphorus-based ligands. The solubility of the prepared cationic ethylene complexes **I-6** and **I-20–I-22** was found limited in CD_2Cl_2 which could be solved utilizing the permethyl-cyclopentadienyl complex **I-26**. The only drawback of **I-26** was the in-house preparation of **I-24** from highly toxic iron pentacarbonyl as the initial step. Thus, a different route with less toxic starting material was sought. According to literature iron(II) chloride was chosen as starting material for the preparation of half sandwich complexes (Scheme 25).[122]

$$FeCl_2 \xrightarrow[\substack{\Delta T \\ 72\ h}]{THF} \underset{\substack{\textbf{I-27} \\ 72\ \%}}{(THF)_3Fe_2Cl_4} \xrightarrow[THF]{L} (L)_2FeCl_2 \xrightarrow[THF]{\textbf{I-28}\ or\ \textbf{I-29}}$$
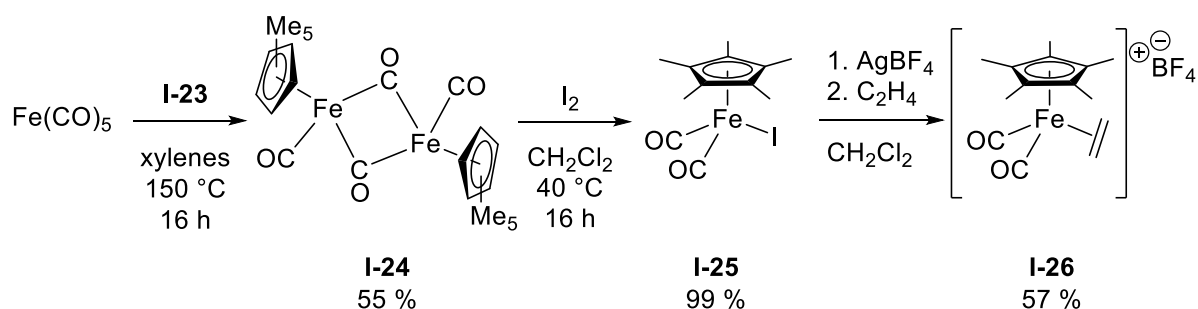
with L =   P(OPh)$_3$ **I-11**
            dppe   **I-14**

TMEDA
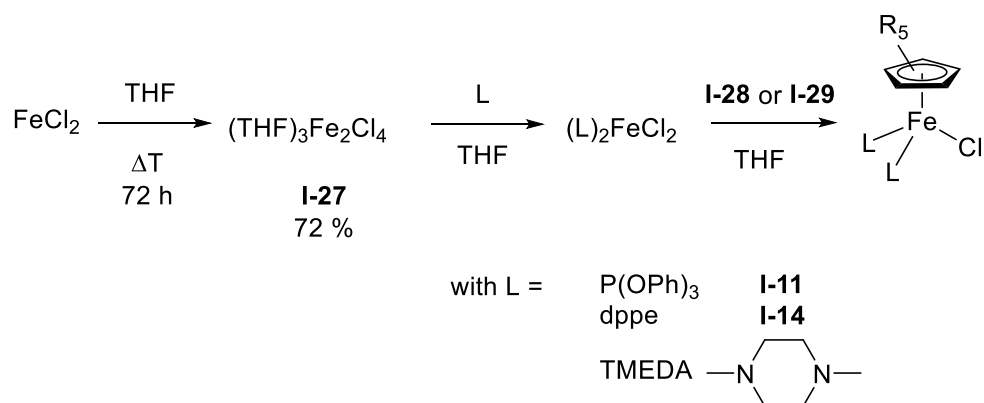
Scheme 25. Strategy for the preparation of piano stool complexes starting from iron(II) chloride.[122-123]

First, anhydrous iron(II) chloride was converted with a continuous extraction with refluxing THF that provided Fe$_2$Cl$_4$(THF)$_3$ (**I-27**) as a tan powder in good yield of 72 %.[122] Subsequent reactions with **I-11**, **I-14** and TMEDA provided oily products that could not be characterized with NMR spectroscopy.[122-123] For **I-11** the follow-up reaction in THF with NaCp (**I-28**) and LiCp* (**I-29**) was attempted to obtain diamagnetic compounds.[122] After 22 h of stirring at room temperature, the solvent was removed and oily dark residue unsuitable for NMR spectroscopy were obtained in both cases. Also treating **I-27** in a one-pot attempt with both **I-11** and **I-28** did not provide the expected piano stool compound. It was expected that the formation of sandwich complexes could be a challenging side reaction, but instead only unidentified products were formed.[122]

3.3.1.5 Attempted modification of the Counterion

A different approach to improve solubility of the cationic iron complexes can be addressed by changing the rather small tetrafluoroborate counter ion.[124] To improve solubility in apolar solvents like CH_2Cl_2, fluorinated tetraphenyl borates were thought to be appropriate. Under the standard conditions no formations of cationic ethylene complexes was observed when $AgBF_4$ was substituted by $AgB(C_6F_5)_4$ (Scheme 26).[109] Due to the success of employing Cp* instead of Cp as ligand (see 3.3.1.3) and limited time, the borate pathway was not further investigated.
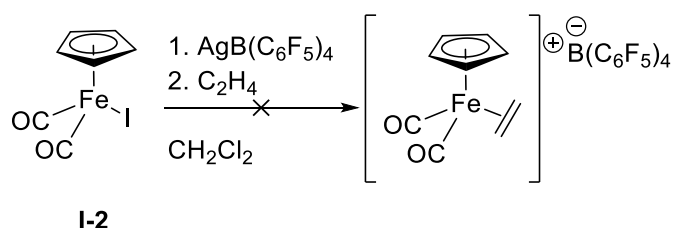
Scheme 26. Attempted preparation of cationic iron ethylene complex with a tetrakis(pentafluorophenyl)borate as counter ion.

3.3.2 Activation of Ethylene – NMR Study

With the cationic iron ethylene complexes **I-5**, **I-20–I-22** and **I-26** in hand, a small set of test reactions was conducted to investigate nucleophilic addition of benzyl amine, triphenyl- and diphenyl phosphine ($HPPh_2$) to the coordinated ethylene. Former investigations by Rosenblum and others suggests the formation of adducts at low temperatures with a variety of nucleophiles, such as carbanions, sulfides, phosphines and amines.[71-75, 106, 125-127] The reactions described in the literature were carried out on a mmol scale with intend of isolating the formed adducts. Our approach was to investigate the nucleophilic addition on the NMR scale with identification of formed intermediates without the need for isolation. In the literature, CH_3CN was chosen as solvent and for characterization CD_3NO_3. Due to limited solubility of **I-5** in CD_3CN, other deuterated solvents were employed at room temperature to ensure reasonable concentrations for NMR spectroscopic measurements.[125-127] In addition, the formed adducts had higher solubility in the chosen solvents. So observation of increased solubility of the iron complex upon addition of a nucleophile was a good indicator for reactivity.
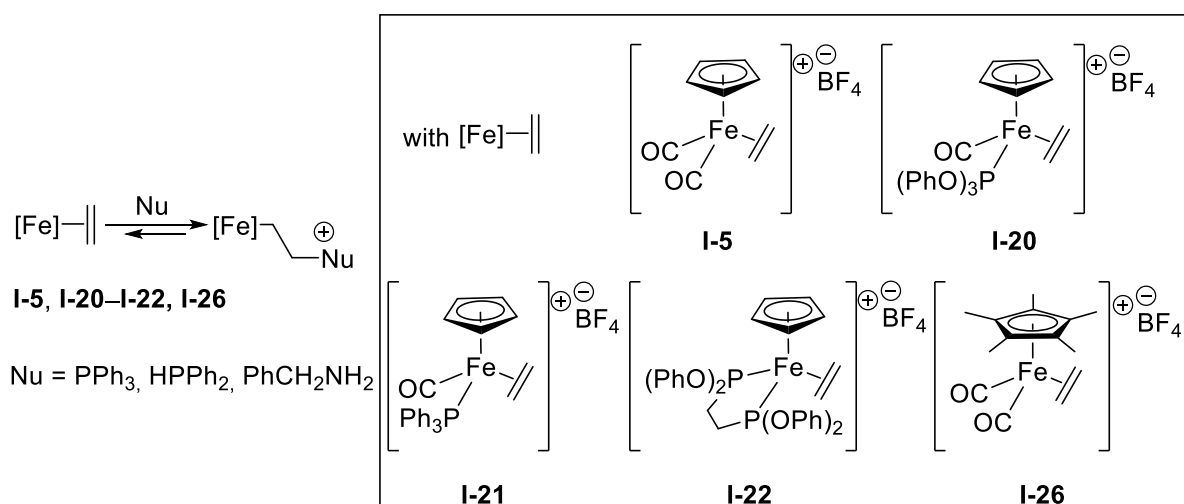
Scheme 27. Schematic nucleophilic addition to cationic iron ethylene complexes.

Initial experiments were carried out with benzyl amine as nucleophile in THF-d_8, acetone-d_6 and CD_2Cl_2. A color change was observed in all reactions but only the NMR spectra in THF-d_8 were found acceptable for interpretation. As shown in Figure 6, the formation of a new C-N and Fe-C bond is indicated by broad signals at 1.18–1.45 ppm and 3.06–3.35 ppm, respectively. Further evidence for a nucleophilic addition is provided by the ^{13}C(APT) NMR spectrum (Figure 7) which shows a new signal at –6.2 ppm that is either a secondary or a quaternary carbon. This characteristic chemical shift is a good indicator for the formation of a Fe-C bond. A second signal for the new aliphatic carbon atom attached to nitrogen was observed at 51.4 ppm, however, it was expected in the region of 20–30 ppm.
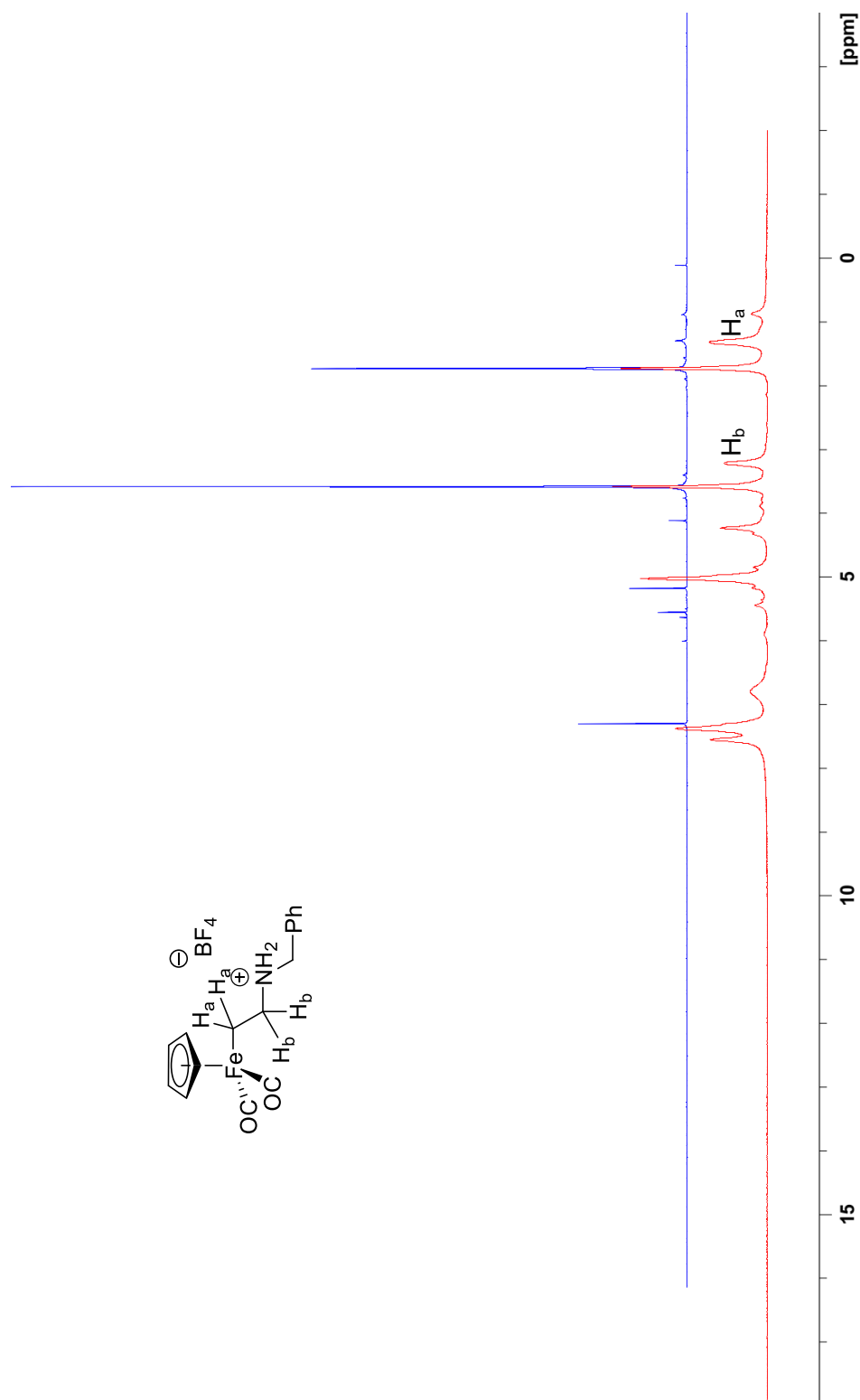
Figure 6. *In situ* ^{1}H NMR spectrum (400.3 Mhz) in THF-d_8: Nucleophilic addition of 1.1 equiv benzyl amine to **I-5** at 25 °C after 1 h (red). The reference spectrum (blue) provides only limited information due to low solubility of **I-5** in THF.
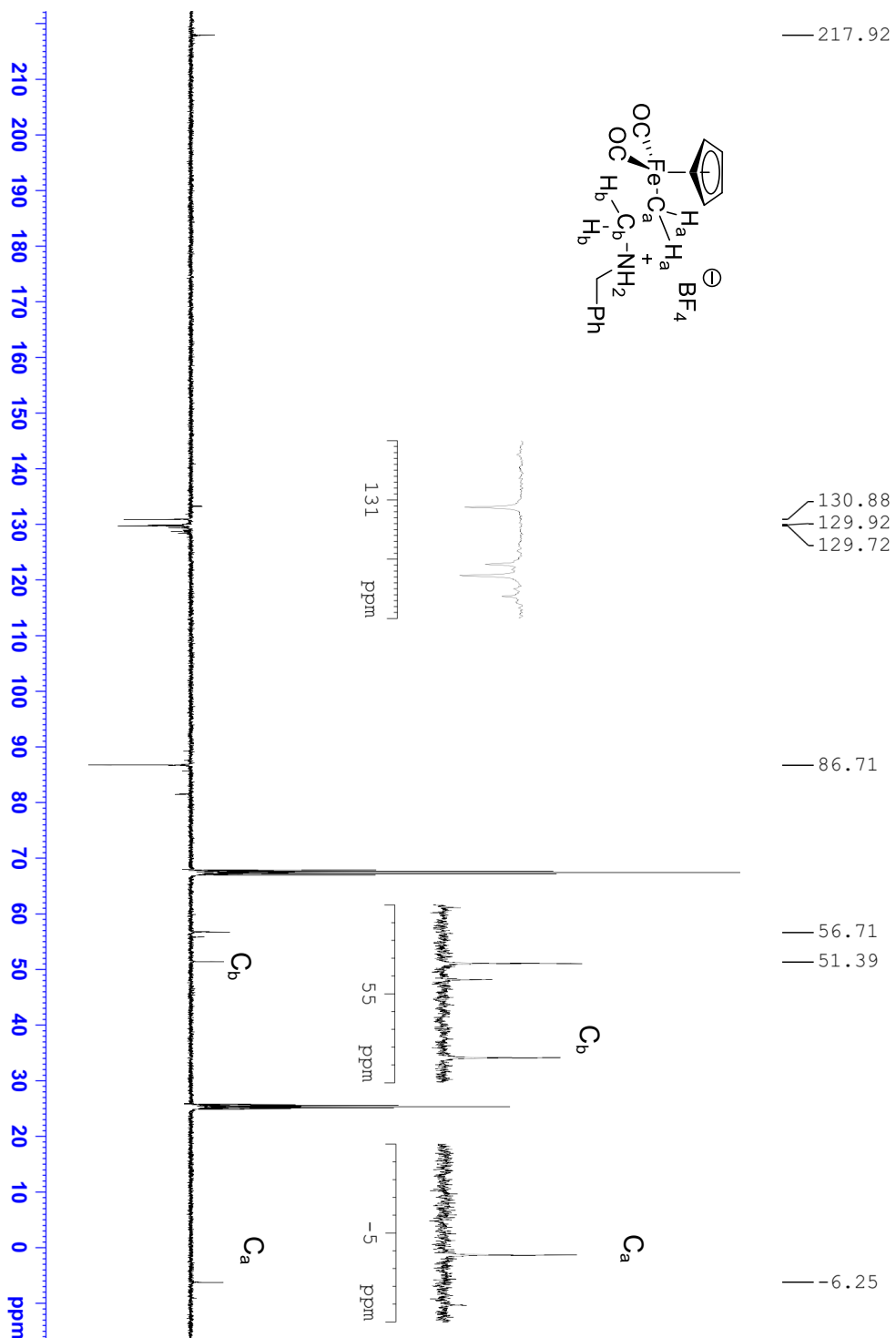
Figure 7. *In situ* ^{13}C(APT) NMR spectrum (100.6 Mhz) in THF-d_8: Nucleophilic addition of 1.1 equiv benzyl amine to **I-5** at 25 °C after 1 h with zoomed areas of interest.

The formed benzyl amine adduct was heated to 80 °C with the intention to either force a 1,3-proton shift providing *N*-ethyl benzyl amine (**pathway A**) or *N*-benzyl ethanimine *via* β-hydride elimation (**pathway B**), respectively.[76]
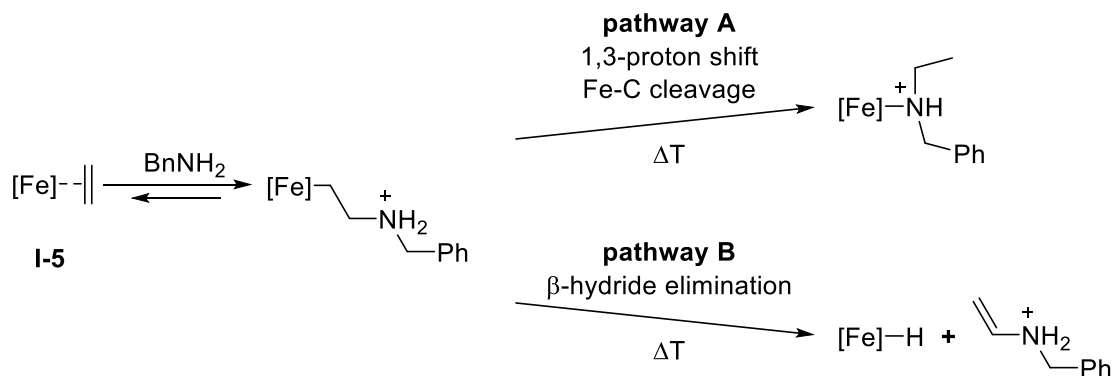
Scheme 28. Proposed thermal decomposition of benzyl amine adduct from **I-5**.[76]

Instead, the adduct decomposed and the formation of crystals was observed after storing the reaction solution at room temperature overnight in THF-d_8 (Scheme 29). The crystals were suitable for X-ray analysis and the obtained crude structure indicates a substitution of ethylene by benzyl amine (Figure 8).
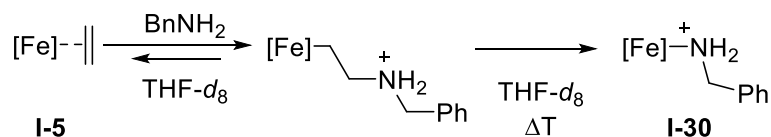
Scheme 29. Thermal degradation of the benzyl amine adduct of **I-5** resulting in a benzyl amine complex **I-30**.
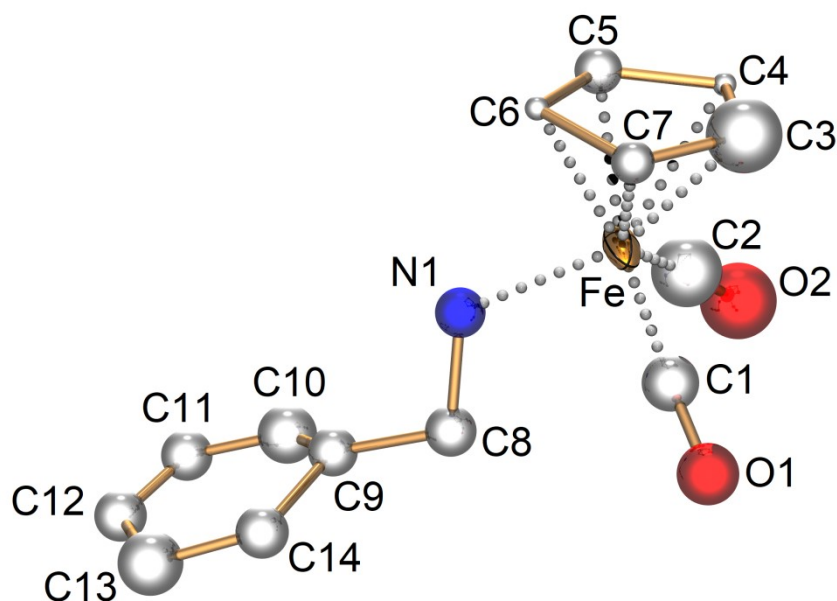
Figure 8. Molecular structure of cationic species [Fp(benzyl amine)]BF$_4$ (**I-30**) with thermal ellipsoids set at 50% probability. The anion BF$_4^-$ and all hydrogen atoms are omitted for clarity.

With the obvious limitations for *in situ* NMR spectroscopic investigation, a different approach with phosphine nucleophiles as NMR probes was chosen. To confirm results from literature,[72, 125-127] triphenyl phosphine was added to **I-5** in CD$_2$Cl$_2$ and the formation of adducts was observed. In the ^{1}H NMR spectrum (Figure 9), new signals at 1.35–1.50 ppm and 3.51–3.74 ppm indicates the formation of new P-C and Fe-C bonds and are in good agreement with previous observations when using benzyl amine (Figure 6). Observations from the ^{31}P{^{1}H} NMR spectrum suggest the formation of a quaternary phosphine with its signal at 19.9 ppm and also partial ligand substitution of CO by PPh$_3$ based on a signal at 61.9 ppm (Figure 10). The ^{13}C(APT) NMR spectrum (Figure 11) showed new signals at −11.3 ppm and 30.9 ppm. The high field shifted signal is a doublet (d, $^3J_{C,P}$ = 17.5 Hz) and the second signal is also expected to show a coupling pattern which is covered by the acetone-d_6 signal. With all observations combined, a successful nucleophilic addition of triphenyl phosphine to ethylene is highly probable.
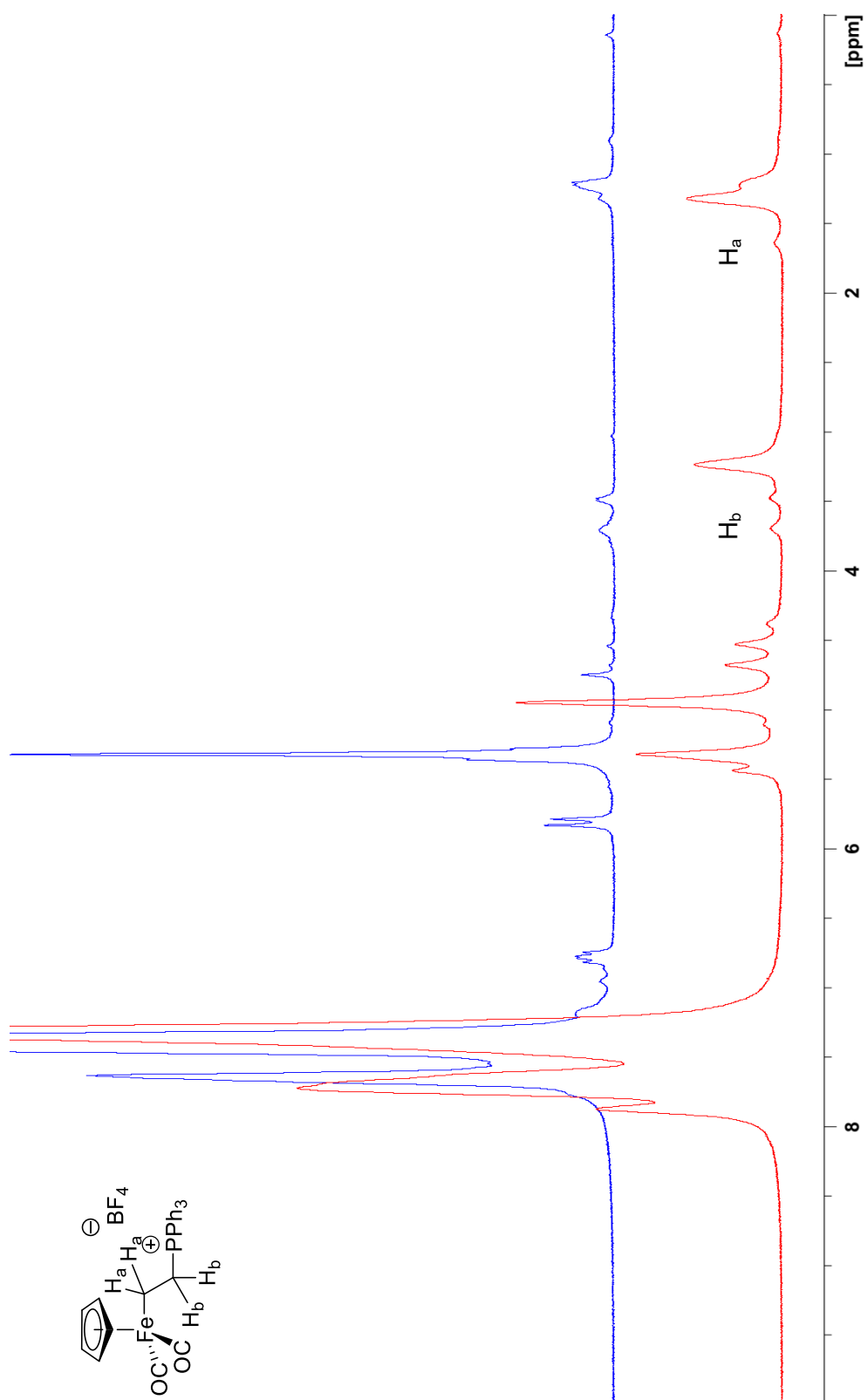
Figure 9. *In situ* ^{1}H NMR spectrum (400.3 MHz, 25 °C) in CD$_2$Cl$_2$: Nucleophilic addition of 1.1 equiv triphenyl phosphine to **I-5** at 25 °C after 1 h (red).. The reference spectrum (blue) was recorded initially after mixing.
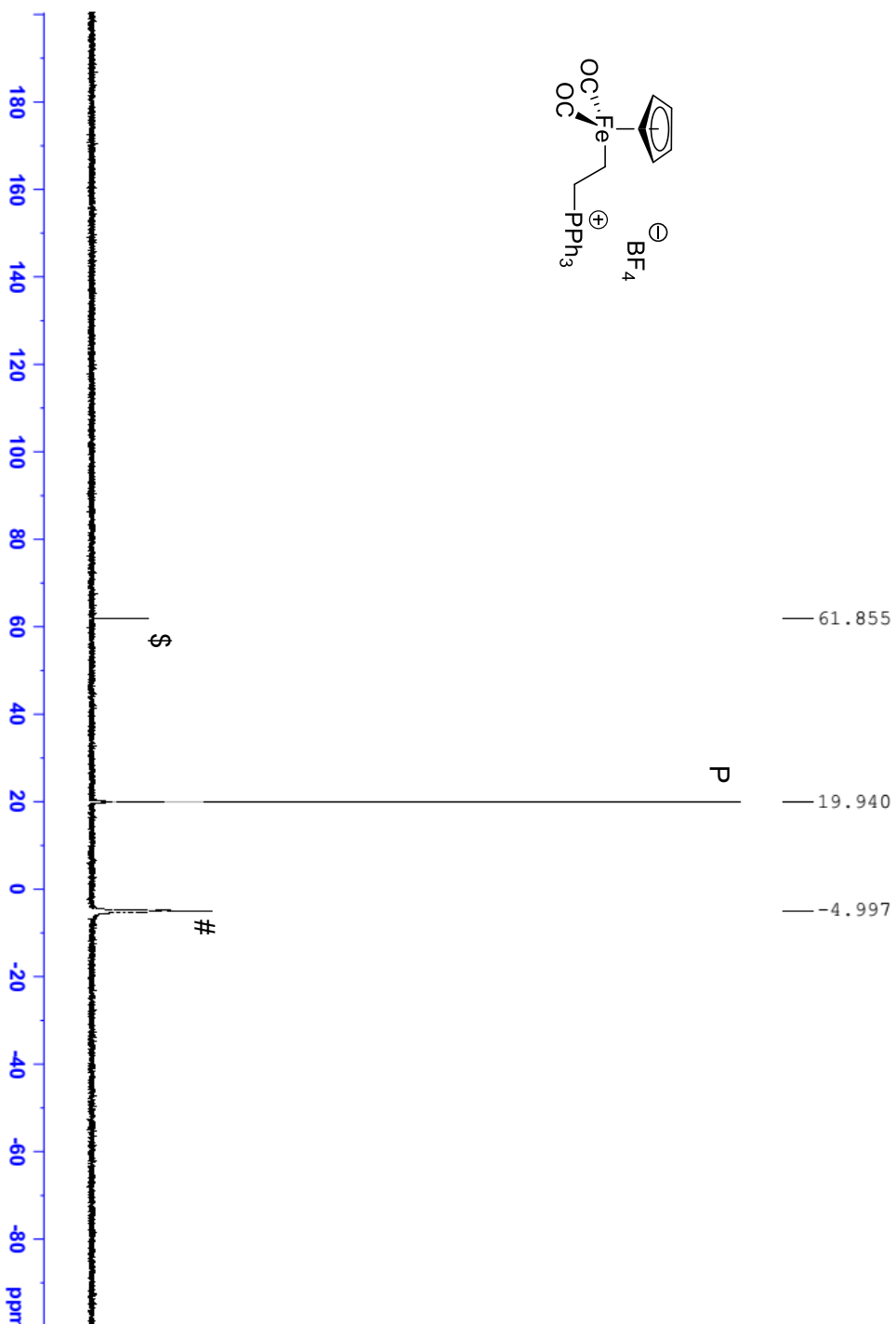
Figure 10. *In situ* ^{31}P{^{1}H} NMR spectrum (162.0 MHz, 25 °C) in CD$_2$Cl$_2$: Nucleophilic addition of 1.1 equiv triphenyl phosphine to **I-5** at 25 °C after 1 h. P – desired phosphine adduct, # - free PPh$_3$, $ - PPh$_3$ coordinated to Fe.
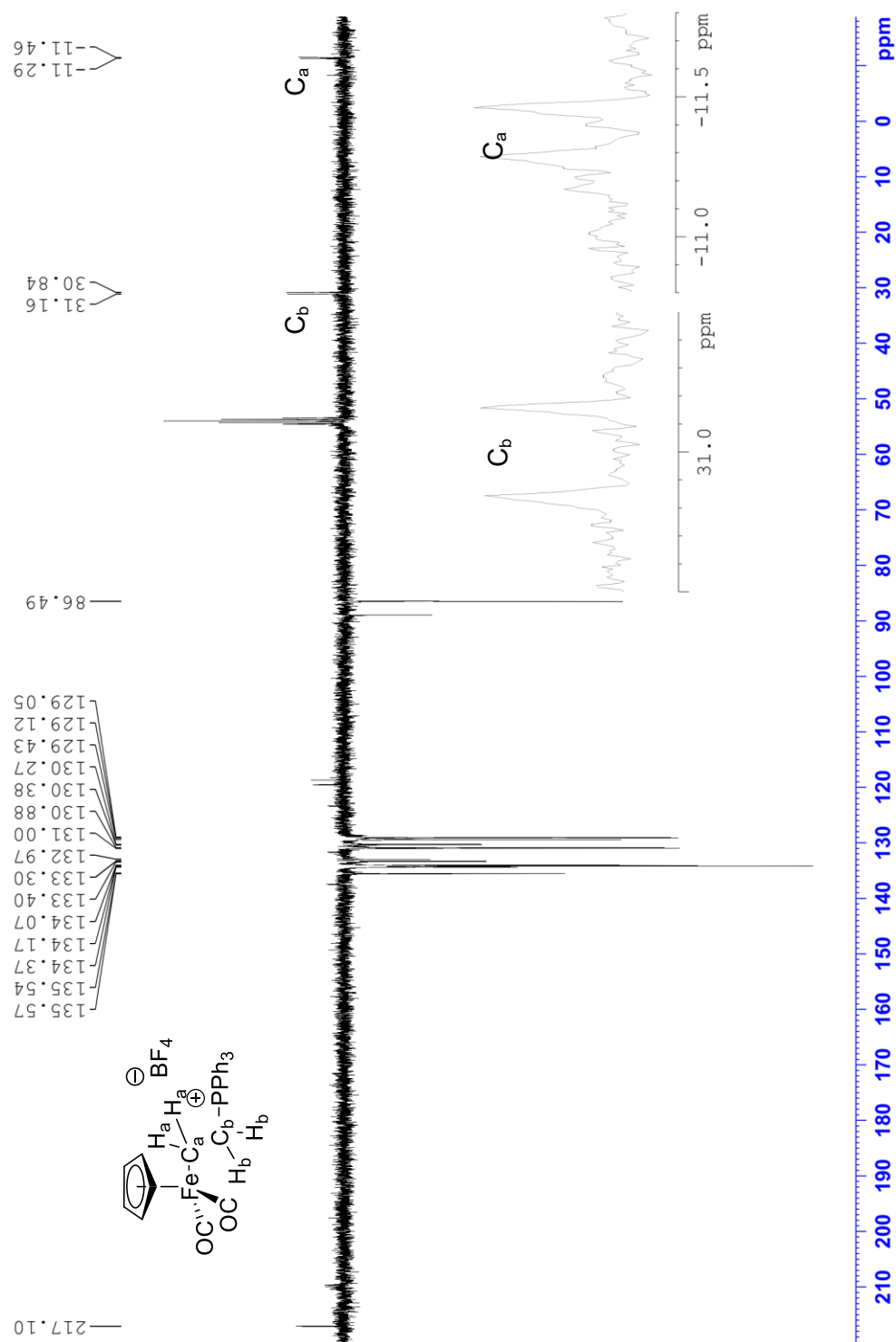
Figure 11. *In situ* ^{13}C(APT) NMR spectrum (162.0 MHz, 25 °C) in CD$_2$Cl$_2$: Nucleophilic addition of 1.1 equiv triphenyl phosphine to **I-5** at 25 °C after 1 h with zoomed areas of interest.

After reproduction of the results from literature, the next approach was the formation of a cationic phosphine adduct that could be deprotonated. $HPPh_2$ was used as logical replacement of triphenyl phosphine for nucleophilic addition to **I-5**. The new substrate provided excellent results in THF-d_8, acetone-d_6, CD_2Cl_2 and C_6D_6 due to the good solubility of the formed adduct. In acetone-d_6 new signals were observed in the ^{1}H NMR spectrum with chemical shifts of 1.08–1.15 ppm and 3.02–3.12 ppm which indicate the formation of P-C and Fe-C bonds. The spectrum shows two separate sets of signals which can be observed best for the Cp signals at 5.06 and 5.07 ppm, respectively. A similar set of two signal was observed in the $^{31}P\{^1H\}$ spectrum with chemical shifts of 19.9 ppm and 28.8 ppm, respectively, which indicates the formation of the two species **I-31** and **I-32** (Scheme 30). In a separate experiment in C_6D_6, the conversion of **I-32** into **I-31** by protonation with 1 equiv of TFA was observed (Figure 12).
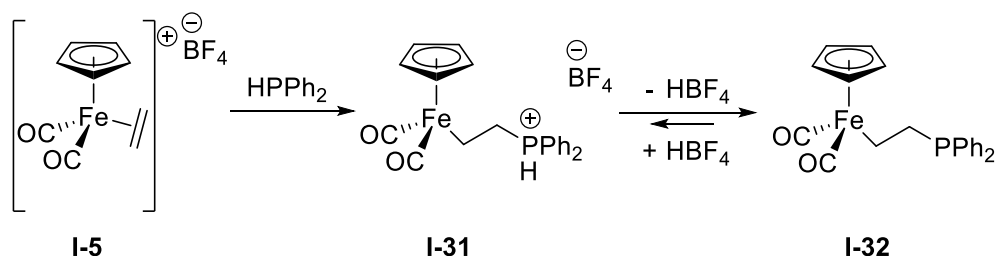
Scheme 30. Nucleophilic addition of $HPPh_2$ to **I-5** providing **I-31** and proposed deprotonation to **I-31** in acetone-d_6 and C_6D_6.

The ^{1}H NMR spectrum intiailly shows two pairs of separate mulitpletts with chemical shifts at 1.07–1.17 ppm and 3.00–3.10 ppm for **I-31**, and at 0.90–0.99 ppm and 3.11–3.20 ppm for **I-32**, respectively (Figure 12). In the $^{31}P\{^1H\}$ NMR spectrum (Figure 13) two separate signals at 17.7 ppm (**I-31**) and 25.2 (**I-32**) ppm respectively, whose intensities are in good agreement with the integrals of the observed signal sets before (Figure 12). The ^{13}C(APT) NMR spectrum (Figure 14) shows confirmingly also two separate sets of signals which is most evident for the ethylene bridge. The signals showed characteristic coupling to phosphorus and were observed at –11.6 ppm (d, $^3J_{C,P}$ = 17.0 Hz) and 27.8 ppm (d, $^2J_{C,P}$ = 30.7 Hz) for **I-31**, and –11.2 (d, $^3J_{C,P}$ = 18.3 Hz) and 24.7 ppm (d, $^2J_{C,P}$ = 25.9 Hz) for **I-32**, respectively. The influence on the Cp and CO ligand was also observed with signals at a chemical shift of 86.3 ppm and 217.3 ppm for **I-31**, and 86.2 ppm and 217.1 ppm, respectively.

It is worth noting, only **I-32** is formed when THF-d_8 is employed as solvent. Most probably the deprotonation of **I-31** to form **I-32** is accelerated due to solvation effects.
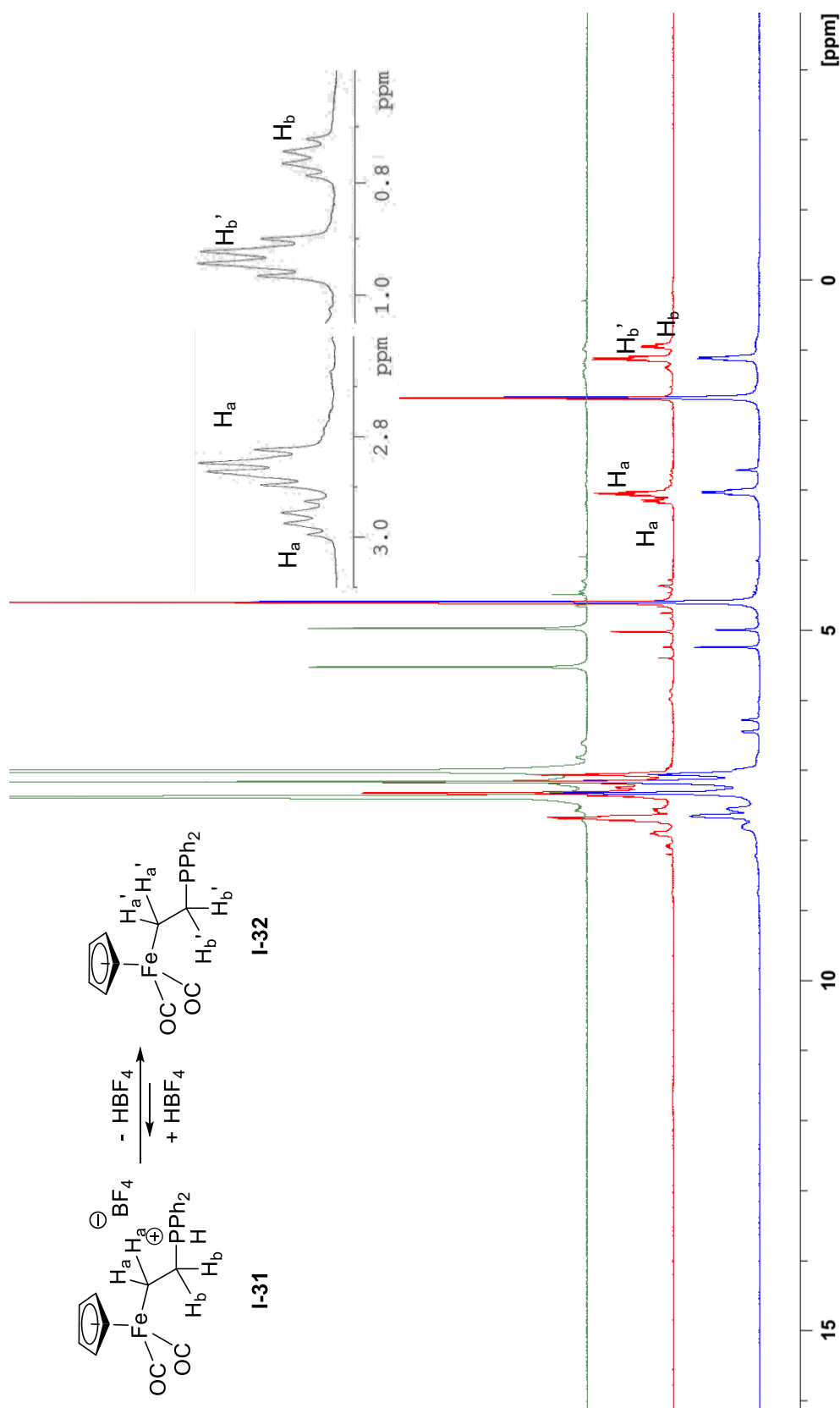
Figure 12. *In situ* ^{1}H NMR spectrum (400.3 MHz, 25 °C) in C_6D_6: Nucleophilic addition of 1.1 equiv $HPPh_2$ to **I-5**. The reference spectrum (green) was recorded initially after mixing and provides only signals of $HPPh_2$ due to low solubility of **I-5** in C_6D_6. Heating to 80 °C for 5 min: formation of **I-31** and **I-32** (red). Addn. of 1 equiv TFA (blue): conversion of **I-32** into **I-31** at 25 °C after 1h.
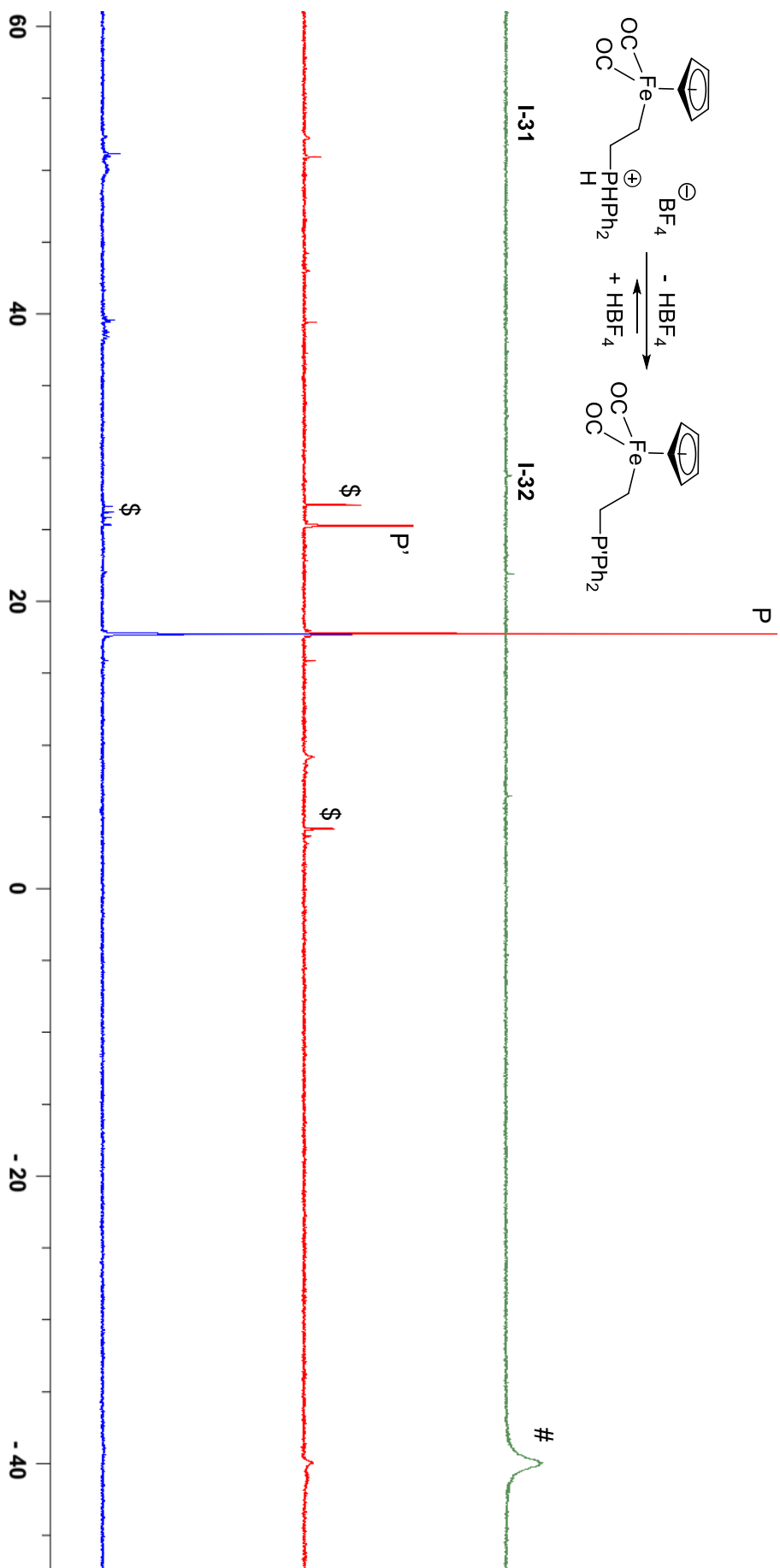
Figure 13. *In situ* $^{31}P\{^1H\}$ NMR spectrum (162.0 MHz, 25 °C) in C_6D_6: Nucleophilic addition of 1.1 equiv $HPPh_2$ to **I-5**. The reference spectrum (green) was recorded initially after mixing and provides only signals of $HPPh_2$ due to low solubility of **I-5** in C_6D_6. Heating to 80 °C for 5 min: formation of **I-31** (P) and **I-32** (P') (red). Addn. of 1 equiv TFA (blue): conversion of **I-32** into **I-31** at 25 °C after 1h; # - $HPPh_2$; $ - unidentified side product.
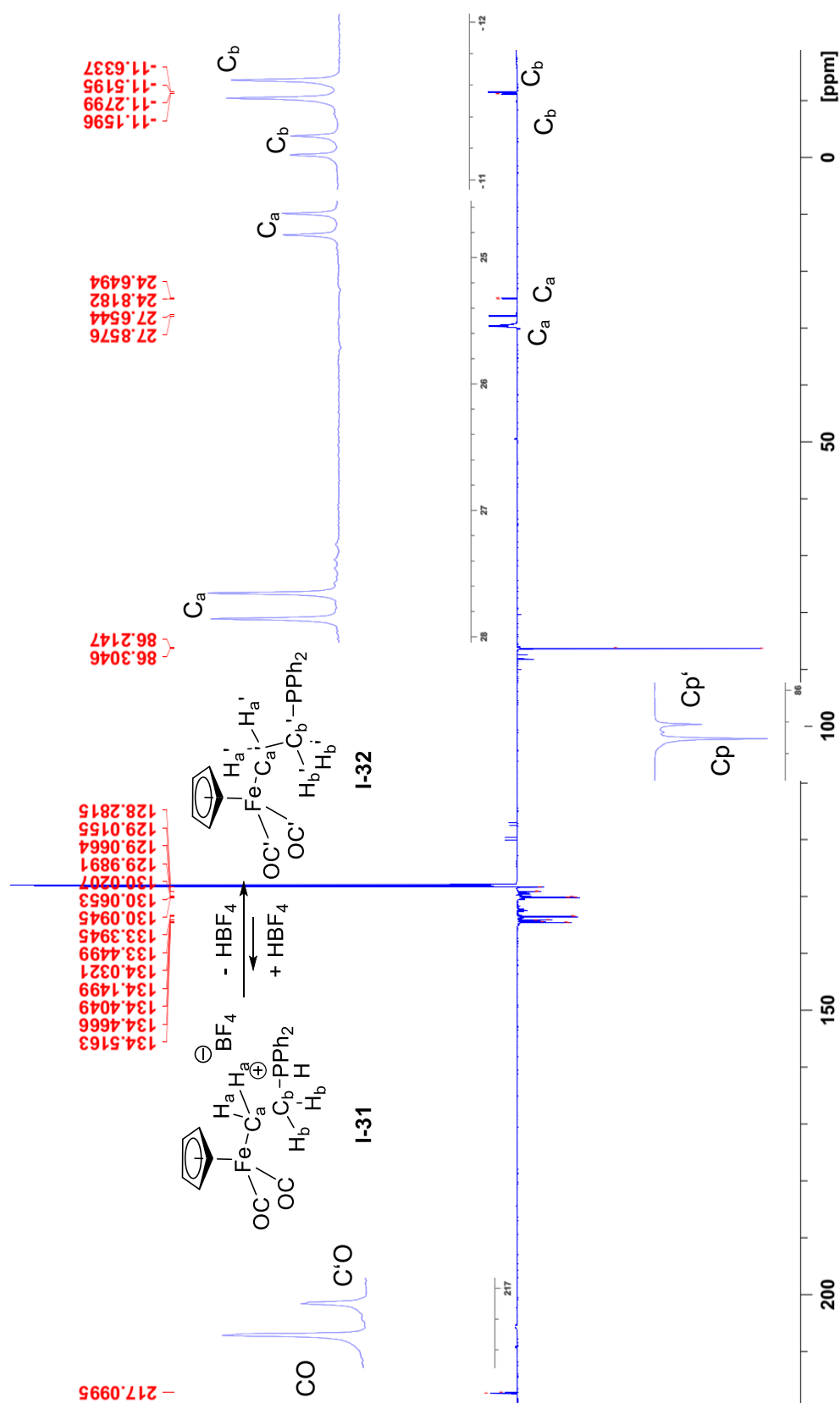
Figure 14. *In situ* ^{13}C(APT) NMR spectrum (162.0 MHz, 25 °C)) in C$_6$D$_6$: Nucleophilic addition of 1.1 equiv HPPh$_2$ to **I-5** after heating to 80 °C for 5 min with zoomed areas of interest; **$** - unidentified side products.

With the promising results in the reaction of **I-5** with HPPh$_2$, the reaction was also attempted with the other iron complexes **I-20**–**I-22** and **I-26**. All reactions were conducted at room temperature in acetone-d_6 with NMR measurements performed 1 h after the addition of HPPh$_2$ for comparability. When **I-20** was employed, the outcome was challenging to quantify, due to two phosphorus atoms in the resulting adduct which led to complicated coupling patterns and a broadening of signals. The ^{1}H NMR spectrum (Figure 15) showed new signals emerging at 0.79–0.86 ppm and 3.02–3.27 ppm, respectively, which were assigned to the formed P-C and C-Fe bonds. Interestingly, the ^{31}P NMR spectrum indicated the formation of different isomers with the major signals being two triplets at 18.9 ppm (t, J = 13.8 Hz) and 19.4 ppm (t, J = 12.4 Hz) ppm (Figure 16). In the ^{13}C(APT) NMR spectrum (Figure 17) the expected signals are shifted to higher field as overlaying multiplets at –12.4—11.9 ppm and doublet of doublets at 27.5 ppm (dd, J = 29.5, 86.7 Hz), and doublet of doublets at –11.1 ppm (dd, J = 17.9, 32.3 Hz) and doublets at 25.7 (d, J = 24.2 Hz), respectively.
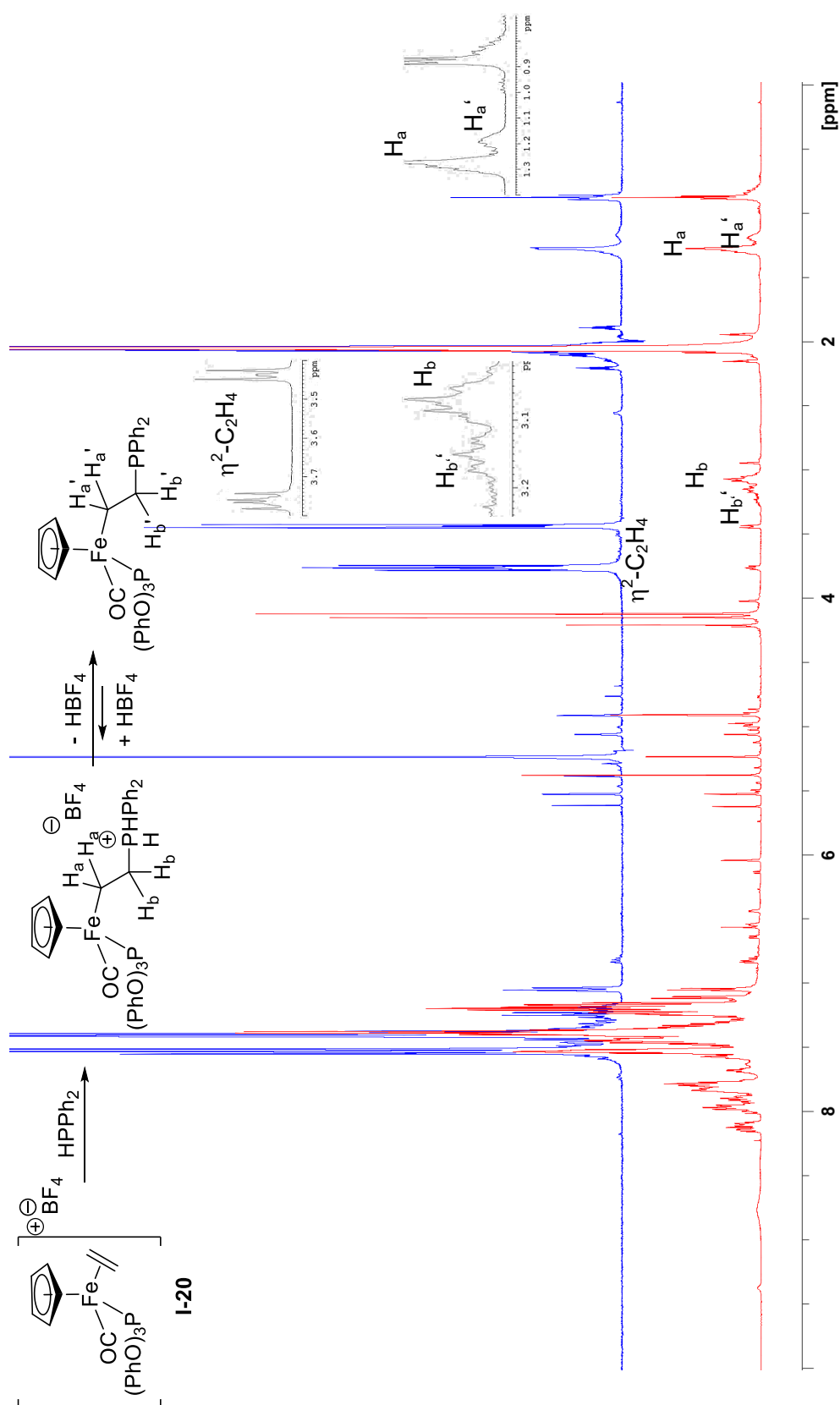
Figure 15. *In situ* ^{1}H NMR spectrum (400.3 MHz, 25 °C) in acetone-d_6: Nucleophilic addition of 1.1 equiv HPPh$_2$ to **I-20** at 25 °C after 1 h with zoomed areas of interest. The reference spectrum (blue) was recorded before addition of HPPh$_2$.
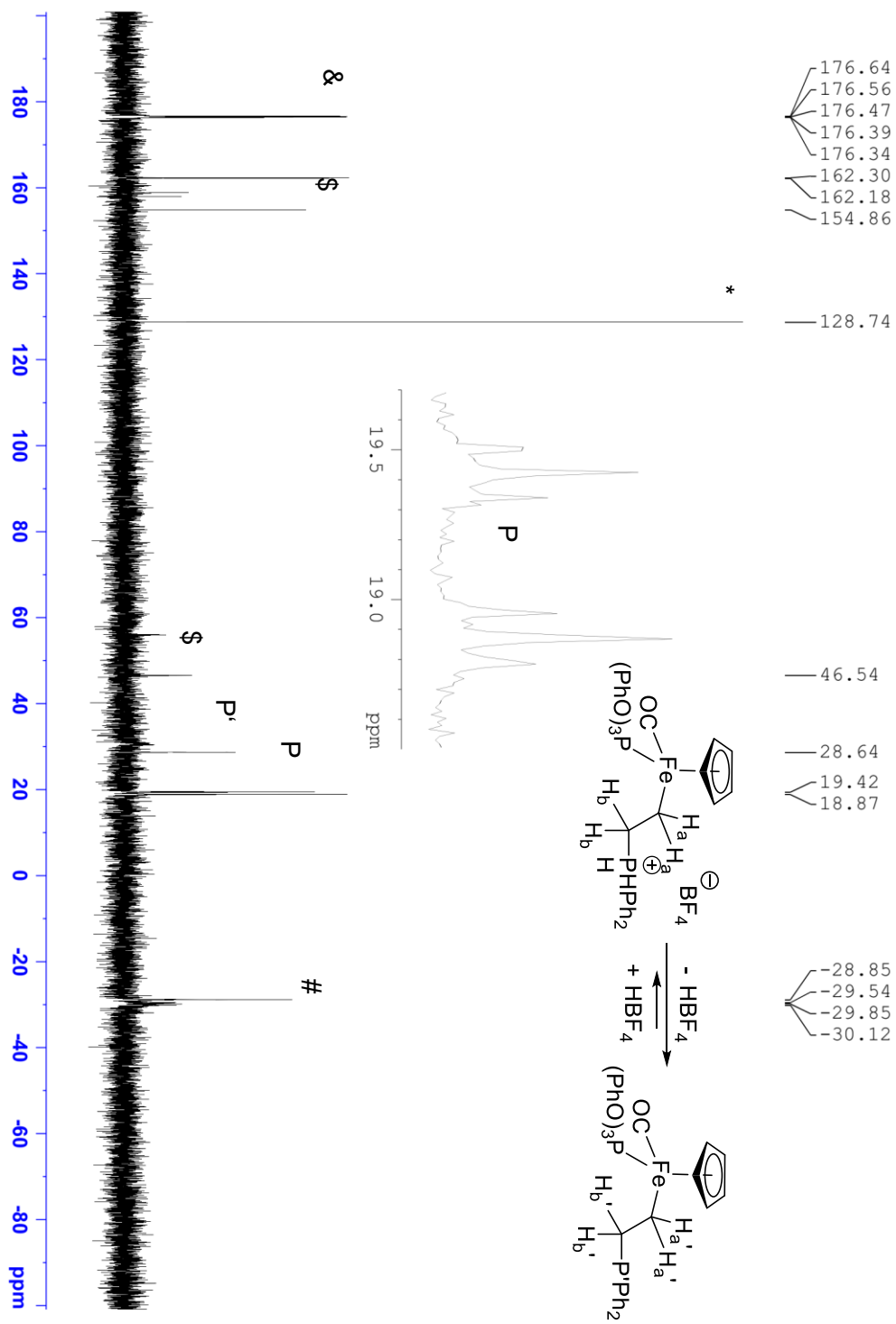
Figure 16. *In situ* ^{31}P NMR spectrum (162.0 MHz, 25 °C) in acetone-d_6: Nucleophilic addition of 1.1 equiv HPPh$_2$ to **I-20** at 25 °C after 1 h with zoomed area of interest; # - HPPh$_2$; P - phosphine adduct; & - coordinated P(OPh)$_3$; * - free P(OPh)$_3$; $ - unidentified side products.
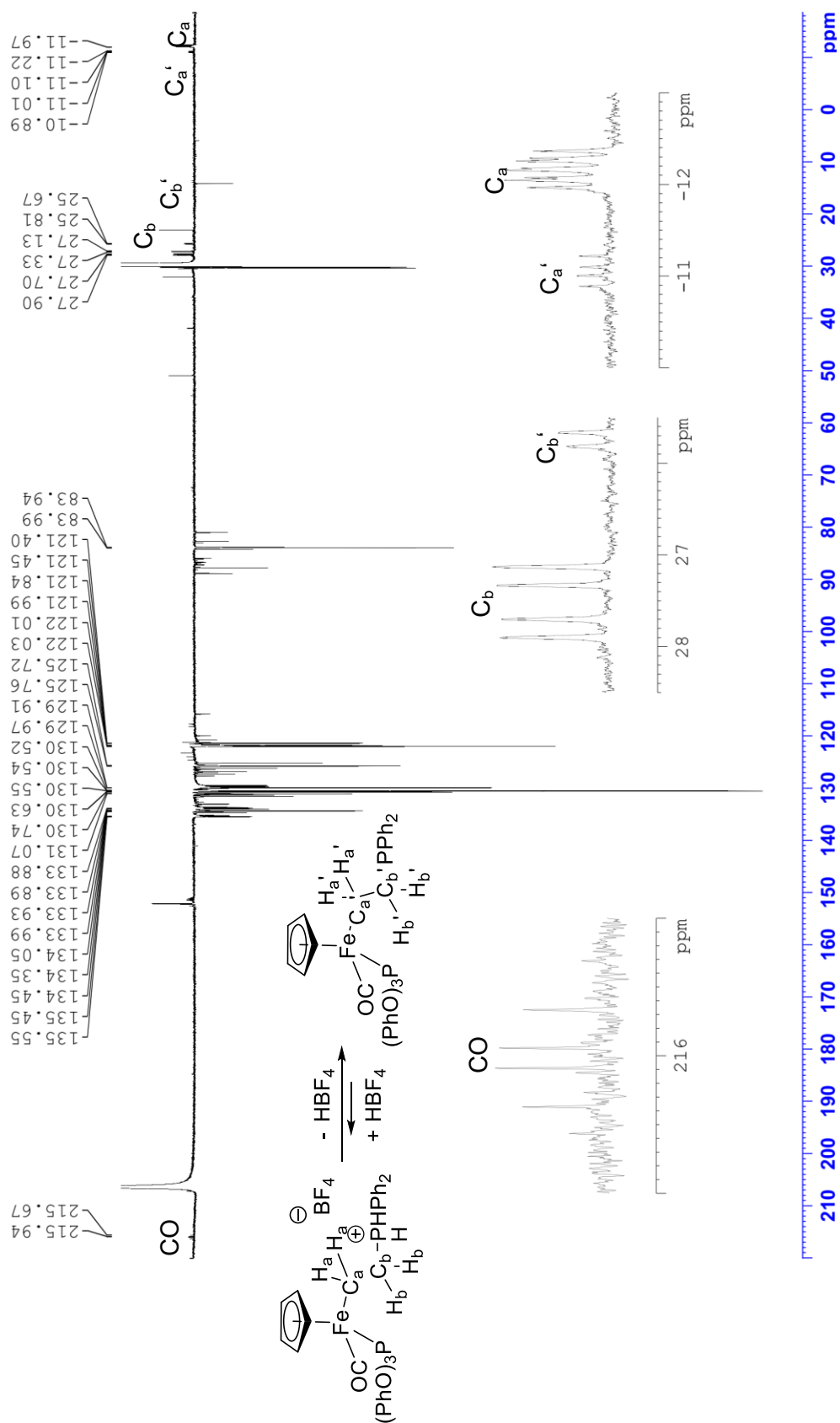
Figure 17. *In situ* ^{13}C(APT) NMR spectrum (162.0 MHz, 25 °C) in acetone-d_6: Nucleophilic addition of 1.1 equiv HPPh$_2$ to **I-20** at 25 °C after 1 h with zoomed areas of interest.

The other cationic iron ethylene complexes with phosphorus-based ligands (**I-21** and **I-22**) did not show any reactivity towards nucleophilic addition with HPPh$_2$. In contrast, complex **I-26** readily reacted with HPPh$_2$.

| | **I-26** | **I-33** | **I-34** |
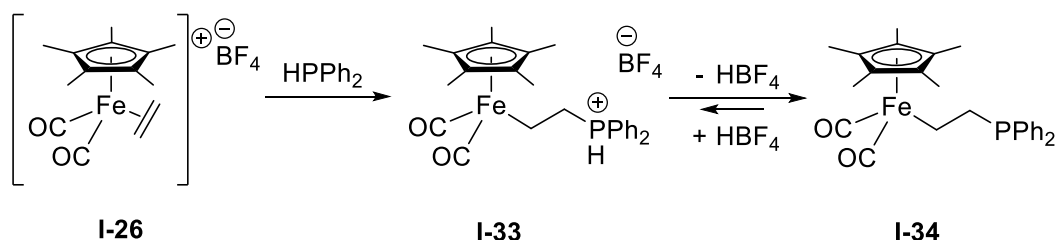
Scheme 31. Nucleophilic addition of HPPh$_2$ to **I-26** providing **I-33** and proposed deprotonation to **I-34**.

The ^{1}H NMR spectrum provided two separate Cp* signals at 1.68 ppm (**I-34**) and 1.61 (**I-33**) ppm in a 2:1 ratio, as well as the characteristic signals for P-CH$_2$ and Fe-CH$_2$ groups. The signals were observed with comparatively high field chemical shifts for P-CH$_2$ at 0.61–0.67 ppm (**I-34**) and 0.68–0.74 ppm (**I-33**) and Fe-CH$_2$ at 2.97–3.04 (**I-33**) and 3.04–3.10 ppm (**I-34**), respectively. This high field shift might be directly connected to the increased electron density at the iron center provided by the Cp* ligand. In the ^{31}P{^{1}H} NMR spectrum (Figure 19) two species with signals at 19.6 ppm (**I-33**) and 28.3 ppm (**I-34**) were identified. The formation of two different species (**I-33** and **I-34**) confirmed with earlier observations (Scheme 31, compare Scheme 30). The ^{13}C(APT) NMR spectrum (Figure 20) also showed the formation of two adduct species at –2.4 ppm (d, $^3J_{C,P}$ = 15.7 Hz) and 26.8 (d, $^2J_{C,P}$ = 35.5 Hz) (**I-33**), and –0.9 (d, $^3J_{C,P}$ = 16.2 Hz) and 25.0 (d, $^2J_{C,P}$ = 28.4 Hz) (**I-34**), respectively.
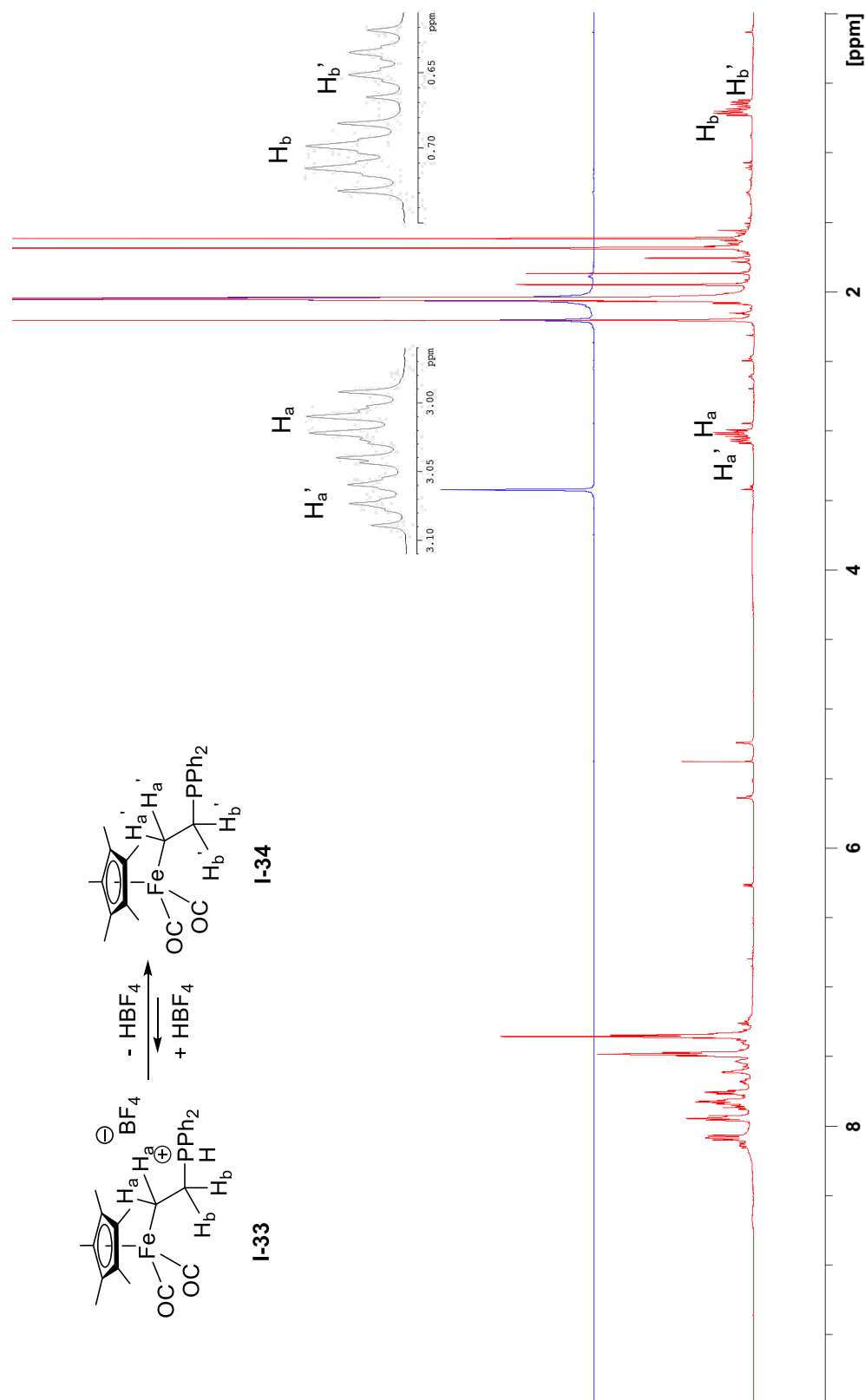
Figure 18. *In situ* ^{1}H NMR spectrum (400.3 MHz, 25 °C) in acetone-d_6: Nucleophilic addition of 1.1 equiv HPPh$_2$ to **I-26** with zoomed areas of interest. The reference spectrum (blue) was recorded before addition of HPPh$_2$.
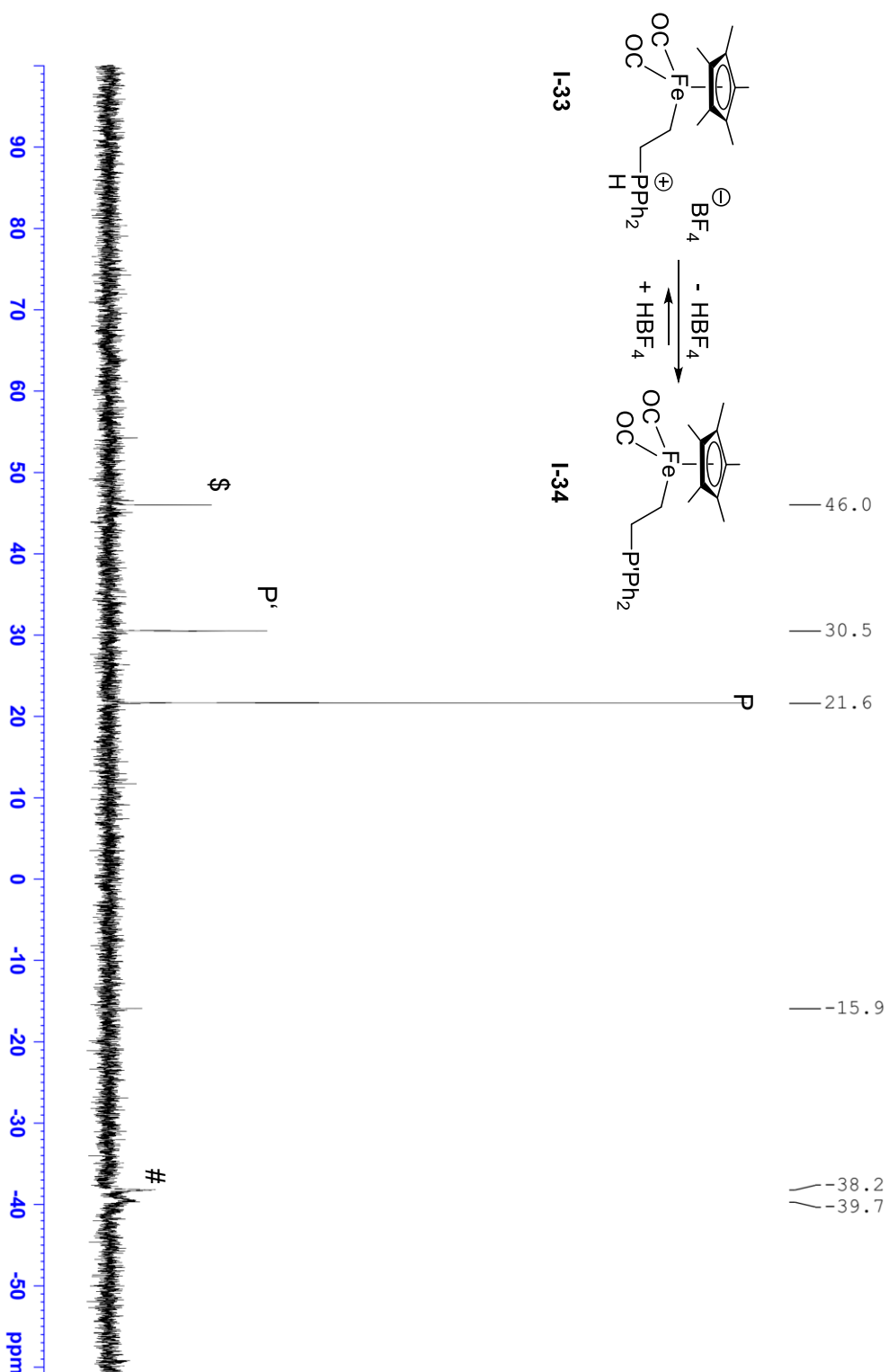
Figure 19. *In situ* $^{31}P\{^1H\}$ NMR spectrum (162.0 MHz, 25 °C) in acetone-d_6: Nucleophilic addition of 1.1 equiv HPPh$_2$ to **I-26** at 25 °C after 1 h. P – desired phosphine adduct **I-33**, P' – phosphine adduct **I-34**, # - free HPPh$_2$, $ - HPPh$_2$ coordinated to Fe
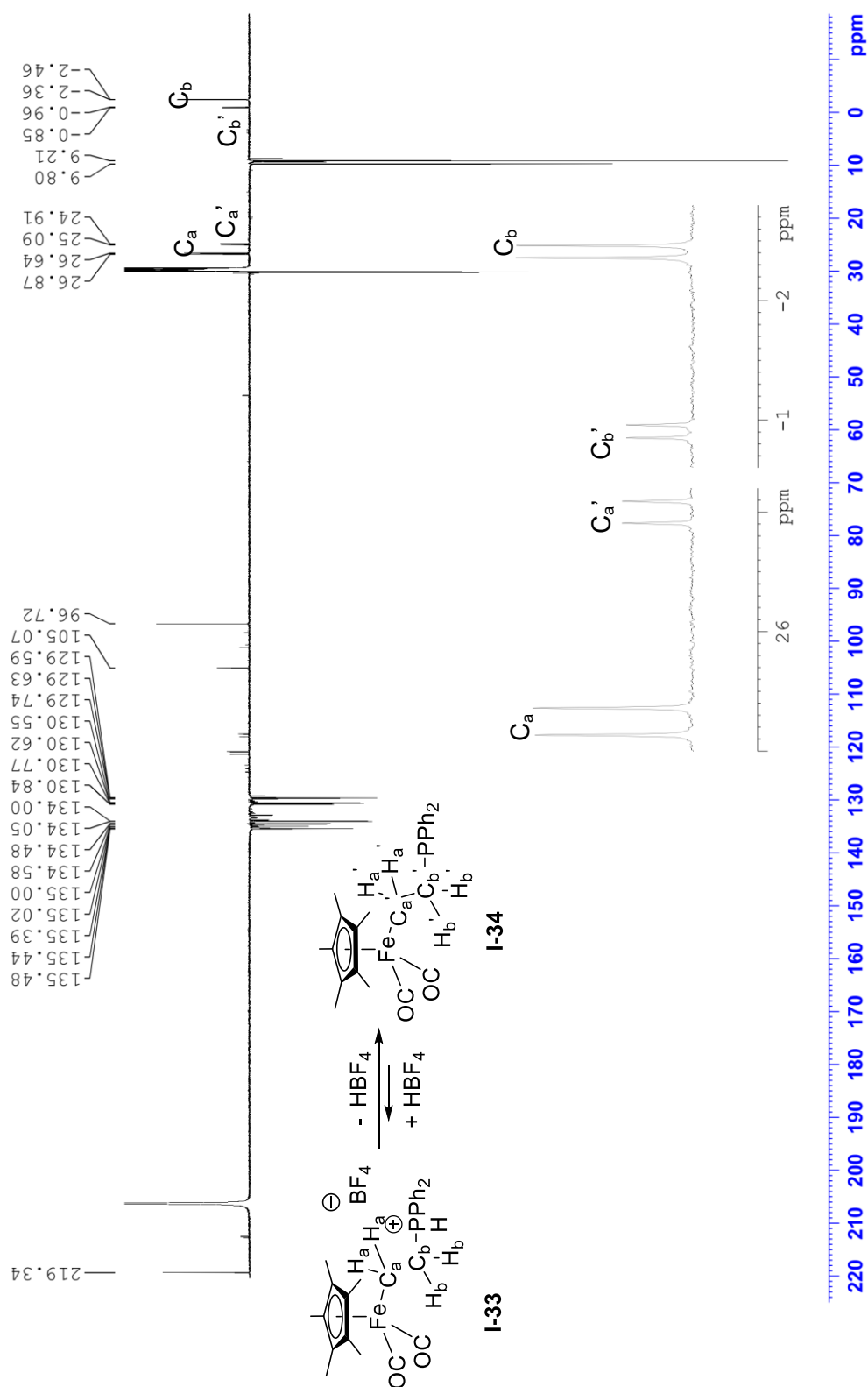
Figure 20. *In situ* ^{13}C(APT) NMR spectrum (162.0 MHz, 25 °C) in acetone-d_6: Nucleophilic addition of 1.1 equiv HPPh$_2$ to **I-26** with zoomed areas of interest.

The study of ethylene activation towards nucleophilic attack with benzyl amine, triphenyl phosphine and $HPPh_2$ was successfully conducted with the complexes **I-5**, **I-20** and **I-26**. Other ethylene complexes **I-21** and **I-22,** as well as, the olefin complexes **I-6** and **I-7** were not found active for nucleophilic additions. The attempted thermal decomposition of all formed adducts to afford aminated or phosphinated products resulted in undesired products. The major product resulted of ethylene substitution (pathway C Scheme 32) with unidentified side products.
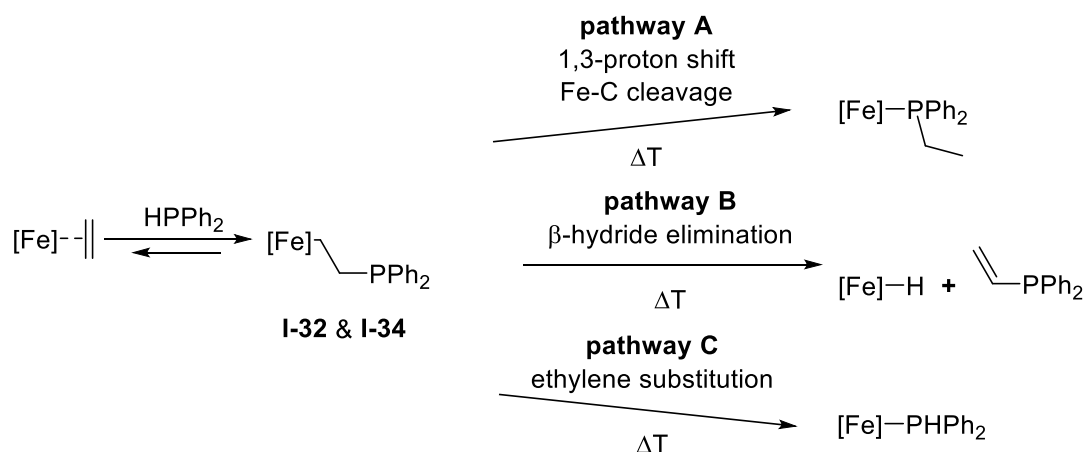
Scheme 32. Proposed pathways thermal decomposition of **I-32** and **I-34**.[76]

We found that $HPPh_2$ adducts degrade in solution when dissolved in acetone-d_6. Removal of the solvent provided a yellow solid that was readily soluble in C_6D_6. The adduct formation was attempted in alkaline medium, employing K_2CO_3 in CD_2Cl_2 and KO^tBu in DMSO-d_6 but no reaction was observed (Scheme 33).
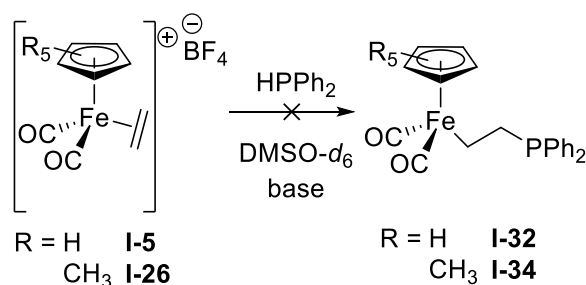
Scheme 33. Attempted formation of phosphine adducts under basic conditions.

In the absence of viable leads, no further reaction under basic alkaline conditions were attempted. With the results of $HPPh_2$ (Scheme 30) and having thermal cleavage of Fe–C bonds for product release ruled out, we then focused on electrophilic bond cleavage.

3.3.3 Investigations of the reactivity of Iron-Carbon bonds

3.3.3.1 Bond Formation

The iron-carbon bond cleavage remains an obstacle for nucleophilic hydrofunctionalization of olefins within the investigated system. Earlier (see chapter 3.3.2) we focused mainly on thermal cleavage, which led mainly to an alkene extrusion with a subsequent alkene substitution by the nucleophile. The literature also reported a potential β-hydride elimination for iron alkyl complexes at elevated temperatures,[76] which is not desired in our case. A different approach is utilizing acids for electrophilic cleavage of iron alkyl compounds. To mimic adducts of ethylene, ethylbenzene was chosen as a model compound.
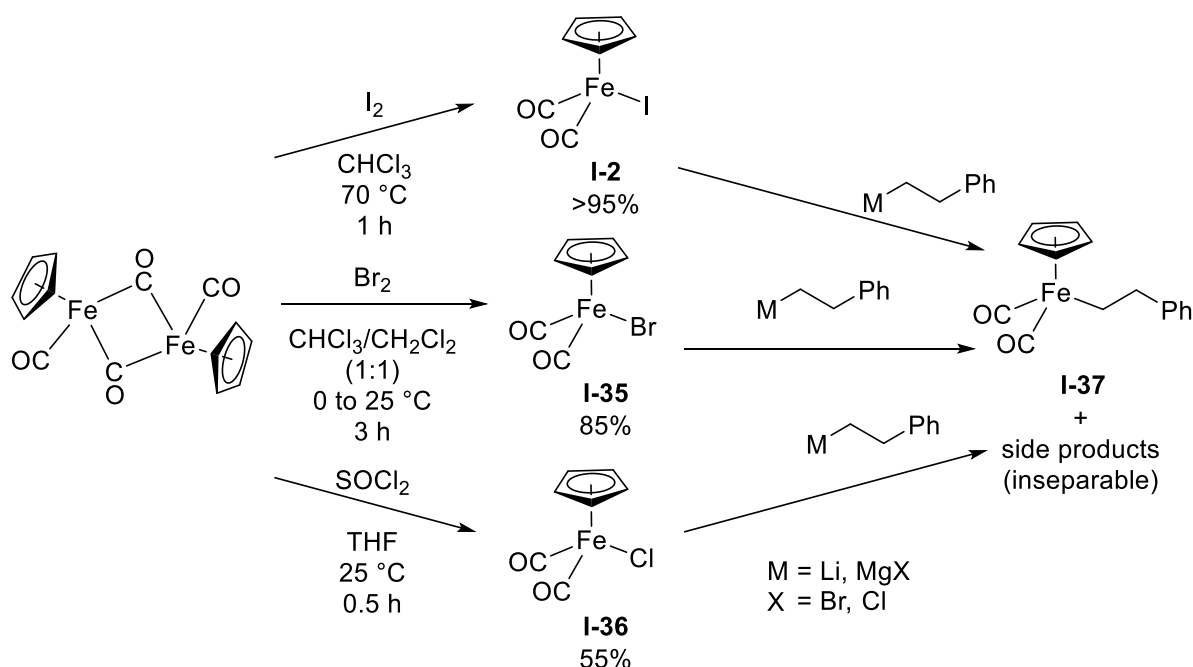
Scheme 34. Preparation of Fp halide and alkyl compounds.[108, 128-133]

In order to create a model compound for iron-carbon cleavage reactions, different Fp halides were prepared. Synthesizing FpI is a simple and high yielding reaction of Fp_2 and I_2, the analogous reaction with Br_2 provided FpBr (**I-35**) in 85 % yield.[129] FpCl (**I-36**) was prepared from Fp_2 and $SOCl_2$ in a 55 % yield with slight impurities of Fp_2 (Scheme 34).[131-132] Spectroscopic comparison of the three halides in terms of electron density at Cp as probe for Fe, revealed only slight differences. However, the reaction with organo-lithium and Grignard reagents only provided crude product mixtures which were found inseparable.
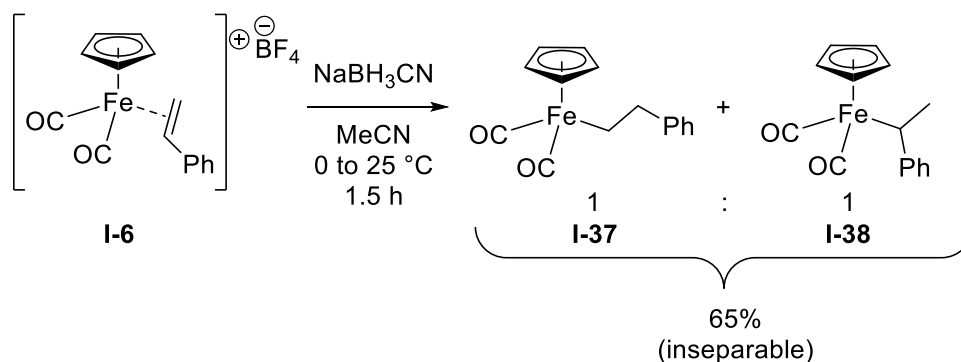
Scheme 35. Reduction of cationic iron olefin complex **I-6** providing iron alkyl compounds **I-37** and **I-38**.[128]

The reduction of a cationic iron olefin complex with a boro-hydride reagent provides a different route to iron alkyl compounds. Test reactions of Fp(η_2-styrene)BF$_4$ (**I-6**) in CD$_3$CN showed that sodium cyanoborohydride undergoes a clean reaction to Fp alkyl compounds **I-37** and **I-38** (Scheme 36) at room temperature.[128] However, the reaction is not regioselective and a 1:1 product mixture of linear (**I-37**) and branched product (**I-38**) is obtained, and the separation of the iron alkyl products remained unsuccessful.
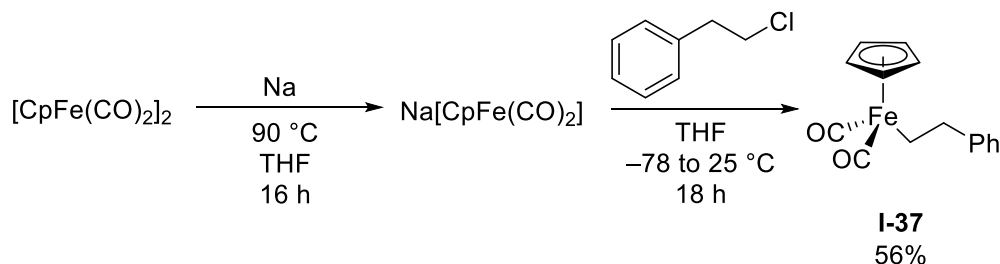
Scheme 36. Preparation of FpC$_2$H$_4$Ph.[128]

As an alternative approach an iron nucleophile was generated *in situ* by treating Fp$_2$ with sodium. The subsequent reaction with chloro-2-phenyl ethane provided the alkyl complex **I-37** in a 56 % yield after workup and the product was moderately stable in air as a solid.[128]

3.3.3.2 Electrophilic Cleavage

The investigation on the cleavage reaction was driven by two major interests: a) the production of ethylbenzene and b) the nature of the formed iron species. The cleavage reactions were performed with the substrate dissolved in deuterated benzene and a 3-5 fold excess of the respective acid was added *via* pipette in air. The outcome of the reaction was evaluated with ^{1}H NMR spectroscopy.

Table 6. Electrophilic cleavage of iron-carbon bond of **I-37** with different acids.
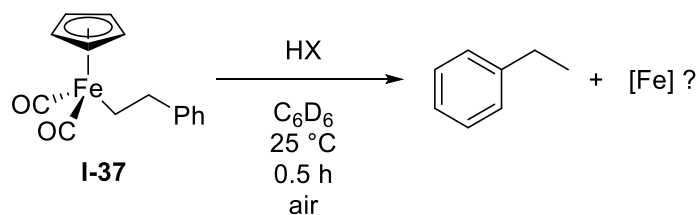
#	HX	pK_A[a]	Conversion to free alkane[b] [%]
1	HI 57 %[c]	-10	-[e]
2	HClO$_4$ 70 %[c]	-10	33
3	HBr 48 %[c]	-8.9	33
4	HCl 38 %[c]	-6	17
5	CH$_3$SO$_3$H	-1.9	-[e]
6	HNO$_3$ 65 %[c]	-1.32	-[e]
7	HBF$_4$ 48 %[c]	-0.4	-[e]
8	HBF$_4$ 55 %[d]	-0.4	13
9	CF$_3$COOH	0.23	89
10	CBr$_3$COOH	0.72	-[e]
11	CBr$_2$HCOOH	1.48	-[e]
12	H$_3$PO$_4$ 85 %[c]	2.13	-[e]
13	HCOOH 85 %[c]	3.77	-[e]
14	C$_2$H$_5$COOH	4.87	-[e]

[a] in water under standard conditions for orientation; [b] determined by ^{1}H NMR spectroscopy in comparison with **I-37**; [c] in water; [d] in Et$_2$O; [e] not observed.[79-80, 134-135]

14 different acids were tested for their reactivity towards iron-carbon bond cleavage. However, a direct correlation between pK_A values and reactivity was not observed. Given that the acidity is measured in water, it might be altered due to the non-polar reaction conditions. Only five acids (Table 6, entries 2–4, 8 and 9) were found to promote the cleavage reaction and only trifluoroacetic acid provided a good conversion of 89 %. Only the free alkane could be identified by the characteristic ^{1}H NMR spectroscopic triplet and quartet pattern, whereas

the produced iron species could not be characterized. It was expected that compounds of the type FpX were formed, but their formation could not be established. Aqueous acids (Table 6, entries 2–4) performed significantly worse with conversions of 17–33 %. While aqueous HBF_4 showed no reactivity, the ethereal complex (Table 6, entry 8) showed a low conversion of 13 %. As mentioned, not only the cleavage reaction but also the nature of the resulting iron species should be investigated. Since most investigations on cationic iron complexes utilized tetrafluoroborate as counter ion, further studies were carried out using etheral HBF_4 in a range of solvents with ranging polarities.

Table 7. Electrophilic cleavage of iron-carbon bond **I-37** with ethereal HBF_4.
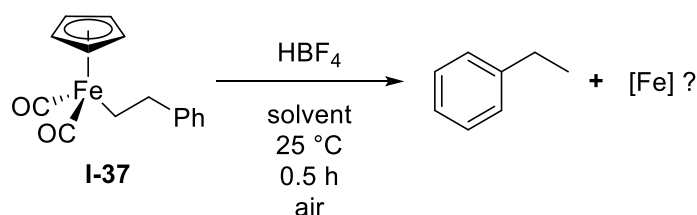
#	Solvent	Dipole Moment [D]	Conversion to free alkane[a] [%]
1	C_6D_6	0.00	9
2	$CDCl_3$	1.04	17
3	CH_2Cl_2	1.60	22
4	MeOH	1.70	-[b]
5	THF	1.75	-[b]
6	Acetone	2.88	29
7	CH_3CN	3.92	15
8	DMSO-d_6	3.96	-[b]

General conditions: **I-37** (0.07 mmol) and HBF_4 (0.29 mmol, 4.1 equiv) in 0.5 mL solvent; [a] determined by ^{1}H NMR spectroscopy in comparison with **I-37**; [b] not observed.

It was observed that the use of deuterated solvents and a short workup with solvent evaporation did not significantly interfere with the reaction outcome. The results suggest acetone (Table 7, entry 6) as the best choice for promoting the reaction providing a conversion of 29 %, while the reaction does not proceed in other solvents (Table 7, entries 4, 5 and 8). A direct correlation of polarity was not observed since not only a more polar solvent (Table 7, entry 7) but also less polar solvents (Table 7, entries 1–3) show a less promoting effect than acetone. It is possible that for non-coordinating solvents a certain correlation to polarity exists since the literature suggests a protonated iron species with a subsequent reductive elimination of the product.[79] Thus, a less polar environment could obstruct the

formation of an ionic iron species while highly coordinating solvents might occupy the protonation site of the iron center in solution.
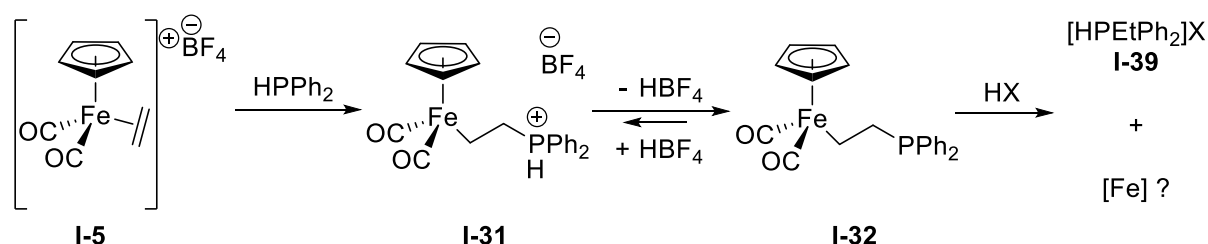
Scheme 37. Schematic depiction of the nucleophilic addition of HPPh$_2$ to the cationic iron ethylene complex **I-5** forming **I-31** and **I-32**. Subsequent formation of a free/coordinated tertiary phosphine *via* electrophilic cleavage.

HPPh$_2$ readily performs nucleophilic addition to cationic iron ethylene complexes in various solvents like acetone, acetonitrile, benzene and dichloromethane (Scheme 37). The obtained adduct was observed both as protonated and deprotonated species that are in an equilibrium, as confirmed by NMR spectroscopy. Additionally, the equilibrium can be shifted by deprotonation with KO^{t}Bu towards the neutral species **I-32**. When acids like HCl, ethereal HBF$_4$ and TFA were employed in a similar manner to earlier investigations (see section 3.2.2) a shift towards the protonated species **I-31** was observed and even heating to high temperatures (>150 °C) did not lead to iron-carbon bond cleavage. The addition of two equiv of TfOH to the phosphine adduct in an NMR tube resulted in formation a of dark precipitate and ^{1}H and ^{31}P{^{1}H} NMR spectroscopic investigations provided new signals. The ^{1}H NMR spectrum provided only broad signals due to the formation of precipitate and challenging to interpret properly (Figure 21). However, the ^{31}P{^{1}H} NMR spectrum suggested the formation of [H$_2$PPh$_2$]$^+$ from residual HPPh$_2$ (-20.9 ppm) and a direct conversion of the phosphine adduct **I-31** (8.3 ppm) to the protonated free phosphine **I-39** (12.2 ppm) (Figure 22).[136] The solids were filtered off and subsequently the ^{1}H NMR spectrum also provided characteristic signals for a terminal ethyl group coupling with phosphorus that match the reference spectrum in the literature (^{1}H NMR (δ in ppm): 2.89 (dq, 2H, PC*H*$_2$CH$_3$), 1.37 (dt, 3H, PCH$_2$C*H*$_3$) (compare to Figure 21).[136] It is noteworthy that the reaction provided mostly desired free phosphine and its protonated form **I-39** which were expected to also coordinate to the iron complex **I-32** to form **I-40** (Scheme 38), however not all observed species could be identified. **I-40** can be observed in the ^{31}P{^{1}H} NMR providing a signal with a chemical shift of 60.5 ppm. This was confirmed by an coordination of ethyl diphenylphosphine to **I-4** in an NMR scale experiment (Scheme 38).
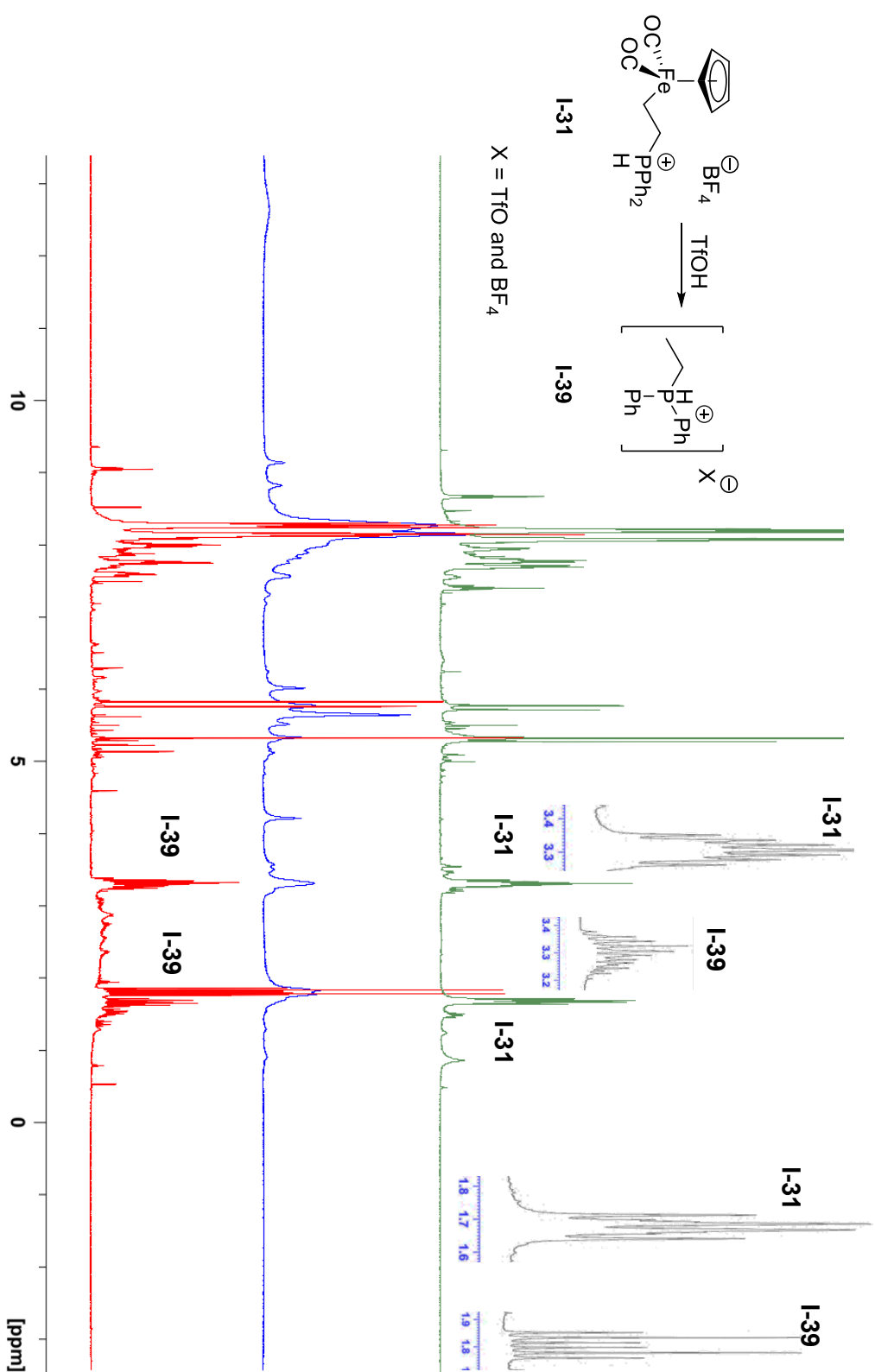
Figure 21. *In situ* ^{1}H NMR spectrum (400.3 Mhz) in CD$_2$Cl$_2$: Electrophilic cleavage of **I-31** with 2 equiv of TfOH providing **I-39** after 1 h at 80 °C. The reference spectrum (green) was recorded before addition of TfOH; directly after the reaction (blue) and after filtration (red). The ethylene signals are zoomed in for clarification.
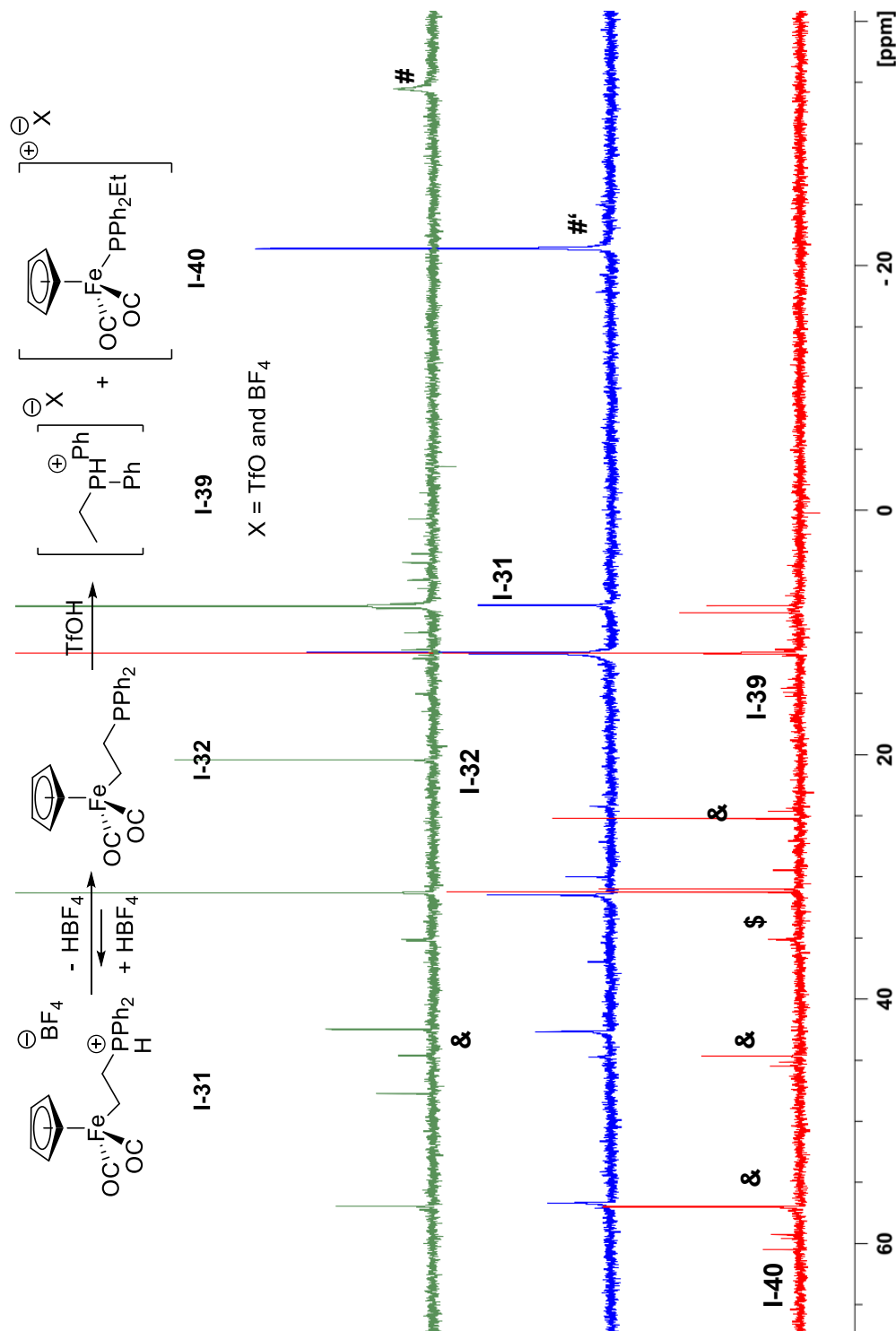
Figure 22. *In situ* $^{31}P\{^1H\}$ NMR spectrum (162.0 Mhz) in CD_2Cl_2: Electrophilic cleavage of **I-31** with 2 equiv of TfOH providing **I-39** after 1 h at 80 °C. The reference spectrum (green) was recorded before addition of TfOH; directly after the reaction (blue) and after filtration (red).; **4** – HPPh$_2$ coordinated to Fe. **#** - free HPPh$_2$, **#'** – [H$_2$PPh$_2$]$^+$. **&** - and **-** not identified side product.
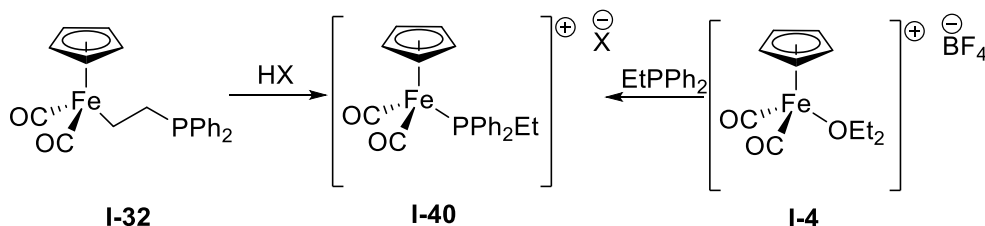
Scheme 38. Proposed formation of cationic iron phosphine complex **I-40** from **I-32** and **I-4**.

Upon treating the unfiltered solution of **I-32** and acid with either atmospheric pressure of ethylene or addition of styrene did not lead to the observation of an olefin complex. It might be worth noting, that iron ethylene complexes were found to be only sparingly soluble in CD_2Cl_2 and formed complexes might have precipitated alongside with other unidentified side products and were lost during the filtration.

The analogous reactions of the iron olefin complexes with styrene (**I-6**) and 1-octene (**I-7**) with HPPh$_2$ only showed a ligand displacement resulting in free styrene and 1-octene, respectively. No further reactivity was observed upon treatment with either NEt$_3$ or TfOH.

3.3.4 Investigation on Hydrophosphination of Styrene

The catalytic transformation of styrene with HPPh$_2$ to diphenyl(phenylethyl)phosphine was observed when applying the reaction conditions of Webster (Scheme 39) in a test reaction.[101]
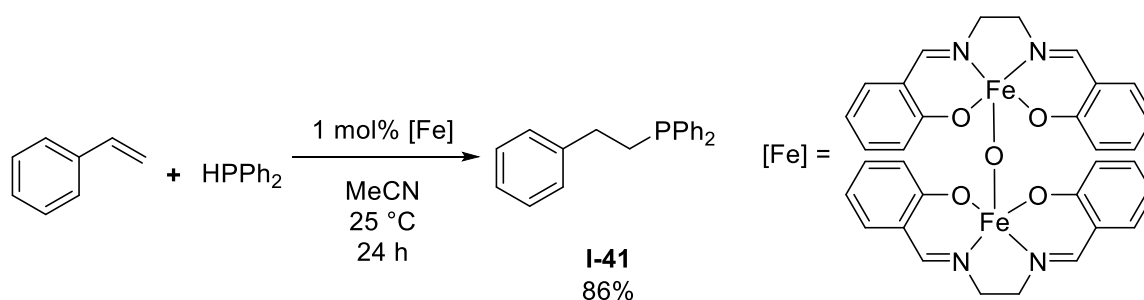
Scheme 39. Iron(III)-salen catalyzed hydrophosphination of styrene.[101]

Instead of iron(III) salen complexes, we applied cationic half-sandwich iron(II) olefin complexes as precatalysts under concentrated conditions. Only limited reactivity was observed at room temperature; therefore, the NMR reaction was heated to 110 °C to investigate catalytic activity (Scheme 40). These drastic temperatures were adapted from Nakazawa who used FpMe as catalyst for double hydrophosphination of terminal alkynes.[102]
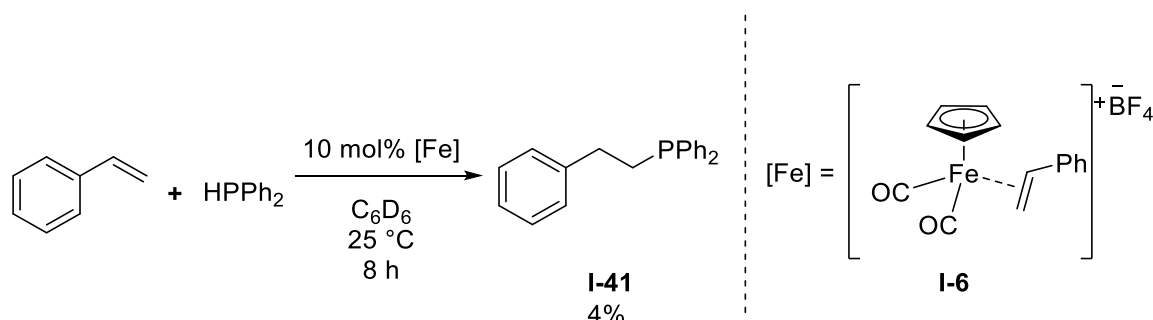
Scheme 40. First results for catalytic hydrophosphination of styrene. [Fe] 87 µmol, $HPPh_2$ 1.72 mmol, Styrene 1.53 mmol, 50 µL C_6D_6 (c(styrene) = 34.5 mol L^{-1}).

When the temperature was increased quantitative conversion was observed after 24 h. Thus the catalyst loading was decreased while the reaction time was increased and different iron precatalysts were investigated. The comparable reaction of 1-octene instead of styrene showed no activity.

Table 8. Hydrophosphination of styrene with different iron complexes.
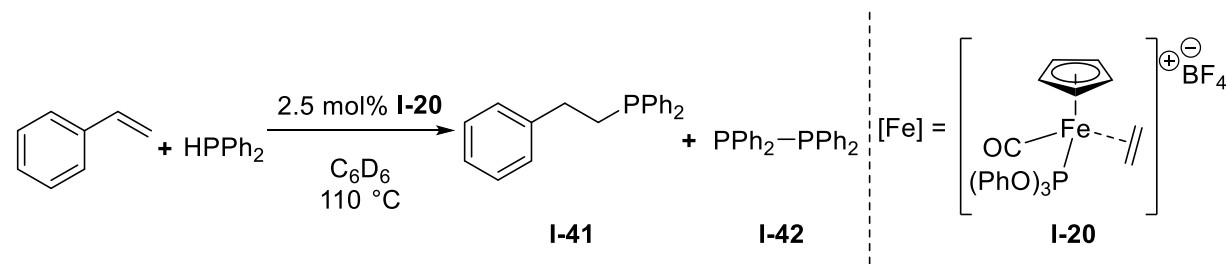
#	Fe complex	conversion[a] [%]	I-41[a] [%]	I-42[a] [%]
1	$[Fp(C_6H_5C_2H_3)]^+BF_4^-$ (**I-6**)	98	88	10
2	$[Fp^{TPOP}(C_2H_4)]^+BF_4^-$ (**I-20**)	>99	92	6
3	$[Fp^*(C_2H_4)]^+BF_4^-$ (**I-26**)	90	84	5
4	none	97	87	7

General conditions: ratio styrene:$HPPh_2$:[Fe] 0.95:1:0.05 in 250 µL C_6D_6 (c(styrene) = 3.61 mol L^{-1}); [a] determined by $^{31}P\{^1H\}$ NMR with [δ in ppm] –40.0 unreacted $HPPh_2$, –20.7 **I-42**, –15.8 **I-41**.

High conversions were obtained in all reactions; even at lower concentrations and in the absence of a catalyst (compare Scheme 40). It is worth noting that employing **I-20** (Table 8, entry 2) resulted in a complete conversion of phosphine while providing a comparable low amount of side product **I-42**. Although, complex **I-6** (Table 8, entry 3) was the only precatalyst containing styrene, no hydrophosphination product of ethylene was observed. For further investigations **I-20** was employed due to being ready accessibility and surprisingly good solubility in substrates and products, while being the most active catalyst. However, the iron complex is only sparingly soluble in CD_2Cl_2 and only free triphenyl phosphite was observed after completion of the reaction.

To get more insight into the rate of the reaction and catalyst activity, a NMR scale reaction under the same conditions as in (Table 8, entry 2) but with a lower catalyst loading was performed. The reaction mixture was heated in an NMR tube in an oil bath and the reaction progress was monitored *via* $^{31}P\{^1H\}$ NMR spectroscopy at room temperature.

Table 9. Hydrophosphination of styrene progress monitored over time.
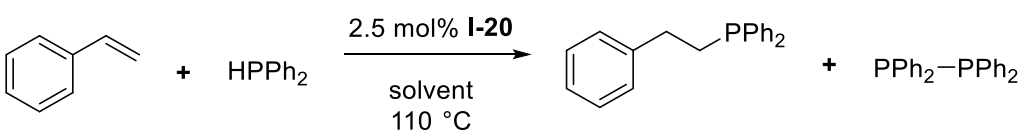
#	t [hh:mm]	conversion[a] [%]	I-41[a] [%]	I-42[a] [%]
1	00:05	3	<1	–[b]
2	01:00	15	10	1
3	03:30	66	57	5
4	17:00	95	82	8
5	18:00	96	85	8

General conditions: ratio styrene:HPPh$_2$:**I-20** 0.95:1:0.025 in 250 µL C$_6$D$_6$ (c(styrene) = 3.61 mol L^{-1}); [a] determined by $^{31}P\{^1H\}$ NMR spectroscopy with [δ in ppm] –40.0 unreacted HPPh$_2$, –20.7 **I-42**, –15.8 **I-41**, [b] not observed.

No catalytic activity was observed right at the beginning of the reaction (Table 9, entry 1) before the reaction was heated to 110 °C. The reaction proceeds relatively fast at elevated temperature and a conversion of 66 % was observed after 3.5 h (Table 9, entry 3). After heating the reaction mixture overnight, a precipitate was observed in the NMR tube, which might explain the observation of catalytic inactivity after 17 h (Table 9, entries 4 and 5). With those results in hand, further investigations were performed with shorter reaction times.

The next step was to study the influence of the solvent on the catalytic activity of the system. Four solvents with different polarities were investigated and a background reaction without catalyst was performed in C$_6$D$_6$.

Table 10. Hydrophosphination of styrene progress monitored over time.

#	solvent	conversion[a] [%]		I-41[a] [%]		I-42[a] [%]	
		1 h	3 h	1 h	3 h	1 h	3 h
1	CD_2Cl_2	44	69	34	54	5	6
2	THF-d_8	34	71	30	65	2	4
3	C_6D_5Br	46	79	42	71	3	5
4	C_6D_6	48	80	44	72	3	5
5	C_6D_6	36	40[b]	34	37[b]	2	2[b]

General conditions: ratio styrene:HPPh$_2$:**I-20** 0.95:1:0.025 in 250 µL C_6D_6 (c(styrene) = 3.61 mol L^{-1}); [a] determined by ^{31}P{^{1}H} NMR with [δ in ppm] −40.0 unreacted HPPh$_2$, −20.7 **I-42**, −15.8 **I-41**; [b] reaction continued at room temperature after 1 h.

The performed reactions (Table 10) showed that benzene and bromobenzene (Table 10, entries 3 and 4) exhibit the most positive effect on the reaction. However, it is worth noting that the differences in activity are not significant and also the advantage over the background reaction in C_6D_6 is within the range of NMR spectroscopic error of measurement. Also the comparable reactions (see Table 9, entry 3 and Table 10, entry 4) exhibit a significant difference in activity which makes the reproducibility questionable. A possible explanation was a slight change in stoichiometry due to insufficient mixing while the reaction proceeds and less substrate is available. Thus, a study at lower temperature with different stoichiometric ratios was conducted to investigate possible effects on activity in an even more dilute system.
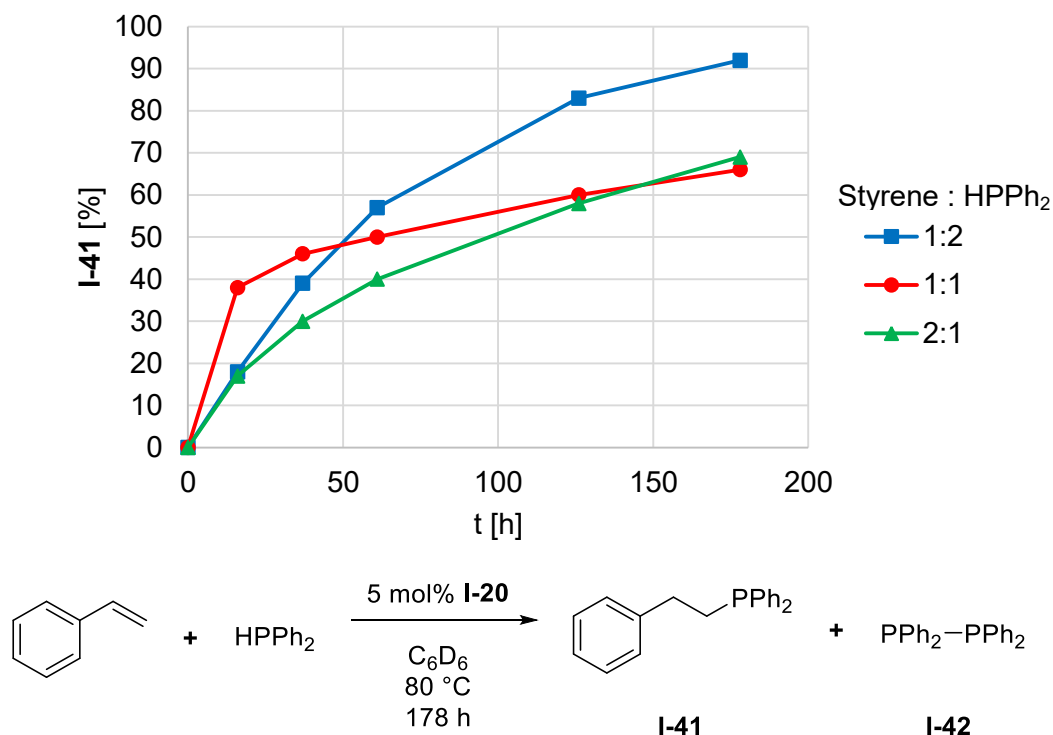
Figure 23. Reaction progress of the Hydrophosphination of styrene with HPPh$_2$ over time *via* ^{31}P{^{1}H} NMR spectroscopy.

Table 11. Hydrophosphination of styrene progress monitored over time.

#	Ratio [equiv]		conv. [%][a,b]	I-41 [%][b]	I-42 [%][b]	Residual ratio[c]	
	Styrene	HPPh$_2$				Styrene	HPPh$_2$
1	1	2	92	43	<1	1.0	14.0
2	1	1	65	66	4	1.2	1.0
3	2	1	36	69	8	4.1	1.0

General conditions: conducted in 450 µL C$_6$D$_6$ (c(1 equiv) = 0.64 mol L^{-1}); [a] determined by the consumption of the limiting reagent; [b] determined by ^{31}P{^{1}H} NMR spectroscopy with [δ in ppm] –40.0 unreacted HPPh$_2$, –20.7 **I-42**, –15.8 **I-41**; [c] determined by ^{1}H NMR spectroscopy.

The graph (Figure 23) shows that the stoichiometric ratio of styrene to HPPh$_2$ has a noticeable effect on the hydrophosphination reaction at 80 °C. An excess of HPPh$_2$ positively influences the conversion of the lesser substrate (Table 11, entry 1), while simultaneously suppressing the formation of the dehydrogenated coupling product. When using the same stoichiometric ratio or even employing an excess of styrene, the conversion of substrates remained on an average level around 66-69 %. Although the initial activity of the equimolar ratio reaction was quite high, it declined during the course of the reaction. It was observed

that an excess of phosphine is beneficial for the catalytic activity while higher concentrations of styrene only increase the amount of the side product **I-42**. However, the formation of ethyl benzene was not observed. Also the effect of dilution resulted in a significantly lower activity, which led to an extended reaction time of 178 h.

Since the aim of the study was the implementation of a system that significantly outperforms the catalytic background reaction, less vigorous conditions were thought to be desirable. The latter experiment exhibited only limited activity in a highly diluted system, so the concentrations of the following screening were increased to investigate the effect of different solvents at 80 °C. Although higher activities with an excess of phosphines were observed, the reaction was conducted using equimolar amounts of styrene and HPPh$_2$ to ensure comparable results.
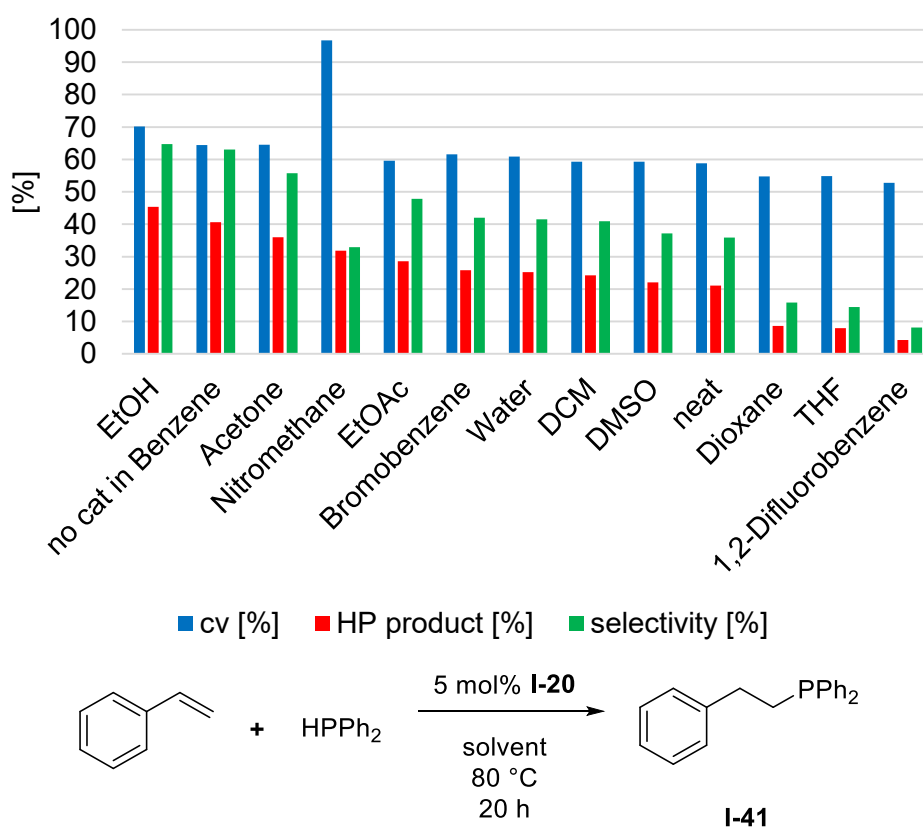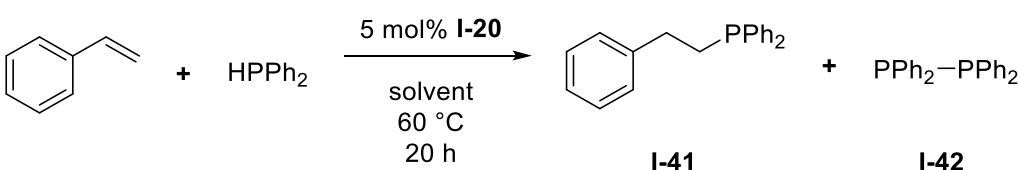
Figure 24. Hydrophosphination of styrene with HPPh$_2$ in different solvents at 80 °C; evaluated by ^{31}P{^{1}H} NMR spectroscopy; General conditions: ratio styrene:HPPh$_2$:**I-20** 1:1:0.05 in 100 µL solvent (c(styrene) = 3.50 mol L^{-1}). Selectivity $= \frac{\textbf{I-41}}{conv.}$

As shown in Figure 24, the hydrophosphination reaction of styrene with HPPh$_2$ catalyzed by **I-20** performed best in ethanol (45 %), followed by acetone (36 %) and nitromethane (32 %). However, the reaction performed in benzene without **I-20** provided

similar results (41 %). It is worth noting that the reaction in nitromethane exhibit a very high conversion of the phosphine (97 %) while only 32 % of the hydrophosphination product **I-41** was observed. Unidentified signals in the $^{31}P\{^1H\}$ NMR spectrum between 20 and 40 ppm were assumed to be oxidized **I-41**, **I-42** and $HPPh_2$. The other solvents provided lower conversions and selectivity, with no noteworthy effects. With lowering the reaction temperature the autocatalytic reactivity was expected to by limited. The concentration of the reaction was left unchanged for comparison.

Table 12. Hydrophosphination of styrene with $HPPh_2$ in different solvents at 60 °C.

#	solvent	conversion[a] [%]	I-41[a] [%]	I-42[a] [%]
1	C_6H_6	32	25	1
2	C_6H_6[b]	43	37	2
3	C_6H_6[c]	21	18	<1
4	C_6H_6[b,c]	26	14	<1
5	Dioxane	22	16	<1
6	MeCN	7	_[d]	_[d]
7	1,2-Difluorobenzene	13	7	<1
8	$MeNO_2$	55	39	2

General conditions: ratio styrene:$HPPh_2$:**I-20** 1:1:0.05 in 100 µL C_6D_6 (c(styrene) = 3.50 mol L^{-1}); [a] determined by $^{31}P\{^1H\}$ NMR spectroscopy with [δ in ppm] –40.0 unreacted $HPPh_2$, –20.7 **I-42**, –15.8 **I-41**; [b] open system; [c] reaction without **I-20** added; [d] not observed.

Hydrophosphination reactions in benzene and nitromethane exhibited the best conversions. Interestingly the reaction in benzene with iron complex **I-20** provides even higher conversion and high selectivity when not performed under inert conditions (Table 12, entries 1 and 2). Whereas the background reaction was debased as it was exposed to non-inert conditions (Table 12, entries 3 and 4). The reactions in 1,2-difluorobenzene, acetonitrile and 1,2-dioxane were only perfomed under argon but their conversion rates did not match the rates in benzene (Table 12, entries 5–7). Only nitromethane provided a slightly higher conversion and also a slightly higher output under inert conditions (Table 12, entry 8). Therefore, nitromethane was suspected to be a non-innocent solvent in the hydrophosphination. It is known that strong Brønsted acids catalyze hydrophosphination, but nitromethane is only slightly acidic (p$K_{a,DMSO}$ = 17.2);[137] so an oxidative reaction was thought

to take place. Since the major side-product **I-43** exhibited a chemical shift around 29 ppm in the $^{31}P\{^1H\}$ NMR and the literature reported 32 ppm.[138]

To investigate a potential effect of nitromethane on the hydrophosphination of styrene, the reactions were repeated at 60 °C with and without the iron complex **I-20**.

Table 13. Hydrophosphination of styrene with HPPh$_2$ in nitromethane at 60 °C.

#	additives	conversion[a] [%]	I-41[a] [%]	I-42[a] [%]	I-43[a] [%]
1	5 mol% **I-20**	95	50	3	27
2	none	74	54	3	14

General conditions: ratio styrene:HPPh$_2$:**I-20** 1:1:0.05 in 100 µL MeNO$_2$ (c(styrene) = 3.50 mol L^{-1}); [a] determined by $^{31}P\{^1H\}$ NMR with [δ in ppm] –40.0 unreacted HPPh$_2$, –20.7 **I-42**, –15.8 **I-41**, 29.0 **I-43**.

The reaction proceeded with high conversion of HPPh$_2$ (Table 13, entry 2) to almost quantitative (Table 13, entry 1) no matter if **I-20** was added or not. However, addition of **I-20** was found to improve the conversion of the substrate to the oxidized product **I-43**. But with the background reactivity in mind, the reaction becomes less selective for the desired product **I-41**. In order to achieve higher selectivity further adjustment of the conditions were implemented.

Table 14. Hydrophosphination of styrene in MeNO$_2$ in different concentrations.

#	c(styrene) [mol L^{-1}]	conversion[a] [%]	I-41[a] [%]	I-42[a] [%]	I-43[a] [%]
1	1.75[b]	47	39	3	5
2	1.75	-[c]	-[c]	-[c]	-[c]
3	3.50	23	20	-[c]	-[c]
4	7.00	30	27	-[c]	-[c]
5	14.00	40	36	<1	-[c]
6	14.00[d]	62	58	-[c]	-[c]

General conditions: ratio styrene:HPPh$_2$:**I-20** 1:1:0.05 in 100 µL MeNO$_2$; [a] determined by ^{31}P{^{1}H} NMR spectroscopy with [δ in ppm] -40.0 unreacted HPPh$_2$, -20.7 **I-42**, -15.8 **I-42**, 29.0 **I-43**; [b] no iron complex added, [c] not observed; [d] 2 equiv of phosphine.

Experiments with and without the iron complex **17** (Table 14, entries 1 and 2) showed an effect on the reaction. Interestingly, the reaction can be conducted at a considerably lower temperature with relatively low concentration of MeNO$_2$, and showed almost 50 % conversion after 20 h. But once a cationic iron complex is added, neither conversion to the desired product nor side-products is observed. However, when the reaction was performed with higher concentrations in MeNO$_2$ an increase in reactivity was observed. Under almost neat conditions with sub-stoichiometric amounts of solvent and 8-fold higher concentration, the conversion to the desired product **I-41** is matched with the reaction without iron additive (Table 14, entries 1 and 5). Interestingly, the amount of side-products was minimized in the course of higher concentrated reactions. These results sparked the idea to run the reaction with a 2:1 excess of phosphine, which led to an even higher conversion of 58 % solely to the desired product. A unknown signal in the ^{31}P{^{1}H} NMR spectrum around 17 ppm is thought to be coordinated product to the iron complex, since coordinated HPPh$_2$ is observed around 35 ppm. This matches with the observation in the ^{1}H NMR spectrum in which the methylene protons show small satellite signals slightly shifted to higher field. It is worth noting that nitromethane might be the active species in this reaction, but the addition of iron complex **I-20** appears to influence the reaction and shifted its selectivity towards **I-41**. Interestingly, adverse effects were observed at higher temperatures (compare Table 13), but seemed to affect the reaction only positively at 40 °C in terms of selectivity.

After extensive investigation of the hydrophosphination of styrene a variety of effects that influence the outcome were observed while modifying the experimental conditions. No phosphine adduct coordinated to iron was observed even when previous experiments with iron ethylene complexes almost exclusively yield the phosphine adduct (Scheme 41). It is possible that the formed phosphine adduct from a nucleophilic addition is not stable in solution and was therefore not detected in NMR spectroscopic investigations. Or the reaction does not follow the proposed outer sphere mechanism which was observed for nucleophilic addition to cationic iron ethylene complexes (see chapter 3.3.2).

R = H   **I-5**   quantitative
Ph   **I-6**   not observed
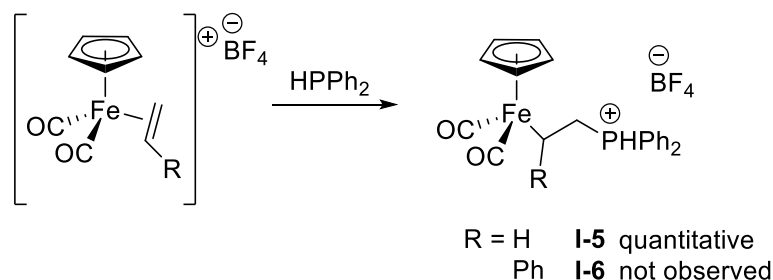
Scheme 41. Comparison of the nucleophilic addition of HPPh$_2$ to cationic iron olefin complexes **I-5** and **I-6**.

Based on the results of Nakazawa phenyl acetylene was tested as a substrate due to its higher susceptibility to nucleophilic additions and also bearing the possibility of double hydrophosphination.[102]
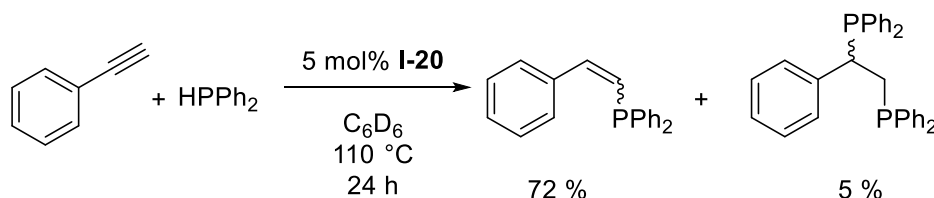
Scheme 42. Phenylacetylene as test substrate for hydrophosphination.[102]

When phenyl acetylene was reacted with HPPh$_2$ using 5 mol% **I-20** as catalyst, reactivity towards mono hydrophosphination and limited reactivity towards double hydrophosphination was observed. In comparision, Nakazawa observed the formation of the double hydrophosphination product using 5 mol% CpFe(CO)$_2$Me as catalyst at 110 °C in a yield of 24 % after 16 h and 94 % after 72 h, respectively.[102] Given the fact, that the hydrophosphination of styrene provided almost quantitative conversion to the product after 18 h while using an equimolar amount of phosphine (see Table 9). Thus, the use of phenyl acetylene as a substrate was not further investigated.

3.4 Conclusion and Outlook

A general protocol for the preparation of different iron olefin complexes was developed. The complexes were successfully employed in the outer-sphere addition of benzyl amine, triphenyl phosphine and diphenyl phosphine to form iron-alkyl complexes. The adduct formation was monitored by NMR spectroscopy which provided partial insight on structural features of the formed iron-alkyl complexes. Diphenyl phosphine was selected for further investigations on nucleophilic additions to facilitate reaction monitoring with ^{31}P{^{1}H} NMR spectroscopy. This enabled structural investigation that provided insight in the formation of two major species when used at room temperature. As a proof-of-concept, liberation of ethyl diphenylphosphine was achieved by electrophilic cleavage of the iron-alkyl bond with trifluoromethanesulfonic acid (Scheme 43).
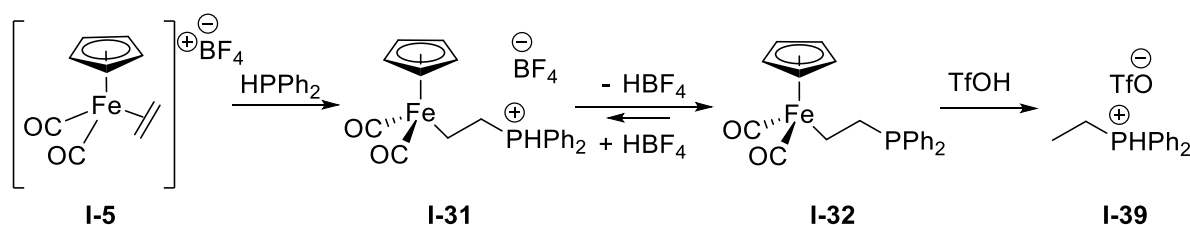
Scheme 43. Stepwise Nucleophilic addition of diphenyl phosphine to an iron-ethylene complex and the subsequent liberation of ethyl diphenylphosphine.

With our findings the work of Rosenblum was extended towards the liberation of a higher phosphine in a stoichiometric manner.[72-75] However, iron complexes of styrene and 1-octene were not susceptible for nucleophilic addition of phosphines or amines under the given conditions. Our approach to implement a catalytic system following an outer-sphere mechanism did not succeed for hydrophosphination of styrene, which confirmed our prior observations.

The next step would be to transfer our structural insights to the nucleophilic addition of different amines to iron ethylene complexes. Further, investigations on the nucleophilic addition to iron olefin complexes should focus on higher olefins like propylene or butylene to investigate regioselectivity. The use of different olefins might also facilitate the regeneration of the iron olefin complex after the liberation of the desired product.

3.6 Experimental section

3.6.1 Working methods

If not explicitly mentioned differently, all reactions were carried out in an inert gas atmosphere under exclusion of air and moisture at room temperature. These conditions were ensured by using the Schlenk-technique or working in a glove box. Solvents used for preparations or analytics were dried with sodium and benzophenone or calcium hydride, and distilled under inert gas. Commercially obtained starting materials were purified if needed. Other reagents were provided by the group and did not need to be purified. NMR spectroscopic experiments were performed on *Bruker AVIII* instruments (400 and 600 MHz). Chemical shifts (δ in ppm) are indicated relative to TMS and were referenced to residual protons in the solvent. Air-tight sealed NMR tubes were used for NMR experiments for compounds that were air or moisture sensitive.

Table 15. Chemical shifts and multiplicities of used deuterated solvents.[139]

Solvent	δ (^{1}H) / ppm (multiplicity)	δ (^{13}C{^{1}H}) / ppm (multiplicity)
CDCl$_3$	7.26 (br s)	77.16 (t)
CD$_2$Cl$_2$	5.32 (t)	53.84 (quint)
C$_6$D$_6$	7.16 (br s)	128.06 (t)
Acetone-d_6	2.05 (m)	206.26 (s)
		29.84 (sept)
DMSO-d_6	2.50 (m)	39.52 (sept)
THF-d_8	3.58 (br s)	67.21 (quint)
	1.73 (br s)	25.31 (quint)

3.6.2 Synthesis of phosphorus compounds

3.6.2.1 Synthesis of 4-ethyl-2,6,7-trioxa-1-phosphabicyclo[2.2.2]-octane[114]
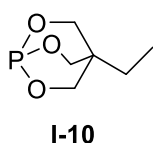
1,1,1-Trimethylolpropane (5.14 g, 38.3 mmol, 1.15 equiv) and triethylphosphite (5.35 mL, 5.52 g, 33.2 mmol, 1.0 equiv) were mixed in a flask and a distillation apparatus was fit on top. Triethylamine (50 µL, 36.3 mg, 0.36 mmol, 0.01 equiv) was added and the mixture was heated (160 °C) for 2 h. Under continuous distillation ethanol was removed from the reaction and the endpoint was identified when the head temperature dropped to 40 °C. The crude product was purified by distillation (11 mbar, T_{bath}: 170 °C, T_{head}: 108 °C), obtained as a low melting colorless solid and characterized by NMR spectroscopy.

Yield: 3.98 g (24.5 mmol, 79 %).

^{1}H NMR (C$_6$D$_6$, 25 °C, 400.3 MHz, ppm): δ = 3.54 (s, 6H, 3 × OCH_2C), 0.34 (q, $^3J_{H,H}$ = 7.21 Hz, 2H, CH_2CH$_3$), 0.16 (t, $^3J_{H,H}$ = 7.21 Hz, 3H, CH$_2$CH_3). ^{31}P{^{1}H} NMR (162.0 MHz, ppm): δ = 93.3 (1P, P(OR)$_3$). The NMR spectroscopic data are in accordance with the literature.[114]

3.6.2.2 Preparation of 1,2-bis-(diphenoxyphosphino) ethane (dpope)[9]
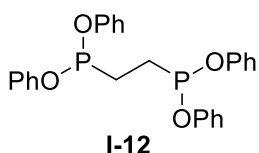
A Schlenk flask was charged with phenol (3.71 g, 39.42 mmol, 4.2 equiv) and triethylamine (7.6 mL, δ = 0.726 g mL^{-1}, 5.52 g, 54.53 mmol, 5.8 equiv) dissolved in Et$_2$O (30 mL). The mixture was cooled to −78 °C and bis-1,2-(dichlorophosphino) ethane (2.19 g, 9.44 mmol, 1.0 equiv) dissolved in 5 mL Et$_2$O was added dropwise over 5 min. The mixture was stirred for 30 min at −78 °C and then let warm to room temperature overnight. The voluminous [Et$_3$NH]Cl is filtered off and the residue is extracted several times with Et$_2$O (6 × 20 mL) until ^{31}P{^{1}H} NMR showed no more product in the residue. After removal of the solvent *in vacuo* no residual phenol or Et$_3$N were detected in the white product which was characterized by ^{1}H/^{13}C NMR spectroscopy.

Yield: 3.487 g (7.54 mmol, 80 %).

^{1}H NMR (C$_6$D$_6$, 25 °C, 400.3 MHz, ppm): δ = 6.54–7.09 (m, 20H, 4 × C$_6$H$_5$), 2.25 (t, $^3J_{H,P}$ = 7.82Hz, 4H, PCH_2CH_2P). ^{31}P{^{1}H} NMR (162.0 MHz, ppm): δ = 179.2. The NMR spectroscopic data are in accordance with the literature.[9]

3.6.2.3 Attempted preparation of 1,2-bis[bis(trifluoromethyl)phosphino]ethylene (dtfmpe)[112]
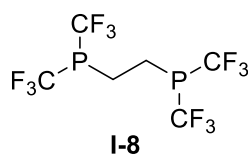
1,2-Bis(diphenoxyphosphino)ethylene (253 mg, 0.55 mmol, 1.0 equiv) and cesium fluoride (166 mg, 1.09 mmol, 2.0 equiv) were suspended in 5 mL Et_2O, and then $TMSCF_3$ (0.41 mL, 394 mg, 2.77, 5.07 equiv) were added dropwise over 5 min. The colorless suspension turned slowly orange after the addition and the mixture was stirred for 24 h at room temperature. The flask was transferred into the glovebox, cesium fluoride (93 mg, 0.61 mmol, 1.12 equiv) was added and the reaction was stirred for another 18 h. The mixture was concentrated *in vacuo* (10^{-2} mbar) at 0 °C and the brown residue was stored in the glovebox for crystallization. Crystals were formed, but upon attempted isolation by washing with cold pentane they degraded to an oily residue. A crude NMR showed a mixture of two different products that remained inseparable.

3.6.4 Synthesis of iron compounds

3.6.4.1 Synthesis of dicarbonyl(η5-cyclopentadienyl)iron(II) iodide (FpI)[108]
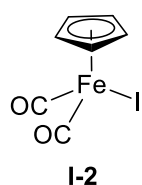
Fp_2 (2.72 g, 8.24 mmol, 1.0 equiv) and I_2 (2.31 g, 9.06 mmol, 1.1 equiv) were placed in a round-bottomed flask, suspended in $CHCl_3$ (20 mL) and refluxed for 1 h. The reaction mixture was let cool to room temperature and stirred overnight. Dark precipitate was collected by filtration and washed with PE (3 × 20 mL). The combined washing solution was stored at −19 °C overnight for follow-up precipitation. The product was obtained as a black crystalline solid that was characterized by ^{1}H/^{13}C NMR spectroscopy and MS.

Yield: 4.20 g (13.8 mmol, 84 %).

^{1}H NMR (CDCl$_3$, 25 °C, 400.3 MHz, ppm): δ = 5.05 (s, 5H, η^5-C$_5$H$_5$). ^{13}C{^{1}H} NMR (100.7 MHz, ppm): δ = 84.2.[1] The NMR spectroscopic data are in accordance with the literature.[108]

HRMS-(ESIpos) (m/z): calc. for C$_7$H$_5$FeIO$_2$: 303.8684, found: 303.8679.

---

[1] No CO signal was observed.

3.6.4.2 Synthesis of dicarbonyl(η^5-cyclopentadienyl)iron(II) bromide (FpBr)[129]

I-35
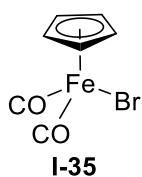
Fp$_2$ (6.94 g, 19.5 mmol, 1 equiv) dissolved in CH$_2$Cl$_2$ (80 mL) and chloroform (160 mL) was cooled and maintained at 0 °C while Br$_2$ (1.15 mL, δ = 3.12 g mL^{-1}, 3.60 g, 22.5 mmol, 1.15 equiv) dissolved in chloroform (80 mL) was added dropwise over 40 min. The reaction mixture was stirred for 3 h at room temperature and then Na$_2$S$_2$O$_4$ (aq. sat., 100 mL) was added to remaining Br$_2$. The organic phase is collected, washed with DI water (3 × 100 mL) and dried over MgSO$_4$ for 2 d. After filtration the solvents were removed at the rotary evaporator and a dark oily residue was obtained. The residue was dissolved in 1:2 chloroform/CH$_2$Cl$_2$ and filtered through 2 cm Al$_2$O$_3$ with follow up extraction with acetone. The dark-red solution was concentrated to 1/3 volume, three equivalents of petrol ether (60/80) was added and the mixture was stored at – 25 °C for crystallization overnight. The product was obtained as brown-red shimmering crystalline solid.

Yield: 2.31 g (8.98 mmol, 23 %).

^{1}H NMR (CDCl$_3$, 25 °C, 400.3 MHz, ppm): δ = 5.06 (s, 5H, η^5-C$_5$H$_5$). ^{13}C{^{1}H} NMR (100.6 MHz, ppm): δ = 212.0 (CO), 86.4 (η^5-Cp). The NMR spectroscopic data are in accordance with the literature.[129]

3.6.4.3 Synthesis of dicarbonyl(η^5-cyclopentadienyl)iron(II) chloride (FpCl)[131-132]

I-36
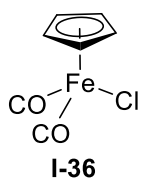
A three-necked round bottomed flask was charged with Fp$_2$ (7.50 g, 21.2 mmol, 1 equiv) dissolved in chloroform (100 mL) and methanol (60 mL). HCl$_{(aq)}$ (2 M, 60 mL, 120 mmol, 5.7 equiv) was added and the brown-red mixture was stirred for 5 min at room temperature. Then O$_2$ is bubbled through the mixture for 1.25 h until the color changed to intensive red. The organic phase was collected and the aqueous phase was extracted with chloroform (5 × 50 mL). The combined organic phases were dried over MgSO$_4$ overnight and then the solvents were removed at the rotary evaporator. The tar-like dark residue was extracted with benzene (5 × 30 mL) and the extracts were filtered through a 2 cm silica plug (60 nm). After concentrating the red-brown mixture to 1/3 volume, petrol ether (150 mL) was added and the mixture was stored for crystallization at –25 °C. The product is obtained as red powder that was dried *in vacuo* and characterized by ^{1}H/^{13}C NMR spectroscopy.

Yield: 3.74 g (17.6 mmol, 42 %).

^{1}H NMR (CDCl$_3$, 25 °C, 400.3 MHz, ppm): δ = 5.05 (s, 5H, η^5-C$_5$H$_5$). ^{13}C{^{1}H} NMR (100.6 MHz, ppm): δ = 211.7 (CO), 84.9 (η^5-Cp). The NMR spectroscopic data are in accordance with the literature.[131-132]

3.6.4.4 Syntesis of (η^5-cyclopentadienyl) bis-(4-ethyl-2,6,7-trioxa-1-phosphabicyclo[2.2.2]-octane) iron(II) iodide[115]
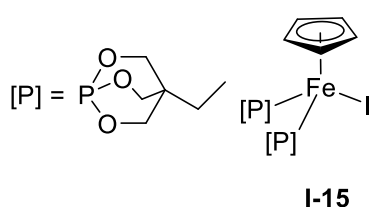
A Schlenk flask was charged with FpI (531 mg, 1.75 mmol, 1.0 equiv), 4-ethyl-2,6,7-trioxa-1-phosphabicyclo[2.2.2]-octane (740 mg, 4.56 mmol, 2.6 equiv) and Fp$_2$ (59 mg, 0.17 mmol, 0.1 equiv) dissolved in toluene (60 mL). The reaction mixture was heated to reflux (130 °C) for 48 h and a color change from red-brown to yellow was observed. The formed precipitate was identified as product; collected by filtration, dried *in vacuo* and characterized by NMR spectroscopy.

Yield: 1.01 g (1.77 mmol, 79 %).[2]

^{1}H NMR (C$_6$D$_6$, 25 °C, 400.3 MHz, ppm): δ = 4.47 (s, 5H, η^5-C$_5$H$_5$), 4.32 (s, 12H, 6 × OCH$_2$C), 1.30 (q, $^3J_{H,H}$ = 7.58 Hz, 4H, 2 × CH$_2$CH$_3$), 0.86 (t, $^3J_{H,H}$ = 7.58 Hz, 3H, 2 × CH$_2$CH$_3$). ^{31}P{^{1}H} NMR (162.0 MHz, ppm): δ = 168.1.

3.6.4.5 Synthesis of carbonyl(η^5-cyclopentadienyl) (triphenylphosphite)iron(II) iodide[115]
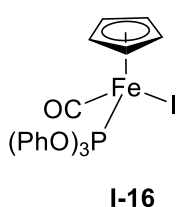
P(OPh)$_3$ (0.38 mL, 449 mg ,1.84 mmol, 1.4 equiv) was added dropwise to a solution of FpI (400 mg, 1.32 mmol, 1.0 equiv) and Fp$_2$ (38 mg, 0.12 mmol, 0.09 equiv) as catalyst in toluene (25 mL). The reaction mixture was refluxed for 1 h and then stirred overnight at room temperature. Precipitate was removed by filtration; the resulting solution was concentrated under reduced pressure and was stored at −19 °C for precipitating. A dark green product was collected by filtration, washed with pentane (3 × 10 mL), dried *in vacuo*.

Yield: 558 mg (0.95 mmol, 72 %).

^{1}H NMR (CDCl$_3$, 25 °C, 400.3 MHz, ppm): δ = 7.48–7.33 (m, 15H, 3 × Ph), 4.19 (s, 5H, η^5-C$_5$H$_5$). ^{31}P{^{1}H} NMR (CDCl$_3$, 25 °C, 162.0 MHz, ppm): δ = 173.0.

HRMS-(ESIpos) (m/z): [M–I]$^+$ calc. for C$_{24}$H$_{20}$FeIO$_4$P: 459.0449, found: 459.0434.

---

[2] 20.7 mol% side product [CpFe(CO)(P(OCH)$_2$)CEt)$_2$]I was observed.

3.6.4.6 Synthesis of (η⁵-cyclopentadienyl)(κ₂-1,2-bis(diphenoxyphosphino)ethylene) iron(II) iodide (Fp^{dpope}I)[116]
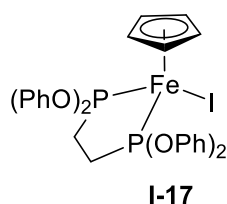
A Schlenk-flask was charged with FpI (107 mg, 352 μmol, 1.0 equiv), 1,2-bis(diphenoxyphosphino)ethylene (163 mg, 353 μmol, 1.0 equiv) and Fp₂ (13 mg, 35 μmol, 0.1 equiv) in the GB. Toluene (25 mL) was added and the solution is refluxed (130 °C) for 48 h and then let cool to room temperature for 36 h. Insoluble precipitate was filtered off and washed with toluene (2 × 10 mL) until colorless washings were observed. The combined washings were combined, volatiles were removed *in vacuo* and the product was obtained as dark brown powder.

Yield: 67 mg (94 μmol, 27 %).

^{1}H NMR (CDCl₃, 25 °C, 400.3 MHz, ppm): δ = 7.54–7.63 (m, 4H, 4 × *p*-Ph), 7.32–7.43 (m, 8H, 4 × *o*-Ph), 7.13–7.32 (m, 8H, 4 × *m*-Ph), 3.93 (s, 5H, η⁵-C₅*H*₅), 2.37–2.67 (m, 4H, PC*H*₂C*H*₂P). ^{13}C{^{1}H}(APT) NMR (100.6 MHz, ppm): δ = 154.0 (+, m, *i*-Ph), 129.7 (−, d, $^2J_{C,P}$ = 61.6Hz, *o*-Ph), 124.5 (−, d, $^2J_{C,P}$ = 69.7Hz, *p*-Ph). 121.8 (−, d, $^2J_{C,P}$ = 227.4Hz, *m*-Ph), 78.3 (−, s, η⁵-C₅*H*₅), 29.5 (+, m, PC*H*₂C*H*₂P), ^{31}P{^{1}H} NMR (162.0 MHz, ppm): δ = 247.8 (*P*CH₂CH₂*P*).

3.6.4.7 Synthesis of carbonyl(η⁵-cyclopentadienyl) (triphenylphosphine)iron(II) iodide[115]
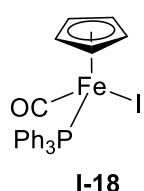
PPh₃ (483 mg, 1.84 mmol, 1.4 equiv) was added to a solution of FpI (400 mg, 1.32 mmol, 1.0 equiv) and Fp₂ (38 mg, 0.12 mmol, 0.09 equiv) as catalyst in toluene (25 mL) and the reaction mixture was refluxed overnight. Precipitate was removed by filtration and the resulting solution was concentrated under reduced pressure. Excess of pentane was added and the suspension was stored at −19 °C for precipitation. A green product was collected by filtration and dried *in vacuo*.

Yield: 432 mg (0.80 mmol, 61 %).

^{1}H NMR (CDCl₃, 25 °C, 400.3 MHz, ppm): δ = 7.64–7.34 (m, 15H, 3 × Ph), 4.49 (s, 5H, η⁵-C₅*H*₅). ^{31}P{^{1}H} NMR (162.0 MHz, ppm): δ = 67.2. The NMR spectroscopic data are in accordance with the literature.[115]

HRMS-(ESIpos) (m/z): [M+Na]$^+$ calc. for C₂₄H₂₀FeIO₄PNa: 560.9544, found: 561.0449.

3.6.4.8 Synthesis of (η⁵-cyclopentadienyl) (ethyl-1,2-diylbis(diphenylphosphane))iron(II) iodide[116]
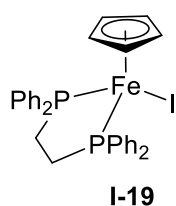
dppe (525 mg, 1.32 mmol, 1.0 equiv) in toluene (5 mL) was added dropwise to a solution of FpI (400 mg, 1.32 mmol, 1.0 equiv) in toluene (15 mL) under reflux at 140 °C. After completion the reaction mixture was kept under reflux for 16 h and then let cool to room temperature. Precipitate was removed by filtration, solvent was removed *in vacuo* and the residue was washed with hexanes (3 × 10 mL). A green product was collected by filtration and dried *in vacuo*.

Yield: 489 mg (0.76 mmol, 58 %).

^{1}H NMR (CDCl$_3$, 25 °C, 400.3 MHz, ppm): δ = 7.49–7.08 (m, 20H, 4 × Ph), 4.26 (s, 5H, η^5-C$_5$H$_5$), 2.84–2.42 (m, 4H, . ^{31}P{^{1}H} NMR (162.0 MHz, ppm): δ = 65.9.

3.6.4.9 Synthesis of bis dicarbonyl(η⁵-1,2,3,4,5-pentamethylcyclopentadienyl)iron(II) (Fp*₂)[120-121]
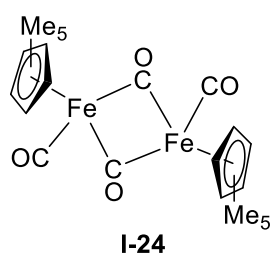
1,2,3,4,5-Pentamethylcyclopentadiene (1.40 g, 10.4 mmol, 1.0 equiv) was transferred to a two-necked round bottomed flask and diluted with xylene (40 mL). Iron pentacarbonyl (4.2 mL, 31.2 mmol, 3.0 equiv) was added over a syringe and the reaction mixture refluxed overnight. The solid was filtered off, washed with toluene (10 mL) and treated with CH$_2$Cl$_2$ until the solution passing the filtered solid became colorless. The solvent was removed under reduced pressure to give the product as dark-purple crystals which was characterized by ^{1}H/^{13}C NMR spectroscopy.

Yield: 1.39 g (2.8 mmol, 55 %).

^{1}H NMR (CDCl$_3$, 25 °C, 400.3 MHz, ppm): δ = 1.69 (s, 30H, 2 × η^5-C$_5$(CH$_3$)$_5$). ^{13}C{^{1}H} NMR (100.6 MHz, ppm): δ = 97.8 (η^5-C$_5$(CH$_3$)$_5$), 8.6 (η^5-C$_5$(CH$_3$)$_5$). The NMR spectroscopic data are in accordance with the literature.[120-121]

3.6.4.10 Synthesis of dicarbonyl(η⁵-1,2,3,4,5-pentamethylcyclopentadienyl)iron(II) iodide (Fp*I)[120-121]
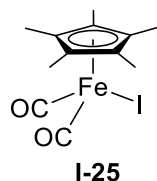
Fp*₂ (661 mg, 1.34 mmol, 1.0 equiv) and I$_2$ (1.4 g, 5.5 mmol, 4.1 equiv) were transferred to a two-necked round bottomed flask set under argon. Dry CH$_2$Cl$_2$ (15 mL) was added *via* a cannula, the reaction mixture was refluxed for 1 h and then stirred at room temperature overnight. The mixture was then filtered and the organic phase was washed three times with saturated Na$_2$S$_2$O$_5$ (20 mL) solution. The

solution was dried over Na_2SO_4, filtered and the solvent removed under reduced pressure to give a dark purple-red, crystalline solid.

Yield: 988 mg (1.32 mmol, 99 %).

^{1}H NMR ($CDCl_3$, 25 °C, 400.3 MHz, ppm): δ = 2.00 (s, 15H, η^5-$C_5(CH_3)_5$). The NMR spectroscopic data are in accordance with the literature.[120-121]

3.6.4.12 Synthesis of dicarbonyl(η5-cyclopentadienyl)iron(II) 2-phenyl ethylene[128]
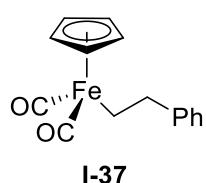
Fp_2 (779 mg, 2.2 mmol, 1 equiv) and sodium sand (235 mg, 10.2 mmol, 4.7 equiv) was mixed in a Schlenk flask in the glovebox and was suspended in THF (70 mL). The reaction mixture was stirred under heating to reflux at 90 °C for 16 h. Then the mixture was cooled to –78 °C and filtered into a separate flask containing 2-phenyl ethylchloride (0.6 mL, 0.64 g, 4.6 mmol, 2.1 equiv) dissolved in THF (5 mL) at –78 °C. The resulting mixture was stirred under cooling at –78°C for 2 h and then the reaction was warmed to room temperature over 16 h. Volatiles were removed *in vacuo* and the grey-green residue was extracted with degassed benzene (3 × 20 mL). Benzene was then removed *in vacuo* and dark-brown product was obtained which solidified after freeze drying.

I-37

Yield: 696 mg (2.45 mmol, 67 %).

^{1}H NMR (C_6D_6, 25 °C, 400.3 MHz, ppm): δ = 7.25–7.12 (m, 5H, Ph), 4.03 (s, 5H, η^5-C_5H_5), 2.76 (t, 2H, Fe-CH_2-CH_2-Ph), 1.69 (t, 2H, Fe-CH_2-CH_2-Ph).

3.6.5 Synthesis of cationic iron olefin complexes

3.6.5.1 Synthesis of dicarbonyl(η⁵-cyclopentadienyl)iron(II) (η²-ethylene) tetrafluoroborate[109]
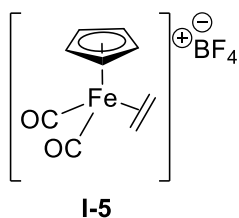
A Schlenk flask was charged with FpI (503 mg, 1.66 mmol, 1.0 equiv), $AgBF_4$ (411 mg, 2.12 mmol, 1.3 equiv), was wrapped with aluminium foil and then CH_2Cl_2 (25 mL) was added. The solution was stirred for 2 h at room temperature. The precipitate was filtered off, extracted with CH_2Cl_2 (3 × 10 mL) and the combined red solutions were collected in a 100 mL flask. The Ar-atmosphere was substituted by an ethylene atmosphere and the mixture was stirred under a dynamic ethylene flow (ca. 5 mbar over ambient pressure) for 2 h. Then the ethylene atmosphere was set static and the mixture was stirred for another 16 h. The resulting orange-brown mixture was concentrated to 10 mL under reduced pressure, Et_2O

I-5

(90 mL) was added and it was stirred for 0.5 h. Orange precipitate was formed, collected by filtration, washed with Et$_2$O (2 × 10 mL) and dried *in vacuo*. The product was stored at –35 °C in the glove box.

Yield: 287 mg (0.98 mmol, 59 %).

^{1}H NMR (CD$_2$Cl$_2$, 25 °C, 400.3 MHz, ppm): δ = 5.62 (br s, 2H, η^2-C$_2$*H*$_4$), 5.31 (s, 5H, η^5-C$_5$*H*$_5$), 3.83 (br s, 2H, η^2-C$_2$*H*$_4$. ^{13}C{^{1}H} NMR (CD$_2$Cl$_2$, 25 °C, 151.0 MHz, ppm): δ = 86.1. The NMR spectroscopic data are in accordance with the literature.[109]

3.6.5.2 Synthesis of dicarbonyl(η^5-cyclopentadienyl)iron(II) (η^2-styrene) tetrafluoroborate[109]

I-6
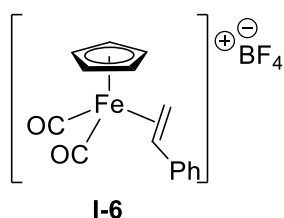
FpI (413 mg, 1.36 mmol, 1 equiv) and AgBF$_4$ (313 mg, 1.61 mmol, 1.2 equiv) were weighed in the glovebox into Schlenk-flask and covered with aluminium foil. CH$_2$Cl$_2$ (25 mL) was added, the red mixture was stirred for 1 h at room temperature and then precipitates were filtered of *via* cannula. Styrene (0.48 mL, 436 mg, 4.19 mmol, 3.0 equiv) was added dropwise under vigorous stirring and a color change to orange was observed. The solution was stirred at room temperature for 3 h and then concentrated to 10 mL total volume under reduced pressure. Et$_2$O (50 mL) was added and a yellow precipitate started to form. After storage at –19 °C overnight, the yellow product was obtained by filtration ans was washed with Et$_2$O (3 × 10 mL).

Yield: 341 mg (0.93 mmol, 68 %).

^{1}H NMR (CD$_2$Cl$_2$, 25 °C, 400.3 MHz, ppm): δ = 7.75 (br s, 5H, Ph), 6.21–6.30 (m, 1H, η^2-C$_2$*H*$_3$-Ph), 5.56 (s, 5H, η^5-C$_5$*H*$_5$), 4.08–4.18 (m, 2H η^2-C$_2$*H*$_3$Ph). The NMR spectroscopic data are in accordance with the literature.[109]

3.6.5.3 Synthesis of dicarbonyl(η^5-cyclopentadienyl)iron(II) (η^2-1-octene) tetrafluoroborate[109]

I-7
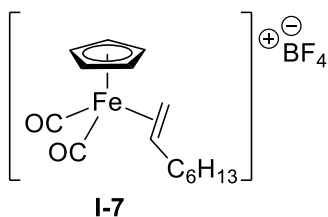
FpI (409 mg, 1.35 mmol, 1 equiv) and AgBF$_4$ (296 mg, 1.52 mmol, 1.2 equiv) were weighed in the glovebox into Schlenk-flask and covered with aluminium foil. CH$_2$Cl$_2$ (25 mL) was added, the red mixture was stirred for 1 h at room temperature and then precipitates were filtered of *via* cannula. 1-Octene (0.65 mL, 464 mg, 4.1 mmol, 3.0 equiv) was added dropwise under vigorous stirring and a color change to orange-red was observed. The solution was stirred at room

temperature for 3 h and then concentrated to 10 mL total volume under reduced pressure. Et$_2$O (50 mL) was added and a yellow precipitate started to form. After storage at –19 °C overnight, the yellow product was obtained by filtration was washed with Et$_2$O (3 × 10 mL).

Yield: 345 mg (0.92 mmol, 68 %).

^{1}H NMR (CD$_2$Cl$_2$, 25 °C, 400.3 MHz, ppm): δ = (s, 5H, η^5-C$_5$H$_5$), 5.34 (m, η^2-5.11 (m, η^2- (br s, η^2- (br s, η^2- (br s, η^2- (br s, η^2-(br s, η^2- (br s, η^2-. The NMR spectroscopic data are in accordance with the literature.[109]

3.6.5.4 Synthesis of (η^5-cyclopentadienyl)(κ$_2$-1,2-Bis(diphenoxyphosphino)ethylene) iron(II) (carbonyl) tetrafluoroborate ([Fp^{dppe}(CO)]BF$_4$)[103]

I-19b
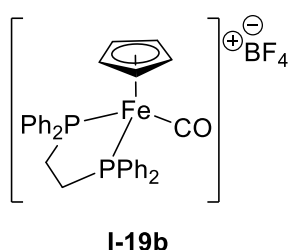
MeCN (6 mL, 115 mmol, 117 equiv) was added to Fp^{dppe}(CO)I (666 mg, 1.03 mmol, 1.0 equiv) dissolved in chloroform (30 mL) while stirring. During the addition a color change from dark brown to golden yellow was observed. Volatiles were removed and the residue was dissolved in MeCN (20 mL). Potassium tetrafluoroborate (259 mg, 2.06 mmol, 2.0 equiv) was added and the mixture was stirred at room temperature for 16 h. Potassium salts were filtered off and volatiles were removed to obtain the product as semi-crystalline orange solid.

Yield: 498 mg (769 µmol, 75 %)

^{1}H NMR (CD$_2$Cl$_2$, 25 °C, 600.3 MHz, ppm): δ = 7.51–7.70 (m, 16H, 4 × p-Ph, 8×o-Ph), 7.25–7.31 (m, 4H, 4 × m-Ph), 4.87 (s, 5H, η^5-C$_5$H$_5$), 2.65–2.95 (m, 4H, PCH$_2$CH$_2$P). ^{13}C{^{1}H}(APT) NMR (151.0 MHz, ppm): δ = 214.0 (+, t, CO), 135.2 (+, dt, i-Ph), 132.2 (−, dt, o-Ph), 132.2 (−, d, p-Ph), 130.0 (−, d, m-Ph), 85.1 (−, s, η^5-C$_5$H$_5$), 29.8 (+, dt, PCH$_2$CH$_2$P). ^{19}F{^{1}H} NMR (564.7 MHz, ppm): δ = −152.9 (s, BF$_4$). ^{31}P{^{1}H} NMR (243.0 MHz, ppm): δ = 92.0 (PCH$_2$CH$_2$P).

3.6.5.5 Synthesis of carbonyl(η^5-cyclopentadienyl)(triphenylphosphite) iron(II) (η^2-ethylene) tetrafluoroborate ([Fp^{tpop}(C$_2$H$_4$)]BF$_4$)[109]
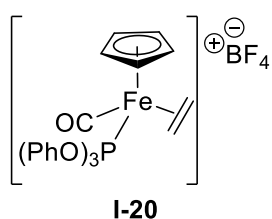
I-20

A Schlenk flask was charged with Fp^{tpop}I (936 mg, 1.60 mmol, 1.0 equiv), AgBF$_4$ (404 mg, 2.08 mmol, 1.3 equiv), was wrapped with aluminium foil and then CH$_2$Cl$_2$ (25 mL) was added. The solution was stirred overnight at rt. Precipitate was filtered off, extracted with CH$_2$Cl$_2$ (3 × 10 mL) and the combined green solutions were collected in a 100 mL flask. Ethylene was bubbled through the reaction mixture for 3 h

using a syringe connected to the gas cylinder. A color change to dark yellow was observed within 15 min. The resulting dark yellow solution was concentrated to 10 mL under reduced pressure, Et$_2$O (90 mL) was added and it was stirred for 0.5 h. A yellow precipitate was formed, collected by filtration, washed with Et$_2$O (2 × 10 mL) and dried *in vacuo*. The product was stored at –35 °C in the glove box.

The product could not be completely characterized by ^{1}H NMR spectroscopy since the ethylene signal was not observed but was confirmed by follow up addition reactions.

Yield: 570 mg (0.99 mmol, 62 %).

3.6.5.6 Synthesis of (η^5-cyclopentadienyl)(κ$_2$-1,2-bis(diphenoxyphosphino)ethylene) iron(II) (η^2-ethylene) tetrafluoroborate ([Fp^{TPP}(C$_2$H$_4$)]BF$_4$)[109]

I-21
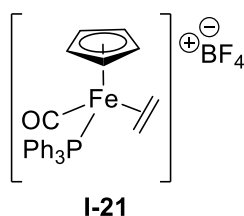
Carbonyl(η^5-cyclopenthadienyl)iodo(triphenylphosphine)iron (II) (0.511 g; 0.95 mmol; 1 equiv) and AgBF$_4$ (0.348 g, 1.79 mmol, 1.9 equiv) were dissolved in CH$_2$Cl$_2$ (15 mL) and stirred for 1 h. The solution, which was green in the start of the reaction, turned light-orange after the stirring. (While stirring the solution, the flask was covered with aluminium foil as AgBF$_4$ is light sensitive.) Then the solution was filtered and ethylene was added in excess while stirring. The addition took place overnight. Then the solution (brownish- orange/yellow) was concentrated under reduced pressure until 2/3 of the volume were removed and then hexane (15 mL) was added to precipitate the product (the solution turned transparent and a brown-orange precipitate appeared). The solution was put in an ice bath and then the product (light brown solid) was filtered and dried under reduced pressure.

Yield: 317 mg (46 μmol, 63 %).

^{1}H NMR (Acetone-d_6, 25 °C, 400.3 MHz, ppm): δ = 7.35–7.80 (m, 15H, Ph), 4.48 (m, 2H η^2-C$_2$H$_4$), 3.74 (m, 5H η^5-C$_5$H$_5$), 1.16 (m, 2H η^2-C$_2$H$_4$). ^{31}P{^{1}H} NMR (162.0 MHz, ppm): δ = 61.5 (PPh$_3$).

3.6.5.7 Synthesis of (η^5-cyclopentadienyl)(κ$_2$-1,2-bis(diphenoxyphosphino)ethylene) iron(II) (η^2-ethylene) tetrafluoroborate ([Fp^{dpope}(C$_2$H$_4$)]BF$_4$)[109]

I-22
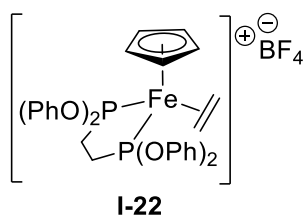
A Schlenk tube was charged with Fp^{dpope}I (64.0 mg, 0.09 mmol, 1.0 equiv), AgBF$_4$ (23.7 mg, 0.12 mmol, 1.4 equiv), was wrapped with aluminium foil and then CH$_2$Cl$_2$ (10 mL) was added. The solution was stirred overnight at rt. Precipitate was filtered off, extracted with CH$_2$Cl$_2$ (3 × 5 mL) and the combined orange

solutions were collected in a 50 mL flask. Ethylene was bubbled through the reaction mixture for 3 h *via* a syringe connected to the gas cylinder. A color change to grey is observed within 15 min. The resulting solution was concentrated to 10 mL under reduced pressure, Et$_2$O (40 mL) was added and it was stirred for 0.5 h. A grey precipitate was formed, collected by filtration, washed with Et$_2$O (2 × 5 mL) and dried *in vacuo*. The product was stored at –35 °C in the glove box.

Yield: 32 mg (46 μmol, 72 %) of a grey powder.

^{1}H NMR (Acetone-d_6, 25 °C, 400.3 MHz, ppm): δ = 7.15–7.75 (m, 20H, Ph), 4.80 (br s, 2H η^2-C$_2$H$_4$), 3.74 (s, 5H, η^5-C$_5$H$_5$), 2.50-2.77 (m, 4H, PC*H$_2$C*H$_2$P), 1.16 (br s, 2H η^2-C$_2$H$_4$). ^{31}P{^{1}H} NMR (162.0 MHz, ppm): δ = 239.6 (*P*CH$_2$CH$_2$*P*).

3.6.5.8 Synthesis of dicarbonyl(η^5-1,2,3,4,5-pentamethylcyclopentadienyl)iron(II) ethylene tetrafluoroborate[109]

I-26
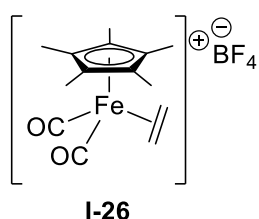
Fp*I (500 mg, 1.37 mmol, 1 equiv) and AgBF$_4$ (338 mg, 1.73 mmol, 1.3 equiv) were weighed in the glovebox into a Schlenk-flask and the flask was covered with aluminium foil. CH$_2$Cl$_2$ (15 mL) was added, the mixture was stirred for 1 h at room temperature and then cannula filtrated. Ethylene gas was then applied overnight. The reaction mixture was concentrated under reduced pressure, the product precipitated from Et$_2$O (15 mL) and was filtered to give a grey solid.

Yield: 289 mg (0.80 mmol, 58 %).

^{1}H NMR (CDCl$_3$, 25 °C, 400.3 MHz, ppm): δ = 3.20 (s, 4H, η^2-C$_2$H$_4$), 1.93 (s, 5H, η^5-C$_5$(CH$_3$)$_5$). ^{13}C{^{1}H} NMR (100.6 MHz, ppm): δ = 212.0 (CO), 59.6 (η^5-*C$_5$*(CH$_3$)$_5$), 10.4(η^2-C$_2$H$_4$), 9.8 (η^5-C$_5$(*C*H$_3$)$_5$).

3.6.6 General procedure for catalysis

3.6.6.1 Hydrophosphination of styrene

In the glovebox a 2 mL vial was charged with $[CpFe(CO)P(OPh)_3(\eta^2\text{-}C_2H_4)]BF_4$ (**I-20**) (5 mg, 8.7 µmol, 1.0 equiv) dissolved in 50 µL of a chosen solvent; and then styrene (16 µL, 174 µmol, 20.0 equiv) and $HPPh_2$ (30 µL, 174 µmol, 20.0 equiv) was added via syringe subsequently. The vial was capped and placed in a Al-heating block on a mangetic stirring plate. After the desired amount of reaction time, the vial was let cool to ambient temperature. The reaction was evaluated by NMR spectroscopy while using an aliquot of the reaction mixture.

4 Chapter II – Borrowing Hydrogen Catalysis

4.1 Introduction

4.1.1 Borrowing Hydrogen Methodology

Redox-reactions are a basic tool in chemistry with the possible division in oxidation and reduction. Those reactions usually resemble electron transfers along the normal potential of reagents. Some processes like the Wacker-Oxidation use combined reduction-oxidation cycles to ensure that the catalyst returns to its active oxidation state (Scheme 44).
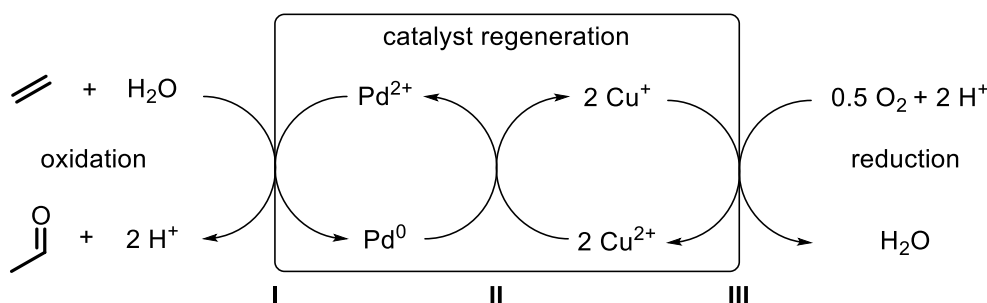
Scheme 44. Wacker-Hoechst process for the oxidation of ethylene. Combination of (**I**) stoichiometric oxidation of ethylene to acetaldehyde (**I**), re-oxidation of palladium with a copper adjuvant (**II**) and re-oxidation of copper under air (**III**).[140]

Most 4d- and 5d-metals are known to undergo two-step oxidation-reduction steps in reversible fashion, which leads to the possibility of connecting different catalytic cycles when comparable conditions are employed.

A prominent example is hydroaminomethylation, a combination of hydroformylation and reductive amination reaction of olefins (Scheme 45).[141-143] In the first step (**I**) a common hydroformylation reactions transforms an olefin into an aldehyde. A consecutive condensation reaction with an amine (**II**) provides an aldimine which is reduced to an amine with the present hydrogen (**III**). The overall reaction consumes two equivalents of hydrogen which shows the dependency on external hydrogen. A complementary reaction which releases hydrogen, instead of relying on external hydrogen, is the dehydrogenative coupling of alcohols with amines providing aldimines or amides.[144]
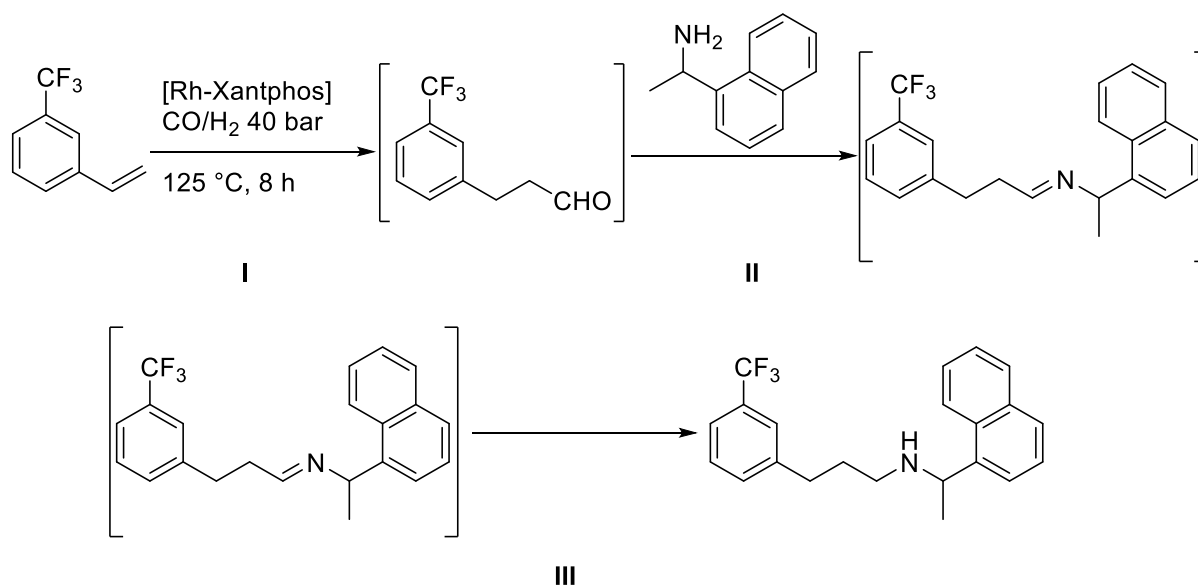
Scheme 45. Amgen's route to Cinacalcet (Mimpara ®, Sensipar ®) employing combined hydroformylation (**I**) and reductive amination (**II** + **III**); the conditions for the reaction cascade are mentioned on the first reaction arrow.[145]

In contrast to both reaction types, the borrowing hydrogen methodology provides an overall reaction that is neutral in terms of hydrogen. As the name states, hydrogen is "borrowed" or transferred in a line of sub-reactions (Scheme 46).
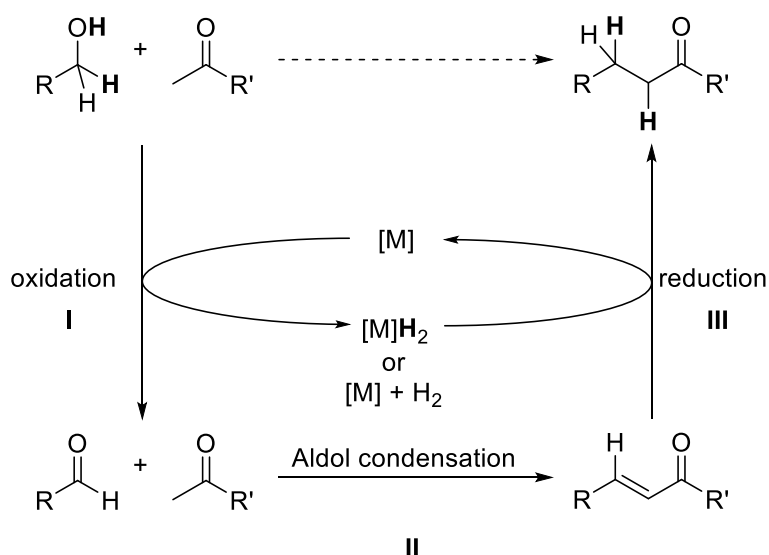
Scheme 46. Schematic depiction of borrowing hydrogen methodology employed in an aldol condensation type reaction.[26]

This methodology is based on the idea that a substrate is oxidized to provide an active reagent for a consecutive reaction (**I**). The second reaction is supposed to occur faster than the equilibrium of oxidation and reduction of the original substrate (**II**). The formed

intermediate is then reduced (**III**) with the abstracted hydrogen that originated from the initial oxidation step (**I**). Depending on the system, hydrogen remains activated on the catalyst or it is liberated as molecular hydrogen, but it is not fully understood yet. In the latter case, molecular hydrogen has to be activated for the conclusion of the borrowing hydrogen cycle.

4.1.2 Metal-Ligand Cooperation

Catalysts for borrowing hydrogen processes are mostly 4d- and 5d-metals, due to their ability of oxidative activation of hydrogen in a two electron process. More abundant 3d-metals prefer one electron transfers, which renders them inactive for borrowing hydrogen in a classic approach.[140]

The classic approach of catalysis in organometallic chemistry is a division of a metal complex into metal and ligand. Ligands are coordinating to one or more metal centers and not only influence the electronic density at the metal center, but more importantly are providing steric hindrance. This hindrance is employed to force substrates into free coordination sites which can be used to influence regio-, stereo- and also enantioselectivity of a reaction.[146] The ligand can be defined as X, L or Z according to its coordination mode which is depending on its electronic characteristic. Multidentate ligands have the possibility of bearing different (X, L or Z) characteristics in one molecule (e.g. η^5-cyclopentadienide (Cp) $\triangleq$ L_2X). During a catalytic cycle the ligand is considered observing or innocent when it remains unchanged at the metal center. In some reactions the ligand can switch in its coordination mode to vacate coordination sites at the metal center (Scheme 47).[147-148]
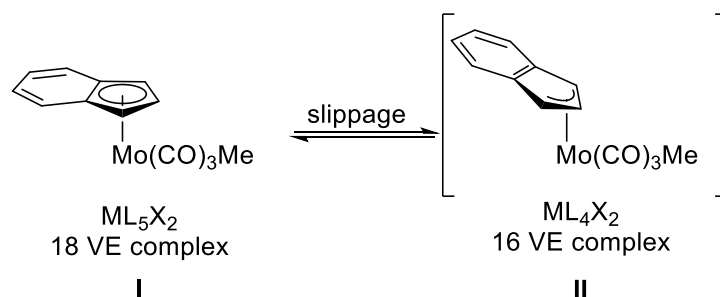
Scheme 47. Example for indenyl ring slippage in a molybdenum complex (**I**). The altered coordination mode of indenyl enables the coordination of other ligands on the metal center (**II**).[147-148]

When the ligand is chemically altered during the reaction and also returning to its original form in the complex, it is considered as part of the catalyst since it is not consumed during the reaction, although a reaction occurred at the ligand. Usual reversible reactions on ligands are protonation/deprotonation and coordination of small molecules. This reaction at

the ligand can be combined with a metal center which is then enabled to undergo a wider range of reactions. It is especially interesting for 3d-metals since their limitation to one electron steps can be extended to formal two electron steps through metal-ligand cooperation. A most prominent example is Knoelker's catalyst that employs a Cp-ligand which is switching between L_2 and L_2X during the reaction (Scheme 48). Knoelker's catalyst is structurally closely related to Shvo's catalyst which is based on the heavier d^8 sibling ruthenium (Figure 25).[149-150]
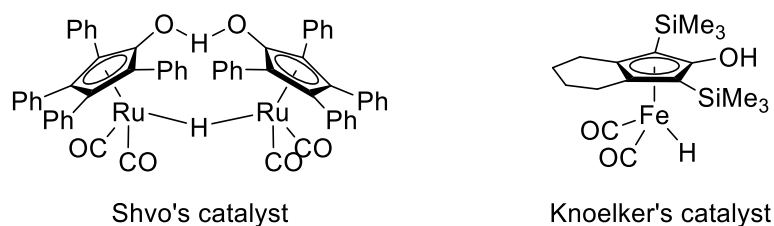
Figure 25. Structurally related d^8-metal Shvo and Knoelker complexes.[150-151]

The metal-ligand cooperation allows the simultaneous abstraction of a proton and a hydride in an overall oxidation reaction.[151-154] Knoelker's catalyst is known to catalyze both reductive aminations with external hydrogen and transfer hydrogenation, which suggests the capability of the activation of molecular hydrogen.
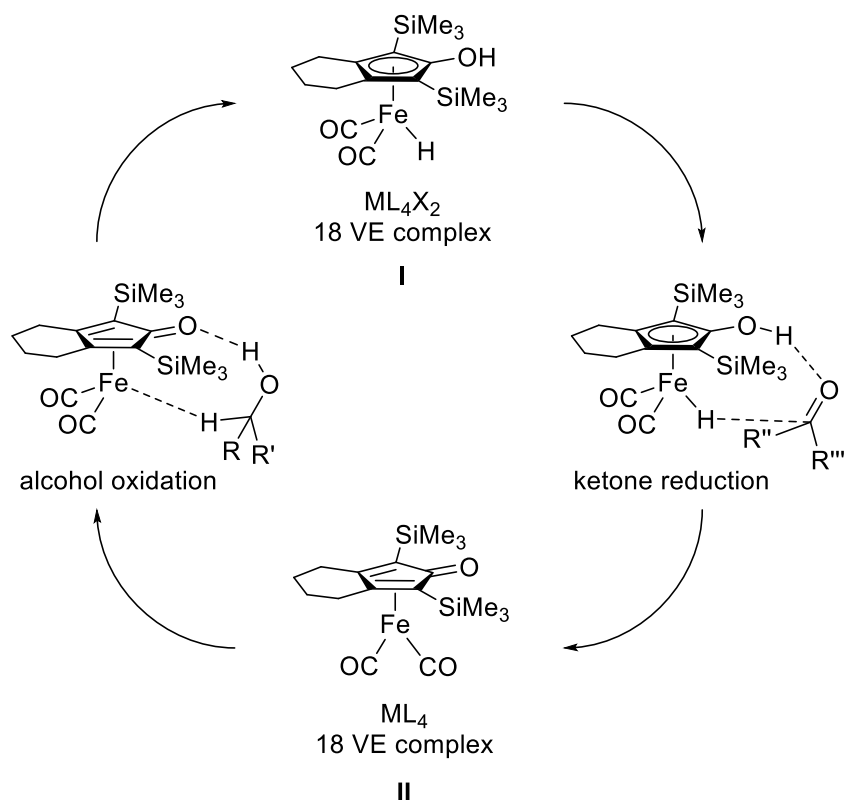
Scheme 48. Simplified depiction of transfer hydrogenation of alcohols and ketones with Knoelker's catalyst. Both coordination states of the Cp ligand as L_2X (**I**) and L_2 (**II**) are shown.[153]

4.1.3 N-Alkylation of Amines with Alcohols (Nucleophilic Substitution of OH)

Nucleophilic substitution is one of the most common reactions and is a principle that organic chemistry heavily relies on. Halogenated alkyl substrates show high activity for substitution reactions, but come with the drawback of high toxicity and mutagenicity for the same reason. Those compounds can be prepared from the corresponding alcohol by treatment with either a strong Brønsted acid or strong Lewis acid which promotes the nucleophilic substitution of a hydroxyl group with a halogen.

In terms of atom-efficiency and number of reaction steps for amination, nucleophilic substitution ranks far behind hydroamination. Hydroxyl groups are non-sufficient leaving groups for amination reactions, but carbonyl compounds are well-known as electrophiles which are desired for nucleophilic addition reactions. So in principle alcohols could be oxidized and then reacted with amines, but resulting aldimines and ketimines need a further reduction step to provide the desired products. This would omit the use of halogens but would further increase the amount of necessary reaction steps. It is noteworthy that

hydroaminomethylation (**I**) can be used to cut down several steps of amine preparation but the reaction relies on noble metals (Scheme 49).[26, 142]

I Hydroaminomethylation

R⌒⌒NHR

II Hydroamination

R⌒NHR

Hydroformylation or Hydratisation

III N-Alkylation

R⌒OH

Halogen Introduction

IV Nucleophilic Substitution

R⌒X
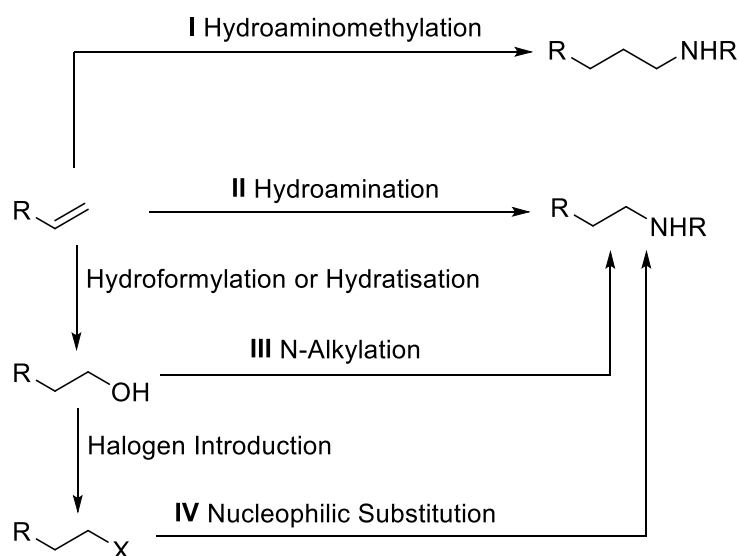
Scheme 49. Simplified comparison of steps for different synthetic strategies.

For the preparation of amines, N-alkylation of amines with alcohols (**III**) can be seen as intermediate solution between direct hydroamination (**II**) and nucleophilic substitution (**IV**) whilst reducing the number of reactions from three steps to two steps. In the process readily accessible alcohols are converted into reactive aldehydes and ketones. The intermediate carbonyl reacts with amines and the formed imine is consecutively reduced to the desired product (Scheme 50).[155]
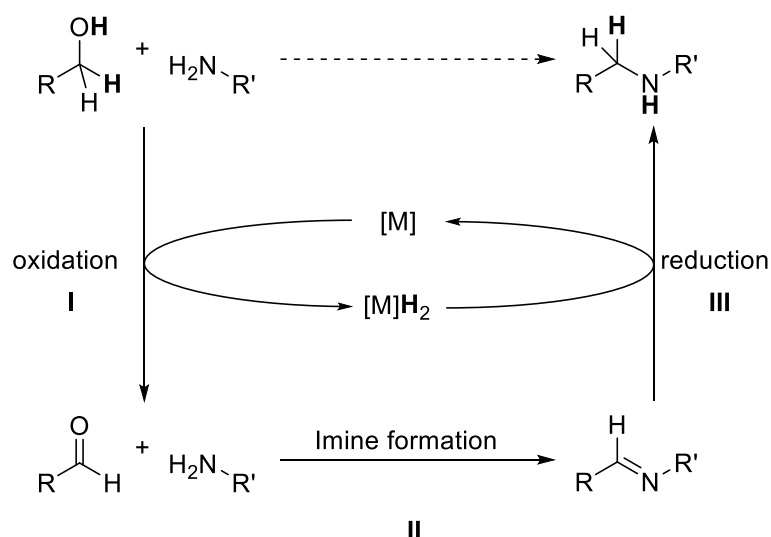
Scheme 50. Simplified depiction of the N-alkylation of amines with primary alcohols using borrowing hydrogen methodology.[156]

The reaction was first reported for noble metals in 1981 with harsh reaction conditions and relatively low catalyst loadings.[27, 157-159] Grigg *et al.* investigated the alkylation of pyrrolidines and reported the catalytic activity of different rhodium and iridium complexes. While complexes of different oxidation states were employed, it was observed that complexes with the oxidation state +I were most suitable catalysts. Ruthenium was also identified as catalytically active but the report focused on rhodium since the preliminary results were pointing in that direction (Table 16).[159]

Table 16. First reported preliminary screening of different homogeneous catalyst for N-methylation of pyrrolidine.[159]

#	catalyst	time [h]	yield[b] [%]
1	$RhH(PPh_3)_4$	4	97
2	$IrCl(PPh_3)_3$	5	87
3	$RhCl(PPh_3)_3$	8	92
4	$IrCl_3 \times 3\ H_2O^{[a]}$	13	80
5	mer-$IrH_3(PPh_3)_3$	24	47
6	$RuH_2(PPh_3)_4$	28	15

General conditions: Pyrrolidine in excess of refluxing methanol. [a] 5 equiv of PPh_3 added; [b] isolated yields.

For rhodium, a broader substrate scope of primary and secondary amines reacting with different primary alcohols was presented. It showed that pyrrolidine is readily alkylated while other secondary substrates are more challenging. Conversion of primary alkyl amines was more facile than of aniline (Scheme 51).[159]
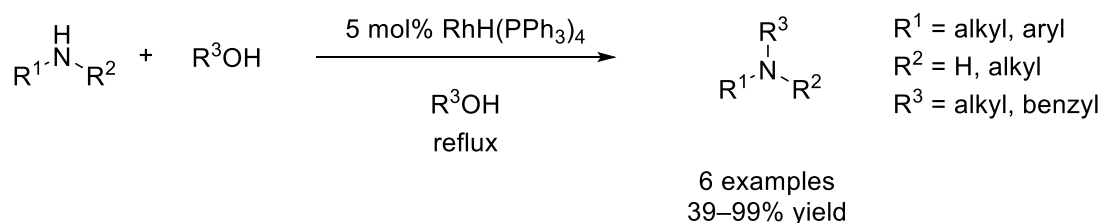
Scheme 51. First reported rhodium catalyzed N-alkylation of different amines.[159]

The groups of Watanabe and Murahashi independently reported N-alkylation with ruthenium (II) complexes.[157-158] Watanabe focused on the preparation of secondary amines with ruthenium chloride and employed this approach in a Doebner-Von Miller type quinolone synthesis. The reaction was observed to provide selective mono-alklyation only for methanol, secondary alcohols and 2,3-unsaturated alcohols (Scheme 52).[160] Watanabe also investigated platinum-based systems for the same catalytic approach. However, his report stated that platinum only provides limited catalytic activity for N-alkylation of anilines.[161]

R = Me   12%
      iPr   25%
      sBu 28%

R = Et   74%
      Pr   88%
      Bu 79%

R = allyl 33%
      crotyl 45%
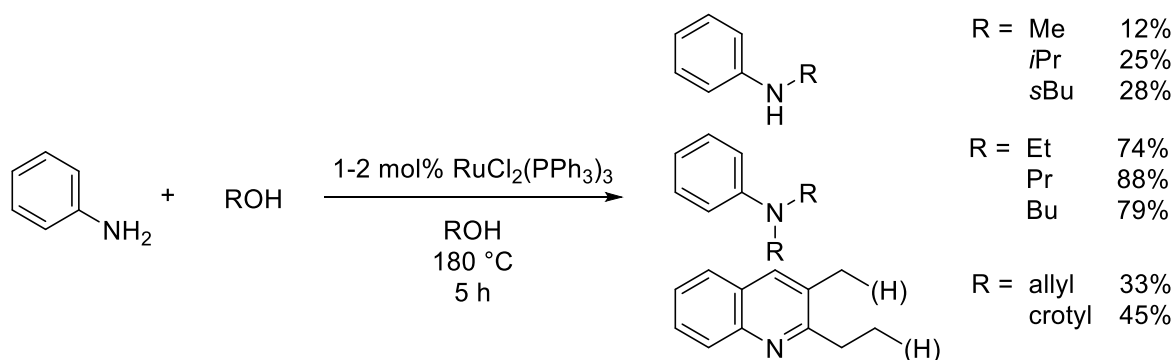
Scheme 52. $RuCl_2(PPh_3)_3$ catalyzed preparation of secondary and tertiary amines, and quinolines by N-alkylation.[157]

Murahashi was mostly focusing on the preparation of tertiary amines with ruthenium hydride complexes and employed his findings in cyclisation reactions (Scheme 53).[158] It is worth noting that the reactions carried out under neat conditions and in stoichiometric ratios.

	NH	N–R
	(A)	(B)	(C)
n = 1	79%	58%	40%
2	89%	80%	83%
3	41%	21%	87%

$R = C_6H_{13}$
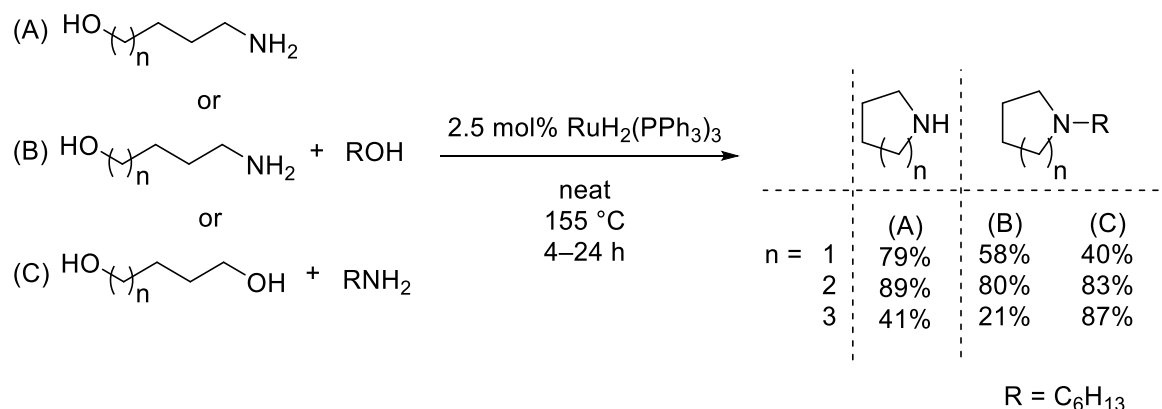
Scheme 53. $RuH_2(PPh_3)_3$ catalyzed preparation of tertiary amines by N-alkylation by cyclization reactions.[158]

Iridium- and ruthenium-based catalytic systems were subject to extensive research in the following years.[26, 162-163] To provide comparability of reported findings, the N-benzylation of aniline was chosen as benchmark reaction. However, no further research in that field was conducted with rhodium and platinum-based systems to the best of our knowledge. The initial finding that iridium (III) salts also catalyzed N-alkylation of amines (Table 16) was further developed. The group of Kempe recently reported an iridium-based catalyst that performs at very low catalyst loadings by employing base additives. This allowed the reaction to proceed under mild conditions and only slight excess of alcohol (Scheme 54).[164]
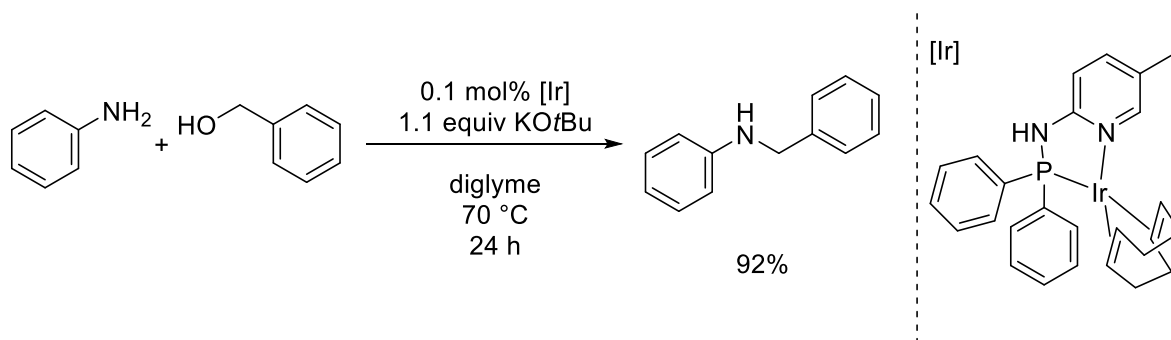
Scheme 54. Iridium catalyzed N-benzylation of different anilines.[164]

For ruthenium, Taddei *et al.* focused on implementing a catalytic system that performs under mild conditions. This was achieved by employing stoichiometric amounts of base and comparatively high catalyst loadings (Scheme 55).[165]
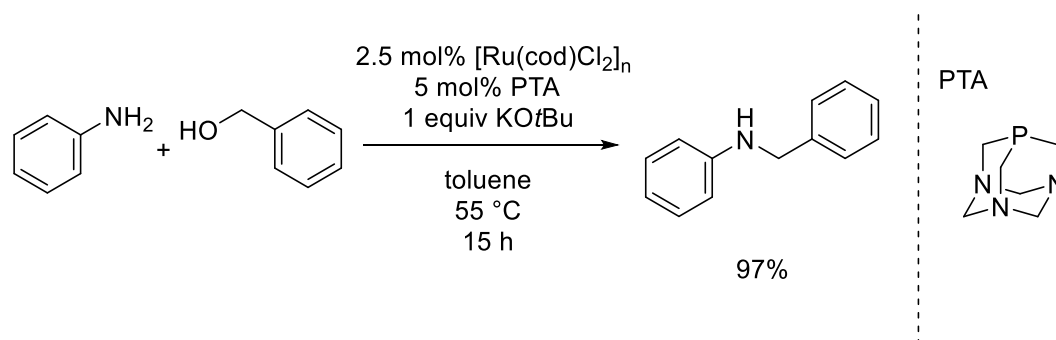
Scheme 55. Ruthenium catalyzed N-benzylation of different anilines under mild conditions.[165]

As a comparison, the group of Bruneau reported a ruthenium system with a carbene ligand which performed at low catalyst loadings. To perform properly, only catalytic amounts of base are needed. However, when a wider scope of substrates was employed stoichiometric amounts of base are necessary (Scheme 56).[166]
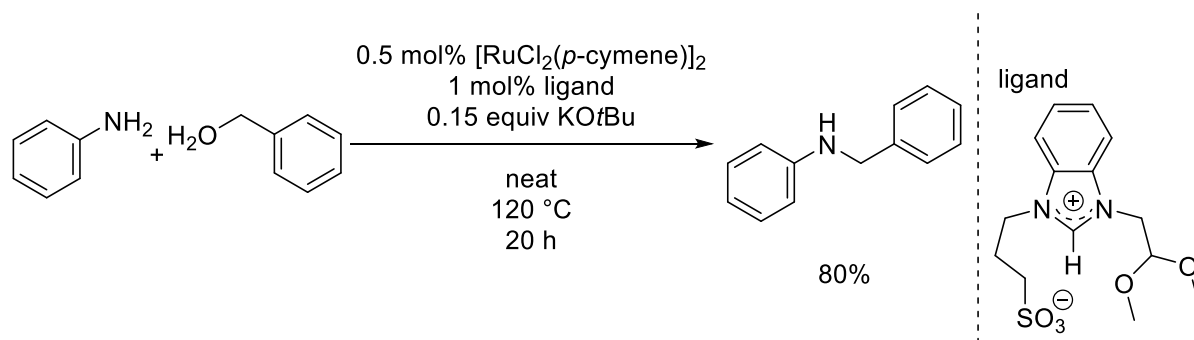
Scheme 56. Ruthenium catalyzed N-benzylation of anilines with low catalyst and base additive loadings under neat conditions.[166]

As discussed, noble metals readily perform reactions with two electron steps like hydrogen activation.[167] Almost 20 years later the iron-based Knoelker's catalyst was introduced as catalyst for hydrogenation and dehydrogenation based on Shvo's catalyst (Figure 25).[149-151] Feringa used the complex for N-alkylation of amines with alcohols in 2014 which created a great interest in the development of base metal catalysts for borrowing hydrogen reactions (Scheme 57).[168]
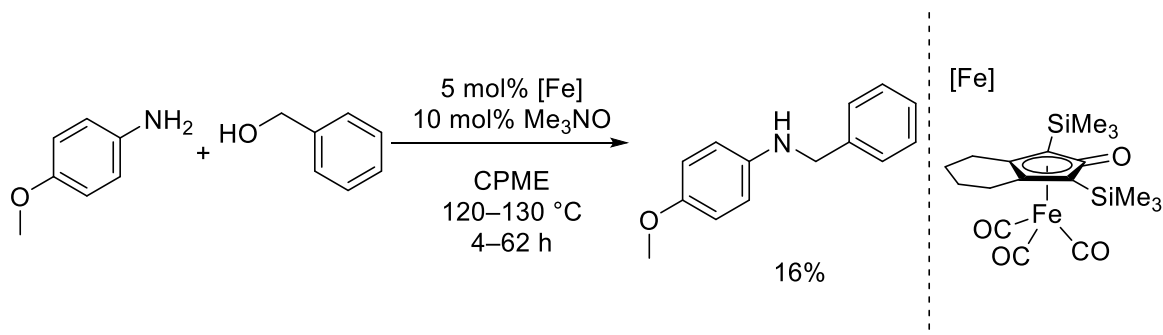
Scheme 57. Iron catalyzed general N-benzylation of anilines with different alcohols.[168]

4.1.4 Recent Developments in Base Metal Catalyzed N-alkylation of Amines

Replacement of Ru with more abundant iron as catalyst was part of a general trend towards more abundant base metals for catalysis.[151, 169-180] Knoelker's catalyst is a prominent example for successful d^8 metal substitution in a piano stool complex (Figure 25). Other approaches focus on ligand systems that are related to the Ru-MACHO catalyst (**I**) and pincer ligands with more rigid phenyl backbones (**II**) (Figure 26).[181-186]
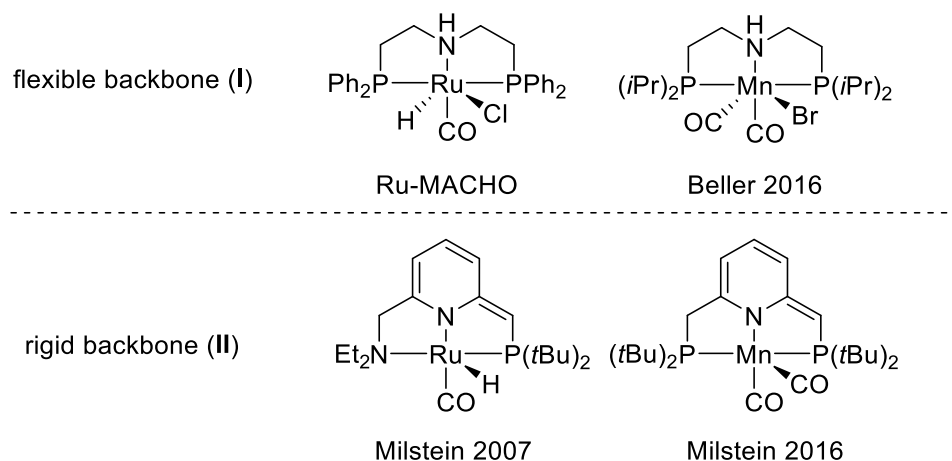
Figure 26. Structural relationship of catalysts with their ruthenium counterparts.[187-192]

Pincer complexes attracted lots of attention since their meridional coordination promotes catalytic activity on metal centers by creating a single site catalyst. In pincer complexes coordination sites are distinguishable as equatorial and apical which also facilitates structural tuning.[140] On the one hand, pincer complexes of iron and cobalt that were known as catalysts for polymerization were investigated more closely in terms of redox mechanisms.[61, 193-203] On the other hand, a different approach was the straight-forward replacement of iridium and ruthenium with cobalt, iron and manganese which provided promising results in comparable reactions.[164, 204-205] Following the results of Feringa *et al.* (Scheme 57), different groups reported base metal pincer catalysts for condensation reactions of alcohols with amines in the following years.[168, 192, 206-209] For comparability, only the intermolecular N-alkylation of aryl amines catalyzed by base metal pincer complexes will be discussed in this section.

A cobalt PNP-pincer catalyst for hydrogenation of C=C, C=N and C=O was introduced by Hanson in 2012 (Scheme 58).[210] Further investigations showed that the cobalt complex is also an active catalyst for acceptorless dehydrogenative coupling (ADC) of alcohols and amines.[211] When the catalyst was combined with molecular sieves as

dehydrating agent, it also performed imine reduction, providing amines as products without any base additive (compare Scheme 50, Scheme 58).[207]
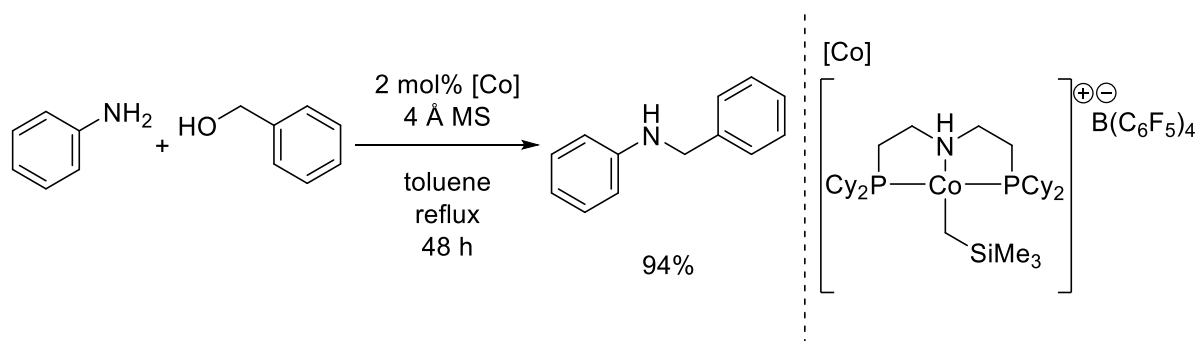
Scheme 58. N-benzylation of aniline catalyzed by a cobalt PNP-pincer complex.[207, 210-211]

The group of Kempe showed that a cobalt PNP-pincer complex with a more rigid backbone is a superior catalyst for C=O hydrogenation compared to its iridium counterpart.[212] Similar to the work of Hanson *et al.* (vide supra), the catalyst was found active for the N-alkylation of amines with alcohols.[207, 210-211] Sodium *tert*-butoxide was employed a base additive, which did not only activate the precatalyst but also allowed for lower temperatures during the reaction (Scheme 59).[213] A study by Kirchner *et al.* showed that for a cobalt pincer catalyzed reaction molecular sieves and strong base additives are interchangeable. However, for a cobalt halide precatalyst a base additive was needed for activation and the reaction temperatures had to be adjusted accordingly.[214]
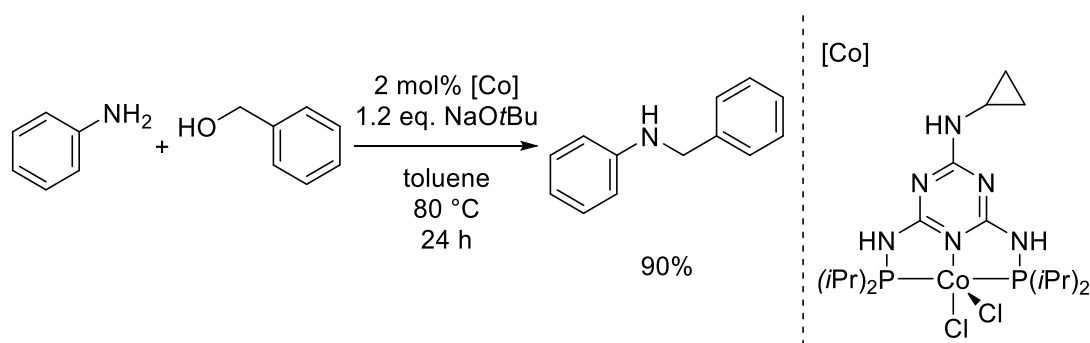
Scheme 59. N-benzylation of aniline catalyzed by a cobalt PNP-pincer complex with base additive.[213]

Kirchner *et al.* also reported on the use of molecular sieves and potassium *tert*-butoxide with iron PNP-pincer complexes as catalysts. Iron-hydride complexes were able to perform N-alkylation in the presence of molecular sieves (compare Scheme 58 and Scheme 60).[206]
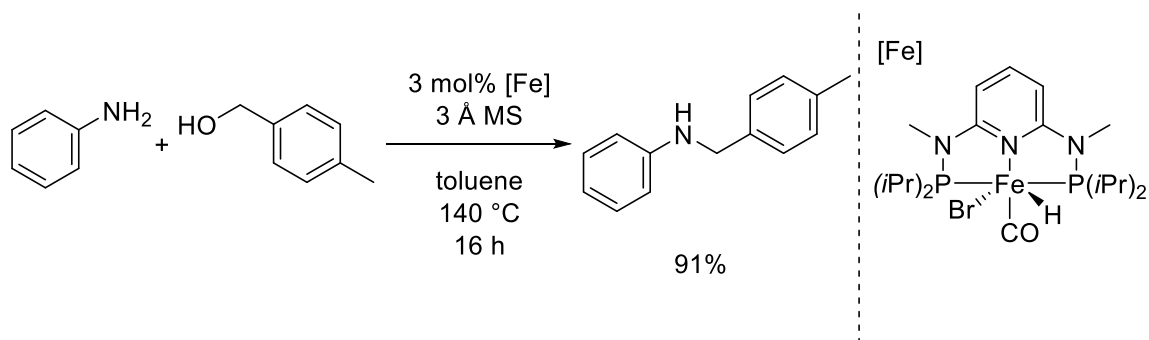
Scheme 60. N-benzylation of aniline catalyzed by an iron PNP-pincer hydride complex.[206]

Kirchner *et al.* also showed, that with potassium *tert*-butoxide as additive, lower catalyst loadings and lower reaction temperatures can be realized (compare Scheme 59 and Scheme 61).[215]
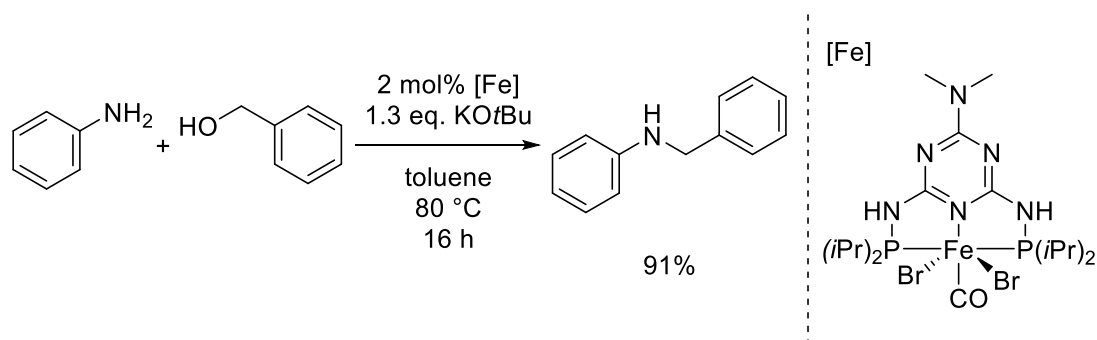
Scheme 61. N-benzylation of aniline catalyzed by an iron PNP-pincer complex with base additive.[215]

For manganese, a multitude of different pincer complexes were introduced since the group of Beller reported the first manganese catalyst in 2016.[216-221] However, manganese complexes were found to perform N-alkylation reactions only with base additives present. All systems share comparable catalyst loadings and reaction times, while the base loading and the reaction temperature seem to be most characteristic for comparison. On one hand, the group of Sortais reported a manganese pincer catalyst that performs N-methylation of anilines with catalytic amounts of base at high temperatures (Scheme 62).[218] However, the N-benzylation of anilines was not discussed. But it is expected that N-methylation with methanol is more challenging according to initial reports of Beller *et al.*.[192, 217]
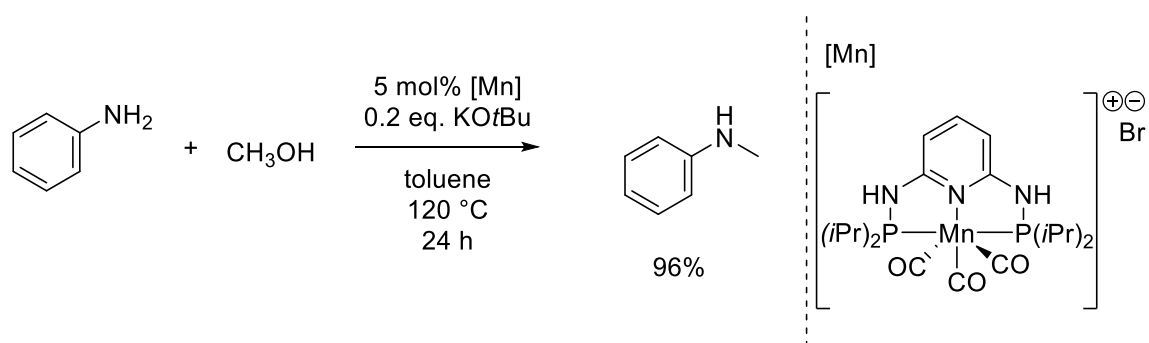
Scheme 62. N-methylation of aniline catalyzed by a manganese PNP-pincer complex with a catalytic amount of base additive.[218]

On the other hand, the group of Ke recently reported a manganese carbene catalyst performing at room temperature with a stoichiometric amount of base (Scheme 63).[221]
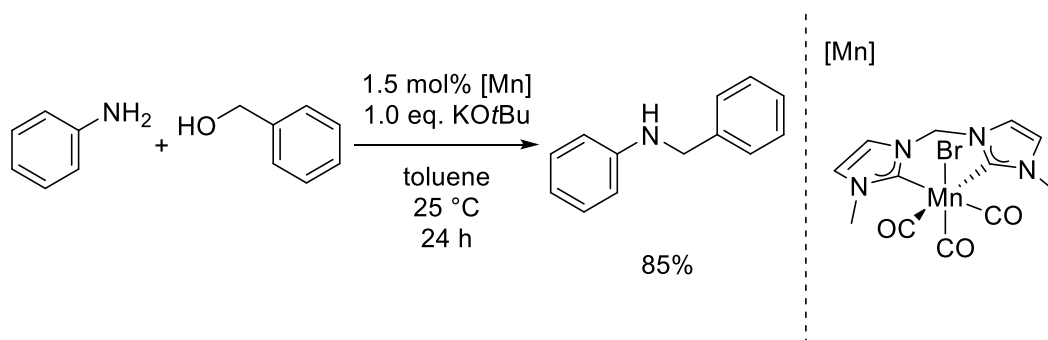
Scheme 63. N-alkylation of aniline by a manganese carbene complex at room temperature.[221]
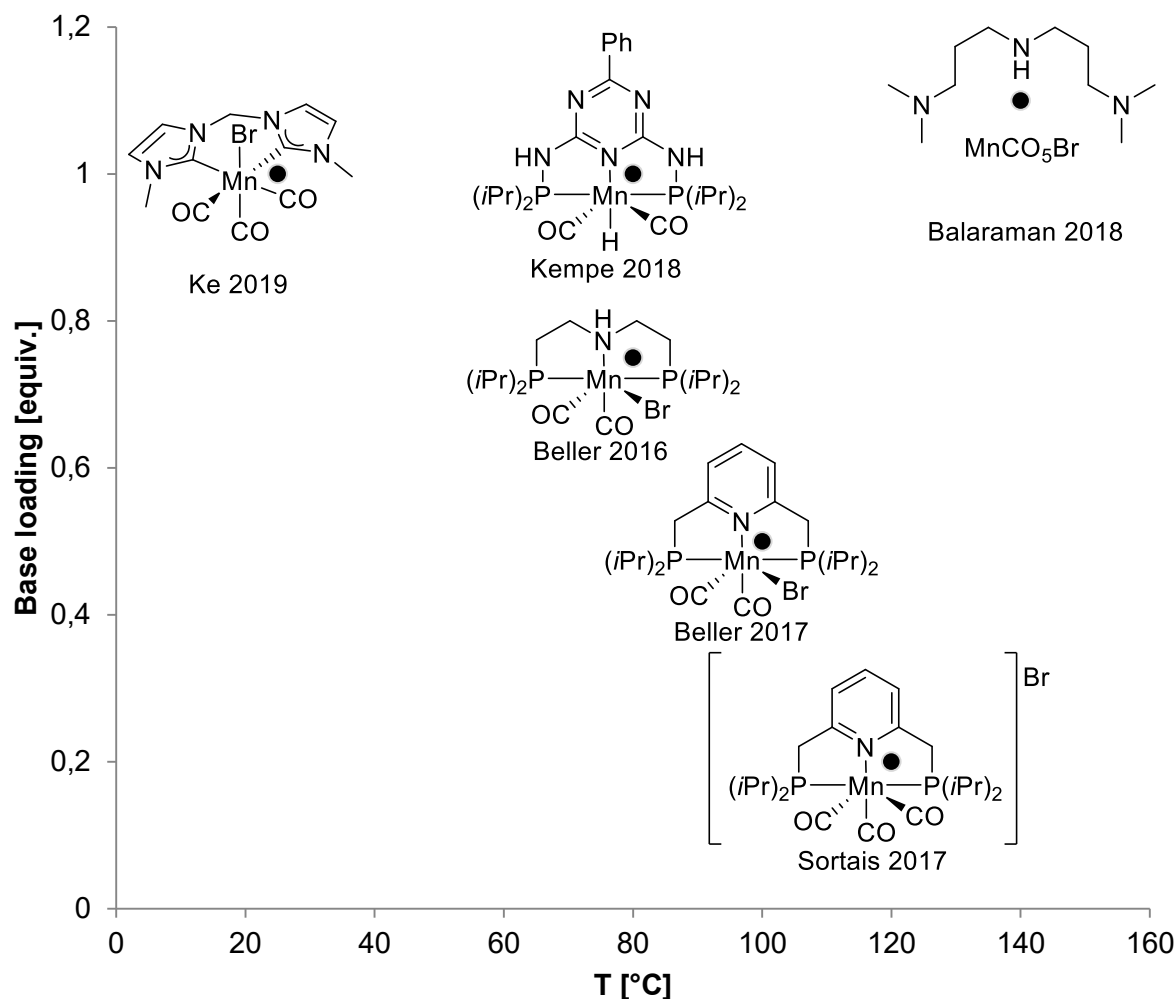
Chart 4. Selected examples of manganese pincer complexes used as catalysts in N-alkylation of aniline with primary alcohols in relation of temperature and base additive dependence.[185-186, 192, 217-223]

To provide an overview for manganese catalyst systems, the N-alkylation of anilines was plotted in terms of temperature and base loading (Chart 4). On the one hand, some systems perform at rather mild conditions, but require strong bases as additives in higher amounts. On the other hand, there are catalytic systems that rely on activated catalysts and perform at harsher conditions, but can reduce the base loading, respectively.[185-186, 192, 217-223] Catalysts that stop at the oxidative coupling of amines and alcohols, yielding imines are not taken into account for this comparison.[191, 206, 219] These recent findings indicate that manganese-based systems are heavily dependent on strong bases and appropriate reaction conditions when applied in borrowing hydrogen-mediated N-alkylation reactions of anilines with alcohols.[175, 206, 219]

4.1.5 Borrowing hydrogen or acceptorless dehydrogenative coupling

As discussed in chapter 4.1.4, N-alkylation of anilines with alcohols catalyzed by manganese pincer complexes was developed enormously recently. However, the acceptorless dehydrogenative coupling (ADC) of amines and alcohols was reported by the group of Milstein in 2016.[191] The manganese PNP-pincer complex only required catalytic amounts of base for the formation of an active species and the reaction proceeded without further base additives (Scheme 64).
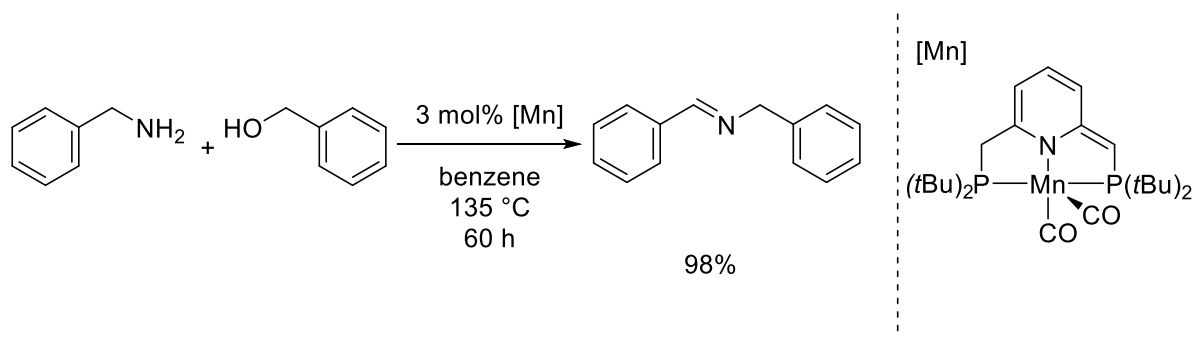
Scheme 64. Dehydrogenative coupling of alcohols with amines without base additive.[191]

It was proposed that the catalytic dehydrogenation of alcohols includes the formation of a manganese hydride complex (Scheme 65).[191, 206, 219] First, deprotonation of the alcohol occurs and an alkoxide complex is formed (**I**). Then the alcohol is oxidized in a β-hydride elimination type mechanism (**II**). In total, the hydrogen is activated in a heterolytic manner through metal-ligand cooperation.[224] The acceptorless dehydrogenative coupling cycle is concluded by release of molecular hydrogen by metal-ligand cooperation and regeneration of the active species (**III**).
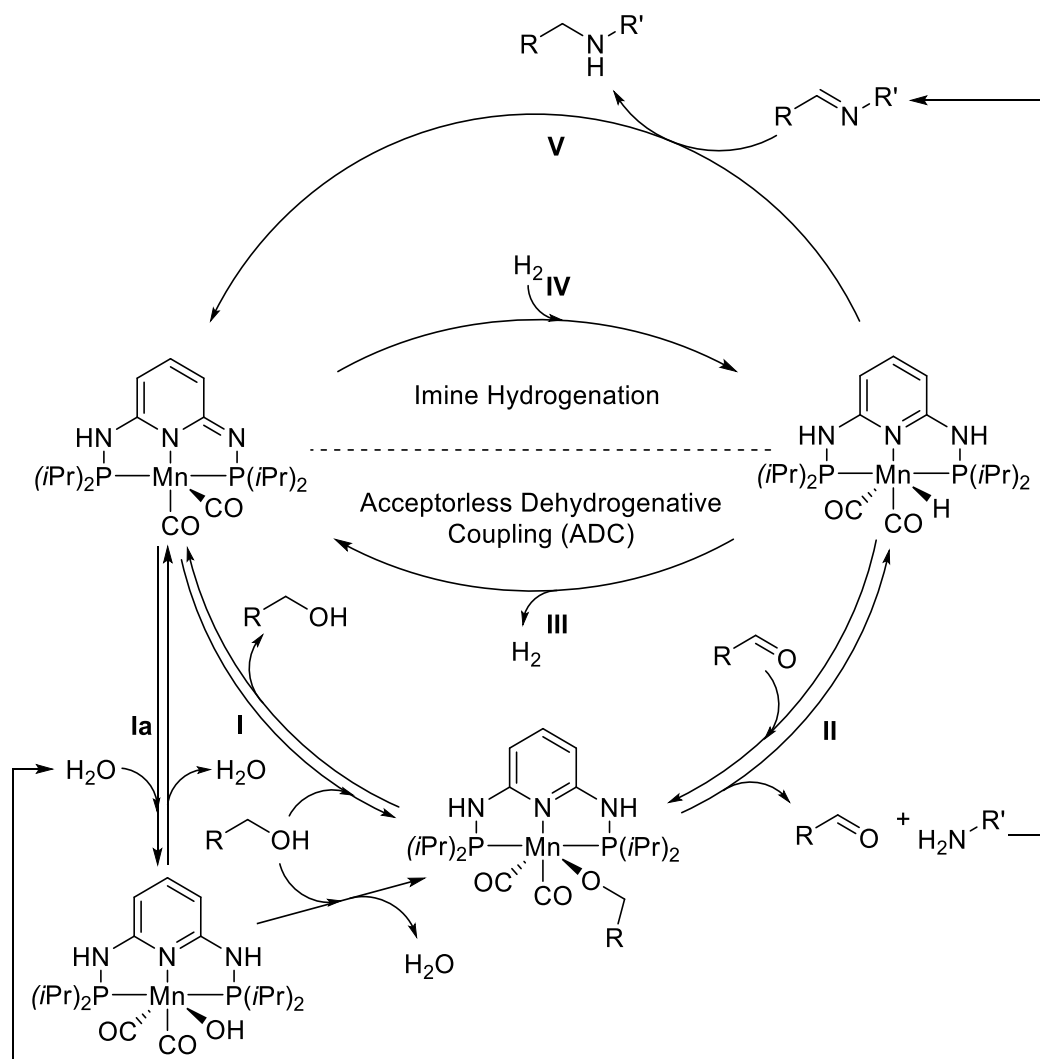
Scheme 65. Schematic exemplary depiction of a proposed borrowing hydrogen cycle composed of acceptorless dehydrogenative coupling (**I**–**III**) and hydrogenation (**IV**–**V**) with a manganese PNP-pincer catalyst.[175, 191, 206, 224-226]

Accordingly, the group of Kirchner reported that a manganese PNP-pincer hydride complex in combination with molecular sieves can be used as catalyst for acceptorless dehydrogenative coupling (Scheme 66).[206]
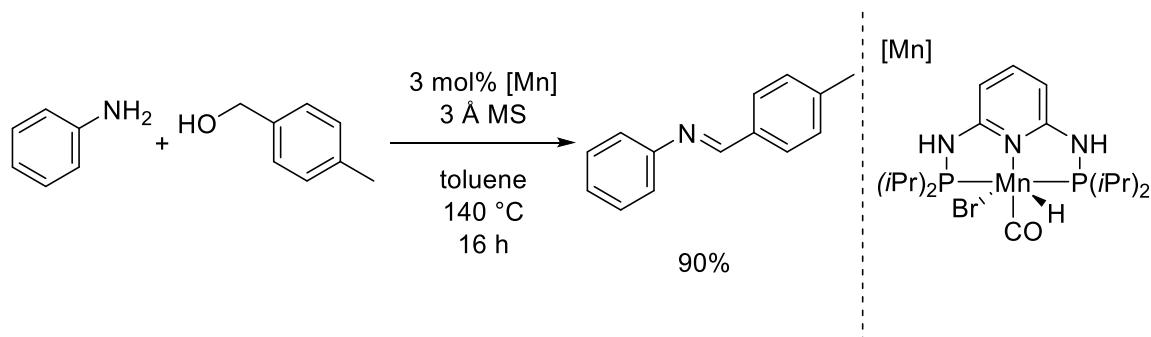
Scheme 66. Dehydrogenative coupling of alcohols with amines catalyzed by manganese hydride complex with molecular sieves.[206]

The main side product of N-alkylation of amines is the formation of imines, which is actually a shortcut of the borrowing hydrogen cycle (Scheme 65). As discussed earlier (Chart 4), a certain combination of base and reaction temperature is necessary to obtain products from the complete borrowing hydrogen cycle. The group of Kempe showed that hydrogen can be activated with manganese PNP-pincer complexes in the presence of potassium *tert*-butoxide, which is active for hydrogenation catalysis (Scheme 67).[226] Also the group of Liu reported that under excess of hydrogen, the active manganese complex activates hydrogen across the complex (Scheme 67).[225] This indicates a second shortcut (**IV**) to a manganese hydride complex.
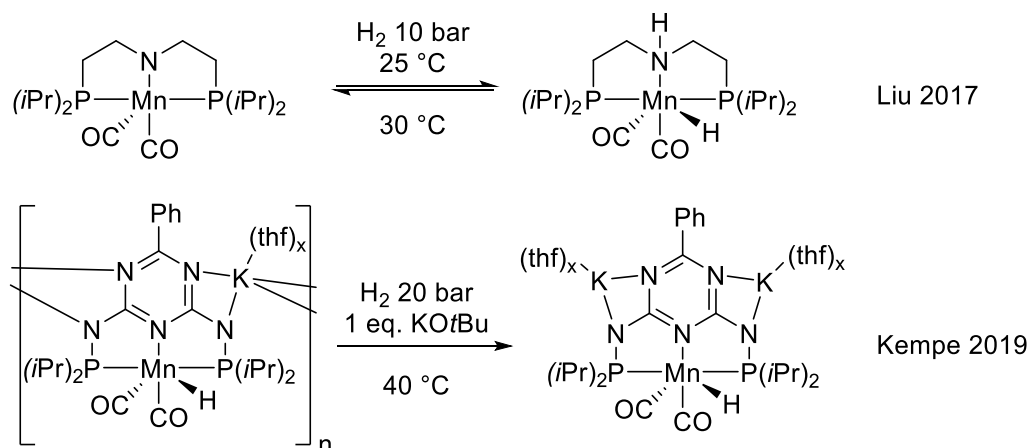
Scheme 67. Two different possibilities for the heterolytic activation of hydrogen across a manganese pincer complex.[225-226]

It is also possible that the formation of a manganese hydroxide complex is a dormant state for the catalyst (**Ia**). Studies have shown that this complex can be converted into alkoxide complexes with alcohols or strong bases by an acid-base reaction (Scheme 68).[225-227] This returns the dormant species into the borrowing hydrogen cycle. However, hydroxide bases also convert the manganese pincer alkoxide complex into a hydroxide complex.
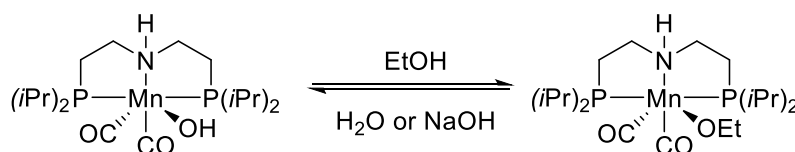
Scheme 68. Equilibrium formation of manganese alkoxide complexes from hydroxide complexes.[225]

The group of Boncella reported that manganese PNP-pincer hydroxide complexes eliminate water with an activation barrier of $\Delta G = 13.3$ kcal (Scheme 69).[224] This could be achieved by performing reactions at high temperature, which are applied in most settings that require less base additive (Chart 4). The formation of dormant species is also a possible explanation for the significant lower amount of base additive needed in transfer hydrogenation and hydrogenation reactions.[185-186, 228]

$$\Delta G_{equilibrium} = \Delta G_+ - \Delta G_- = -0.2 \text{ kcal}$$

$$\Delta G_+ = 13.1 \text{ kcal}$$
$$\Delta G_- = 13.3 \text{ kcal}$$
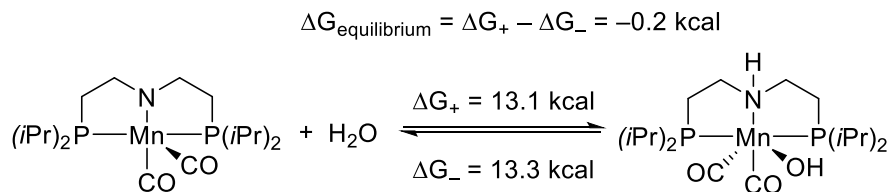
Scheme 69. Equilibrium of manganese complexes and water forming a hydroxide species.[224]

Since all reports include the formation of imines, it might be possible that the borrowing hydrogen cycle is actually performing in dependence of the reaction mixture. While primary alcohols are present, the reaction mostly performs through the acceptorless dehydrogenative coupling shortcut (see Scheme 65, **I–III**) and hydrogen is released.[191, 206] Also the dormant species can be regenerated with alcohols even when hydroxide bases are present (Scheme 68).[225] For the conclusion of the full borrowing hydrogen cycle the produced imine has to be hydrogenated. This is not only depending on the substrate availability in the reaction but also from the stability of the manganese PNP-pincer hydride complex. When the primary alcohol is depleted, the reaction switches predominantly to the conclusion of the borrowing hydrogen cycle. A manganese hydride complex is formed (see Scheme 65, **IV**) and present imines are hydrogenated to provide amines (see Scheme 65, **V**).

3 mol% [Mn]
5 mol5 KO*t*Bu

THF
110 °C
24 h

92%

[Mn]
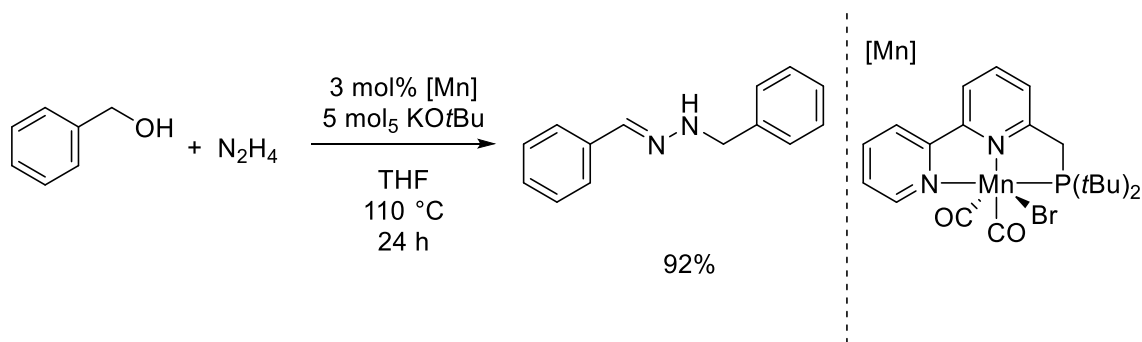
Scheme 70. Manganese catalyzed preparation of N-substituted hydrazones from hydrazine by combination of borrowing hydrogen and acceptorless dehydrogenative coupling.[175]

When the intermediate is highly susceptible to hydrogenation, the shortcut (**III**) can be omitted with a faster competitive reaction (**V**). A good example for that case is the work by Milstein *et al.* on the preparation of N-substituted hydrazones. The reaction features both borrowing hydrogen cycle and acceptorless dehydrogenative coupling in one product (Scheme 70).[175] The intermediate hydrazone is readily hydrogenated to provide benzylhydrazine, while the final N-benzyl hydrazone remains untouched by hydrogenation.

Another example is the N-methylation of anilines with methanol, which employs an excess of methanol. Even if the intermediate is highly unstable, a vast amount of methanol as hydrogen source (**I–III**) provides a shift towards the hydride species.[217-218]

4.2 Motivation

Based on pioneering work by Milstein, Beller, Zheng, Kirchner and Sortais different pincer ligand scaffolds were sought that enable catalytic transformations at milder conditions.[175, 191-192, 206-207, 214-215, 217-218, 229] With that intention established pyridine based ligands systems should be compared to different ligands with an emphasis on pyridine linkers and its influence on reactivity. This semi-empirical approach is expected to provide insight into structure dependence of reactivity. To the best of our knowledge, pincer ligands for metal-ligand cooperated catalysis rely on protic sites (CH_2 or NH) (Chart 5).[230] Thus, this study should cover a rational approach from identifying most promising linkers towards the application of the insight in the preparation of new catalyst. It would also provide experimental insight according to the DFT studies of Ke which were conducted on ruthenium-based systems.[36, 231-236]

Table 17. Comparison of DFT calculation values of the free energy ΔG for de-aromatization of different ligand scaffolds.[236]

#	R	X	ΔG [kcal×mol^{-1}]
1	(tBu)$_2$P	CH	−9.9
2		N	−6.0
3		CH	−9.3
4		N	−5.8

According to DFT studies, NH linkers in pyridine based pincer complexes are beneficial for the MLC mechanism, since their deprotonation and de-aromatization of the pyridine ring requires less energy than with CH_2 linkers (Table 17).[236] Since deprotonation and de-aromatization only occurs once per ligand, the energy demand for symmetric and non-C_2-symmetric ligands are on comparable levels. Also an electron richer substituent R seems to facilitate the de-aromatization of the central pyridine moiety. Thus, this insight can be employed for the preparation of non-C_2-symmetric ligand systems which are then to be used in catalysis.

Beller **2016**
Rueping **2019**
Morrill **2019**

Milstein **2016**
Beller **2017**
Rueping **2019**

Kirchner **2016**
Kempe **2015**
Sortais **2017**

Balaraman **2018**

Milstein **2017**

Rueping **2018**

Milstein **2018**

Balaraman **2018**

R = alkyl, aryl
R' = alkyl, aryl, amine
X = C, N
L = PR_2, NHR, NR_2

Chart 5. Recently reported L_3-pincer ligand systems for Mn, Fe and Co systems which catalyze borrowing hydrogen and acceptorless dehydrogenative coupling processes to a certain extend.[34, 170, 175, 185-186, 191-192, 204, 206, 213-215, 217-220, 222, 226, 237-242]

A most common reaction of N-alkylation of anilines was chosen as benchmark since it resembles a baseline in recent published catalytic systems. The goal was to investigate pincer complexes in terms of reactivity and to optimize potential reactions in terms of conditions. Also a look beyond at new reactions and potential synergetic effects was planned, since borrowing hydrogen methodology resembles borrowed knowledge from established noble metal systems to a certain extend.[26, 156]

4.3 Results and Discussion

4.3.1 Investigation on different C_2-symmetric L_3-type Pincer Ligands

4.3.1.1 Preparation of different ligands

A small library of different ligand scaffolds based on a rigid 2,6-substituted pyridine were to be synthesized and investigated for their reactivity in the N-alkylation of aniline with benzyl alcohol (Figure 27). The selected ligand scaffolds **II-1** and **II-2** were used by Milstein and Kirchner in their studies and the other scaffolds **II-3** and **II-4** are known, but were used in different applications.[191, 206, 243-245]
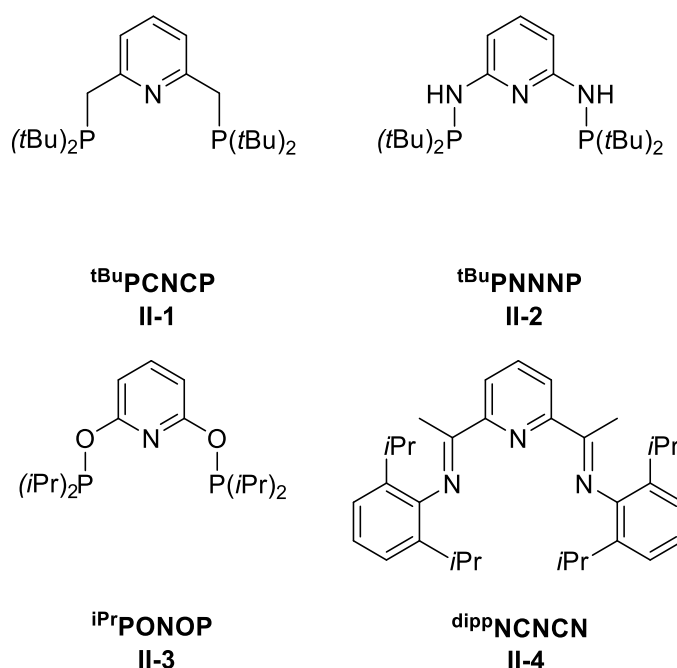
Figure 27. Library of prepared ligands with 2,6-substituted pyridine backbone.[191, 206, 243-245]

In the literature, pincer ligand system nomenclature is dominated by the coordinating atoms which would make all ligands **II-1**–**II-3** PNP ligands and hard to distinguish. The nomenclature was adapted by taking bridging nitrogen's into account which resulted in the abbreviation PN^{3}P for ligand **II-2**.[246] In this part of the thesis the nomenclature is taking coordinating atoms, substituents and bridging atoms into account.
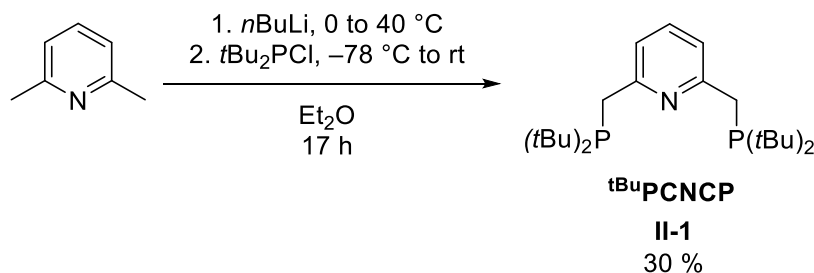
Scheme 71. Preparation of ligand ^{tBu}**PCNCP** (**II-1**).[191]

Firstly, literature known ^{tBu}**PCNCP** was synthesized by metalation of 2,6-lutidine with *n*BuLi and subsequent salt metathesis with *t*Bu$_2$PCl (Scheme 71). The off–white product was obtained analytically pure after recrystallization in a fair yield. The product was found to be highly air sensitive and the oxidized ligand was the main side-product. Even multiple attempts did not provide improved yields since the weak spot is the aqueous workup of the strong base which was conducted with great caution and with freshly degassed water.

With the most prominent pyridine based ligand **II-1** in manganese borrowing hydrogen catalysis in hand, the next step was inspired by Kirchner by substituting methylene linkers with amine linkers.[206] It was expected that an amine linker would come with higher susceptibility towards deprotonation and therefore would facilitate a MLC catalytic process.
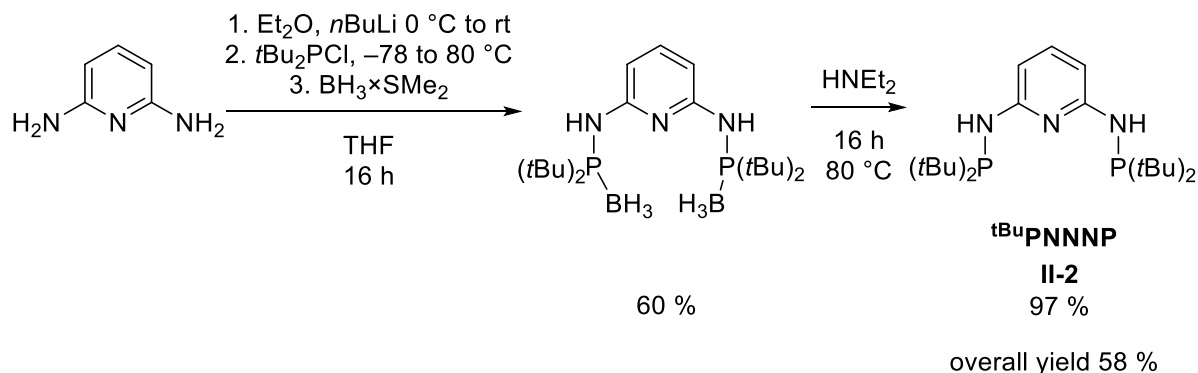
Scheme 72. Stepwise preparation of ligand ^{tBu}**PNNNP** (**II-2**).[206]

^{tBu}**PNNNP** was prepared by adapting the procedure of Kirchner and treating 2,6-diamino pyridine with NEt$_3$ and *t*Bu$_2$PCl in THF in combination with *n*BuLi at elevated temperatures (Scheme 72).[206] The high susceptibility to oxidation was a major issue when purifying the product since the oxidized side product was inseparable by crystallization. So the crude mixture was treated with an excess of borane dimethyl sulfide and stirred at room temperature until no further gas evolution was observed. The product was then successfully

purified by column chromatography, deprotected with $HNEt_2$ and obtained in a 58 % overall yield.

In order to prove the theory of the linker influence on MLC effects in borrowing hydrogen catalysis, non-protic ether linkages were introduced to compare the activity with protic methylene and amine linkers.
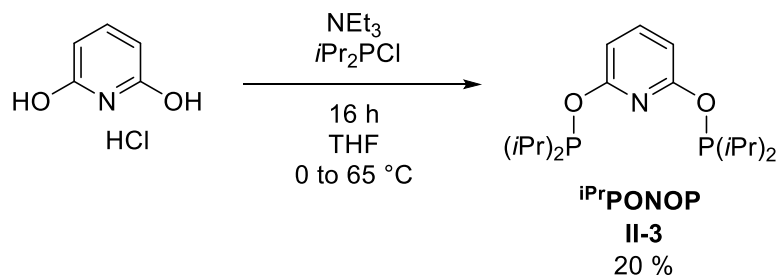
Scheme 73. Preparation of ^{iPr}PONOP (**II-3**).[243]

^{iPr}**PONOP** was prepared by combination of NEt_3 as acid scavenger and iPr_2PCl at elevated temperature (Scheme 73). **II-3** was obtained as an oil which was found inseparable with precipitation attempts unlike described in the literature. Thus the product was collected as highly air sensitive colorless oil by high vacuum distillation in 20% yield.[243]

A different approach was to investigate ^{dipp}**NCNCN** which is known for its susceptibility to reduction which could also be exploited for MLC borrowing hydrogen catalysis.[199]
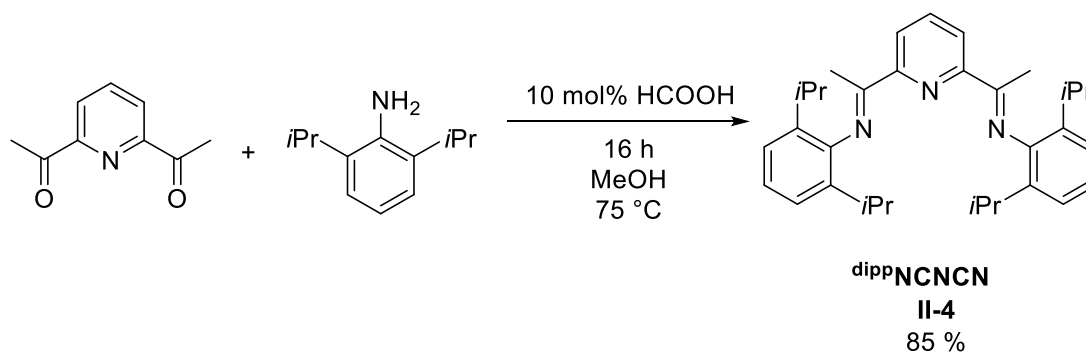
Scheme 74. Preparation of ^{dipp}**NCNCN** (**45**).[194]

The preparation of ^{dipp}**NCNCN** was conducted by double ketimine condensation reaction by combining diacetyl pyridine with di-*iso*-propylanilin (dipp) in methanol with a catalytic amount of formic acid. The product readily precipitated from the reaction and was obtained as yellow solid in a 85 % yield.[194]

4.3.1.2 Preparation of Mn(CO)₅Br

The manganese(I) precursor Mn(CO)$_5$Br (**II-5**) was prepared by treating dimanganese decacarbonyl with bromine in carbon tetrachloride at 50 °C, which provided an orange crystalline product with a moderate yield of 76 %. The complex was successfully characterized by HRMS and also some identification via ^{13}C NMR spectroscopy was possible.

$$Mn_2(CO)_{10} \xrightarrow[\substack{CCl_4 \\ 1\ h \\ 50\ °C}]{Br_2} Mn(CO)_5Br$$

$$\textbf{II-5}$$
$$76\ \%$$
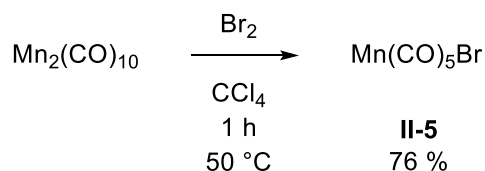
Scheme 75. Preparation of Mn(CO)$_5$Br (**II-5**).[247]

4.3.1.4 Complexation reactions

All prepared ligands **II-1**–**II-4** were employed in complexation reactions with **II-5** on the NMR scale. A test tube was charged with the corresponding ligand, metal precursor and THF-d_8 at room temperature, agitated and left overnight.[191]

	II-1, II-6	X = CH$_2$	L = tBu$_2$P
	II-2, II-7	X = NH	L = tBu$_2$P
	II-3, II-8	X = O	L = iPr$_2$P
	II-4, II-9	X = CCH$_3$	L = dippN
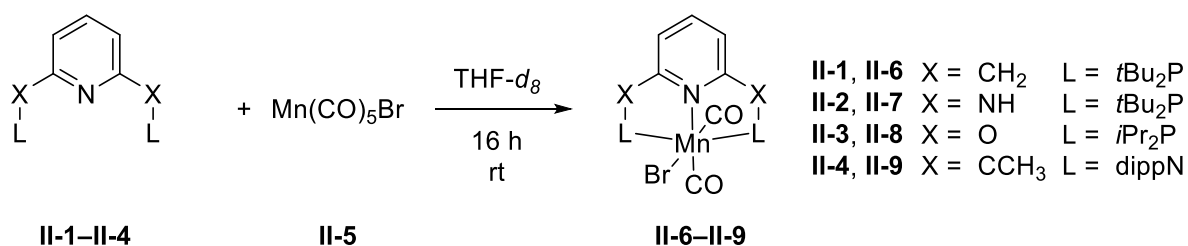
Scheme 76. Complexation of different ligands **II-1**–**II-4** to obtain manganese pincer complexes **II-6**–**II-9**.

Due to the limited solubility of the orange starting material **II-5** in THF, all reactions were set up as suspensions. Complete dissolution, color changes from orange and also evolving gas was taken as signs of complexation. Reactions of ^{tBu}**PCNCP**, ^{iPr}**PONOP** and ^{dipp}**NCNCN** showed distinct color changes within 1 h and interestingly ^{tBu}**PNNNP** did not provide a change of color nor showed improved solubility. Since a manganese complex of ^{iPr}**PNNNP** is known in literature, the sterically more demanding *tert*-butyl groups might obstruct the formation of a metal complex at the given conditions.
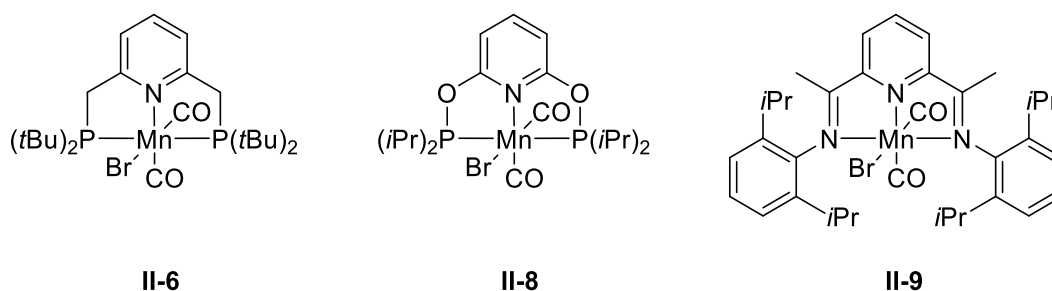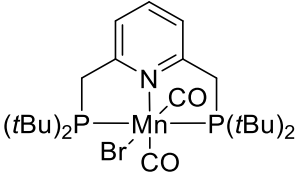
Figure 28. Prepared manganese pincer complexes **II-6**, **II-8** and **II-9**.

Complexes **II-6** and **II-8** were successfully characterized by ^{1}H/^{31}P{^{1}H} NMR spectroscopy with distinct alteration of chemical shifts observable in the ^{31}P{^{1}H} NMR spectrum and all signals being in good accordance with the literature.[191, 243] The reaction providing **II-9** showed distinctive color changes, but the NMR spectroscopic investigation gave ambiguous results. All shifts were comparable with the free ligand without any distinct changes, which could be explained by weak bonding and the remote placement of protons relative to manganese. Due to low solubility it was impossible to record a proper ^{13}C NMR spectrum so the NMR data was interpreted as not confirmed for all complexes since it might also be an NMR inactive complex and the NMR just shows free ligand in solution. With two confirmed complexes **II-6**, **II-8** and the potential complex **II-9** in hand, their catalytic activity in the N-alkylation of aniline benchmark reaction was tested.

4.3.1.5 Investigations on N-alkylation of Amines with Alcohols

Complex **II-6** was employed as catalyst in the reported formation of aldimines in the earlier proposed benchmark reaction, in order to confirm results from literature.[191] The conditions for the N-alkylation of anilines from Beller *et al.* were applied as well, to compare the experimental outcome.[192]

Table 18. First benchmark reactions for N-alkylation of amines with manganese catalyst **II-6**.
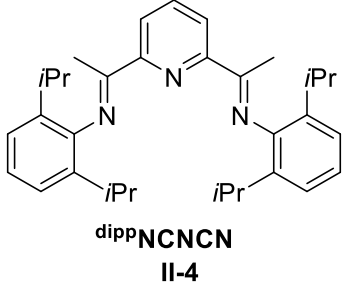
#	z [mol%]	n	T [°C]	t [h]	conv.[a] [%]	ratio **A** : **I**[a]
1	5	0	130	96	96	only **I**
2	75	0	90	24	96	44 : 56
3	75	1	90	24	98	only **I**

General conditions: Conducted in toluene 0.5 mL, ratio amine:alcohol:**II-6** 1:1.2:0.05 in NMR scale (1 mol L^{-1}); [a] determined by GC-MS analysis, referenced to amine consumption.

The conditions for dehydrogenative coupling were successfully applied and the desired aldimine **I** was obtained (Table 18, entry 1). When the conditions from a different catalyst system (Chart 4 and Table 18, entry 2) were employed with significant reduced reaction time, lower reaction temperature and near stoichiometric amount of base, it was observed that the reaction provided also high conversion but an almost 1:1 mixture of amine **A** and aldimine **I**. When benzyl amine was used, only the formation of aldimine **I** was observed. Since the potential catalysts were formed but were impossible to isolate, all reactions were conducted with *in situ* created complexes. This brief investigation was conducted before Beller published its insights and they are in good agreement which the observed results.[217] Recent results by Kempe showed a base-switchable catalyst system and the general observation of the production of both aldimine and N-alkylation product were confirmed (Chart 4).[219] At first sight it seemed that higher loadings of base enable a shift towards the desired N-alkylation of amines, which separates dehydrogenative coupling from borrowing hydrogen methodology. Interestingly, the more nucleophilic benzyl amine was

found to only provide aldimines which was also reported in the literature for other manganese catalysts.[185, 222, 228]

Table 19. N-alkylation of aniline with benzyl alcohol catalyzed by different metal precursors combined with **II-4** on NMR scale.

#	metal precursor	solvent	conv.[a] [%]	ratio **A** : **I**[a]
1	CoCl$_2$	THF	n.r.[b]	n.r.[b]
2	CoCl$_2$	C$_6$H$_6$	4	42 : 58
3	Fe(CO)$_4$Br$_2$	THF	4	62 : 38
4	Fe(CO)$_4$Br$_2$	C$_6$H$_6$	6	33 : 67
5	Mn(CO)$_5$Br	THF	6	83 : 17
6	Mn(CO)$_5$Br	C$_6$H$_6$	5	only **A**

General conditions: Conducted in 0.5 solvent, ratio amine:alcohol:metal:**II-4** 1:1:0.025:0.025 (1 mol L^{-1}); [a] determined by GC-MS analysis, referenced to amine consumption; [b] n.r. = no conversion of the substrates was observed.

More forcing conditions were applied for the investigation of **II-4** as suitable ligand for different metal precursors in borrowing hydrogen catalysis, since the earlier investigations (Table 18) showed a beneficial effect of higher base loadings.[214-215] All attempts with different metal precursors showed only very limited to no reactivity for the desired N-alkylation of aniline. The reaction was conducted in THF and C$_6$H$_6$ to investigate dissolving effects on the reactivity, since KOtBu is only sparingly soluble in non-polar solvents like toluene or C$_6$H$_6$. Interestingly, the reactions proceed slightly better in C$_6$H$_6$ for iron and cobalt. For manganese the conversion was slightly better in THF, but the reduction of the product to amine was quantitative in C$_6$H$_6$. Thus manganese was used for further investigations. The limited reactivity can be explained by the missing protic site in the pincer ligand. Since this

would obstruct MLC, the literature suggests a single electron reduction of the complex forming a sp^2-radical at the linker.
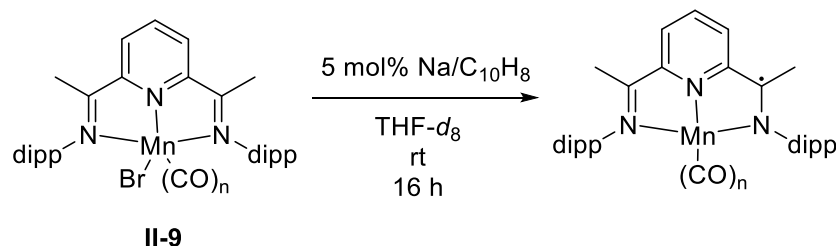
Scheme 77. Attempted reduction of **II-9** with sodium naphthalene.[199]

According to the literature, sodium naphthalenide was used as reducing agent for the manganese complex (**II-9**). Prior NMR experiments remained unsuccessful due to the possible formation of a paramagnetic complex. Thus, it was attempted to create and reduce the complex *in situ* for catalysis.

Table 20. N-alkylation of aniline with benzyl alcohol catalyzed by **II-9** and sodium naphthalenide as additive.
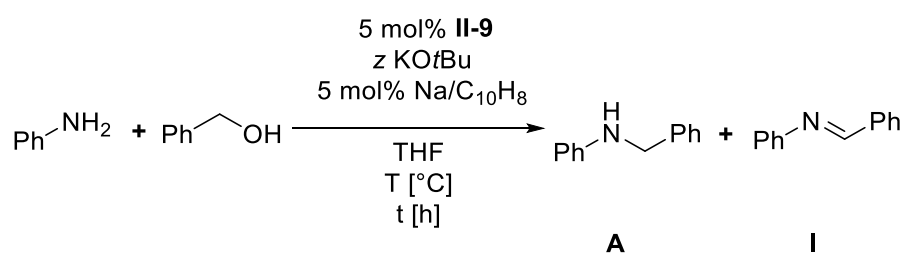
#	z [mol%]	T [°C]	t [h]	conv.[a] [%]	ratio **A** : **I**[a]
1	100	80	24	28	9 : 91
2[b]	100	100	22	14	54 : 46
3	50	80	24	30	9 : 91
4[c]	50	80	24	38	17 : 83
5[b]	50	100	22	26	53 : 47

General conditions: conducted in 1 mL THF, ratio amine:alcohol:**II-9** 1:1:0.05 (1 mol L^{-1}); [a] determined by GC-MS analysis, referenced to amine consumption; [b] reaction was continued; [c] performed in a closed 1.7 mL vial with stirring.

Once sodium naphthalenide is employed in the reaction, a mixture of multiple products was obtained with most of them unidentifiable by GC-MS analysis. Thus the conversions of aniline were determined and also products **A** and **I** were found, but the reaction was not selective. The reaction was observed as reversible at higher temperatures since the continued reactions (Table 20, entries 2 and 5) showed lower conversion, but with selectivity shifted towards production of **A**. Also it was observed that conducting the reactions

in 1.7 mL screw cap vials equipped with magnetic stirring bars was beneficial for the reaction (Table 19, entries 3–4). Despite the low selectivity, the reaction showed greatly improved conversions, so the next step was to investigate of the additives.

Table 21. Combinatory effects of additives in N-alkylation of aniline with benzyl alcohol catalyzed by **II-9**.
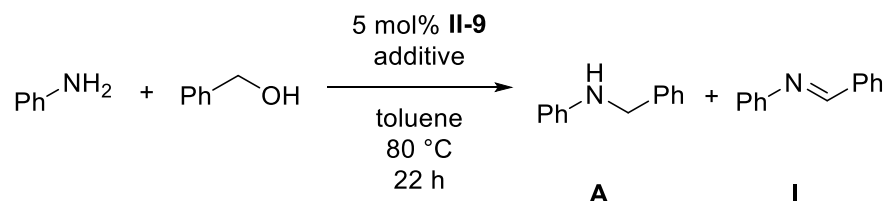
#	Na/$C_{10}H_8$ [mol%]	KO*t*Bu [mol%]	conv. [a] [%]	ratio **A** : **I**[a]
1	5	100	27	68 : 32
2	5	-	14	29 : 71
3	-	100	n.r.[b]	n.r.[b]

General conditions: conducted in 1 mL toluene, ratio amine:alcohol:**II-9** 1:1:0.05 (1 mol L^{-1}); [a] determined by GC-MS analysis, referenced to amine consumption; [b] no conversion of the substrates was observed.

In toluene, the potential catalyst remains inactive for alcohol oxidation without the addition of an equimolar amount of sodium naphthalenide (Table 21, entry 2–3). Addition of KO*t*Bu seems to promote imine reduction as an additive, since the ratio of amine to imine is significantly higher when the base is present (Table 21, entry 1). The reaction was not selective and a range of unidentified side products were observed during GC-MS analysis. With the low selectivity and the limited reactivity compared to earlier test reactions (Table 18), this insight was taken as confirmation that protic sites in the pincer complex are promoting MLC mechanisms and, therefore, are more suitable for catalytic reactions that are governed by borrowing hydrogen. Thus, the third prepared complex **II-8** was not employed in test reactions.

4.3.2 Investigation on non-C_2-symmetric L$_3$-type Pincer Ligands

4.3.3.1 Preparation of different ligands

According to the calculations of Ke, NH is the most suitable linker for pincer ligands in MLC mechanisms.[236] Also the deprotonation only occurs on one side of the ligand which opens the opportunity of preparing non-C_2-symmetric ligands (Table 17). The calculations suggest a beneficial effect of electron donating groups attached to the central pyridine, so a set of different ligands was planned for preparation (Chart 6).

PONCP **PCNNP** **PONNP** **NCNNP**
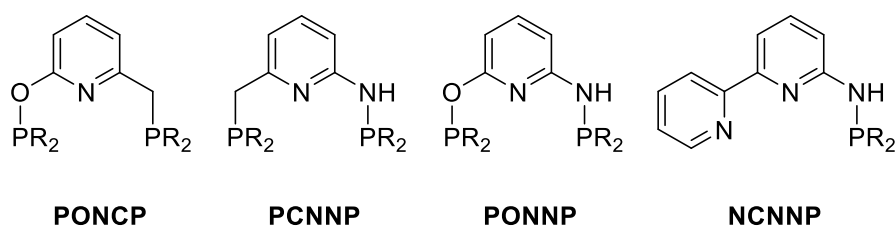
Chart 6. Planned set of non-C_2-symmetric pyridine based L$_3$-type pincer ligand scaffolds.

In addition to bis-phosphine pincer ligands (**PONCP**, **PCNNP** and **PONNP**) a fourth structure based on a bis-pyridine (**NCNNP**) was added based on the findings of Ke. Also the ligand with a methylene linker (NCNCP) was already reported for manganese catalysis earlier, so the amine linker that is known for ruthenium was chosen.[36, 175, 232-234, 246] For the attempted preparation of the desired bis-phosphine ligands the earlier adapted literature procedure for **PNNNP** (Scheme 72) was employed.

X = OH, CH$_3$
Y = CH$_3$, NH$_2$
R = tBu
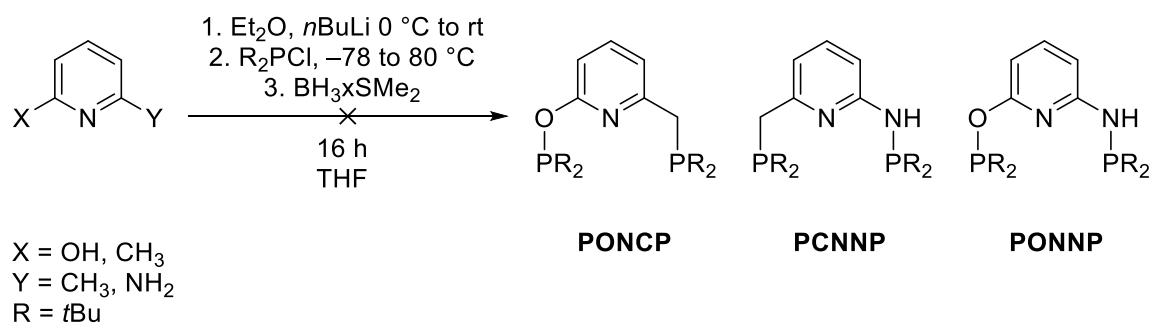
PONCP **PCNNP** **PONNP**

Scheme 78. Attempted preparation of different pyridine based bis-phosphine ligands **PONCP**, **PCNNP** and **PONNP**.

All of the preparations were unsuccessful even after numerous attempts. Recently it was reported that due to the significant difference in pK_a of the linkers X and Y, the reaction stops halfway after introduction of one phosphine moiety.[248] Those findings suggest isolation of the intermediate and a follow-up reaction with a second equivalent of di-$tert$-butylchlorophosphine and sodium hydride.
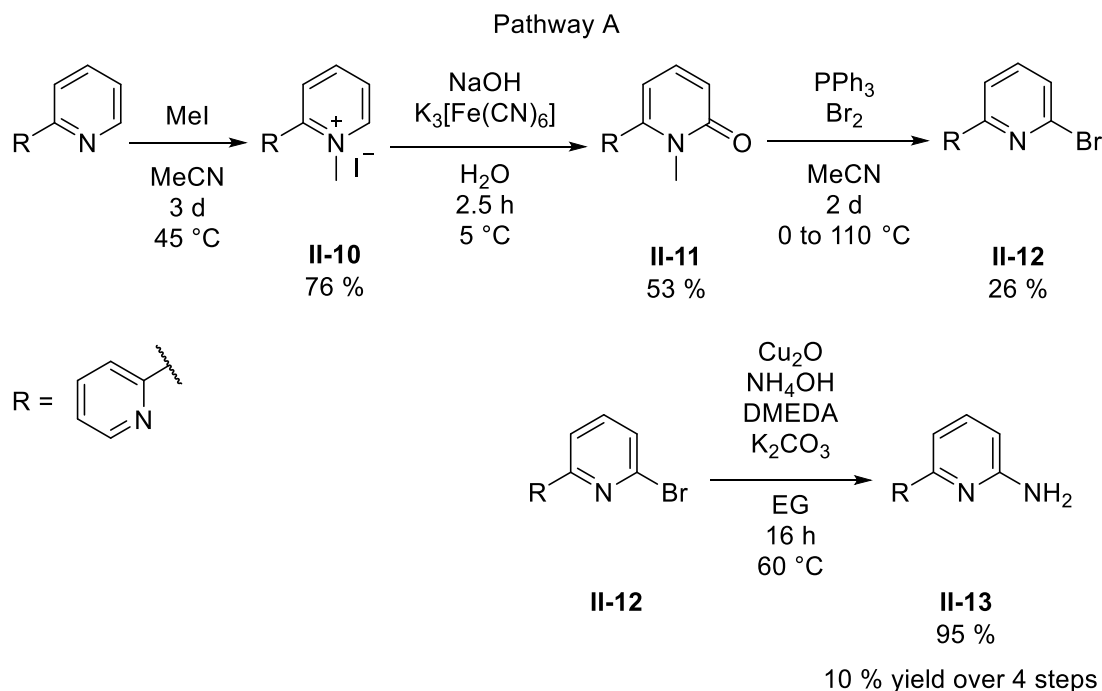
Pathway A

Scheme 79. Pathway A for the preparation of 6-amino-2,2'-bipyridine (**II-13**).[249-250]

For the preparation of **NCNNP** the desired 6-amino-2,2'-bipyridine had to be prepared beforehand. Since direct amination of 2,2'-bipyridine (bpy) was unsuccessful with the Chichibabin synthesis for aminopyridines, two different pathways that were presented in literature were investigated. The first pathway was adapted from a patent that claimed an easy high yielding route starting from the 6-bromo-2,2'-bipridine (**II-12**) (Scheme 79).[251] **II-12** was prepared according to a literature procedure.[250] Firstly, bpy was methylated with methyl iodide providing [bpy-[1]Me]I (**II-10**) in a 76 % yield. Subsequently, **II-10** was oxidized with potassium hexacyanoferrate(III) under strong basic conditions and 1-methyl-[2,2'-bipyridin]-6(1*H*)-one (**II-11**) was obtained in a 53 % yield. For the third step, triphenylphosphonium dibromide was prepared *in situ* and then the dissolved bipyridine was added dropwise. After two days of refluxing, **II-12** was obtained in a low 26 % yield after several purification steps to remove triphenylphosphine oxide. With **II-12** in hand the originally planned amination reaction with copper was more challenging than expected, since the attempted reactions with Cu(0) were unsuccessful.[251] A different procedure employing Cu(I) was adapted and provided **II-13** in excellent 95 % yield.[249] With the most efficient step last, the four step synthesis starting from bpy provided an overall yield of 10 % with the introduction of bromine as most inefficient but also penultimate step.
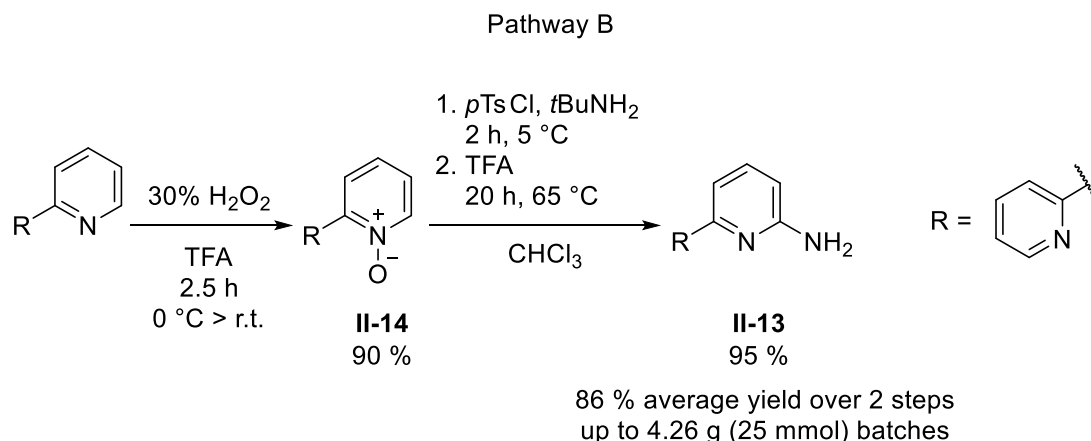
Pathway B

Scheme 80. Pathway B for the preparation of 6-amino-2,2'-bipyridine (**II-13**).[252-253]

Another strategy was employed in pathway B, which was adapted from a procedure for the 2-amination of pyridines and quinolines.[253] During the course of this work, the preparation of **II-13** was also reported in the literature employing similar conditions.[252] For this route, firstly 2,2'-bipyridyl-*N*-oxide (**II-14**) was prepared by treating bpy with hydrogen peroxide in TFA. The product was obtained in a high yield as a white crystalline solid with slight impurities of remaining starting material. The starting material was recovered by column chromatography and was used for subsequent reactions. Treatment of **II-14** with excess of *p*TsCl and *t*BuNH$_2$ in chloroform afforded 6-(*N-tert*-butyl)-amino-2,2'-bipyridine (bpy-^{6}NH-*t*Bu) which was directly transformed with TFA to the unprotected **II-13**. To obtain analytically pure product, most impurities were removed by phase transfer separation with HCl and two subsequent of column chromatographies. The side product was found to be bpy-^{6}NH-*t*Bu, which could be isolated and was readily transformed to **II-13** upon treatment with TFA. Thus, it was possible to recycle the side product in following reactions as the deprotection with TFA is part of the transformation of **II-14** to **II-13**. With both steps being highly selective and the starting material as well as side products recyclable, it also provided a good overall yield of 86 % in gram scale reactions.
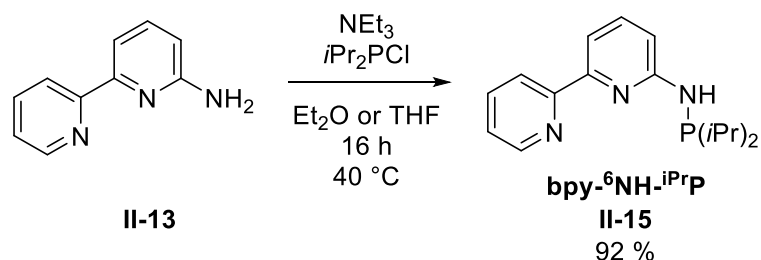
Scheme 81. Preparation of the **NCNNP** scaffold as **bpy-⁶NH-ⁱᴾʳP (II-15)**.[164]

The final step for the ligand preparation was the reaction of **II-13** with a stoichiometric amount of $i\text{Pr}_2\text{PCl}$ in the presence of NEt_3 as acid scavenger in Et_2O (Scheme 81). This reaction provided bpy-⁶NH-ⁱᴾʳP (**II-15**) in a high yield as slightly yellow oil that solidified when scratched of the flask walls with a pipette.

The reaction was readily occurring at room temperature, as indicated by precipitation of $[\text{HNEt}_3]\text{Cl}$. When di-*tert*-butyl-, diphenyl- or dicyclohexyl substituted chloro phosphines were employed, the reaction had to be heated to 60 °C for a precipitate to form. $^{31}\text{P}\{^1\text{H}\}$ NMR spectroscopic investigations showed incomplete conversions of the starting materials. In the literature the use of $n\text{BuLi}$ along with NEt_3 is reported to obtain full conversion of the substrates to the desired PN^3 ligand.[254]

4.3.3.2 Complexation of bpy-⁶NH-ⁱᴾʳP
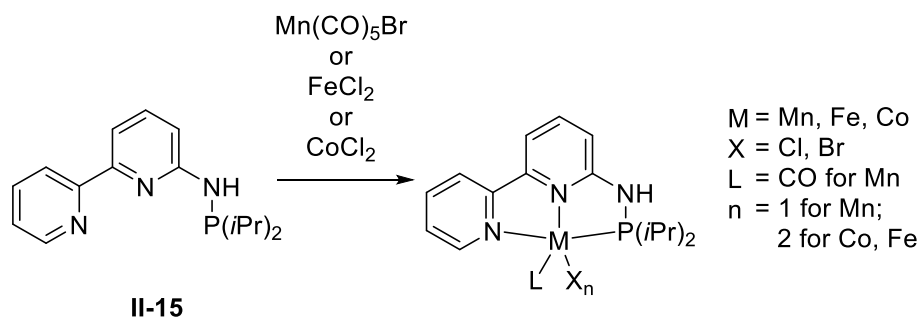
Scheme 82. Complexation reaction of different metal precursors with **II-15**.

When ligand **II-15** was employed in first complexation reactions, formation of a complex was observed with all metal precursors. It was possible to form a deep red manganese complex *in situ* in solution, which was suitable for $^1\text{H}/^{31}\text{P}/^{13}\text{C}$ NMR spectroscopic investigations. When other metal precursors were employed the color of the reaction mixture changed significantly from turbid yellow to red (FeCl_2) and green (CoCl_2), which was taken as sign for complexation. The obtained products were sparingly soluble in THF-d_8 and other deuterated solvents, but seemed NMR-inactive.

The manganese complex appeared stable in solution, although formation of a black precipitate was observed after 30 min at room temperature. Attempts to isolate the complex by crystallization afforded bright orange crystals of Mn(II) species, which were stripped from carbonyl ligands and had a second bromine attached. The complexation reaction was tested in different solvents and it seemed that ethers promote the formation of a complex. The formation of a precipitate was observed at all times, which might indicate the formation of insoluble species during the complexation. The structure of Mn(II) was obtained from several different crystallization approaches (Figure 29). No precipitation was observed in chlorinated solvents like CH_2Cl_2. However, the obtained crystals indicate incorporation of chlorine. None of the crystals indicate the formation of a Mn(0) complex.
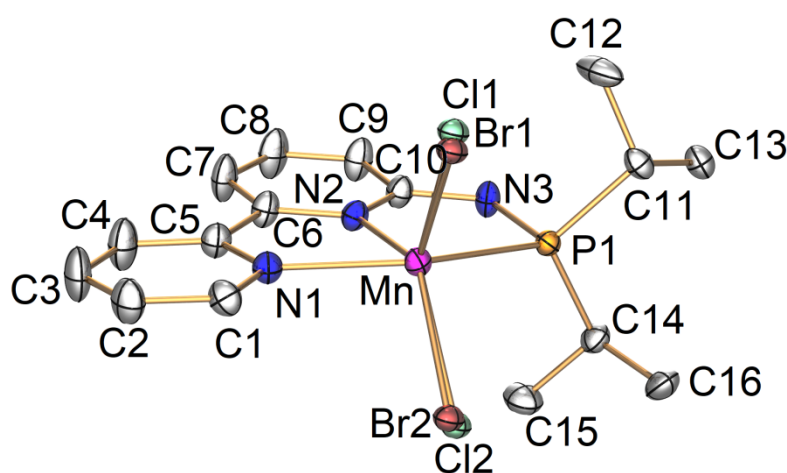
Figure 29. Crystal structure of [(bpy-^{6}NH-^{iPr}P)MnX$_2$] with both bromide and chloride present.

An intermediate of the complexation was obtained when the reaction was carried out carefully in DME under dilute conditions, subsequently layered with pentanes and then stored at –35 °C overnight. Bright red crystals were obtained that showed the coordination of a Mn(I) center of the bpy moiety with the amino-phosphine arm being rotated outwards and coordinated to a different Mn(I) center with carbonyls still attached (Figure 30). With this isolated intermediate a potential degradation upon complexation could occur when the amino-phosphine arm eventually rotates to the Mn(I) center that is coordinated to the bpy moiety to form a pincer complex. The then released Mn(CO)$_4$Br fragment might undergo degradation reactions that include disproportionation, which might explain the formation of the precipitate and Mn(II) species.
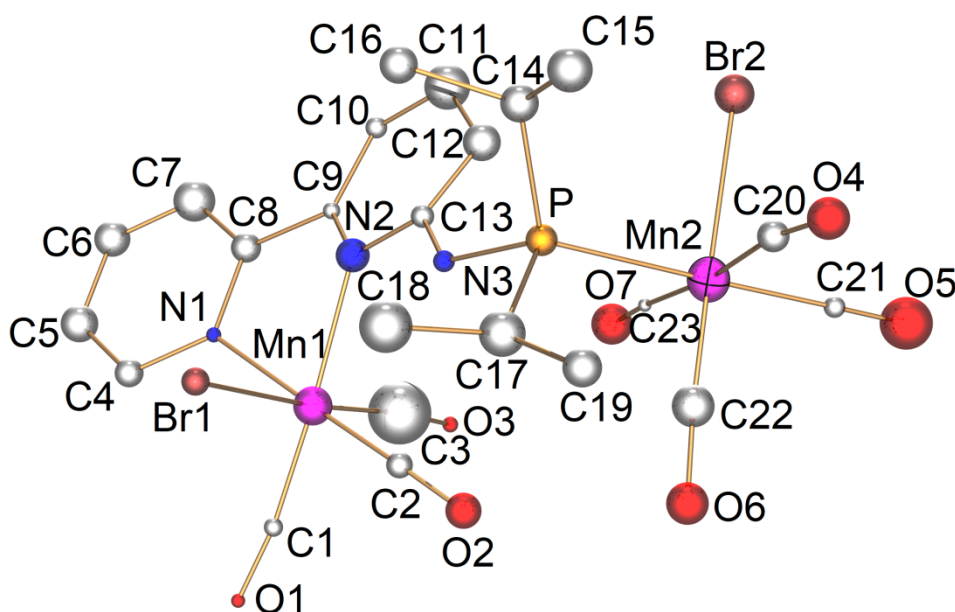
Figure 30. Crystal structure of the complexation intermediate [(CO)$_3$BrMn(κ^2-bpy-^{6}NH-κ^1-^{iPr}P)Mn(CO)$_4$Br].

A successful complexation of Mn(I) was performed in DME without the use of additional pentanes as crystallizing agent. For this attempt all precipitates were filtered off after 1 h of stirring and the resulting solution was stored at –35 °C overnight, which provided red crystals. The structure showed two cationic Mn(I) pincer complexes with a di-anionic Mn(II) counter ion (Figure 31).
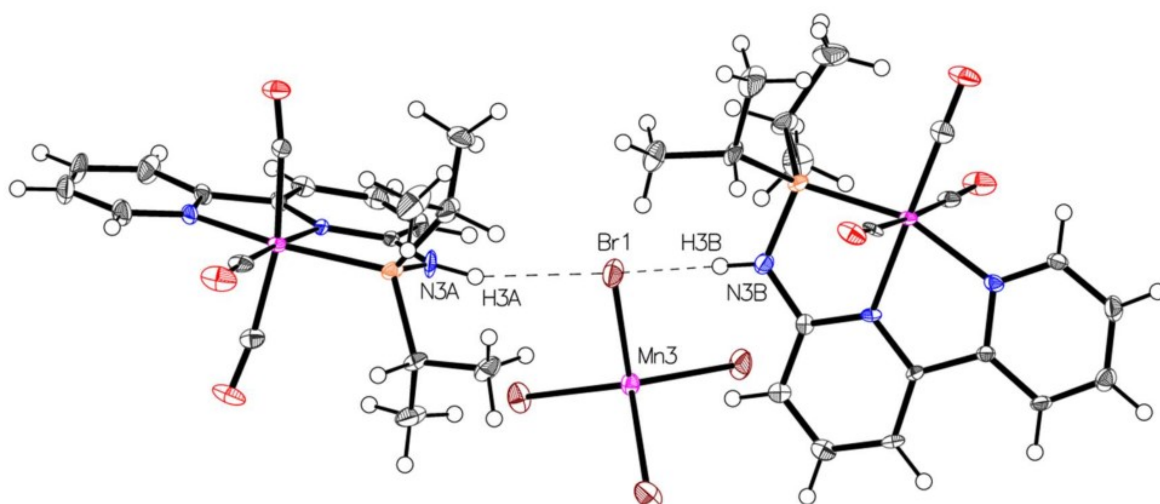
Figure 31. Molecular structure of the cationic species [(bpy-^{6}NH-^{iPr}P)Mn(CO)$_3$] with thermal ellipsoids set at 50% probability. The anion [MnBr$_4$]$^{2-}$ is orientated towards the NH groups of both pincer complexes.[255]
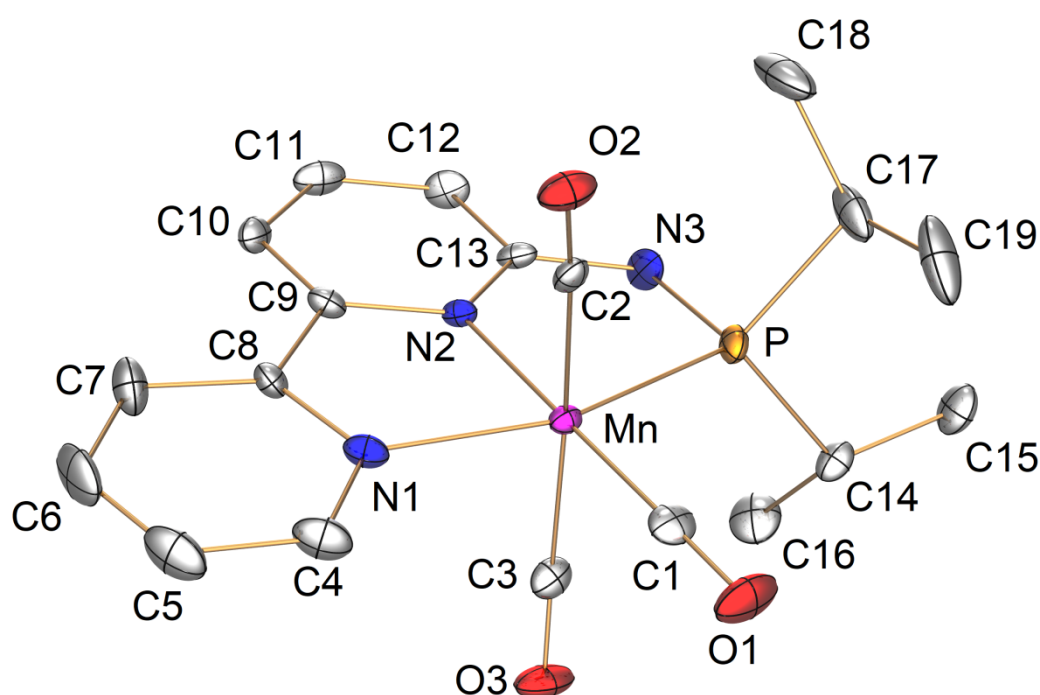
Figure 32. Molecular structure of the cationic species [(bpy-^{6}NH-^{iPr}P)Mn(CO)$_3$] with thermal ellipsoids set at 50% probability. The anion [MnBr$_4$]$^{2-}$, a second cationic Mn(I) pincer moiety and all hydrogen atoms, except for the hydrogen attached to N3a, are omitted for clarity. Selected bond lengths [Å]: Mn1A–P1A 2.2622(13), Mn1A–N1A = 2.049(4), Mn1A–N2A = 2.026(3), Mn1A–C1A = 1.799(5), Mn1A–C2A =1.861(4), Mn1A–C3A = 1.849(4), P1A–N3A = 1.705(4), C1A–O1A = 1.153(5), C2A–O2A = 1.134(5), C3A-O3A = 1.138(5). Selected angles [°]: N1A-Mn1A-P1A = 159.85(11), N2A-Mn1A-P1A = 81.58(10), N2A-Mn1A-N1A = 78.27(14), C1A-Mn1A-N2A = 177.04(19), C1A-Mn1A-P1A = 96.20(15), C3A-Mn1A-C2A = 166.98(18), C2A-Mn1A-P1A = 96.33(13), C3A-Mn1A-P1A = 94.12(15).[255]

The obtained structure is in good accordance with the ruthenium complex that is reported in the literature.[234] With a slightly distorted octahedral coordination, the bpy-^{6}NH-^{iPr}P is coordinated in a planar meridional fashion. The manganese center is pushed out of the plane which results in an angle of 159.85(11)° and might be explained by steric hindrance. Interestingly, also the apical CO ligands are not linear aligned with the manganese center with both angles towards the phosphine slightly exceeding 90°. This might be explained by the steric demand of the *iso*-propyl groups on the phosphine moiety.
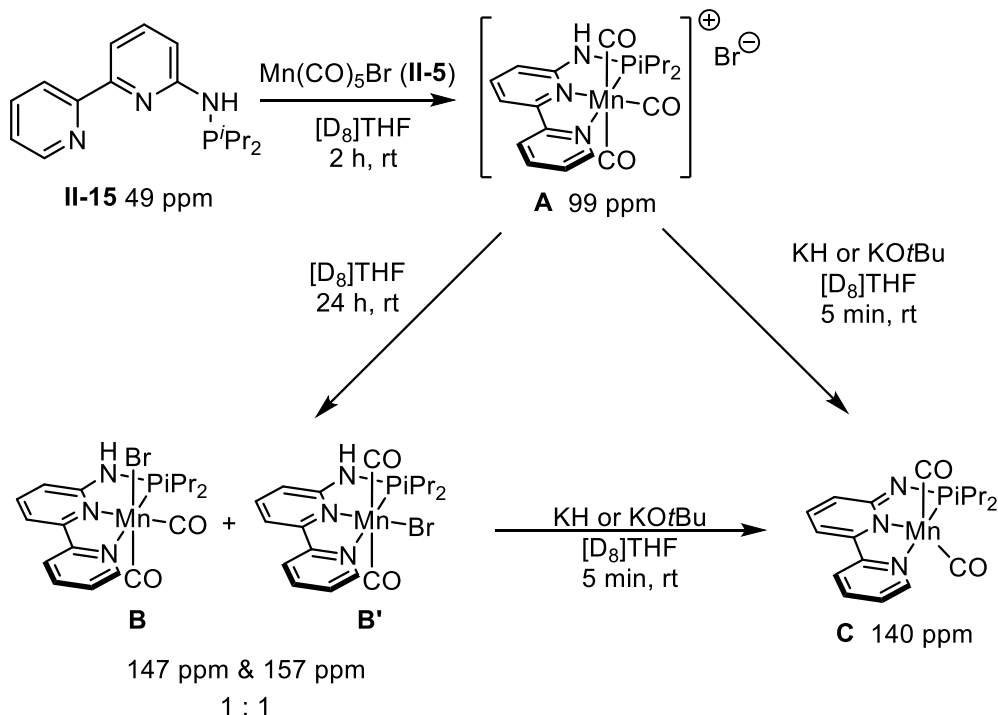
Scheme 83. The formation of different species **A**–**C** observed in the ^{31}P{^{1}H} NMR spectrum during the complexation of **II-5** with **II-15**.[255]
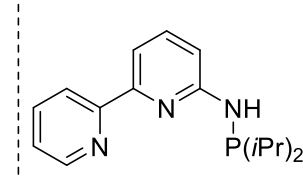
In ^{31}P{^{1}H} NMR spectroscopic measurements different signals were observed during the complex formation (Scheme 83). Initially, a main signal is observed at 99 ppm which is accounted to complex **A**. After 24 h at room temperature, the formation of two different species **B** and **B'** at 147 and 157 ppm in a 1:1 ratio is observed. It was assumed that in the absence of free ligand at 49 ppm, the two species might be originating from differently coordinated bromides.[256] When a strong base was added, the two signals in the ^{31}P{^{1}H} NMR converged to a single signal at 140 ppm accounted to structure **C**, which supported the assumption of differently coordinating bromides resulting in two different complexes.[255] Since the complexation reactions provided various different species, another attempt was to crystallize the complex formed *in situ* after treatment with a strong base, as stated above, to obtain the deprotonated manganese complex.[191] However, the resulting complex did not

crystallize from mixtures of ethers and pentane at various temperatures and numerous attempts yielded only complex degradation.

4.3.3.3 Initial Investigations on Reactivity towards N-Alkylation of Amines with Alcohols

With the prepared ligand bpy-^{6}NH-^{iPr}P (**II-15**) in hand and its confirmed complexation with Mn(CO)$_5$Br providing a manganese pincer complex, the system was tested for catalytic activity. Based on the insight from the complexation, the catalyst mixture was initially prepared *in situ* in toluene with the loading determined by the amount of ligand and metal precursor. The potential degradation was not quantified and, therefore, not included in the calculations. Initially, rather forcing conditions were applied to gage the activity of the system.[214]

Table 22. First reaction mapping of N-alklyation of aniline with benzyl alcohol loadings.

#	R	z [mol%]	T [°C]	conv.[a] [%]	ratio **A** : **I**[a]
1	H	10	120	49	94 : 6
2	H	50	120	83	98 : 2
3	H	100	120	87[b]	only **A**
4	H	100	25	18	only **A**
5	Me	100	120	13[c]	23 : 77

General conditions: 0.5 mmol aniline, 0.5 mmol alcohol, 0.5 mL (50 µmol mL^{-1}, 25 µmol) Mn(CO)$_5$Br and **II-15** in toluene; [a] determined by GC-MS analysis, referenced to amine consumption; [b] benzyl alcohol was consumed; [c] aldol condensation (0.2 : (**A+I**), (m/z 224.0) and formation of significant amounts (3.3 : **A+I**) of an unidentified side product (m/z 209.1) was observed.
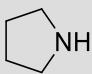
The test reactions with the system based on **II-15** combined with Mn(CO)$_5$Br provided very promising results for the N-alkylation of aniline with benzyl alcohol. Different loadings of KO*t*Bu were employed for the reaction which affected the conversion as well as the ratio of the formed amine and imine. This led to conversions from 49 % with a 94:4 ratio (Table 22, entry 1), through 83 % with a 98:2 ratio (Table 22, entry 2), to a complete conversion of benzyl alcohol and only providing *N*-benzyl aniline as product (Table 22, entry 3). The

reaction was also conducted at room temperature over the same time frame, providing a significantly smaller conversion of 18 % with exclusive formation of *N*-benzyl aniline. When a secondary alcohol was employed, the substrate seemed less reactive and the GC-MS analysis evaluation of the reaction indicated that the imine formation might be the limiting step, since free benzophenone and its aldol condensation product, as well as a significant amount of an unidentified product were found. Assuming that the unknown product was not derived from aniline, a 13 % conversion with a 23:77 ratio of amine to imine was observed. With those first results in hand, the following reactions were conducted with a slight excess (1.2:1 ratio) of benzyl alcohol to ensure a proper monitoring of the reaction.

In order to further investigate secondary alcohols and amines as substrates, reactions were performed under milder conditions (80 °C), but over an increased period of time (68 h) and in the presence of molecular sieves to facilitate imine condensation.

Table 23. Combination of different substrates other than aniline and benzyl alcohol for N-alkylation reactions.
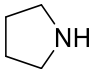
#	R	R'	R''	conv.[a] [%]	ratio A : I[a]
1	Bn	H	H	15	only I
2[b]	Bn	H	H	40	only I
3	Ph	Me	H	n.r.[c]	-
4[b]	Ph	Me	H	n.r.[c]	-
5	Ph	H	Me	2[d]	only I
6[b]	Ph	H	Me	2[e]	only I
7	Bn	H	Me	2	only I
8[b]	Bn	H	Me	5	only I
9	(pyrrolidine NH)		Me	n.r.[c]	-
10			Me	2[f]	only A

General conditions: 0.5 mmol amine, 0.6 mmol alcohol, 0.05 mmol KO*t*Bu, 0.5 mL (50 µmol mL^{-1}, 25 µmol) Mn(CO)$_5$Br and **II-15** in toluene, 100 mg MS 3Å; [a] determined by GC-MS analysis, referenced to amine consumption; [b] after opening to air for GC-MS analysis the reaction was continued for 22 h at 120 °C; [c] no conversion of the substrates was observed; [d] 1 : 0.01 of aniline to free ketone; [e] 1 : 0.2 of aniline to free ketone; [f] referenced to BnOH.

It was found that an increased reaction time and use of molecular sieves do neither outweigh stoichiometric use of base nor lower reaction temperature. The observed activities were all limited and in a comparable range for benzyl amine and aniline at least (compare Table 22, entry 1 and Table 23, entry 1). *N*-methyl aniline was found to be inactive for further alkylation (Table 23, entry 3) but some activity was found for pyrrolidine (entry 9) as secondary amine. In account of secondary alcohol oxidation, the catalyst produced free ketones in both cases (Table 23, entries 5 and 7) that were not consumed by imine condensation. Since the alcohol oxidation is believed to be reversible, the low conversion

might be explained by a very slow imine condensation. Thus, different amines were tested with a higher base loading.

Table 24. N-alkylation of 1-phenyl ethanol with different amines.

#	R	R'	conv.[a] [%]	PhC(O)Me : amine	ratio **A : I**[a]
1	Ph	H	32	0.03	only **I**
2	Bn	H	6	0.07	only **I**
3		NH	n.r.[b]	n.d.[c]	-
4	Ph	Me	n.r.[b]	-	-

General conditions: 0.5 mmol amine, 0.6 mmol alcohol, 0.5 mmol KO*t*Bu, 0.5 mL (50 µmol mL^{-1}, 25 µmol) Mn(CO)$_5$Br and **II-15** in toluene, 50 mg MS 3Å; [a] determined by GC-MS analysis, referenced to amine consumption; [b] no conversion of the substrates was observed; [c] pyrrolidine eluted earlier than the solvent.

Even at higher base loading the catalytic oxidation of 1-phenyl ethanol was only partially successful in the presence of molecular sieves. It was observed that with aniline a significant higher conversion is obtained even though benzyl amine being more nucleophilic (Table 24, entries 1 and 2). When employing secondary amines, no reactivity towards imine condensation was observed. The condensation reaction of amines with acetophenone seems hindered by steric influences of the phenyl ring, since free acetophenone was observed in the product mixture. These test results led to the decision that the optimization of the reaction conditions for the N-alkylation of anilines with primary alcohols was prioritized.

4.3.3.4 Optimization of the Reaction Conditions for N-Alkylation of Anilines with Alcohols

In order to screen other metals and potential influences of molecular sieves, **II-15** was also combined with cobalt and iron precursors and employed in the catalytic benchmark reaction of aniline with benzyl alcohol with reduced reaction time and lowered temperature.

Table 25. N-alkylation of aniline with benzyl alcohol with **II-15** and different metal precursors.

#	metal precursor	MS 3Å [mg]	conv.[a] [%]	ratio **A** : **I**[a]
1	Mn(CO)$_5$Br	-	>99	only **A**
2	Mn(CO)$_5$Br	50	>99	only **A**
3	CoCl$_2$	-	21	9 : 91
4	CoCl$_2$	50	9	only **I**
5	Fe(CO)$_4$Br$_2$	-	19	only **I**
6	Fe(CO)$_4$Br$_2$	50	4	only **I**

General conditions: 0.5 mmol amine, 0.6 mmol alcohol, 0.5 mmol KO*t*Bu, 25 µmol metal precursor, 25 µmol **II-15**, 0.5 mL toluene; [a] determined by GC-MS analysis, referenced to amine consumption.

The reactivity of the manganese complex surpasses by far the tested cobalt and iron complexes in activity towards N-alkylation of amines with benzyl alcohol providing exclusively *N*-benzyl aniline in quantitative GC-MS analysis yield. The addition of molecular sieves is not beneficial to the reaction since the conversion was significantly lower for cobalt and iron (Table 25, entries 4 and 6). Thus, our further investigations focused on manganese complexes.

To investigate the boundaries of the catalytic activity, the temperature and reaction time were left unchanged, while the catalyst and base loading were reduced. Also the effect of molecular sieves in combination with manganese was not fully understood, so some reference reactions were performed under the same conditions.

Table 26. Effects of different catalyst and base loadings, and molecular sieves on N-alkylation of aniline.

$$x \; Mn(CO)_5Br$$
$$y \; \textbf{II-15}$$
$$z \; KOtBu$$

Ph—NH$_2$ + Ph⌒OH $\xrightarrow[\substack{40\ °C \\ 22\ h}]{toluene}$ Ph—N(H)—⌒—Ph + Ph—N=⌒—Ph

A   **I**

#	MS 3Å [mg]	x [mol%]	y [mol%]	z [mol%]	conv.[a] [%]	ratio **A** : **I**[a]
1	-	5	5	100	71	98 : 2
2	-	3	3	100	59	98 : 2
3	-	1	1	100	63	only **A**
4	50	1	1	100	65	97 : 3
5	-	3	3	70	14	93 : 7
6	-	3	3	50	8	57 : 43
7	50	3	3	50	7	only **I**

General conditions: 0.5 mmol amine, 0.6 mmol alcohol, 0.5 mL toluene; [a] determined by GC-MS analysis, referenced to amine consumption.

The catalytic system provided considerable activity at lower temperature (Table 26). When the catalyst loading was reduced only little lower activity was observed (Table 26, entries 1–3) and molecular sieves were observed to have a detrimental effect on the reduction cycle. It is possible that water from the condensation reaction is necessary for a successful reduction (e.g. as proton source) (Table 26, entries 4 and 7). Unlike the variable catalyst loading, the base is needed in quantitative amounts since even slightly lower loadings resulted in significant lower activity towards alcohol oxidation (Table 26, entries 5 and 6). Also the reduction of imine to amine is positively influenced by the base loading, whereas the ratio of base to catalyst seems to be also important (Table 26, entries 1–3).

Further investigations on lower catalyst loading were conducted next at slightly higher temperature with varying base loadings to learn about the temperature dependency of the reaction. Also a blank reaction was performed to identify autocatalytic activity under strong basic conditions.

Table 27. Influence of lowered base loading on the conversion and product ratio.

#	z [mol%]	conv.[a] [%]	ratio **A** : **I**[a]
1	100	76	98 : 2
2[b]	100	15[c]	only **I**
3	90	78	97 : 3
4	80	70	92 : 8
5	70	53	93 : 7

General conditions: 0.5 mmol amine, 0.6 mmol alcohol, 0.5 mL (50 µmol mL^{-1}, 25 µmol) Mn(CO)$_5$Br and **II-15** in toluene; [a] determined by GC-MS analysis, referenced to amine consumption; [b] no catalyst; [c] a range of unidentified side products with **I** as main species.

Low catalyst loadings provide moderate conversion of the substrates in almost all cases (Table 27). The amount of employed base seems to have a significant influence on the imine reduction, since even slightly less than stoichiometric amounts of base resulted in a noticeable lower amine to imine ratio (Table 27, entries 1 and 3). However, in the absence of the manganese catalyst a significantly lower conversion of the substrates was observed, providing only **I** with a range of side products. Unlike the limited background reaction, presence of manganese provides exclusively the amine **A** and the imine **I**. Thus, the next step was investigation of potential improvement at slightly elevated temperature.

Table 28. Linear dependency of base additive loading and conversion.

#	x [mol%]	y [mol%]	z [mol%]	conv.[a] [%]	conv./z	ratio **A** : **I**[a]
1	3	3	100	84	84	98 : 2
2	3	3	50	38	76	85 : 15
3	1	1	100	78	78	99 : 1
4	1	1	50	41	82	81 : 19
5	1	1	10	8	80	only **I**
6[b]	1	1	10	5	50	only **I**

General conditions: 0.5 mmol amine, 0.6 mmol alcohol, Mn(CO)$_5$Br and **II-15** in 0.5 mL toluene; [a] determined by GC-MS analysis, referenced to amine consumption; [b] 10 mol% CsF as additive.

As shown above (Table 28), it was again confirmed that the catalyst loading is almost negligible in terms of activity and that a stoichiometric amount of KO*t*Bu is key for the borrowing hydrogen reaction. In this reaction, an almost linear correlation between conversion and base loading can be observed. A slightly lower activity was observed when cesium fluoride was used as an additive (Table 28, entry 6). The reaction conditions were found to be optimized with 1 mol% catalyst loading and stoichiometric employment of base (Table 28, entry 3) which provided a good conversion with excellent amine to imine ratio. The next step was the investigation of dilution effects on the overall reactivity.

Table 29. The effect of concentration on conversion and selectivity.

#	toluene [mL]	conv.[a] [%]	ratio **A : I**[a]
1	neat	94	only **A**
2	0.1	93	99 : 1
3	0.5	76	97 : 9
4	1.0	60	96 : 4
5	1.5	39	89 : 11

General conditions: 0.5 mmol amine, 0.6 mmol alcohol, 0.5 mmol KOtBu, 0.005 mmol Mn(CO)$_5$Br, 0.005 mmol **II-15**; [a] determined by GC-MS analysis, referenced to amine consumption.

The dilution screening showed that more concentrated reaction mixtures provide by far better reactivity and when running the reaction without solvent even slightly higher activity was observed (Table 29, entry 1). This leads to the assumption that the manganese complex is formed *in situ* when dissolved in the rather polar substrates. Also the reduction of imine to amine was influenced so that a general reciprocal relation of amount of solvent to reactivity can be seen (Table 29, entries 2–5). The three most active reaction mixtures were employed in subsequent reactions by loading the vial with another batch of substrates and base to investigate potential catalyst degradation and reusability (Table 29).

Table 30. Continued N-alkylation of aniline with benzyl alcohol with sequential addition of substrate.

$$
\text{Ph}^{\nearrow}\text{NH}_2 \; + \; \text{Ph}^{\frown}\text{OH} \xrightarrow[\substack{\text{toluene} \\ T \, [\text{°C}] \\ t \, [\text{h}]}]{\substack{1 \text{ mol\% Mn(CO)}_5\text{Br} \\ 1 \text{ mol\% } \mathbf{II\text{-}15} \\ z \text{ KO}t\text{Bu}}} \; \underset{\mathbf{A}}{\text{Ph}^{\nearrow}\overset{\text{H}}{\text{N}}^{\frown}\text{Ph}} \; + \; \underset{\mathbf{I}}{\text{Ph}^{\nearrow}\text{N}^{\diagup\diagdown}\text{Ph}}
$$

#	toluene [mL]	PhNH₂/BnOH [equiv][a]	z [mol%][a]	T [°C]	t [h]	conv. total[a,b] [%]	conv. step[b] [%]	TON	ratio A : I[b]
1	0.1	100/120	100	50	18	93	93	93	99 : 1
2	0.1	200/220	200	50	17	89	85	178	only **A**
3	0.1	400/420	400	150	3	76	63	304	only **A**
4	0.5	100/120	100	50	18	76	76	76	97 : 3
5	0.5	200/220	200	50	17	54	32	108	97 : 3
6	neat	100/120	100	50	18	94	94	94	only **A**
7	neat	200/220	100	50	17	70	46	140	96 : 4
8	neat	400/420	400	150	3	83	96	332	only **A**

General conditions: Initial mixture: 0.25 mmol aniline, 0.30 mmol benzyl alcohol, 0.25 mmol KO*t*Bu 0.25 µmol Mn(CO)₅Br and **II-15**, sequential addition of aniline, benzyl alcohol and KO*t*Bu; [a] in relation to catalyst loading; [b] determined by GC-MS analysis, referenced to amine consumption.

The catalytic species remains active for days, since addition of more substrate provided the desired products **A** and **I**. A link between alcohol and base loading is almost striking, since addition of substrates without addition of base led to a diminished amine-imine ratio and significantly reduced yield (Table 30, compare entries 2 and 6). The more dilute system was found to be less active for recycling, so only the initial 2.5 mM and the neat reactions were used for a third cycle. The third cycle was performed at 150 °C for 3 h, resulting in 126 catalytic turnovers (TOF 41 h⁻¹) and 192 turnovers (TOF 64 h⁻¹), respectively, which shows the potential to perform reactions under more forcing conditions to reduce the reaction time with this highly active catalytic system. Limited reactivity at lower temperatures might be caused by relatively high melting products in this particular reaction (**A** m.p. 35–38 °C, **I** m.p. 52–54 °C).

It was observed that this catalyst system performs well in the presence of a large excess of products **A** and **I**. This indicates the potential of employing lower catalyst loadings

for performing reactions. Although neat reactions provided the highest activity, the melting points of substrates and products were identified as obstacles at the desired lower reaction temperatures. Thus, different solvents with disregard on potential reactivity under strongly basic conditions were investigated in terms of suitability compared to neat reactions.

Table 31. Screening of different solvents with comparison of initial and continued conversion.

$$\text{Ph}\overset{\text{NH}_2}{} + \text{Ph}\overset{}{\text{OH}} \xrightarrow[\substack{\text{solvent} \\ 50\,°\text{C} \\ t\,[\text{h}]}]{\substack{0.5\ \text{mol\%}\ \text{Mn(CO)}_5\text{Br} \\ 0.5\ \text{mol\%}\ \textbf{II-15} \\ 100\ \text{mol\%}\ \text{KO}t\text{Bu}}} \underset{\textbf{A}}{\text{Ph}\overset{\text{H}}{\underset{}{\text{N}}}\text{Ph}} + \underset{\textbf{I}}{\text{Ph}\overset{}{\text{N}}\text{Ph}}$$

#	solvent	conv.$_{3\,h}$ [%] [a]	ratio **A** : **I** [a]	conv.$_{24\,h}$ [%] [a]	ratio **A** : **I** [a]
1	Toluene	80	50 : 50	86[c]	99 : 1
2	THF	87	68 : 32	98	only **A**
3	MeCN	35	only **I**	–[b]	-
4	1,2-Difluorobenzene	67	63 : 37	70[b]	97 : 3
5	Nitromethane	7	79 : 21	14	only **A**
6	DME	87	63 : 37	>99	only **A**
7	Acetone	17[b]	55 : 45	4[b]	41 : 59
8	DMF	71[b]	89 : 11	75[b]	89 : 11
9	DMSO	48	only **I**	12	only **A**
10	1,4-Dioxane	74	44 : 56	85[c]	only **A**
11	Propylene carbonate	43[b]	17 : 83	43[b]	17 : 83
12	Pentane	73	52 : 48	75	only **A**
13	Nitrobenzene	78[b]	only **I**	86[b]	only **I**
14	*i*PrOH	64	70 : 30	75[b]	only **A**
15	neat	82	76 : 24	93	99 : 1

General conditions: 1.0 mmol amine, 1.2 mmol alcohol, 0.1 mL solvent, 50 µmol Mn(CO)$_5$Br and **II-15**; [a] determined by GC-MS analysis, referenced to amine consumption; [b] side reactions with solvent; [c] no residual alcohol detected.

14 different solvents were compared in their suitability for the N-alkylation of amines with benzyl alcohol with the neat reaction as benchmark. Since prior investigations (Table 30) suggested that the reaction is occurring faster at elevated temperatures, the conversion was determined after 3 h and 24 h. This was also sought to provide some insight into the rate determining steps of the borrowing hydrogen cycle. Decreasing conversion rates might be explained with inhomogeneous sampling of the reaction mixture (Table 31, entries 7–8). In

general all screened solvents can be divided in three different groups. Firstly, MeCN, 1,2-difluorobenzene, DMF and cyclic propylene carbonate provided excellent solvation of the catalyst, but due to the strong basic conditions, undesired side reactions occurred which rendered those solvents unsuitable for the reaction (Table 31, entries 3–4, 8 and 11).

Secondly, solvents that were unsuitable due to interfering with the borrowing hydrogen methodology were acetone, nitrobenzene and *iso*-propanol (Table 31, entries 7 and 13–14). Acetone acted strongly debasing on the reaction in general as a hydrogen accepting agent and as a potential substrate for the condensation reaction with the amine substrate. Nitrobenzene did not interfere with the imine formation, but the hydrogenation of the solvent seemed more favorable and formation of **A** was not observed. When *iso*-propanol was employed, it acted also as hydrogen donator and the exclusive formation of **A** was observed. However, the acetone formed in the reaction was found a competitive agent for the condensation reaction with the amine (*vide supra*). Interestingly, nitromethane did not produce undesired side products despite its relatively low pK_a combined with a potentially hydrogen accepting nitro group (Table 31, entry 5).

The third group of solvents, which tolerated the reaction conditions and did not interfere with the borrowing hydrogen process, were the non-polar toluene and pentane (Table 31, entries 1 and 12), as well as ethers THF, DME and 1,2-dioxane (Table 31, entries 2, 6 and 10) and the rather polar DMSO. Reactions in DMSO provided unsatisfactory results; however, the observed selective production of 48 % **I** after 3 h and of 12 % **A** after 24 h, respectively, seems noteworthy (Table 31, entry 9). Pentane and toluene provided similar activity as solvents, with both systems showing high initial conversions of the substrates after 3 h with an average 50 : 50 **A** : **I** ratio (Table 31, entries 1 and 12). The conversion did not improve significantly over 24 h but the formed imine **I** was almost completely hydrogenated to provide desired **A**. The neat reaction was only outperformed by the employment of ethers, which also provided high initial conversions of the substrates after 3 h with significant amounts of desired **A** already observable (Table 31, entries 2 and 6). After 24 h all reactions conducted in ethers provided almost quantitative conversion of the substrates and the exclusive formation of the desired amine **A**. A possible explanation is the solvation of the base additive, which is assumed to promote the reactivity. Thus, a range of bases were tested to investigate potential alternatives to KO*t*Bu, which is most commonly used in the literature.

Table 32. Screening of different base additives.

0.5 mol% Mn(CO)$_5$Br
0.5 mol% **II-15**
z mol% base additive

Ph–NH$_2$ + Ph–OH $\longrightarrow$ (DME, 50 °C, 24 h) → **A** + **I**

#	base additive	conv.$_{z=10}$ [a] [%]	ratio **A** : **I** [a]	conv.$_{z=50}$ [a] [%]	ratio **A** : **I** [a]
1	KOH	3	only **A**	9	only **A**
2	NaOH	n.r. [b]	-	9 [c]	86 : 14
3	KH	n.r. [b]	-	>99	only **A**
4	NaH	6	only **A**	58	96 : 4
5	NaNH$_2$	2	only **A**	13 [c]	57 : 43
6	KOtBu	5	38 : 62	79	99 : 1
7	NaOtBu	2	only **A**	62	96 : 4
8	Cs$_2$CO$_3$	n.r. [b]	-	2	only **A**
9	K$_2$CO$_3$ [d]	n.r. [b]	-		

General conditions: 0.5 mmol amine, 0.6 mmol alcohol, 0.1 mL solvent, 25 µmol Mn(CO)$_5$Br and **II-15**; [a] determined by GC-MS analysis, referenced to amine consumption; [b] no conversion of the substrates was observed; [c] no alcohol left; [d] performed earlier neat with z = 100 mol%.

Different base additives that are employed in the literature for comparable catalytic systems were employed.[185, 228] In general poor activity was observed for all base additives with 10 mol% loading. K$_2$CO$_3$ was identified earlier as non-suitable base additive, while KOH, NaOH, NaNH$_2$ and Cs$_2$CO$_3$ provided slight activity at 50 mol% loading under the employed conditions (Table 32, entries 1–2, 5 and 8–9). However, it is noteworthy that the reaction with KOH as additive provided exclusively **A,** despite its limited activity. Hydrides and *tert*-butoxides were identified as most promising base additives under the given conditions. Potassium cations seem to have a promoting effect on the reactivity, since both KH and KOtBu provide better conversions and better **A** : **I** ratios at 50 mol% base loading compared to their sodium counterparts (Table 32, entries 3–4 and 6–7). With a new base identified, different loadings were investigated to ensure fully optimized reaction conditions.

Table 33. Dependency of conversion and base loading.

#	z [mol%]	conv.[a] [%]	ratio A : I[a]
1	10	9	63 : 17
2	20	25	90 : 10
3	30	56	94 : 6
4	40	78	97 : 3
5	50	99	only A

General conditions: 0.5 mmol amine, 0.6 mmol alcohol, 0.1 mL solvent, 25 µmol Mn(CO)$_5$Br and **II-15**; [a] determined by GC-MS analysis, referenced to amine consumption.

With different loadings of KH employed at slightly shorter reaction times, a significant drop in activity was observed with decreasing amount of base (Table 33, entries 1–5). Thus, 50 mol% loading of KH was considered optimized for the desired reaction conditions with DME as the solvent of choice (Table 33, entry 5).

Table 34. Employment of different metal precursors under the optimized conditions.

#	metal precursor	x [mol%]	conv.[a] [%]	ratio **A** : **I**[a]
1	Mn(CO)$_5$Br	0.5	95	98 : 2
2	MnCl$_2$	1	1	only **A**
3	FeCl$_2$(THF)$_{1.5}$	1	n.r.[b]	-
4	CoCl$_2$	1	1	38 : 62
5[c]	Mn(CO)$_5$Br	1	3	90 : 10
6[d]	-	-	n.r.[b]	-
7[e]	Mn(CO)$_5$Br	1	n.r.[b]	-
8[f]	-	-	4	only **A**

General reaction conditions: 0.5 mmol aniline, 0.6 mmol benzyl alcohol, 1:1 ratio (x) ligand to metal precursor, in 0.1 mL DME; [a] determined by GC-MS analysis, referenced to aniline consumption; [b] no conversion of substrates was observed; [c] no ligand **II-15** added; [d] without metal precursor; [e] no base added; [f] without catalyst.

The optimized conditions were employed in a cross check with different metal precursors as well as in blank reactions to confirm that the optimization of conditions was not based on background reactivity. Mn(CO)$_5$Br was confirmed as a superior metal precursor under the optimized conditions, while other selected precursors exhibited little to no reactivity (Table 34, entries 1–4). Also very little to no activity was observed in the absence of metal precursor, ligand or base (Table 34, entries 5–8).

Table 35. Influence of stoichiometric ratios on N-alkylation of aniline.

#	PhNH$_2$ [equiv]	BnOH [equiv]	conv.[a] [%]	ratio A : I[a]
1[b,c]	1	1	22	91 : 9
2	1	1	99	99 : 1
3	1.5	1	92	only A
4	1	1.5	43	96 : 4
5[d]	1	1	65	only I

General conditions: 1 equiv ≡ 0.5 mmol, 0.1 mL solvent, 0.1 mL (c = 250 µmol mL^{-1}, 25 µmol) Mn(CO)$_5$Br and 56 in DME; [a] determined by GC-MS analysis, referenced to consumption of limiting reagent; [b] amine added first; [c] reaction at 25 °C; [d] open system.

With the optimized reaction conditions in hand, the ratio of substrates as well as the order of addition was investigated. The reaction provided significantly lower conversions, when aniline was added first and conducting the reaction at room temperature (Table 35, entry 1). In terms of stoichiometry, a slight excess of aniline was beneficial for the reaction, providing exclusively amine **A** in good conversion of substrates (Table 35, entries 2–3). When benzyl alcohol was employed in moderate excess, not only the conversion dropped significantly, but also the provided amine to imine ratio (**A : I**) dropped slightly (Table 35, entry 4). This might be explained by the proportionate lower base loading, which reduce the effective benzyl alcoholate concentration (compare Table 35, entries 2 and 4). Interestingly, the reaction also performed in an open vial under air providing exclusively imine **I**. This reaction demonstrates that molecular hydrogen is generated during the reaction and that it can escape the system when it is not sealed. The lower conversion might result from water getting into the reaction mixture from ambient air humidity or catalyst degradation.

With all the gained insight the investigated catalyst system was considered optimized for the N-alkylation of aniline with benzyl alcohols.[255]

4.3.3.5 Application of the optimized catalytic system for a range of substrates[255]

Figure 33. Substrate screening of different alcohols for N-alkylation with aniline. General conditions: 1.1 mmol aniline, 1 mmol alcohol, 0.1 mL DME, 24 h, 60 °C, Ar. Yields determined by GC-FID with *p*-xylene as standard; [a] 36 h; [b] 48 h; [c] 80 °C; [d] 100 °C.[255]

The optimized reaction conditions were employed to perform N-alkylation with broad substrate scope (Figure 33). Benzyl alcohols with different substituents as substrates showed that the reactivity for N-alkylation reactions is correlating with electron density and steric hindrance. However, prolonged reaction times and elevated reaction temperatures provided satisfactory results. Aliphatic alcohols exhibited slower conversion and methanol could only be converted under relatively forcing conditions. This might be explained by the

low stability of formaldehyde under forcing basic conditions. Secondary alcohols provided good results while the main side product was the ketimine, which is formed as an intermediate. We think that the oxidation of the alcohol that provides the ketone moiety and the subsequent condensation reaction with the amine are relatively fast. However, hydrogenation of the ketimine seems to be the limiting step in this reaction.
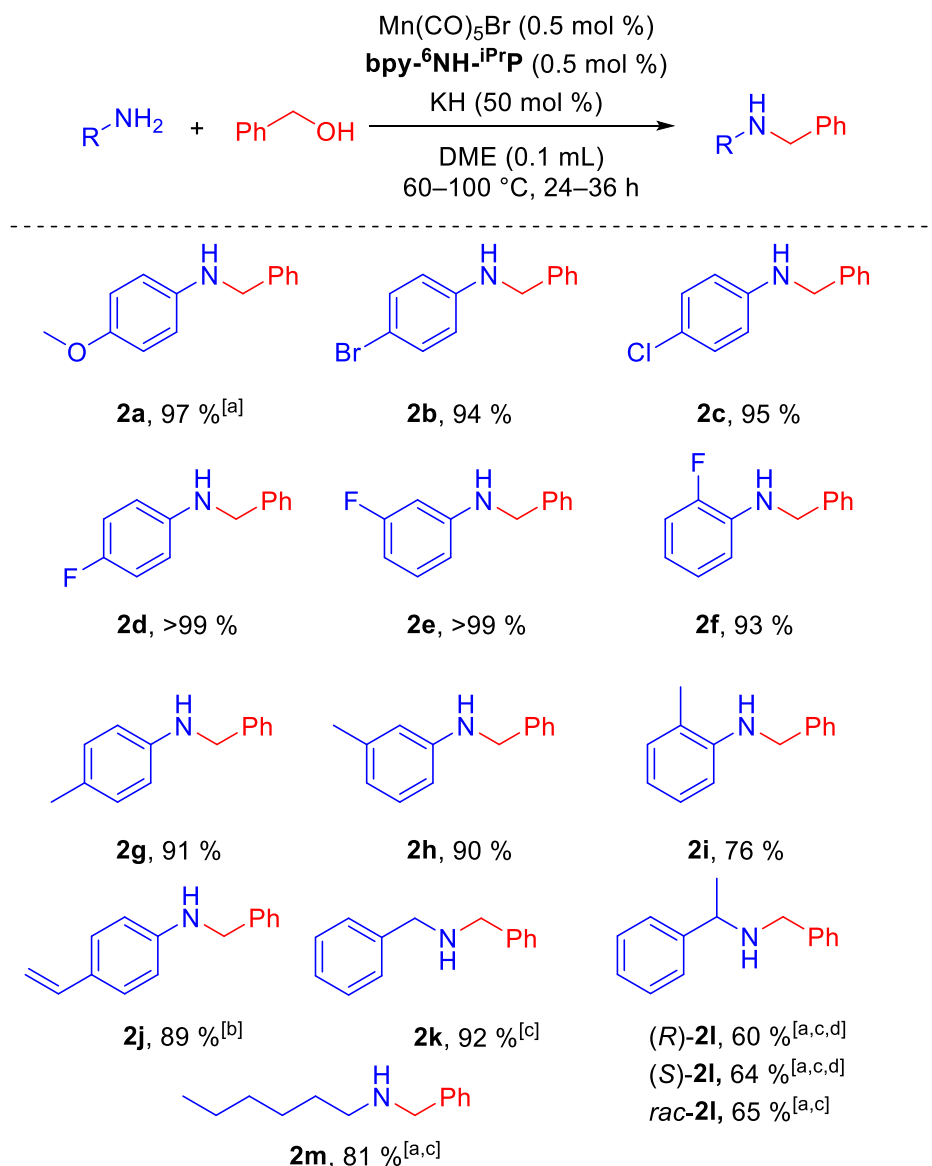
Figure 34. Substrate screening of different amines for the N-alkylation of benzyl alcohol. General conditions: 1.1 mmol amine, 1 mmol benzyl alcohol, 0.1 mL DME, 24 h, 60 °C, Ar. Yields determined by GC-FID with *p*-xylene as standard; [a] 36 h; [b] 1% *N*-(4-ethylphenyl)-1-phenylmethanimine, 6 % *N*-benzyl 4-ethylaniline; [c] 100 °C; [d] Partially racemized ((*R*)-**2l** 84 % ee, (*S*)-**2l** 80 % ee).[255]

Different anilines exhibited high activity throughout the screening even if *o*-methyl aniline exhibited slightly lower yield (Figure 34). More nucleophilic amines also reacted

readily with benzyl alcohol forming an aldimine but the hydrogenation reaction seemed limiting at this step. Higher basicity of the amine substrate could indicate an electron donate effect on the formed C=N bond which might impede hydrogenation reactions.[175, 226, 257]

Interestingly, when ethanol and benzylamine were combined in a reaction, a 1:1 mixture of *N*-ethyl benzylamine and benzyl acetamide was obtained (not shown).[174]
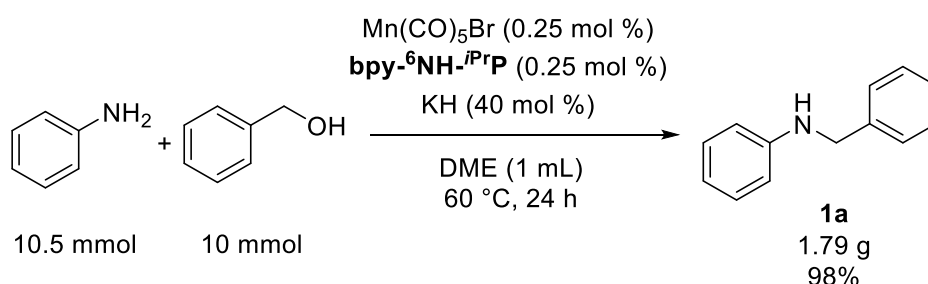
Scheme 84. Exemplary gram scale preparation of *N*-benzyl aniline. [255]

In addition to the tolerated broad substrate scope, the catalytic system and its optimized reaction conditions could also be applied for the gram scale synthesis of *N*-benzyl aniline (Scheme 84). Considering the reaction volume and amount of catalyst that was used, even lower catalyst and base additive loadings were tolerated.
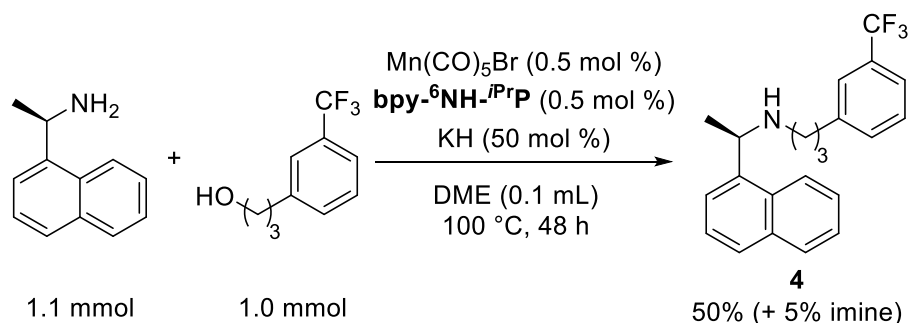
Scheme 85. Exemplary preparation of Cinacalcet ®.[255]

In the light of optimizing synthetic strategies (see chapter 1.2), the exemplary 1-step preparation of the active pharmaceutical ingredient Cinalcalcet ® was performed (Scheme 85). The usual pathway consists of a 3-step synthesis with condensation and reduction in separate steps.[258] The reaction conditions were not completely optimized and still underline the flexibility of the discovered manganese-based catalyst system in terms of substrate scope.

It was observed that moieties with a lower pK_a than the employed primary or secondary alcohols (eg. carboxylic acids and phenols) interfere with the reaction by the

formation of unreactive and mostly insoluble salts. In addition, nitro- and nitrile substituents undergo "competitive" hydrogenation under the given conditions leading to unidentified oligomeric side products (compare 4.3.3.10 and 4.3.3.11).

4.3.3.6 N-Alkylation of Aniline with Methanol

During the investigation on intermolecular N-alkylation of amines with alcohols, methanol was identified as a challenging substrate. The readily available methanol is highly desired as an N-methylation agent and subject to research.[216-218, 259] Its employment in the developed system was further investigated using a different base additive in combination with molecular sieves.

Table 36. Catalytic N-methylation of aniline with methanol.
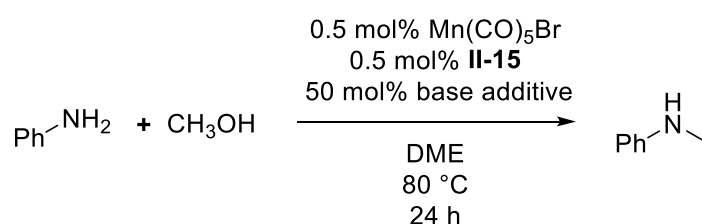
#	base additive	molecular sieves 3Å [mg]	conv. [%][a]
1	KOtBu	-	50
2	KOtBu	50	45
3	NaOtBu	-	28
4	NaOtBu	50	27
5	NaOMe	-	30
6	NaOMe	50	36
7	KH	-	8
8	KH	50	5

General conditions: 1.1 mmol aniline, 1.0 mmol methanol, 5 µmol Mn(CO)$_5$Br, 5 µmol **II-15** in 0.1 mL DME; [a] determined by GC-FID with *p*-xylene as standard.

Conversion to N-methyl aniline was most satisfying with KOtBu, which is commonly used, though overall conversion remained mediocre (Table 35, entries 1–2). Both sodium containing base additives resulted in lower conversions (Table 35, entries 3–6). Potassium hydride was unsuitable for N-methylation reactions with methanol (Table 35, entries 7–8), due to the highly exothermic reaction between methanol and KH. Interestingly, addition of molecular sieves diminishees conversion for both butoxide base additives (Table 35, compare entries 1–4) but improves the conversion for sodium methoxide (Table 35, entries 5–6). While manganese catalyzed N-alkylation reactions with methanol are commonly performed at 100–120 °C,[217-218] the employed system Mn(CO)$_5$Br/**II-15** requires only heating to 80 °C.

4.3.3.7 Intramolecular N-Alkylation Reaction of Aminoalcohols

In extension to the studies of intermolecular reactions, amino alcohols were investigated as substrates for intramolecular reactions. The preparation of indole from 2-(2-aminophenyl)-ethan-1-ol was successfully achieved in 24 h at 80 °C (Scheme 86). When the reaction mixture was stirred for additional 24 h at 100 °C, the indole was found to be hydrogenated to provide indoline in 77 % GC-MS yield.
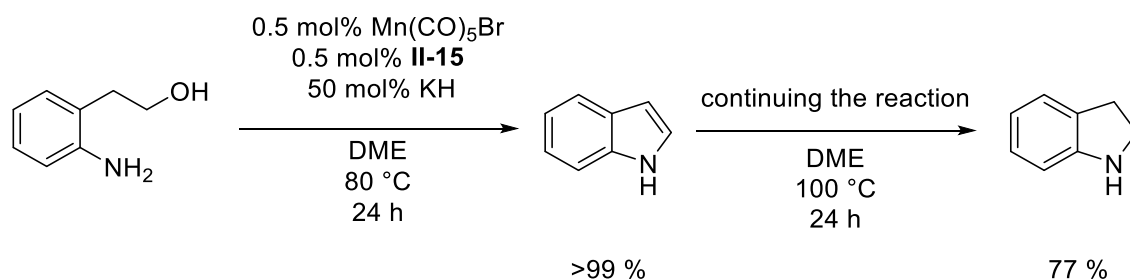
Scheme 86. Intramolecular N-alkylation providing indole and indoline; yields were determined by GC-MS analysis.

When 4-amino-butan-1-ol was employed as substrate the immediate formation of a white precipitate was observed in preparative scale and NMR-scale experiments (Scheme 87). GC-MS analysis of the reaction mixture did not provide any trace of the desired products, nor was unreacted substrate present, indicating that oligomerization of the linear amino alcohol is favored over the formation of 1-pyrrol or pyrrolidine.
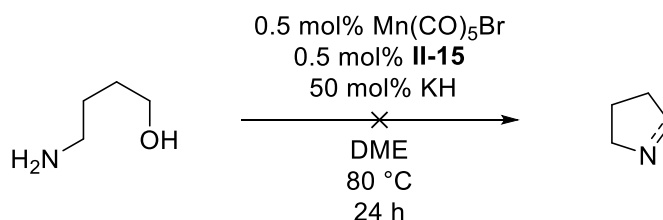
Scheme 87. Attempted cyclisation condensation 4-amino-butan-1-ol.

4.3.3.8 C-Alkylation Reaction of Alcohols

A test reaction towards C-C bond formation combining borrowing hydrogen methodology with an aldol type condensation was conducted. Since the reaction is known in the literature, only a general confirmation of activity was desired. In non-optimized conditions, the reaction of 1-phenyl ethanol with benzyl alcohol was studied using KOtBu as base additive (Scheme 88).[185]
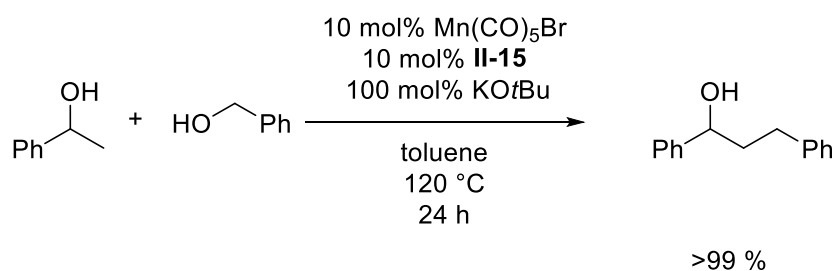
Scheme 88. C-C bond formation combining borrowing hydrogen methodology with an aldol type condensation reaction, providing 1,3-diphenyl-propan-1-ol;[185] yields were determined by GC-MS analysis.

The reaction provided exclusively the α-alkylated alcohol in quantitative yield. This was taken as confirmation that the developed system not only performs N-alkylation but also C-alkylation reactions with a full borrowing hydrogen cycle (Scheme 50), and providing exclusively the fully hydrogenated products.

4.3.3.9 Amides as Subtrates for N- and C-Alkylation reactions

Since the catalyst system showed reactivity for both N- and C-alkylation reactions, acetamide was tested as substrate, which offered both a primary amine group as well as an active site for aldol reactions.[204, 260]
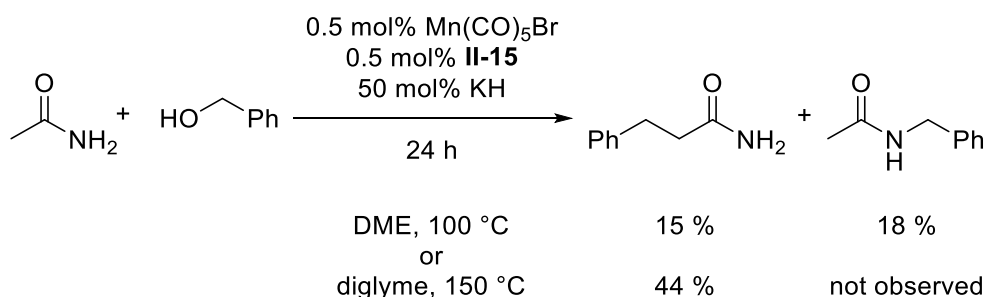
Scheme 89. Exploratory test reaction employing acetamide as bifunctional substrate; yields were determined by GC-MS analysis.

Interestingly, the reaction provided the C- and N-alkylation products in approximately 1 : 1 ratio. Although both C- and N-alkylation reactions take place, no further alkylation was detected. Also the amide moiety was not observed to be hydrogenated in the process. It was observed that the selectivity could be pushed towards the C-alkylation when the reaction conditions were slightly adjusted but not completely optimized.[204]

In the literature, the N-alkylation of sulfonamides[237] is discussed as well as the C-alkylation of amides.[204, 261-262] However, N-alkylation of amides with alcohols has not been reported for manganese based catalysis before.[263] To demonstrate N-alkylation without potential competitive C-alkylation, benzamide was tested as substrate (Scheme 90).
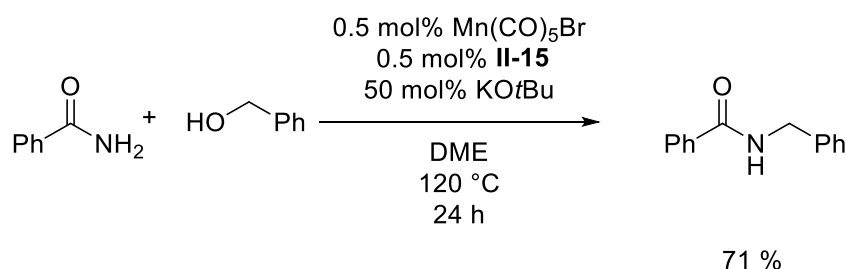
Scheme 90. N-alkylation of benzamide with benzyl alcohol; yield was determined by GC-MS analysis.

The N-alkylation of benzamide was readily performed with the applied conditions and provided a good conversion of the substrates to give exclusively *N*-benzylbenzamide. With the promising N-alkylation results in hand, urea was chosen as substrate that offers two sites

for an N-alkylation reaction. It is worth noting, that urea is mostly employed as ammonia surrogate and only limited results on N-alkylation of urea have been published.[26, 263-264]
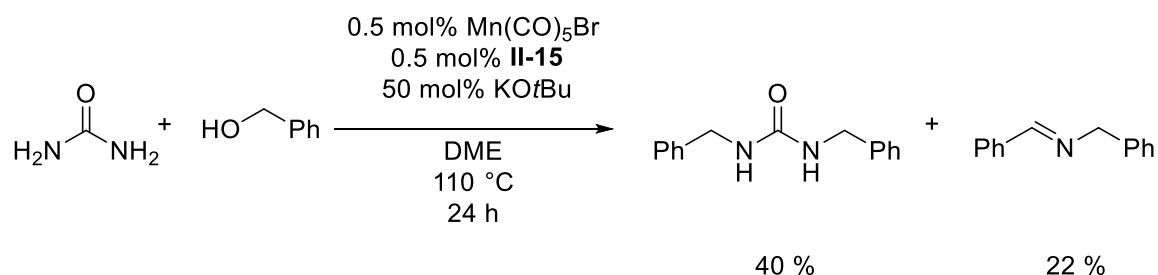
Scheme 91. N-alkylation of urea with benzyl alcohol; yields were determined by GC-MS analysis.

When urea was employed as substrate, it was readily *N*-alkylated and the reaction provided the double alkylated 1,3-dibenzylurea. Interestingly, also the formation of *N*-benzyl-1-phenylmethanimine was observed, which might be a hydrolysis product of the either the intermediate mono-alkylated species, in which urea acted as ammonia surrogate,or the 1,3-dibenzylurea (Scheme 92).[227] The imine formation can then be rationalized by manganese catalyzed dehydrative coupling of benzylamine with benzyl alcohol under the employed conditions.[174, 255]
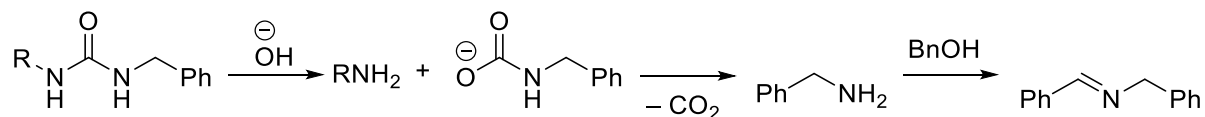
Scheme 92. Proposed hydrolysis of mono- and dialkylated urea to provide benzylamine.[227]

4.3.3.10 Reduction of Nitrobenzene

The borrowing hydrogen methodology can also be extended to hydrogen transfer reactions which are well-known for manganese-based pincer complexes employed in ketone hydrogenation.[185, 228, 265] The idea was to combine transfer hydrogenation with N-alkylation in a one-pot reaction cascade.[216] Thus, observations made during the solvent screening (Table 31) were pursued in the reaction of nitrobenzene with methanol under borrowing hydrogen conditions (Table 37).

Table 37. Transfer hydrogenation of nitrobenzene with methanol.

#	MeOH[a] [equiv]	t [h]	T [°C]	conv.[c] [%]	ratio **AOB : AB**[b]
1	3	24	50	>99	only **AOB**
2[a]	3	24	80	>99	86 : 14
3[b]	13	72	120	>99	10 : 90

General conditions: 0.5 mmol nitrobenzene, 25 µmol Mn(CO)₅Br, 25 µmol 56 in 0.1 mL DME, all entries derive from a singular reaction mixture; [a] the sample from entry 1 was heated for another 24 h at 80 °C; [b] the sample from entry 2 was heated for another 72 h at 120 °C; [c] determined by GC-MS analysis, referenced to consumption of nitrobenzene.

It was observed that the manganese catalyst system readily reduces nitrobenzene quantitatively to azoxybenzene (**AOB**) in the presence of methanol at 50 °C (Table 37, entry 1). When the reaction is extended by 24 h and heated to 80 °C, the formation of azobenzene (**AB**) was observed (Table 37, entry 2). After the addition of more equivalents of methanol and a further extension of the reaction time by 72 h in combination with higher temperature of 120 °C, further conversion of **AOB** to **AB** was observed.[265-266] No hydrazine or aniline was detected by GC-MS analysis, which inidicates that transfer hydrogenation with methanol is limited to the formation of **AOB** and **AB** under the given conditions. Autocatalytic activity for the formation of **AOB** from nitrobenzene in the presence of *iso*-propanol at 100 °C has been reported in the literature;[267] therefore, background activity for the reaction between nitrobenzene and methanol without catalyst and base can be assumed. Observations from made in the N-alkylation of aniline with benzyl alcohol in the presenece of nitrobenzene

(Table 31), indicate that the hydrogenation of nitrobenzene providing **AOB/AB**, is more facile than the reduction of imines providing amines.

4.3.3.11 Hydrogenation of Imines and Nitriles

The developed catalytic system was also tested for its suitability in hydrogenation reactions employing external hydrogen. C=N bonds were successfully reduced using 10 mol% NaO*t*Bu as base at 120 °C (Scheme 93).

$$\text{0.5 mol\% Mn(CO)}_5\text{Br}$$
$$\text{0.5 mol\% } \textbf{II-15}$$
$$\text{10 mol\% NaO}t\text{Bu}$$
$$\text{50 bar H}_2$$

toluene
120 °C
24 h

R = H   >99 %
CH$_3$ 38 %
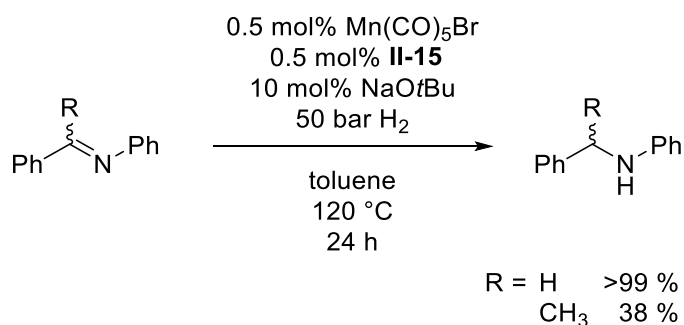
Scheme 93. Exemplary hydrogenation of *N*,1-diphenylmethanimine (R = H) and *N*,1-diphenylethan-1-imine (R = CH$_3$); yield was determined by GC-MS analysis.

While hydrogenation of the aldimine was quantitative, the hydrogenation of the ketimine was found more challenging under the given conditions. This is in good agreement with the observation, that 1-phenyl ethanol provides most ketimine in attempted N-alkylation reactions of aniline.[255] The test reactions were conducted to implement suitable transfer hydrogen processes that were also observed during the solvent screening (Table 31). Also different groups have recently reported the activity of manganese complexes for transfer hydrogenation of aldimines and ketimines, [257, 268] which confirm our observations.

Further investigations on C-N bond reduction was targeting nitrile reduction, which is a reaction well known in the literature.[269]

$$\text{Ph}-\text{CN} \xrightarrow[\substack{\text{toluene} \\ 120\ °C \\ 24\ h}]{\substack{0.5\ \text{mol\% Mn(CO)}_5\text{Br} \\ 0.5\ \text{mol\% II-15} \\ 10\ \text{mol\% NaO}t\text{Bu} \\ 50\ \text{bar H}_2}} \text{Ph}\diagup\text{N}\diagup\diagup\text{Ph}$$

>99 %
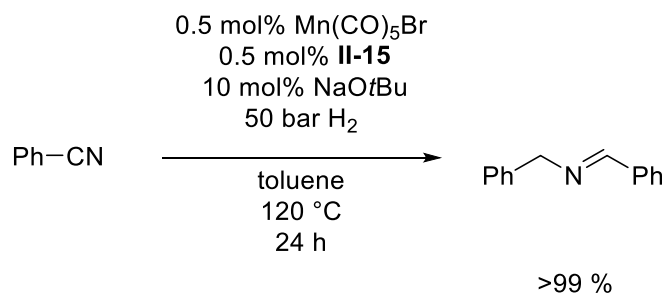
Scheme 94. Exemplary hydrogenation of benzonitrile providing *N*-benzyl-1-phenylmethanimine; yield was determined by GC-MS analysis.

Instead of the desired production of benzyl amine, the hydrogenation of benzonitrile provided exclusively the condensation product *N*-benzyl-1-phenylmethanimine in quantitative GC-MS analysis conversion. Interestingly, the obtained aldimine was not hydrogenated further to dibenzyl amine, in contrast to our observations for *N*,1-diphenylmethan imine (Scheme 93). This reaction outcome was also reported in the literature when iron catalysts were employed.[270-271]

4.3.4 Extended PN^3 Ligand System Development

4.3.4.1 Preparation of bpy-^{6}NH-$^{(R)\text{-BINOL}}$P

After the identification and development of the bpy-^{6}NH-^{iPr}P ligand, the pyridine based PN^3 scaffold was further investigated with exploratory structural adaptions.[233, 246]
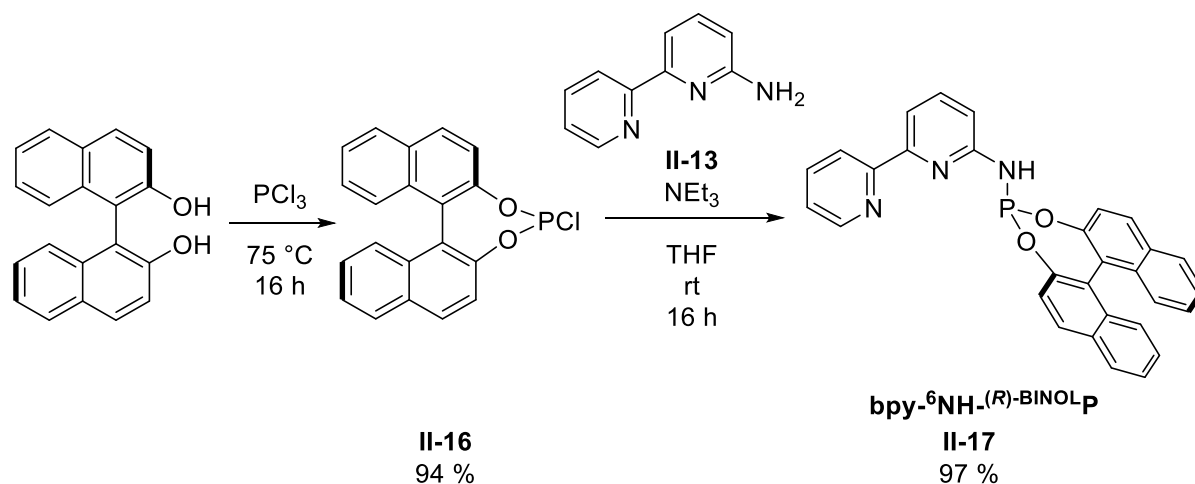
Scheme 95. Two-step preparation of **bpy-^{6}NH–$^{(R)\text{-BINOL}}$P (II-17)**.[272]

Firstly, the alkyl substituents on the phosphine moiety were replaced with BINOL to investigate not on the effect of different electron density at the phosphine and the effect of a stereogenic center on the enantioselectivity for selected reactions. The first step in the ligand synthesis was treatment of (R)-BINOL with an excess of PCl$_3$ while refluxing over 16 h which provided the desired chlorophosphite **II-16** in a good yield (Scheme 95).[272] Subsequently, reaction of **II-16** with the **II-13** using NEt$_3$ as base produced the desired product **II-17** in an excellent yield. The slight yellow oily product was found sufficiently pure by NMR spectroscopic investigation. A characteristic signal shift in the ^{31}P{^{1}H} NMR spectrum was observed with 13.4 ppm for **II-16** and 150.2 ppm for **II-17**, which indicated a successful conversion of **II-16**. A complexation experiment with Mn(CO)$_5$Br monitored by ^{31}P{^{1}H} NMR spectroscopy led to the formation of a new species at 183.5 ppm (Figure 35). Upon treatment with one equivalent of KH a new species with a chemical shift of 227.8 ppm along with a small signal at 165.6 ppm was observed (compare to Scheme 83). The formed species could not be clearly identified in the recorded ^{1}H or ^{13}C{^{1}H} NMR spectras. However, the observed alteration of the ^{31}P{^{1}H} NMR spectrum was taken as indication for complex formation.
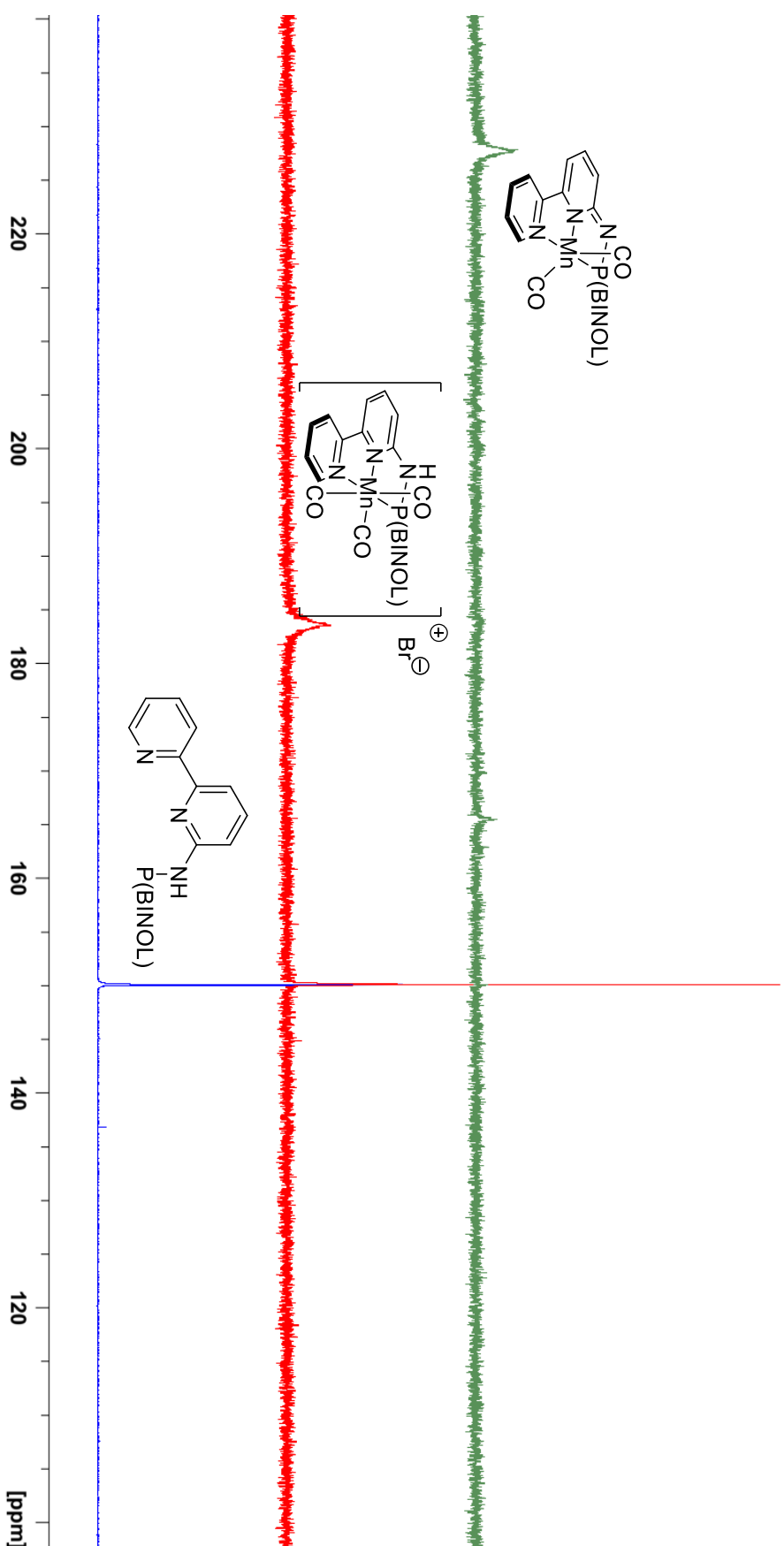
Figure 35. Complexation reaction of **bpy-⁶NH–(R)-BINOLP (II-17)** with Mn(CO)₅Br monitored by ³¹P{¹H} NMR spectroscopy (162.0 Mhz) in THF-*d₈*: ligand **II-17** (blue); combination with Mn(CO)₅Br after 5 min (red); treatment with 1 equiv KH (green).

4.3.4.2 Preparation of phen-^{2}NH-^{iPr}P
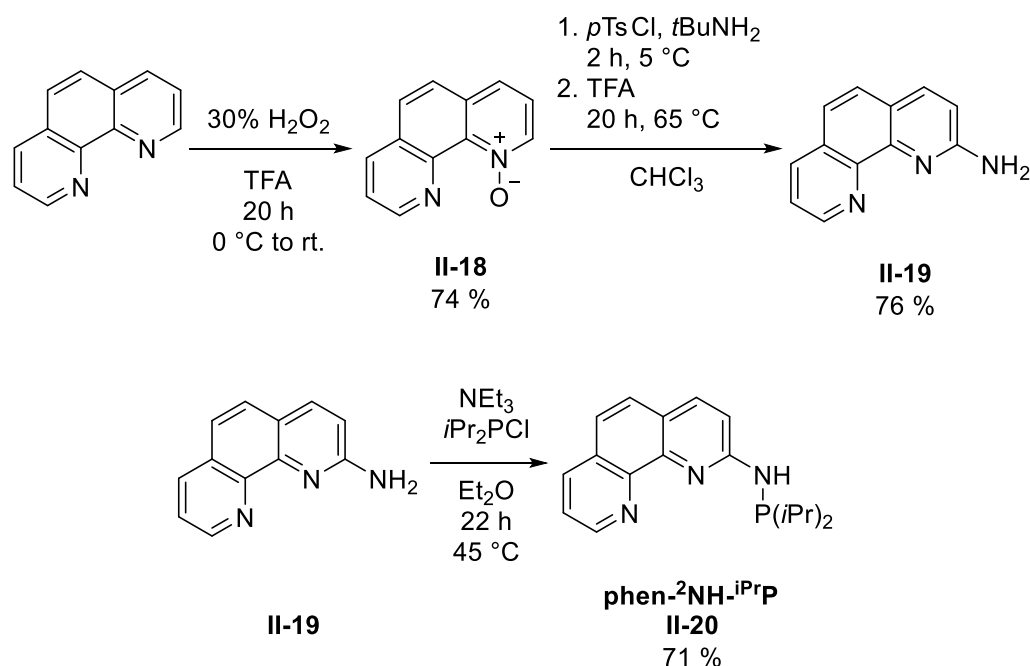
Scheme 96. Three-step preparation of **phen-^{2}NH-^{iPr}P** (**II-20**).

The preparation of the 1,10-phenanthroline-based ligand (**II-20**) followed the earlier optimized route for the preparation of **II-15** (compare Scheme 80). The reaction sequence was conducted without further optimization, since average yields were obtained for all three steps to provide **II-20** in an acceptable overall yield of 40 % (Scheme 96). The product was isolated as an off-white low melting solid, which was isolated with approximately 5 mol% impurities according to the ^{31}P{^{1}H} NMR spectrum. However, similar impurities were observed for **II-15** which vanished during complex formation. The ^{31}P{^{1}H} NMR spectroscopic investigation of **II-20** showed signals with comparable chemical shifts (48.8 ppm) as for **II-15** (48.9 ppm). As for the preliminary nature of this synthesis, we assumed that the complexation behavior of **II-20** would match the complexation behavior of **II-15**.

4.3.4.2 Preparation of oxazoline-pyridine ligands
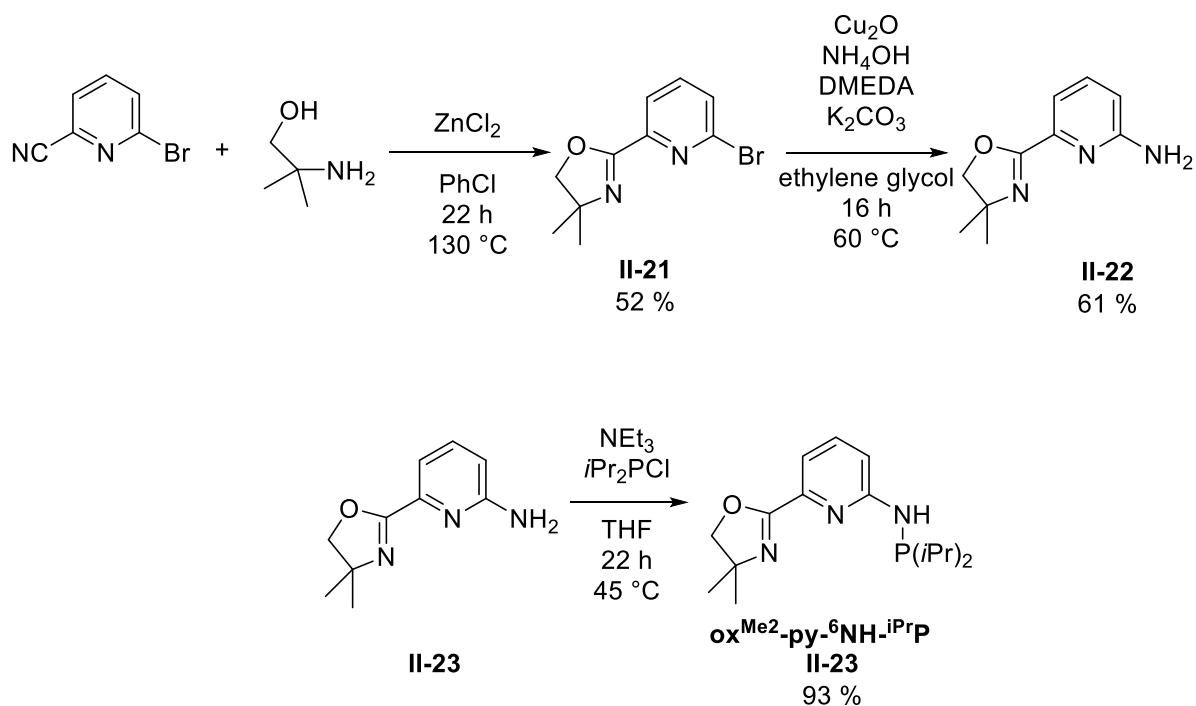
Scheme 97. Three-step preparation of **ox^{Me2}-py-⁶NH-^{iPr}P (II-23)**.[249, 273]

The preparation of the oxazoline substituted ligand **ox^{Me2}-py-⁶NH-^{iPr}P (II-23)** was conducted in three consecutive steps (Scheme 97, see also Scheme 79). First, a well-known preparation strategy for pyridine bis-oxazoline ligands was adapted providing **II-21** in a 52 % yield.[273] Attempts to optimize the conditions by altering the reaction time and temperature remained unsuccessful. A copper(I) catalyzed amination was employed to obtain **II-22** in a 61 % yield.[253] The starting material **II-21** was completely consumed providing **II-22** and a side product in 39 % GC yield was formed which could be removed by column chromatography. However, it could not be characterized by NMR spectroscopic investigations. GC-MS analysis suggested a molecular mass difference of 2 compared to **II-22** which could originate from a hydrogenation reaction. Since the reaction provided **II-22** in an average yield, it was not further optimized at this point. The last step, introduction of the phosphine group, provided **ox^{Me2}-py-⁶NH-^{iPr}P (II-23)** in a good yield of 93 %. The product was obtained as yellow oil which solidified at –35 °C with slight impurities visible in the ^{1}H NMR-spectrum. Attempts to follow the established synthetic route for **bpy-⁶NH (II-13)** (Scheme 80) with the preparation of an N-oxide remained unsuccessful.[274] Instead hydrolysis of the oxazoline upon treatment with per-acids was observed (Scheme 98, compare with Scheme 80).
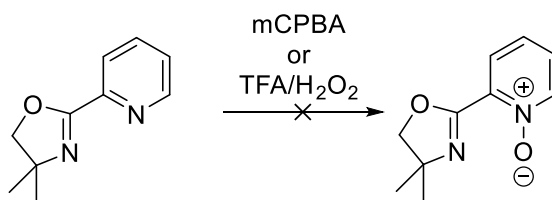
Scheme 98. Attempted N-oxidation of ox^{Me,Me}-py.[274]

II-(R)-24	R = H	R' = iPr	79 %
II-(S)-25	R = iPr	R' = H	66 %
II-(S)-26	R = CH$_2$iPr	R' = H	70 %
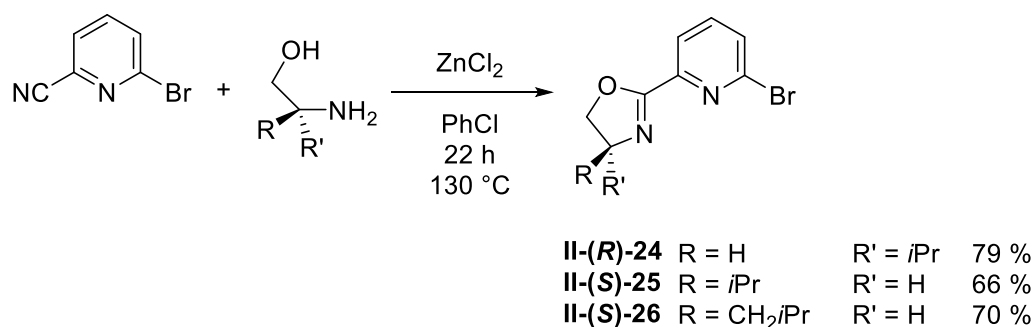
Scheme 99. Exemplary preparation of different chiral **ox^{R,R}-py-Br** (**II-24–II-26**) ligand precursors.

The advantage of employing pyox ligands is their structural tunability by using chiral amino alcohols that derive from amino acids. Thus, a small set of different chiral **ox^{R,R}-py-Br** (**II-24–II-26**) was prepared exemplary (Scheme 99), which can serve as building blocks for potential chiral pincer ligands in future studies.

A complexation experiment of **II-23** with Mn(CO)$_5$Br monitored by ^{31}P{^{1}H} NMR spectroscopy showed the formation of a new species at 96.9 ppm (Figure 36). Upon treatment with one equivalent of NaBEt$_3$H a new species with a chemical shift of 142.6 ppm was observed (compare to Scheme 83).[206] The formed species could not be clearly identified in the recorded ^{1}H or ^{13}C{^{1}H} NMR spectras. However, the observed changes in of the ^{31}P{^{1}H} NMR spectrum was taken as indication for complex formation.
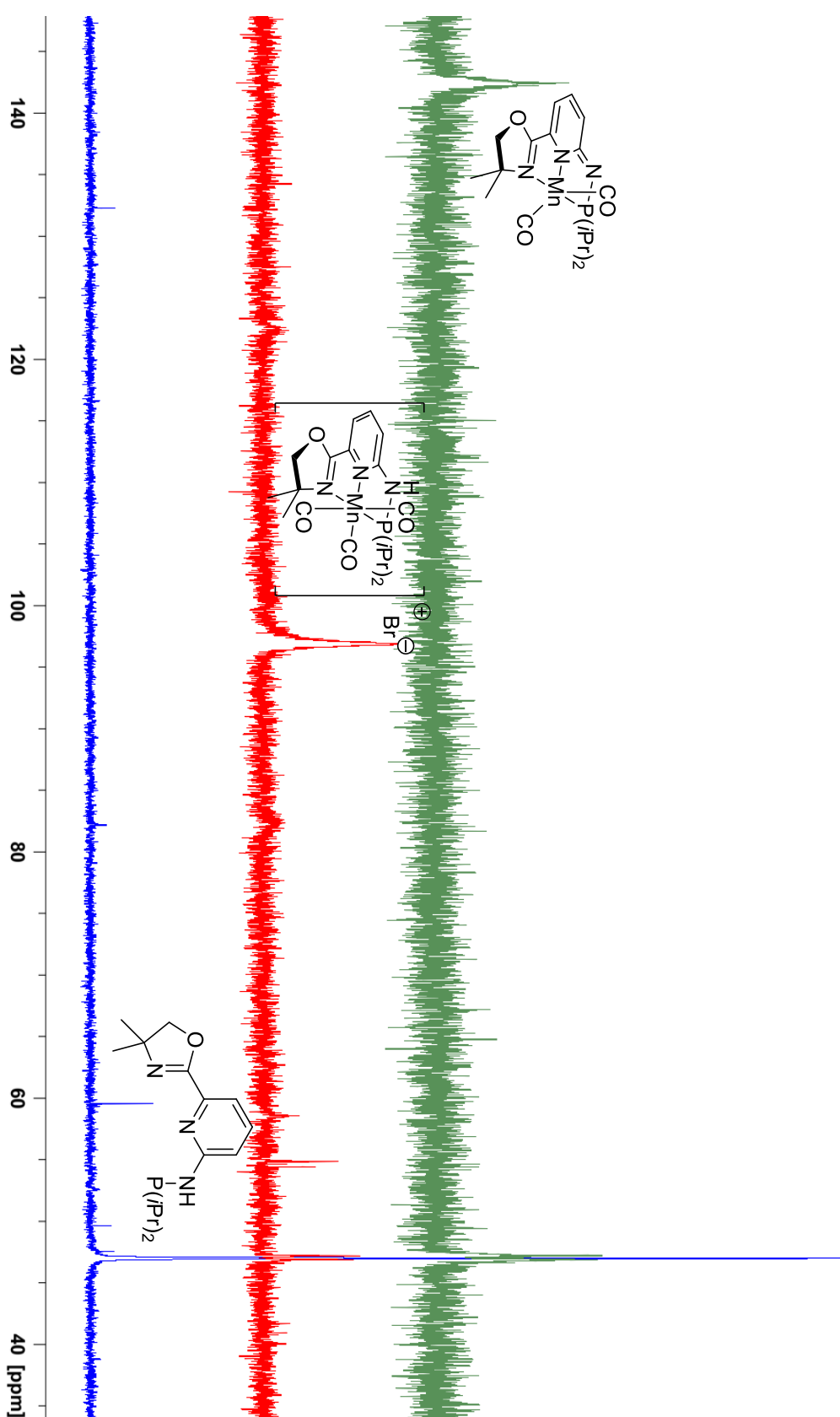
Figure 36. Complexation reaction of **ox^{Me2}-py-^{6}NH-^{iPr}P (II-23)** with Mn(CO)$_5$Br monitored by ^{31}P{^{1}H} NMR spectroscopy (162.0 Mhz) in THF-d_8: ligand **II-23** (blue); combination with Mn(CO)$_5$Br after 5 min (red); treatment with 1 equiv NaBEt$_3$H (green).

4.3.4.4 Application of prepared PN^3 in Borrowing Hydrogen Catalysis

With a set of 4 different PN^3-ligands in hand, their reactivity as catalysts for the N-alkylation of anilines with benzyl alcohol was compared.[255] The reaction conditions for **II-17**, **II-20** and **II-23** were chosen more forcing than for **II-15**, since preliminary tests indicated lower catalytic activity.

Table 38. Different PN^3-ligands employed in N-alkylation of aniline with benzyl alcohol.

#	ligand	structure	conv.[a] [%]	ratio **A : I**[a]
1	**bpy-^{6}NH$^{-(R)BINOL}$P** (**II-17**)		74	only **A**
2	**phen-^{2}NH-^{iPr}P** (**II-20**)		>99	only **A**
3	**ox^{Me2}-py-^{6}NH-^{iPr}P** (**II-23**)		88	only **A**
4[b]	**bpy-^{6}NH-^{iPr}P** (**II-15**)		>99	only **A**

General conditions: 1.1 mmol aniline, 1.0 mmol benzyl alcohol, 30 µmol Mn(CO)$_5$Br, 30 µmol ligand in 0.1 mL DME; [a] determined by GC-FID with *p*-xylene as standard; [b] 50 mol% KH, 0.5 mol% Mn(CO)$_5$Br/**II-15** at 50 °C.[255]

All PN^3 ligands readily catalyzed the N-alkylation of aniline with benzyl alcohol at the chosen reaction conditions (Table 38, entries 1–3). Since the reactions were carried out under more forcing conditions compared to the system based on **bpy-^{6}NH-^{iPr}P** (Table 38, entry 4), the ligand systems **II-17** and **II-23** seem less active for this type of reaction. For **II-17**

not only the steric hindrance of the BINOL group might affect the reactivity, but also the lower electron density of a phosphoramidite compared to an aminophosphine (as in **II-15**) could have a debasing effect on the reactivity. The lower reactivity when **II-23** is employed compared to **II-15** and **II-20** might be explained with a smaller aromatic system limited to the pyridine moiety. Since larger delocalized aromatic system were found to promote the MLC effect better, enhancing its reactivity.[36, 231]

Also the newly discovered N-alkylation of anilines with secondary alcohols was investigated with the new ligands **II-17** and **II-23**. *sec*-Butanol was chosen as substrate (Table 39) due to the potential implementation of a chiral complex to eventually prepare chiral amines with a PN^3-ligated manganese pincer complex. The reaction conditions were taken from the optimized system that was published earlier.[255]

Table 39. Different PN^3-ligands employed in N-alkylation of aniline with *sec*-butanol.

#	ligand	structure	conv.[a] [%]	ratio **A** : **I**[a]
1	**bpy-^{6}NH$^{-(R)BINOL}$P** (**II-17**)		8	only **I**
2	**ox^{Me2}-py-^{6}NH-^{iPr}P** (**II-23**)		7	only **I**
3	**bpy-^{6}NH-^{iPr}P** (**II-15**)		57	only **A**

General conditions: 1.1 mmol aniline, 1.0 mmol *s*BuOH, 5 μmol Mn(CO)$_5$Br, 5 μmol ligand in 0.1 mL DME; [a] determined by GC-FID with *p*-xylene as standard.

The application of a secondary alcohol in the N-alkylation is a challenging task for ligands **II-17** and **II-23** since they both exhibited limited catalytic activity. Low conversions to

dehydrogenative aldimine coupling product was observed exclusively (Table 39, entries 1–2). It seems, that a ligand employed in this reaction should provide both a comparatively electron rich aminophosphine moiety (Table 39, entry 1 vs 3) as well as an extended aromatic system (Table 39, entry 2 vs 3). Thus, attempts to introduce chirality into the PN³-ligand scaffold should focus on derivatives of **II-15** or **II-20**.

4.4 Conclusion and Outlook

A manganese-based catalyst for the N-alkylation of amines with alcohols was successfully implemented. The system was optimized in a multi-dimensional manner, which lead to a system that performed with substoichiometric amounts of potassium hydride as base additive at temperatures as low as 60 °C for N-benzylation of aniline. It was found that both neat reactions as well as reactions in ethers provide excellent results, which allowed us to work with catalyst loadings as low as 0.25 mol%. The optimized conditions were found suitable for a range of different benzyl alcohols and anilines, and the reaction could easily be performed at gram scale. Moreover, we successfully employed secondary alcohols as well as nucleophilic amines by adjusting the reaction temperature or the reaction time.

Exemplary investigations were conducted on the applicability of our developed system for other reactions and we confirmed activity for the C-alkylation of secondary alcohols and amides, which was already presented in literature with other manganese.[204, 238, 261-262, 275-276] Further, different potential applications of our developed system were briefly investigated. This included intramolecular N-alkylation reactions, the combined C- and N-alkylation of ureas and amides, and the preparation of azobenzene from nitrobenzene. The preliminary indicate that the developed catalytic system can be applied in a manifold of reactions with proper adjustment of the reaction conditions.

Aside from applying the borrowing hydrogen methodology in different types of reactions, some challenges have to still to be addressed. Primary amines show excellent activity for the N-alkylation while secondary amines could not be implemented as substrates yet. Also the preparation of ligand system that performs enantioselective N-alkylation is still being sought. Transfer hydrogenation of imines with manganese based catalysts has already been reported and the next step would be an asymmetric process.[257]

As a first step for following investigations, the structural tuneability of PN^3 ligands for manganese-based catalyst systems was presented. This provides the opportunity to introduce chirality at different positions in the ligand for potential asymmetric catalytic applications.

4.6 Experimental section

4.6.1 Working methods

If not explicitly mentioned differently, all reactions were carried out in an inert gas atmosphere under exclusion of air and moisture at room temperature. These conditions were ensured by using the Schlenk-technique or working in a glove box. Solvents used for preparations or analytics were dried with sodium and benzophenone or calcium hydride, and distilled under inert gas atmosphere. Commercially obtained starting materials were purified if needed. GC analyses were carried out using an *Agilent Technologies 7890A* system equipped with a *HP-5* column (30 m, 320 μm, 0.25 μm) or *Shimadzu GC-2010 Plus* equipped with a *HP-5* column (30 m, 320 μm, 0.25 μm). GC-FID conditions: (Inlet temp.: 270 °C, carrier gas flow: He at 34.9 cm s^{-1}; oven temperature: 50 °C (2.25 min) to 300 °C at 25 °C min^{-1} (hold 5 min) for a total run time of 17.25 min). GC-MS analyses were carry out on an Agilent 7820A/MSD 5977B system equipped with a *HP-5MS* column (30 m, 250 μm, 0.25 μm). GC-MS conditions: Inlet temp.: 270 °C, carrier gas flow: He at 39.8 cm s^{-1}; oven temperature: 45 °C (2.25 min) to 300 °C at 25 °C min^{-1} (hold 0.55 min) for a total run time of 13 min). NMR spectroscopic experiments were performed on *Bruker AVIII* and *Bruker AVIII* HD instruments (400, 600 and 700 MHz). Chemical shifts (δ in ppm) are indicated relative to TMS and were referenced to residual protons in the solvent. Air-tight sealed NMR tubes were used for NMR experiments for compounds that were air or moisture sensitive. NMR experiments were performed at room temperature (25 °C) if not explicitly mentioned otherwise. *Merck* aluminum oxide 90 active basic (0.063–0.200 mm particle size, activity stage I) was used for column chromatography.

Table 40. Chemical shifts and multiplicities of used deuterated solvents.[139]

Solvent	δ (^{1}H) / ppm (multiplicity)	δ (^{13}C{^{1}H}) / ppm (multiplicity)
CDCl$_3$	7.26 (br s)	77.16 (t)
CD$_2$Cl$_2$	5.32 (t)	53.84 (quint)
C$_6$D$_6$	7.16 (br s)	128.06 (t)
Acetone-d_6	2.05 (m)	206.26 (s)
		29.84 (sept)
DMSO-d_6	2.50 (m)	39.52 (sept)
THF-d_8	3.58 (br s)	67.21 (quint)
	1.73 (br s)	25.31 (quint)
toluene-d_8	2.08 (quint)	20.43 (sept)
	6.97 (br s)	125.13 (t)
	7.01 (br s)	127.96 (t)
	7.09 (br s)	128.87 (t)
		137.48 (s)

4.5.2 Synthesis of pincer ligands

4.5.2.1 Synthesis of 2,6-bis((di-*tert*-butylphosphaneyl)methyl)pyridine (*tBu*PCNCP)[191]
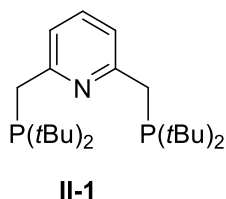
A solution of 2,6-Lutidine (0.75 mL, 692 mg, 6.45 mmol, 1.0 equiv) in Et$_2$O (10 mL) was cooled to 0 °C in an ice bath and *n*BuLi (5.3 mL, 2.5 M in hexane, 13.25 mmol, 2.05 equiv) was added slowly to the solution. The mixture was allowed to warm to room temperature and eventually refluxed at 40 °C overnight. After cooling to -78 °C, *t*Bu$_2$PCl (3.0 mL, 2.85 g, 15.79 mmol, 2.44 equiv) was added dropwise over 5 min and let warm to room temperature under stirring. Freshly degassed water (10 mL) was added and the supernatant organic phase was collected by removing the aqueous phase with a syringe. Degassed MgSO$_4$ was added in the glovebox and the organic phase was left for drying overnight. The drying agent is removed by filtration with a cannula and extracted with Et$_2$O (3 × 3 mL). The combined organic fractions were concentrated under reduced pressure until precipitation began and then stored for crystallization at -18 °C overnight. The product was obtained as pale yellow crystals after removal of the mother liquor and drying *in vacuo*.

Yield: 760 mg (1.92 mmol, 30 %).

^{1}H NMR (C$_6$D$_6$, 25 °C, 400.3 MHz, ppm): δ = 7.24 (br m, 1H, ^{4}Py-*H*), 7.23 (br m, 2H, ^{3,5}Py-*H*), 3.11 (s br, 4H, 2 × C*H$_2$*), 1.12 (d, 36H, 4 × *t*Bu). ^{31}P{^{1}H} NMR (C$_6$D$_6$, 25 °C, 162.0 MHz, ppm): δ = 35.2. The NMR spectroscopic data are in accordance with the literature.[191]

4.5.2.2 Preparation of *N^2,N^6*-bis(di-tert-butylphosphaneyl)pyridine-2,6-diamine di borane (*tBu*PNNNP×(BH$_3$)$_2$)
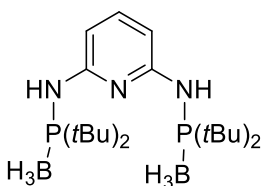
Diaminopyridine (138 mg, 1.27 mmol, 1.0 equiv) was dissolved in 15 mL toluene and triethylamine (0.35 mL, 256 mg, 2.52 mmol, 2.0 equiv) was added at once. The solution was cooled down to 0 °C and *t*Bu$_2$PCl (456 mg, 0.48 mL, 2.53 mmol, 2.0 equiv) was added. The reaction temperature was lowered to –78°C and *n*BuLi (1.1 mL, 2.33 M in hexane, 2.56 mmol, 2 equiv) was added dropwise. The reaction mixture was allowed to warm to room temperature and then heated to 80 °C overnight. The precipitate was removed by cannula filtration and all volatiles were removed *in vacuo*. The crude product mixture was dissolved in 15 mL Et$_2$O and BH$_3$×SMe$_2$ (0.55 mL >90 % in SMe$_2$, 0.45 g, 6.52 mmol, 5.1 equiv) was added at once. The reaction mixture was stirred at room temperature for 2 h until no further gas evolution was observed. All volatiles were removed *in vacuo* leaving a colorless oil. The residue was purified by column chromatography (SiO$_2$, EtOAc : hept 1:1) and an off-white low melting product was obtained.

Yield: 324 mg (0.76 mmol, 60 %).

^{1}H NMR (CDCl$_3$, 25 °C, 400.3 MHz, ppm): δ = 7.35 (t, 1H, ^{4}Py-*H*), 6.82 (d, 2H, ^{3,5}Py-*H*), 4.69 (s br, 2H, 2 × N*H*), 1.33 (m, 36H, 4 × *t*Bu) ^{31}P{^{1}H} NMR (CDCl$_3$, 25 °C, 162.0 MHz, ppm): δ = 82.36.

4.5.2.3 Preparation of ^{tBu}PNNNP
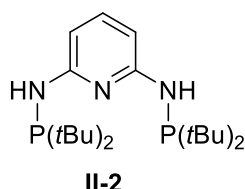
*t*BuPNNNP×(BH$_3$)$_2$ was dissolved in freshly degassed Et$_2$NH (12 mL, 8.52 g, 116.5 mmol, 153 equiv) and heated to 70 °C for 16 h. Subsequently all volatiles were removed *in vacuo* and colorless oil was obtained as product. ^{31}P{^{1}H} NMR did not show any residual borane protected species.

Yield: 294 mg (0.74 mmol, 97 %).

^{1}H NMR (C$_6$D$_6$, 25 °C, 400.3 MHz, ppm): δ = 7.02 (t, $^3J_{H,H}$ = 7.9 Hz, 1H, ^{4}Py-*H*), 6.85 (dd, $^3J_{H,H}$ = 7.9 Hz, 2H, ^{3,5}Py-*H*), 4.88 (d, $^2J_{H,P}$ = 11.2 Hz, 2H, 2 × N*H*), 1.02 (d, 36H, 4 × *t*Bu) ^{31}P{^{1}H} NMR (C$_6$D$_6$, 25 °C, 162.0 MHz, ppm): δ = 57.10.

4.5.2.4 Synthesis of 2,6-bis((di-*iso*-propylphosphaneyl)oxy)pyridine (^{iPr}PONOP)[243]
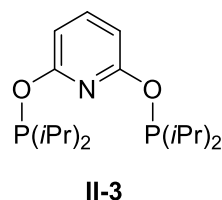
2,6-Hydroxypyridine hydrochloride (0.74 g, 5.01 mmol, 1.0 equiv), TMEDA (1.5 mL, 1.16 g, 10.00 mmol, 1.99 equiv) and triethylamine (4.26 mL, 3.09 g, 30.54 mmol, 6.1 equiv) were dissolved in THF (60 mL) and cooled to 0 °C. *i*Pr$_2$PCl (2.2 mL, 2.11 g, 13.83 mmol, 2.76 equiv) was added dropwise, the mixture was let warm to room temperature over 1 h and then heated to 65 °C overnight. The formed precipitate was removed by filtration and all volatiles were removed under reduced pressure subsequently. The yellow residue was extracted with benzene (3 × 15 mL) and the solvent was removed *in vacuo* subsequently. The residue was distilled through a vigreux column (155 °C/10^{-2} mbar) yielding a slightly yellow oily product.

Yield: 398 mg (0.99 mmol, 20 %).

^{1}H NMR (C$_6$D$_6$, 25 °C, 400.3 MHz, ppm): δ = 7.02 (t, J = 7.8 Hz, 1H, ^{4}Py-*H*), 6.19 (d, J = 7.8 Hz, 2H, ^{3,5}Py-*H*), 1.22 (sept, J = 7.0 Hz, 4H, 4 × C*H*(CH$_3$)$_2$), 1.09 (d, J = 7.1 Hz, 24H, 4 × CH(C*H$_3$*)$_2$). ^{31}P{^{1}H} NMR (C$_6$D$_6$, 25 °C, 162.0 MHz, ppm): δ = 148.22. The NMR spectroscopic data are in accordance with the literature.[243]

4.5.2.5 Preparation of *N*-(di-*iso*-propylphosphaneyl)-[2,2'-bipyridin]-6-amine ([bpy-[1]N-Me]I)[250]
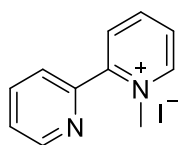
2,2'-Bipyridin (1.06 g, 6.97 mmol, 1.0 equiv) was dissolved in MeCN (16 mL), methyliodide (1.2 mL, 2.75 g, 19.28 mmol, 2.8 equiv) was added at once and the reaction mixture was stirred at 45 °C for 3 d. A color change to canary yellow was observed after 1 h of reaction time, although the reaction was left stirring under the noted conditions. A yellow crystalline product was obtained by filtration and careful washing with CH_2Cl_2 (4 × 3 mL). The yield was increased by precipitation from the mother liquor through addition of Et_2O and storage at 5 °C overnight.

II-10

Yield: 1.58 g (5.30 mmol, 76 %).

^{1}H NMR (C_6D_6, 25 °C, 400.3 MHz, ppm): δ = 9.43 (m, 1H), 8.71 (m, 1H), 8.47 (m, 1H), 8.10 (m, 1H), 8.03 (m, 1H), 7.94 (m, 2H), 7.48 (m, 1H), 4.43 (s, 3H, NCH_3). The NMR spectroscopic data are in accordance with the literature.[250]

4.5.2.6 Synthesis of 1-methyl-[2,2'-bipyridin]-6(1*H*)-one[250]
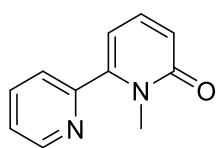
1-methyl-2.2'-bipyridinium iodide (1.61 g, 5.38 mmol, 1.0 equiv) and sodium hydroxide (4.33 g, 108.1 mmol, 20.0 equiv) were separately dissolved in water (20 mL) and cooled to 5 °C. Potassium hexacyanoferrate (III) (4.31 g, 13.08 mmol, 2.4 equiv) dissolved in water (25 mL), cooled to 5 °C and then both mixtures prepared earlier were added dropwise through Teflon cannulas over 30 min simultaneously. After addition, the flask was sealed with a septum and the reaction was kept for additional 2 h at 5 °C while stirring. Although a color change from yellow to deep red was observed, a TLC suggested residual starting material. So the reaction was allowed to warm to room temperature and stirring was continued overnight. The aqueous reaction mixture was extracted with CH_2Cl_2 (4 × 20 mL), the organic phases were combined and dried over $MgSO_4$. Volatiles were removed under reduced pressure providing the product as a brown oil that slowly solidified at room temperature.

II-11

Yield: 531 mg (2.85 mmol, 53 %).

^{1}H NMR (CDCl$_3$, 25 °C, 400.3 MHz, ppm): δ = 8.73 (ddd, J = 4.9 Hz, 1.8 Hz, 0.9 Hz, 1H, [6']Py-*H*), 7.83 (dt, J = 7.7 Hz, 1.8 Hz, 1H, [4']Py-*H*), 7.45 (dt, J = 7.7 Hz, 1.1 Hz, 1H, [3']Py-*H*), 7.38 (ddd, J = 7.7 Hz, 4.9 Hz, 1.1 Hz, 1H, [5']Py-*H*), 7.36 (dd, J = 8.9 Hz, 6.8 Hz, 1H, [4]Py-*H*), 6.65 (dd, J = 8.9 Hz, 1.4 Hz, 1H, [5]Py-*H*), 6.20 (dd, J = 6.8 Hz, 1.4 Hz, 1H, [3]Py-*H*), 3.45 (s, 3H, N-CH_3). The NMR spectroscopic data are in accordance with the literature.[250]

4.5.2.7 Synthesis of 6-bromo-2,2'-bipyridine[250]
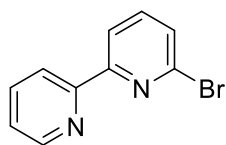
Freshly recrystallized PPh$_3$ (3.99 g, 15.2 mmol, 1.4 equiv) was dissolved in 15 mL MeCN, cooled to 0 °C and Br$_2$ (0.72 mL, 2.25 g, 14.1 mmol, 1.3 equiv) was added dropwise. A yellow suspension was formed after 0.5 h of stirring and 1-methyl-[2,2'-Bipyridin]-6(1H)-one (2.00 g, 10.7 mmol, 1.0 equiv) dissolved in 5 mL MeCN was added at once. The resulting brown reaction mixture was let warm to room temperature and then refluxed at 110 °C for 48 h. Then the mixture was poured into 50 mL ice water, filtered cold and treated with 50 mL saturated aqueous Na$_2$CO$_3$ solution. 60 mL CH$_2$Cl$_2$ were added to the mixture, the organic phase was separated and the aqueous phase was extracted with CH$_2$Cl$_2$ (4 × 60 mL). The combined organic phases were dried over MgSO$_4$ and concentrated under reduced pressure. The off-white residue was purified by column chromatography (SiO$_2$, EtOAc : heptanes 1:1) to remove residual phosphorus compounds. An off-white amorphous powder was obtained as product after removing all volatiles *in vacuo*.

Yield: 649 mg (2.76 mmol, 26 %).

^{1}H NMR (CDCl$_3$, 25 °C, 400.3 MHz, ppm): δ = 8.66 (m, 1H, $^{6'}$Py-*H*), 8.39 (m, 2H, ^{4}Py-*H* & $^{4'}$Py-*H*), 7.82 (m, 1H, $^{3'}$Py-*H*), 7.67 (m, 1H, ^{3}Py-*H*), 7.49 (m, 1H, ^{5}Py-*H*), 7.32 (m, 1H, ^{5}Py-*H*). The NMR spectroscopic data are in accordance with the literature.[250]

4.5.2.8 Synthesis of 6-amino-2,2'-bipyridine from II-12[249]
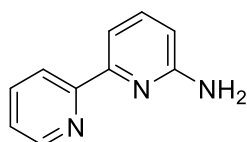
A Schlenk-tube was charged with 6-Bromo-2,2'-bipyridine (137 mg, 0.58 mmol, 1.0 equiv) dissolved in ethane-1,2-diol (1 mL) and degassed by three freeze-pump-thaw cycles. The solution was stirred and ammonium hydroxide (3.6 mL, 28 wt% in water, 907 mg, 25.9 mmol, 45 equiv), copper(I) oxide (4.2 mg, 0.029 mmol, 0.05 equiv) and N,N'-dimehtylethane-1,2-diamine (6.2 µL, 5.1 mg, 0.058 mmol, 0.1 equiv) were added subsequently. The reaction was stirred for 5 min, K$_2$CO$_3$ (16 mg, 0.116 mmol, 0.2 equiv) was added, the Schlenk-tube was closed and the mixture was heated to 60 °C and stirred for 16 h behind a blast shield. The reaction was allowed to reach room temperature and was extracted with EtOAc (4 × 20 mL). The combined organic phases were dried over MgSO$_4$, concentrated *in vacuo* and purified by column chromatography (Al$_2$O$_3$, hept : EtOAc 99:1 to 1:99, then EtOAc : MeOH 99:1 to 80:20). An off-white product was obtained whose ^{1}H NMR spectroscopic signals were in good accordance with the product prepared from **II-14**.

Yield: (95 mg, 0.55 mmol, 95 %).

^{1}H NMR (CDCl$_3$, 25 °C, 400.3 MHz, ppm): δ = 8.65–8.67 (m, 1H), 8.25–8.29 (m, 1H), 7.75–7.81 (m, 1H), 7.71–7.74 (m, 1H), 7.55–7.60 (m, 1H), 7.24–7.28 (m, 1H), 6.53–6.56 (m, 1H), 4.49 (br s, NH_2); ^{13}C{^{1}H} NMR (CDCl$_3$, 25 °C, 100.6 MHz, ppm): δ = 158.1 (^{6}C$_q$-NH$_2$), 156.6 (^{2}C$_q$), 154.8 ($^{2'}$C$_q$), 149.3 ($^{6'}$CH), 138.7 (^{4}CH), 136.8 ($^{4'}$CH), 123.4 ($^{5'}$CH), 121.1 ($^{3'}$CH), 111.8 (^{3}CH), 109.0 (^{5}CH). The NMR spectroscopic data are in accordance with the literature.[249]

4.5.2.9 Synthesis of 2,2'-bipyridine *N* monoxide[252-253]

II-14
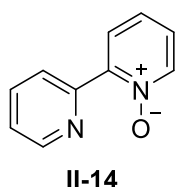
A round bottom flask was charged with 2,2'-bipyridine (4.57 g, 29.3 mmol, 1.0 equiv), TFA (20 mL, 29.8 g, 261.4 mmol, 8.9 equiv) was added and then the reaction mixture was cooled to 0 °C. A septum was fitted on the round bottom flask and then H$_2$O$_2$ (4.5 mL, 30 wt% in water, 1.50 g, 44.0 mmol, 1.5 equiv) was added dropwise over 15 min. The reaction was allowed to reach room temperature and was stirred for 2.5 h. CHCl$_3$ (100 mL) was added for dilution, the organic phase was collected by phase separation and carefully washed with NaOH (6 M, 4 × 30 mL). The combined aqueous phases were extracted with CH$_2$Cl$_2$ (3 × 50 mL), combined and dried over MgSO$_4$. All volatiles were removed under reduced pressure, leaving an off white amorphous product.

Yield: (4.536 g, 26.3 mmol, 90 %).

^{1}H NMR (CDCl$_3$, 25 °C, 400.3 MHz, ppm): δ = 8.89–8.91 (m, 1H, ^{6}Py-*H*), 8.71–8.72 (m, 1H, $^{6'}$Py-*H*), 8.30–8.31 (m, 1H, ^{4}Py-*H*), 8.16–8.19 (m, 1H, $^{4'}$Py-*H*), 7.80–7.84 (m, 1H, ^{3}Py-*H*), 7.32–7.37 (m, 2H, ^{4}Py-*H* & $^{4'}$Py-*H*), 7.24–7.28 (m, 1H, $^{3'}$Py-*H*). The NMR spectroscopic data are in accordance with the literature.[252-253]

### 4.5.2.10 Synthesis of 6-amino-2,2'-bipyridine from II-14[252-253]

II-13
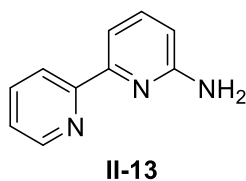
II-14 (4.50 g, 26.1 mmol, 1.0 equiv) and *t*BuNH$_2$ (17.3 mL, 12.11 g, 165.6 mmol, 6.3 equiv) were dissolved in CHCl$_3$ (100 mL) and degassed with 3 freeze-pump-thaw cycles. The mixture was cooled to 5 °C, TsCl (12.50 g, 65.6 mmol, 2.5 equiv) was added at once and then the reaction mixture was stirred for 2 h at 5 °C. TFA (50 mL, 74.50 g, 653.4 mmol, 25.0 equiv) was added at once and the reaction was heated to 65 °C for 20 h. The reaction mixture was allowed to cool to room temperature and all volatiles were removed under reduced pressure, leaving a brown oily residue. The residue was dissolved in MTBE (20 mL), treated with HCl (4 M, 26 mL) and the aqueous phase was separated. The organic phase was extracted with water (3 × 20 mL) and the combined aqueous phases were then treated with NaOH (2 M, 60 mL). Subsequently, saturated aqueous Na$_2$CO$_3$ solution was added to adjust the pH >7. The formed organic phase was diluted with CH$_2$Cl$_2$ (50 mL), separated and

the aqueous phase was extracted with CH_2Cl_2 (3 × 50 mL). The combined organic phases were concentrated under reduced pressure. Purification by column chromatography (Al_2O_3, hept : EtOAc 99:1 to 1:99, then EtOAc : MeOH 99:1 to 80:20) provided analytically clean off-white powder as product.

Yield: 4.26 g (24.9 mmol, 95 %).

^{1}H NMR (CDCl$_3$, 25 °C, 400.3 MHz, ppm): δ = 8.65–8.67 (m, 1H), 8.25–8.29 (m, 1H), 7.75–7.81 (m, 1H), 7.71–7.74 (m, 1H), 7.55–7.60 (m, 1H), 7.24–7.28 (m, 1H), 6.53–6.56 (m, 1H), 4.49 (br s, NH_2); ^{13}C{^{1}H} NMR (CDCl$_3$, 25 °C, 100.6 MHz, ppm): δ = 158.1 (^{6}C$_q$-NH$_2$), 156.6 (^{2}C$_q$), 154.8 (^{2}C$_q$), 149.3 (^{6}CH), 138.7 (^{4}CH), 136.8 ($^{4'}$CH), 123.4 (^{5}CH), 121.1 (^{3}CH), 111.8 (^{3}CH), 109.0 (^{5}CH). The NMR spectroscopic data are in accordance with the literature.[252-253]

4.5.2.11 *N*-(di-*iso*-propylphosphaneyl)-[2,2'-bipyridin]-6-amine (bpy-^{6}NH–^{iPr}P)[164]
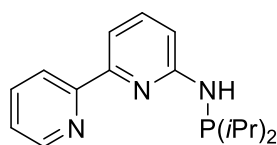
II-15

II-13 (334 mg, 1.95 mmol, 1.0 equiv) was dissolved in THF (10 mL) and degassed, NEt$_3$ (0.25 mL, 238 mg, 2.35 mmol, 1.2 equiv) was added at once. *i*Pr$_2$PCl (0.34 mL, 326 mg, 2.14 mmol, 1.1 equiv) was added dropwise and the reaction mixture was stirred at room temperature for 16 h. The precipitate was filtered off, the residue was extracted with THF (3 × 5 mL) and all volatiles were removed *in vacuo* at 60 °C. The product was obtained as slightly yellow oil that solidified and became an off-white powder upon scratching with a spatula.

Yield: 518 mg (1.80 mmol, 92 %).

^{1}H NMR (THF-d_8, 25 °C, 600.3 MHz, ppm): = 8.56–8.58 (m, 1H), 8.38–8.41 (m, 1H), 7.82–7.84 (m, 1H), 7.73–7.77 (m, 1H), 7.51–7.55 (m, 1H), 7.22–7.25 (m, 1H), 7.04–7.07 (m, 1H), 5.68 (d, $^2J_{H,P}$ = 9.3 Hz, 1H, NH), 1.88–1.95 (m, 2H, 2 × CH(CH$_3$)$_2$), 1.06–1.14 (m, 12H, 2 × CH(CH_3)$_2$); ^{13}C{^{1}H} NMR (THF-d_8, 25 °C, 150.9 MHz, ppm): δ = 161.5 (d, $^2J_{C,P}$ = 18.4 Hz, ^{6}C$_q$), 157.5 (^{2}C$_q$), 155.2 (d, $^4J_{C,P}$ = 0.9 Hz, ^{2}C$_q$), 149.7 (^{6}CH), 138.4 (d, $^4J_{C,P}$ = 1.9 Hz, ^{4}CH), 136.8 ($^{4'}$CH), 123.8 (^{5}CH), 121.1 (^{3}CH), 111.9 (^{3}CH), 109.9 (d, $^3J_{C,P}$ = 15.2 Hz, ^{5}CH), 27.2 (d, $J_{C,P}$ = 12.4 Hz, ^{7}CH), 19.3 (d, $J_{C,P}$ = 21.2 Hz, ^{8}CH$_3$), 17.8 (d, $J_{C,P}$ = 8.5 Hz, ^{8}CH$_3$); ^{31}P{^{1}H} NMR (THF-d_8, 25 °C, 243.0 MHz, ppm): δ = 48.9.

4.5.2.12 *N*-(di-*tert*-butylphosphaneyl)-[2,2'-bipyridin]-6-amine (bpy-[6]NH–[tBu]P)[164, 251, 254]

The reaction was conducted according to 4.5.2.11. The obtained product was found inseparable from unconverted starting material so no yield is provided.
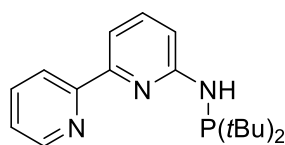
$^{31}P\{^{1}H\}$ NMR (THF-d_8, 25 °C, 243.0 MHz, ppm): δ = 61.7. The NMR spectroscopic data are in accordance with the literature.[251]

4.5.2.13 *N*-(dicylohexylphosphaneyl)-[2,2'-bipyridin]-6-amine (bpy-[6]NH–[Cy]P)[164, 254]

The reaction was conducted according to 4.5.2.11. The obtained product was found inseparable from unconverted starting material so no yield is provided.
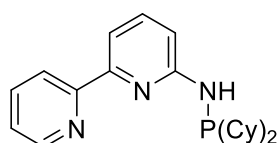
$^{31}P\{^{1}H\}$ NMR (THF-d_8, 25 °C, 243.0 MHz, ppm): δ = 41.3.

4.5.2.14 *N*-(diphenylylphosphaneyl)-[2,2'-bipyridin]-6-amine (bpy-[6]NH–[Ph]P)[164, 254]

The reaction was conducted according to 4.5.2.11. The obtained product was found inseparable from unconverted starting material so no yield is provided.
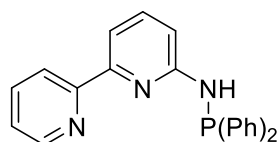
$^{31}P\{^{1}H\}$ NMR (THF-d_8, 25 °C, 243.0 MHz, ppm): δ = 25.4. The NMR spectroscopic data are in accordance with the literature.[254]

4.5.2.15 Synthesis of 1,1'-(pyridine-2,6-diyl)bis(*N*-(2,6-di-*iso*-propylphenyl)ethan-1-imine) ([dipp]NCNCN)[194]
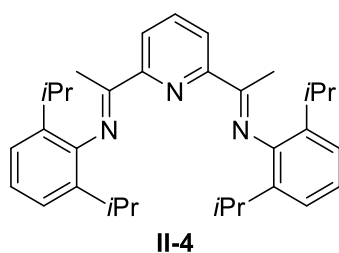
1,1'-(pyridine-2,6-diyl)bis(ethan-1-one) (1.698 g, 10.41 mmol, 1.0 equiv), 2,6-di-i*so*-propylaniline (4.324 g, 24.40 mmol, 2.0 equiv) and formic acid (40 µL, 49 mg, 1.06 mmol 0.1 equiv) were dissolved in MeOH (250 mL) and heated to reflux (75 °C) overnight. The reaction mixture was cooled to -18 °C in the freezer for 4 h. Slightly yellow product was collected by filtration and subsequent washing with cold MeOH (3 × 25 mL).

Yield: 4.279 g (8.89 mmol, 85 %).

^{1}H NMR (C$_6$D$_6$, 25 °C, 400.3 MHz, ppm): δ = 8.50 (d, 2H), 7.30 (t, 1H), 7.14–7.24 (m, 6H), 2.92 (m, 4H, 4 × C*H*(CH$_3$)$_2$), 2.28 (s, 6H, 2 × CH$_3$), 1.20 (d, 12H, 4 × CH(C*H*$_3$)$_2$), 1.16 (d, 12H, 4 × CH(C*H*$_3$)$_2$). The NMR spectroscopic data are in accordance with the literature.[194]

4.5.2.16 Synthesis of 1,10-phenanthroline *N* monoxide

II-18
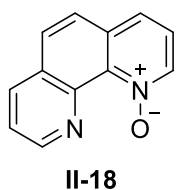
1,10-phenanthroline (1.00 g, 5.55 mmol, 1.0 equiv) was dissolved in TFA (10 mL, 14.9 g, 86.5 mmol, 15.6 equiv) and cooled to 0 °C. A septum was fitted on the round bottom flask and H_2O_2 (0.8 mL, 30 wt% in water, 267 mg, 7.8 mmol, 1.4 equiv) was at once and the reaction was stirred at 0 °C for 30 min. The reaction was allowed warm to room temperature over 20 h, stopped by dilution with CH_2Cl_2 (50 mL) and its pH was adjusted by subsequent addition of NaOH (2.5 M, 40 mL) and Na_2CO_3 (aq. sat. 150 mL). The organic phase was separated and the aqueous phase was extracted with CH_2Cl_2 (4 × 70 mL). The combined organic phases were dried over $MgSO_4$ and all volatiles were removed providing an analytically pure yellow solid.

Yield: 809 mg (4.12 mmol, 74 %).

^{1}H NMR (CDCl$_3$, 25 °C, 400.3 MHz, ppm): δ = 9.32 (dd, $J_{H,H}$ = 1.8 Hz & 4.3 Hz, 1H), 8.74 (dd, $J_{H,H}$ = 6.3 & 0.9 Hz, 1H), 8.23 (dd, $J_{H,H}$ = 8.1 & 1.9 Hz, 1H), 7.81 (m, 1H), 7.74 (m, 2H), 7.66 (dd, $J_{H,H}$ = 7.9 & 4.3 Hz, 1H), 7.45 (dd, $J_{H,H}$ = 8.2 & 6.1 Hz, 1H); ^{13}C{^{1}H} NMR (CDCl$_3$, 25 °C, 100.6 MHz, ppm): δ = 150.1, 140.9, 135.9 (aryl), 135.4 (C$_q$), 129.1 (aryl), 128.9 (C$_q$), 126.5, 124.4, 123.2, 122.9 (aryl). The NMR spectroscopic data are in accordance with the literature.[277]

4.5.2.17 Synthesis of 2-amino-1,10'-bipyridine

II-19
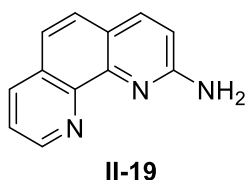
II-18 (809 mg, 4.12 mmol, 1.0 equiv) and *t*BuNH$_2$ (2.2 mL, 1.54 g, 21.06 mmol, 5.1 equiv) were dissolved in CHCl$_3$ (20 mL) and degassed with 3 freeze-pump-thaw cycles. The mixture was cooled to 5 °C, TsCl (1.57 g, 8.23 mmol, 2.0 equiv) was added at once and then the reaction mixture was stirred for 2 h at 5 °C. TFA (40 mL, 59.60 g, 522.7 mmol, 126.8 equiv) was added at once and the reaction was heated to 65 °C for 20 h. The reaction mixture was allowed to cool to room temperature and all volatiles were removed under reduced pressure, leaving a brown oily residue. The residue was dissolved in MTBE (20 mL), treated with HCl (4 M, 10 mL) and the aqueous phase was separated. The organic phase was extracted with water (3 × 10 mL) and the combined aqueous phases were then treated with NaOH (2 M, 30 mL). Subsequently, saturated aqueous Na_2CO_3 solution was added to adjust the pH >7. The formed organic phase was diluted with CH_2Cl_2 (50 mL), separated and the aqueous phase was extracted with CH_2Cl_2 (3 × 50 mL). The combined organic phases were concentrated under reduced pressure. Purification by column chromatography (Al$_2$O$_3$, hept : EtOAc 99:1 to

1:99, then EtOAc : MeOH 99:1 to 80:20) provided analytically clean off-white powder as product.

Yield: 610 mg (3.12 mmol, 76 %).

^{1}H NMR (CDCl$_3$, 25 °C, 400.3 MHz, ppm): δ = 9.01 (dd, $J_{H,H}$ = 4.3 & 1.7 Hz, 1H), 8.06 (dd, $J_{H,H}$ = 18.3 & 1.7 Hz, 1H), 7.82 (d, $J_{H,H}$ = 8.7 Hz, 1H), 7.52 (d, $J_{H,H}$ = 8.2 Hz, 1H), 7.43 (dd, $J_{H,H}$ = 8.1 & 4.3 Hz, 1H), 7.40 (d, $J_{H,H}$ = 8.7 Hz, 1H), 6.80 (d, $J_{H,H}$ = 8.5 Hz, 1H), 5.23 (br s, 2H, NH_2); ^{13}C NMR (CDCl$_3$, 25 °C, 100.6 MHz, ppm): δ = 157.8 (C$_q$), 149.2 (CH), 145.5 (C$_q$), 144.8 (C$_q$), 137.9 (CH), 135.8 (CH), 129.1 (C$_q$), 126.3 (CH), 122.6 (C$_q$), 122.2 (CH), 121.6 (CH), 111.9 (CH). The NMR spectroscopic data are in accordance with the literature.[277]

4.5.2.18 *N*-(di-iso-propylphosphaneyl)-[1,10-phenanthroline]-2-amine (phen-^{2}NH–^{iPr}P)

II-20
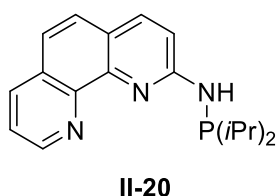
In a glovebox **II-19** (200 mg, 1.02 mmol, 1.0 equiv) was suspended in THF (10 mL) and degassed NEt$_3$ (0.20 mL, 146 mg, 1.44 mmol, 1.4 equiv) was added at once. The suspension was stirring for 10 min at 45 °C to dissolve most of the substrates. *i*Pr$_2$PCl (0.18 mL, 164 mg, 1.07 mmol, 1.05 equiv) was added dropwise and the reaction mixture was stirred at 45 °C for 22 h. The precipitates was filtered off, the residue was extracted with Et$_2$O (3 × 6 mL) and all volatiles were removed *in vacuo* at 60 °C. The product was obtained as an off-white oil which solidified at –35 °C.

Yield: 226 mg (0.73 mmol, 71 %).

^{1}H NMR (C$_6$D$_6$, 25 °C, 400.3 MHz, ppm): δ = 8.99 (dd, $J_{H,H}$ = 4.2 & 1.8 Hz, 1H), 7.71 (dd, $J_{H,H}$ = 3.9 & 2.9 Hz, 1H), 7.68 (dd, $J_{H,H}$ = 8.1 & 1.8 Hz, 1H), 7.57 (d, $J_{H,H}$ = 8.8 Hz, 1H), 7.28 (d, $J_{H,H}$ = 8.7 Hz, 1H), 7.15 (d, $J_{H,H}$ = 6.9 Hz, 1H), 6.92 (dd, $J_{H,H}$ = 8.1 & 4.2 Hz, 1H), 5.45 (br s, 1H, NH), 1.50 (dd, $J_{H,H}$ = 7.0 & 1.8 Hz, 2H, 2 × CH(CH$_3$)$_2$), 0.91 (m, 12H, 2 × CH(CH_3)$_2$); ^{31}P{^{1}H} NMR (C$_6$D$_6$, 25 °C, 162.0 MHz, ppm): δ = 48.8.

4.5.2.19 Synthesis of 2-(6-bromopyridin-2-yl)-4,4-dimethyl-4,5-dihydrooxazole[273]

II-21
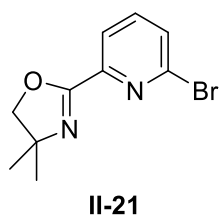
In a glovebox 2-Bromo-6-pyridine (753 mg, 4.11 mmol, 1.0 equiv) and 2-amino-2-methylpropan-1-ol (380 mg, 4.26 mmol, 1.04 equiv) were weighed in a Schlenk-flask and dissolved in chlorobenzene (20 mL). Zinc(II) chloride (30 mg, 0.22 mmol, 0.05 equiv) was added at once and the reaction was stirred under reflux for 22 h connected to a silicon oil filled bubbler. The reaction was allowed to cool to room temperature and concentrated under reduced pressure. The residue was diluted with CH$_2$Cl$_2$ (50 mL), washed with water (3 × 25 mL) and dried over MgSO$_4$. Unreacted substrate can be recovered from the aqueous

phase and used for further reactions. The organic phase was concentrated in vacuum and a light-brown product was obtained.

Yield: 548 mg (2.15 mmol, 52 %).

^{1}H NMR (CDCl$_3$, 25 °C, 400.3 MHz, ppm): δ = 8.01 (dd, $J_{H,H}$ = 7.1 & 1.4 Hz, 1H), 7.60 (m, 2H), 7.29 (m, 3H), 4.19 (s, 2H, CH_2), 1.40 (s, 6H, 2 × CH_3). ^{13}C NMR (CDCl$_3$, 25 °C, 100.6 MHz, ppm): δ = 160.2 (C$_q$), 148.1 (C$_q$), 142.1 (C$_q$), 138.8 (CH), 128.7 (CH), 123.0 (CH), 80.0 (CH_2), 68.3 (C$_q$), 28.5 (2 × CH_3).

4.5.2.20 Synthesis of 6-(4,4-dimethyl-4,5-dihydrooxazol-2-yl)pyridin-2-amine[249]
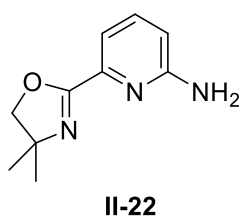
In a glovebox a Schlenk-tube was charged with **II-21** (534 mg, 2.09 mmol, 1.0 equiv) dissolved in ethane-1,2-diol (4 mL) and degassed by three freeze-pump-thaw cycles. The solution was stirred and ammonium hydroxide (13.7 mL, 28 wt% in water, 3.45 g, 98.5 mmol, 47 equiv), copper(I) oxide (14.9 mg, 0.104 mmol, 0.05 equiv) and N,N'-dimehtylethane-1,2-diamine (23 µL, 18.8 mg, 0.209 mmol, 0.1 equiv) were added subsequently. The reaction was stirred for 5 min, K$_2$CO$_3$ (59 mg, 0.42 mmol, 0.2 equiv) was added, the Schlenk-tube was closed and the mixture was heated to 60 °C and stirred for 16 h behind a blast shield. The reaction was allowed to reach room temperature and was extracted with EtOAc (5 × 20 mL). The combined organic phases were dried over MgSO$_4$, concentrated *in vacuo* and purified by column chromatography (Al$_2$O$_3$, EtOAc : MeOH 80:20). The product was obtained as colorless oil.

Yield: 245 mg (1.28 mmol, 61 %).

^{1}H NMR (CDCl$_3$, 25 °C, 400.3 MHz, ppm): δ = 7.48 (br t, $J_{H,H}$ = 7.9 Hz, 1H), 7.35 (dd, $J_{H,H}$ = 7.5 & 0.8 Hz, 1H), 6.57 (dd, $J_{H,H}$ = 8.3 & 0.7 Hz, 1H), 4.63 (br s, 2H, NH_2), 4.14 (s, 2H, CH_2), 1.39 (s, 6H, 2 × CH_3); ^{13}C NMR (CDCl$_3$, 25 °C, 100.6 MHz, ppm): δ = 161.5 (C$_q$), 158.4 (C$_q$), 145.4 (C$_q$), 138.2 (CH), 114.5 (CH), 111.2 (CH), 79.6 (CH_2), 68.0 (C$_q$), 28.5 (2 × CH_3).

4.5.2.21 Synthesis of N-(di-*iso*-propylphosphanyl)-6-(4,4-dimethyl-4,5-dihydrooxazol-2-yl)pyridin-2-amine (ox^{Me2}-py-^{2}NH–^{iPr}P)
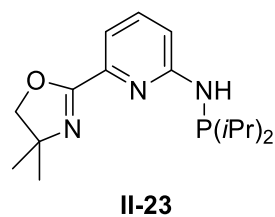
In a glovebox **II-22** (245 mg, 1.28 mmol, 1.0 equiv) was suspended in THF (10 mL) and degassed NEt$_3$ (234 µL, 171 mg, 1.69 mmol, 1.3 equiv) was added at once. *i*Pr$_2$PCl (227 µL, 208 mg, 1.37 mmol, 1.07 equiv) was added dropwise and the reaction mixture was stirred at 45 °C for 22 h. The precipitates was filtered off, the residue was

extracted with Et_2O (3 × 6 mL) and all volatiles were removed *in vacuo* at 60 °C. The product was obtained as slightly yellow oil.

Yield: 365 mg (1.19 mmol, 93 %).

^{1}H NMR (C_6D_6, 25 °C, 400.3 MHz, ppm): δ = 7.68 (dd, $J_{H,H}$ = 7.5 & 0.6 Hz, 1H), 7.35 (ddd, $J_{H,H}$ = 8.4, 2.6 & 0.7 Hz, 1H), 7.06 (ddd, $J_{H,H}$ = 8.4, 7.4 & 0.5 Hz, 1H), 4.87 (d, $J_{H,P}$ = 9.8 Hz, 1H, N*H*), 3.78 (s, 2H, C*H*$_2$), 1.40 (dsept, $J_{H,H}$ = 7.0 & 2.1 Hz, 2H, 2 × C*H*(CH$_3$)$_2$). 1.18 (s, 6H, 2 × C*H*$_3$), 0.85 (m, 12H, 2 × CH(C*H*$_3$)$_2$); ^{31}P{^{1}H} NMR (C_6D_6, 25 °C, 162.0 MHz, ppm): δ = 48.3.

4.5.2.22 Synthesis of (*R*)-BINOL-PCl[272]

II-16
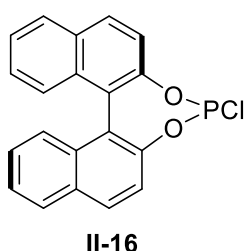
In a Schlenk-flask (*R*)-BINOL (1.63 g, 5.7 mmol, 1.0 equiv) was suspended in trichloro phosphine (10 mL, 15.7 g, 114 mmol, 20 equiv) and heated to 75 °C under stirring over 16 h with the exhaust connected to a silicon oil filled bubbler. The reaction mixture was allowed to cool to room temperature, benzene (10 mL) was added to wash the reaction mixture off the flask walls and all volatiles were removed under vacuum subsequently. The low melting off-white amorphous product was freeze dried in two freeze-crush-pump cycles.

Yield: 1.87 g (5.3 mmol, 94 %).

^{1}H NMR (C_6D_6, 25 °C, 600.2 MHz, ppm): δ = 7.57 (br d, $J_{H,H}$ = 8.1 Hz, 1H), 7.55 (br d, $J_{H,H}$ = 9.1 Hz, 1H), 7.47 (br d, $J_{H,H}$ = 8.8 Hz, 1H), 7.38 (br d, $J_{H,H}$ = 8.7 Hz, 1H), 7.36 (d, $J_{H,H}$ = 8.7 Hz, 1H), 7.34 (d, $J_{H,H}$ = 8.7 Hz, 1H), 7.13 (dd, $J_{H,H}$ = 8.1 & 0.9 Hz, 1H), 7.12 (dd, $J_{H,H}$ = 2.7 & 1.0 Hz, 1H), 7.11 (dd, $J_{H,H}$ = 6.9 & 1.2 Hz, 1H), 6.89 (m, 1H); ^{13}C{^{1}H} NMR (C_6D_6, 25 °C, 150.9 MHz, ppm): δ = 148.3 (d, $J_{C,P}$ = 3.2 Hz, C$_q$), 147.9 (d, $J_{C,P}$ = 4.7 Hz, C$_q$), 133.3 (d, $J_{C,P}$ = 1.9 Hz, C$_q$), 133.0 (d, $J_{C,P}$ = 1.5 Hz, C$_q$), 132.4 (C$_q$), 132.0 (C$_q$), 131.3, 130.5, 128.8, 128.7, 128.4, 127.4, 127.3, 127.0, 126.8, 125.8, 125.7 (aryl), 125.0 (d, $J_{C,P}$ = 5.5 Hz, C$_q$), 123.6 (d, $J_{C,P}$ = 1.9 Hz, C$_q$), 122.0, 121.3 (aryl); ^{31}P{^{1}H} NMR (C_6D_6, 25 °C, 243.0 MHz, ppm): δ = 13.35. The NMR spectroscopic data are in accordance with the literature.[272]

4.5.2.23 Synthesis of bpy-⁶NH–^{(R)-BINOL}P
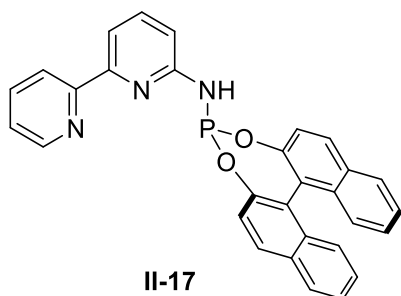
II-13 (49 mg, 286 μmol, 1.0 equiv) was dissolved in THF (5 mL) and degassed NEt₃ (50 μL, 36 mg, 359 μmol, 1.3 equiv) was added at once. (*R*)-BINOL-PCl (101 mg, 288 μmol, 1.0 equiv) was added dropwise and the reaction mixture was stirred at room temperature for 16 h. Precipitates were filtered off, the residue was extracted with THF (3 × 5 mL) and all volatiles were removed *in vacuo* at 60 °C. The product was obtained as slightly yellow oil that solidified upon storage at –35 °C.

II-17

Yield: 135 mg (282 μmol, 97 %).

¹H NMR (THF-*d*₈, 25 °C, 400.3 MHz, ppm): δ = 8.60 (dq, $J_{H,H}$ = 4.8 & 1.0 Hz, 1H), 8.51 (dt, $J_{H,H}$ = 8.1 & 1.1 Hz, 1H), 8.06 (m, 2H), 7.99 (br d, $J_{H,H}$ = 8.2 Hz, 1H), 7.93 (br d, $J_{H,H}$ = 8.2 Hz, 1H), 7.90 (br d, $J_{H,H}$ = 8.7 Hz, 1H), 7.77 (m, 2H), 7.64 (br t, $J_{H,H}$ = 7.8 Hz, 1H), 7.59 (dd, $J_{H,H}$ = 8.8 & 0.6Hz, 1H), 7.41 (m, 5H), 7.30 (m, 4H), 6.64 (dd, $J_{H,P}$ = 8.0 Hz & $J_{H,H}$ = 0.6 Hz, 1H, N*H*), 6.89 (m, 1H); ¹³C{¹H} NMR (THF-*d*₈, 25 °C, 100.6 MHz, ppm): δ = 157.2 (d, $J_{C,P}$ = 13.3 Hz, C_q), 156.9 (aryl), 155.2 (d, $J_{C,P}$ = 1.5 Hz, C_q), 150.3 (C_q), 149.8 (aryl), 149.1 (d, $J_{C,P}$ = 4.4 Hz, C_q), 139.4, 137.3 (aryl), 133.8 (d, $J_{C,P}$ = 4.4 Hz, C_q), 132.7 (C_q), 132.2 (C_q), 131.2 (C_q), 130.4, 129.6, 129.2, 127.6, 127.3, 127.0, 126.8, 125.8, 125.7, 125.4 (d, $J_{C,P}$ = 4.7 Hz, C_q), 124.6 (d, $J_{C,P}$ = 1.9 Hz, C_q), 124.3, 123.5, 122.6, 121.7, 113.6 (aryl), 111.16 (C_q), 111.14 (C_q); ³¹P{¹H} NMR (THF-*d*₈, 25 °C, 162.0 MHz, ppm): δ = 150.16.

4.5.3 Synthesis of complexes

4.5.3.1 Synthesis of Mn(CO)₅Br[247]

A flask was charged with Mn₂(CO)₁₀ (1.01 g, 2.58 mmol, 1.0 equiv) and wrapped with Al-foil. CCl₄ (20 mL) was added, the mixture was stirred until complete solution of all solids and subsequently 3 freeze-pump-thaw cycles were applied. Br₂ (0.18 mL, 0.56 g, 3.49 mmol, 1.4 equiv) was added dropwise and the reaction temperature was increased to 50 °C for 1 h. Subsequently the reaction was let cool to room temperature and all volatiles were removed under reduced pressure. Sublimation of orange product was observed in the cold trap. The orange residue was washed with water (3 × 10 mL) and subsequently extracted with CH₂Cl₂ (4 × 15 mL). The resulting orange solution was concentrated to ~5 mL, pentane (10 mL) was added and it was stored at -18°C for crystallization. The product was as an orange crystalline solid.

Yield: 1.08 g (3.92 mmol, 76 %).

[55]Mn NMR (CDCl$_3$, 25 °C, 148.9 MHz, ppm): δ = –1141.9. The NMR spectroscopic data are in accordance with the literature.[278]

4.5.3.2 Complexation of Mn(CO)$_5$Br with II-15 in NMR scale

An NMR tube was charged with **II-15** (11.2 mg, 3.90 µmol, 1.0 equiv), Mn(CO)$_5$Br (10.7 mg, 3.89 µmol, 1.0 equiv) and C$_6$D$_6$ (0.5 mL). The tube was shaken and the compounds slowly dissolved. An NMR after 5 min suggested the first formation of the desired complex, on the next day precipitate had formed and the NMR suggested full complexation of the ligand.

^{1}H NMR (C$_6$D$_6$, 25 °C, 400.3 MHz, ppm): δ = 8.51 (m, 1H), 8.16 (m, 2H), 7.01 (m, 1H), 6.84 (m, 1H), 6.67 (m, 1H), 6.25 (m, 1H), 3.46 (m, 1H, N*H*), 1.90 (m, 2H, 2 × C*H*(CH$_3$)$_2$), 1.14 (m, 12H, 2 × CH(C*H*$_3$)$_2$); ^{31}P{^{1}H} NMR (C$_6$D$_6$, 25 °C, 162.0 MHz, ppm): δ = 99.29.

^{1}H NMR (400.3 MHz, THF-d_8, 298 K): δ = 8.60–8.67 (br m, 1H), 8.14–8.21 (br m, 1H), 8.02–8.09 (br m, 1H), 7.79–7.89 (br m, 1H), 7.65–7.74 (br m, 1H), 7.27–7.35 (br m, 1H), 6.76–6.82 (br d,1H), 6.63–6.72 (br d, 1H, N*H*), 3.68–3.82 (m, 2H, 2 × C*H*(CH3)2), 1.33–1.48 (m, 12H, 2 × CH(C*H*3)2); ^{13}C{^{1}H} NMR (100.6 MHz, THF-d_8, 298 K): 185.1 (C$_q$), 157.5 (d, [2]$J_{C,P}$ = 12 Hz, C$_q$), 156.8 (C$_q$), 155.7 (C$_q$), 150.3 (CH), 139.9 (CH), 137.6 (CH), 124.4 (CH), 121.0 (CH), 114.8 (CH), 113.1 ([3]$J_{C,P}$ = 5 Hz, CH), 31.6 (d, $J_{C,P}$ = 24 Hz, CH), 19.3, 18.7 (d, $J_{C,P}$ = 5 Hz, CH3); ^{31}P{^{1}H} NMR(162 MHz, THF-d_8, 298 K): δ = 98.0.

4.5.4 General procedures for catalysis

4.5.4.1 Exemplary preparation of a catalyst stock solution

In the glovebox a 4 mL vial was charged with Mn(CO)$_5$Br (37.1 mg, 135 µmol, 1 equiv) and **II-15** (38.8 mg, 135 µmol, 1 equiv), followed by addition of DME (2.7 mL) to prepare a stock solution. After 30 min of stirring at room temperature a distinct color change from light orange to brown was observed and this stock solution was used without any further purification.

4.5.4.1 Exemplary *N*-alkylation of aniline with benzyl alcohol

In the glovebox, a 2 mL vial was charged with KH (20.0 mg, 0.5 mmol, 0.5 equiv) and catalyst stock solution (100 µL, c = 50 µmol mL–1 in DME, 5 µmol, 0.005 equiv). Benzyl alcohol (104 µL, 108.1 mg, 1 mmol, 1.0 equiv) was added dropwise via syringe and hydrogen was allowed to evolve for 1 min. Aniline (99 µL, 102.0 mg, 1.1 mmol, 1.1 equiv) was added via syringe at once subsequently. The vial was capped and placed in a metal-block on a heated stirring plate. After the desired amount of reaction time, the vial was allowed to cool to ambient temperature. *p*-Xylene (100 µL) was added as standard, the reaction mixture was treated with water (0.5 mL) and extracted with EtOAc (3 × 0.7 mL). The sample was

analyzed by GC-MS and GC-FID. The product (*N*-benzyl aniline) was isolated by flash column chromatography on Al_2O_3 using (9:1) heptanes/ CH_2Cl_2, yielding 144.7 mg (0.79 mmol, 79 %) of a colorless oil.

4.5.4.3 Representative GC-FID and GC-MS
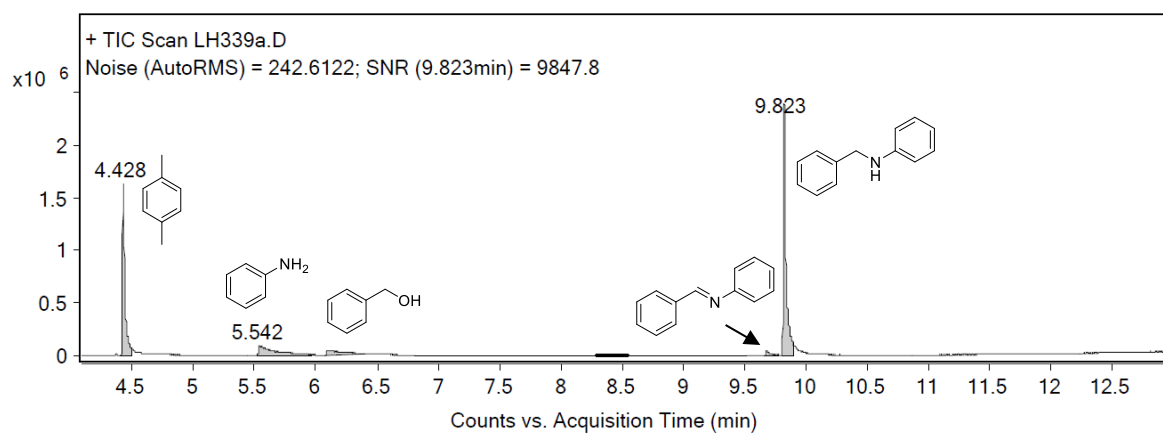
Figure 37. GC-MS trace of the N-benzylation of aniline.
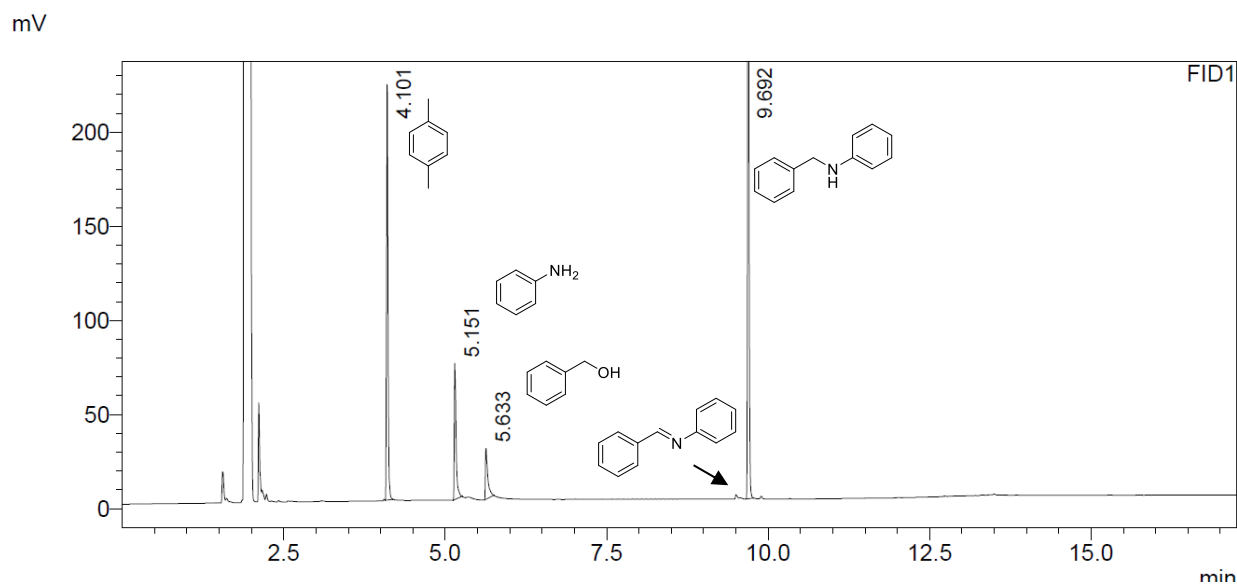
Figure 38. GC-FID trace of the N-benzylation of aniline.

4.5.5 Characterization of N-alkylation products 1-4[255]

4.5.5.1 *N*-benzylaniline (1a)
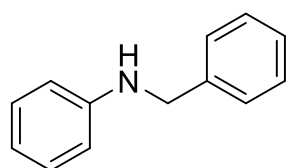
Pale yellow oil. Yield: 144.7 mg (0.79 mmol, 79 %), GC-FID: 99 %.

^{1}H NMR (400.3 MHz, CDCl$_3$, 298 K): δ = 7.33–7.42 (m, 4H, Ar), 7.26–7.32 (m, 1H, Ar), 7.15–7.22 (m, 2H, Ar), 6.70–6.76 (m, 1H, Ar), 6.63–6.68 (m, 2H, Ar), 4.34 (s, 2H, Ar-CH_2-NH), 4.03 (br s, 1H, CH$_2$-NH-Ar); ^{13}C{^{1}H} NMR (100.6 MHz, CDCl$_3$, 298 K): δ = 148.3 (C$_q$), 139.6 (C$_q$), 129.4, 128.8, 127.7, 127.4, 117.7, 113.0 (aryl), 48.5 (CH$_2$). The NMR spectroscopic data are in accordance with the literature.[192]

HRMS (ESI) m/z calcd. for [C$_{13}$H$_{14}$N, M+H]$^+$: 184.1126; Found: 184.1118.

GC-FID Retention time (min): 9.692.

4.5.5.2 *N*-benzyl-4-methoxyaniline (2a)
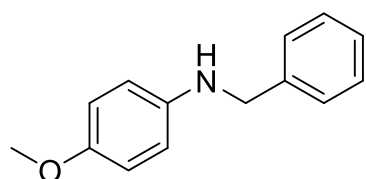
Light brown oil. Yield: 107.7 mg (0.50 mmol, 50 %), GC-FID: 94 %.

^{1}H NMR (400.3 MHz, CDCl$_3$, 298 K): δ = 7.37–7.47 (m, 4H, Ar), 7.31–7.36 (m, 1H, Ar), 6.82–6.87 (m, 2H, Ar), 6.63–6.68 (m, 2H, Ar), 4.33 (s, 2H, Ar-CH_2-NH), 3.79 (br s, 4H, OCH_3 & CH$_2$-NH-Ar); ^{13}C{^{1}H} NMR (100.6 MHz, CDCl$_3$, 298 K): δ = 152.3 (C$_q$), 142.6 (C$_q$), 139.8 (C$_q$), 128.6, 127.6, 127.2, 115.0, 114.2 (aryl), 55.8 (OCH$_3$), 49.3 (CH$_2$). The NMR spectroscopic data are in accordance with the literature.[192]

HRMS (ESI) m/z calcd. for [C$_{14}$H$_{16}$NO, M+H]$^+$: 214.1232; Found: 214.1227.

GC-FID Retention time (min): 11.820.

4.5.5.3 *N*-benzyl-4-bromoaniline (2b)
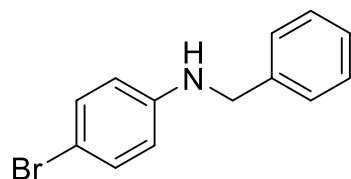
Dark brown oil. Yield: 107.7 mg (0.50 mmol, 50 %), GC-FID: 97 %.

^{1}H NMR (400.3 MHz, CDCl$_3$, 298 K): 7.32–7.36 (m, 4H, Ar), 7.26–7.31 (m, 1H, Ar), 7.21–7.26 (m, 2H, Ar), 6.48–6.52 (m, 2H, Ar), 4.30 (br s, 2H, Ar-CH_2-NH), 4.06 (br s, 1H, CH$_2$-NH-Ar); ^{13}C{^{1}H} NMR (100.6 MHz, CDCl$_3$, 298 K): δ = 147.2 (C$_q$), 139.0 (C$_q$), 132.1, 128.8, 127.54, 127.53, 114.6 (C$_q$), 109.3 (aryl), 48.4 (CH$_2$). The NMR spectroscopic data are in accordance with the literature.[192]

HRMS (ESI) m/z calcd. for [$C_{13}H_{13}BrN$, M+H]$^+$: 262.0231; Found: 262.0221.

GC-FID Retention time (min): 12.280.

4.5.5.4 *N*-benzyl-4-chloroaniline (2c)
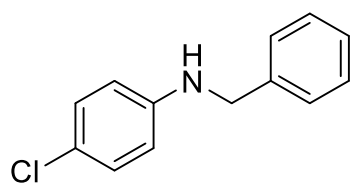
Orange-brown oil. Yield: 190.0 mg (0.87 mmol, 87 %), GC-FID: 95 %.

^{1}H NMR (400.3 MHz, CDCl$_3$, 298 K): δ = 7.33–7.39 (m, 4H, Ar), 7.27–7.33 (m, 1H, Ar), 7.09–7.14 (m, 2H, Ar), 6.53–6.58 (m, 2H, Ar), 4.29–4.33 (m, 2H, Ar-C*H*$_2$-NH), 4.06 (br s, 1H, CH$_2$-N*H*-Ar);

^{13}C{^{1}H} NMR (100.6 MHz, CDCl$_3$, 298 K): δ = 146.8 (C$_q$), 139.1 (C$_q$), 129.2, 128.8, 127.6, 127.5, 122.3 (C$_q$), 114.1 (aryl), 48.5 (CH$_2$). The NMR spectroscopic data are in accordance with the literature.[278]

HRMS (ESI) m/z calcd. for [$C_{13}H_{13}ClN$, M+H]$^+$: 218.0736; Found: 218.0728.

GC-FID Retention time (min): 11.797.

4.5.5.5 *N*-benzyl-4-fluoroaniline (2d)
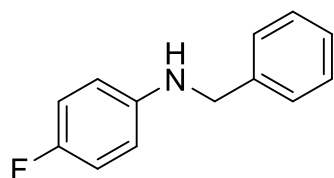
Dark yellow oil. Yield: 198.7 mg (0.99 mmol, 99 %), GC-FID: >99 %.

^{1}H NMR (400.3 MHz, CDCl$_3$, 298 K): δ = 7.34–7.47 (m, 4H, Ar), 7.27–7.32 (m, 1H, Ar), 6.85–6.93 (m, 2H, Ar), 6.55–6.61 (m, 2H, Ar), 4.30 (s, 2H, Ar-C*H*$_2$-NH), 3.93 (br s, 1H, CH$_2$-N*H*-Ar); ^{13}C{^{1}H} NMR (100.6 MHz, CDCl$_3$, 298 K): δ = 156.0 (C$_q$, d, $^1J_{F,C}$ = 234.9 Hz), 144.6 (C$_q$, d, $^4J_{F,C}$ = 2.1 Hz) , 139.4 (C$_q$), 128.8, 127.6, 127.4, 115.8 (d, $^2J_{F,C}$ = 22.3 Hz), 113.8 (d, $^3J_{F,C}$ = 7.3 Hz, aryl), 49.0 (CH$_2$); ^{19}F NMR (659.0 MHz, CDCl$_3$, 298 K): –127.96 (m). The NMR spectroscopic data are in accordance with the literature.[279]

HRMS (ESI) m/z calcd. for [$C_{13}H_{13}FN$, M+H]$^+$: 202.1032; Found: 202.1026.

GC-FID Retention time (min): 10.660.

4.5.5.6 *N*-benzyl-3-fluoroaniline (2e)
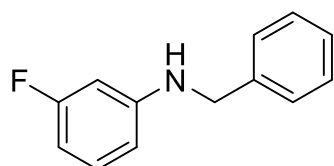
Orange oil. Yield: 199.0 mg (0.99 mmol, 99 %), GC-FID: >99 %.

^{1}H NMR (400.3 MHz, CDCl$_3$, 298 K): δ = 7.42–7.49 (m, 4H, Ar),

7.36–7.42 (m, 1H, Ar), 7.15–7.22 (m, 1H, Ar), 6.45–6.55 (m, 2H, Ar), 6.38–6.44 (m, 1H, Ar), 4.37 (s, 2H, Ar-CH_2-NH), 4.20 (br s, 1H, CH$_2$-NH-Ar); ^{13}C{^{1}H} NMR (100.6 MHz, CDCl$_3$, 298 K): δ = 164.2 (C$_q$, d, $^1J_{F,C}$ = 242.8 Hz); 150.0 (C$_q$,d, $^3J_{F,C}$ = 10.4 Hz), 138.9 (C$_q$), 130.4 (d, $^3J_{F,C}$ = 10.2 Hz), 128.8, 127.5, 127.4, 108.8 (d, $^4J_{F,C}$ = 2.2 Hz), 103:9 (d, $^2J_{F,C}$ = 21.5 Hz), 99.6 (d, $^2J_{F,C}$ = 25.3 Hz, aryl), 48.2 (CH$_2$); ^{19}F NMR (659.0 MHz, CDCl$_3$, 298 K): –112.78 (m). The NMR spectroscopic data are in accordance with the literature.[220]

HRMS (ESI) m/z calcd. for [C$_{13}$H$_{13}$FN, M+H]$^+$: 202.1032; Found: 202.1025.

GC-FID Retention time (min): 10.760.

4.5.5.7 *N*-benzyl-2-fluoroaniline (2f)
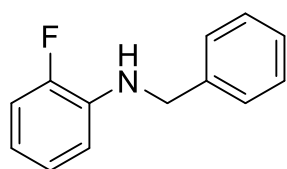
Pale yellow oil. Yield: 184.8 mg (0.92 mmol, 92 %), GC-FID: 93 %.

^{1}H NMR (400.3 MHz, CDCl$_3$, 298 K): δ = 7.44–7.53 (m, 4H, Ar), 7.37–7.44 (m, 1H, Ar), 7.05–7.16 (m, 2H, Ar), 6.72–6.84 (m, 2H, Ar), 4.46 (br s, 3H, Ar-CH_2-NH & CH$_2$-NH-Ar); ^{13}C{^{1}H} NMR (100.6 MHz, CDCl$_3$, 298 K): δ = 151.6 (C$_q$, d, $^1J_{F,C}$ = 238.4 Hz), 139.0 (C$_q$), 136.7 (C$_q$,d, $^2J_{F,C}$ = 18.5 Hz), 128.8, 127.42, 127.40, 124.7 (d, $^3J_{F,C}$ = 3.7 Hz), 116.9 (d, $^3J_{F,C}$ = 11.2 Hz), 114.5 (d, $^2J_{F,C}$ = 18.5 Hz), 112.4 (d, $^4J_{F,C}$ = 2.9 Hz, aryl), 47.9 (CH$_2$); ^{19}F NMR (659.0 MHz, CDCl$_3$, 298 K): –136.50 (m). The NMR spectroscopic data are in accordance with the literature.[279]

HRMS (ESI) m/z calcd. for [C$_{13}$H$_{13}$FN, M+H]$^+$: 202.1032; Found: 202.1024.

GC-FID Retention time (min): 10.356.

4.5.5.8 *N*-benzyl-4-methylaniline (2g)
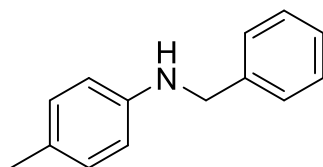
Orange oil. Yield: 135.8 mg (0.69 mmol, 69 %), GC-FID: 91 %.

^{1}H NMR (400.3 MHz, CDCl$_3$, 298 K): δ = 7.46–7.57 (m, 4H, Ar), 7.39–7.46 (m, 1H, Ar), 7.12–7.19 (m, 2H, Ar), 6.67–6.76 (m, 2H, Ar), 4.43 (s, 2H, Ar-CH_2-NH), 4.00 (br s, 1H, CH$_2$-NH-Ar), 2.42 (s, 3H, CH$_3$); ^{13}C{^{1}H} NMR (100.6 MHz, CDCl$_3$, 298 K): δ = 146.0 (C$_q$), 139.8 (C$_q$), 129.8, 128.6, 127.5, 127.2, 126.7 (C$_q$), 113.1 (aryl), 48.6 (CH$_2$), 20.5 (CH$_3$). The NMR spectroscopic data are in accordance with the literature.[192]

HRMS (ESI) m/z calcd. for [C$_{14}$H$_{16}$N, M+H]$^+$: 198.1283; Found: 198.1279.

GC-FID Retention time (min): 11.106.

4.5.5.9 *N*-benzyl-3-methylaniline (2h)
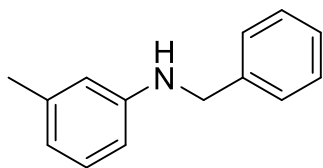
Brown oil. Yield: 166.7 mg (0.85 mmol, 85 %), GC-FID: 91 %.

^{1}H NMR (400.3 MHz, CDCl$_3$, 298 K): δ = 7.45–7.53 (m, 4H, Ar), 7.39–7.44 (m, 1H, Ar), 7.18–7.24 (m, 1H, Ar), 6.68–6.72 (m, 1H, Ar), 6.55–6.61 (m, 2H, Ar), 4.43 (s, 2H, Ar-C*H$_2$*-NH), 4.04 (br s, 1H, CH$_2$-N*H*-Ar), 2.42 (s, 3H, CH$_3$); ^{13}C{^{1}H} NMR (100.6 MHz, CDCl$_3$, 298 K): δ = 148.3 (C$_q$), 139.7 (C$_q$), 139.0 (C$_q$), 129.2, 128.7, 127.6, 127.2, 118.6, 113.7, 110.0 (aryl), 48.4 (CH$_2$), 21.7 (CH$_3$). The NMR spectroscopic data are in accordance with the literature.[220]

HRMS (ESI) m/z calcd. for [C$_{14}$H$_{16}$N, M+H]$^+$: 198.1283; Found: 198.1277.

GC-FID Retention time (min): 11.070.

4.5.5.10 N-benzyl-2-methylaniline (2i)
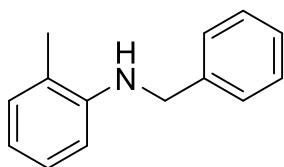
Pale yellow oil. Yield: 123.1 mg (0.62 mmol, 62 %), GC-FID: 76 %.

^{1}H NMR (400.3 MHz, CDCl$_3$, 298 K): δ = 7.33–7.42 (m, 2H, Ar), 7.26–7.32 (m,1H, Ar), 7.06–7.14 (m, 2H, Ar), 6.65–6.71 (m, 1H, Ar), 6.60–6.65 (m, 1H, Ar), 4.38 (s, 2H, Ar-C*H$_2$*-NH), 3.86 (br s, 1H, CH$_2$-N*H*-Ar), 2.18 (s, 3H, CH$_3$); ^{13}C{^{1}H} NMR (100.6 MHz, CDCl$_3$, 298 K): δ = 146.2 (C$_q$), 139.7 (C$_q$), 130.2, 128.8, 127.7, 127.4, 127.3, 122.1 (C$_q$), 117.3, 110.1 (aryl), 48.5 (CH$_2$), 17.7 (CH$_3$). The NMR spectroscopic data are in accordance with the literature.[278]

HRMS (ESI) m/z calcd. for [C$_{14}$H$_{16}$N, M+H]$^+$: 198.1283; Found: 198.1275.

GC-FID Retention time (min): 10.972.

4.5.5.11 *N*-benzyl-4-vinylaniline (2j)
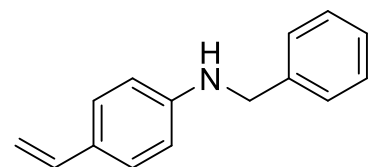
Orange oil. Yield: 91.2 mg (0.44 mmol, 44 %), GC-FID: 89 %.

^{1}H NMR (400.3 MHz, CDCl$_3$, 298 K): δ = 7.26–7.41 (m, 7H, Ar), 6.64 (t, $^3J_{H,H}$ = 11.0 Hz, 1H, C*H*=CH$_2$), 6.59–6.64 (m, 2H, Ar), 5.54 (dd, $^3J_{transH,H}$ = 17.6 Hz, $^2J_{H,H}$ = 1.0 Hz, 1H, CH=C*H$_2$*), 5.04 (dd, $^3J_{cisH,H}$ = 10.9 Hz, $^2J_{H,H}$ = 1.0 Hz, 1H, CH=C*H$_2$*), 4.37 (s, 2H, Ar-C*H$_2$*-NH), 4.12 (br s, 1H, CH$_2$-N*H* -Ar); ^{13}C{^{1}H} NMR (100.6 MHz, CDCl$_3$, 298 K): δ = 148.0 (C$_q$), 139.4 (C$_q$), 136.8 (CH, vinyl), 128.8, 127.59, 127.58, 127.51, 127.4, 112.9 (aryl), 109.7 (CH$_2$, vinyl), 48.3 (CH$_2$). The NMR spectroscopic data are in accordance with the literature.[192]

HRMS (ESI) m/z calcd. for [C$_{15}$H$_{16}$N, M+H]$^+$: 210.1283; Found: 210.1269.

GC-FID Retention time (min): 10.869.

4.5.5.12 Dibenzylamine (2k)
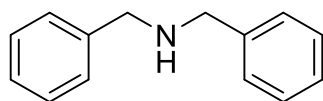
Pale yellow oil. Yield: 127.0 mg (0.64 mmol, 64 %), GC-FID: 95 %.

^{1}H NMR (400.3 MHz, CDCl$_3$, 298 K): δ = 7.28–7.34 (m, 8H, Ar), 7.22–7.27 (m, 2H, Ar), 3.81 (s, 4H, 2 CH$_2$), 1.60 (br s, 1H); ^{13}C{^{1}H} NMR (100.6 MHz, CDCl$_3$, 298 K): δ = 140.6 (C$_q$), 128.6, 128.4, 127.2 (aryl), 53.4 (CH$_2$). The NMR spectroscopic data are in accordance with the literature.[280]

HRMS (ESI) m/z calcd. for [C$_{14}$H$_{16}$N, M+H]$^+$: 198.1277; Found: 198.1277.

GC-FID Retention time (min): 9.646.

4.5.5.13 *N*-benzyl-1-phenylethan-1-amine (2l)
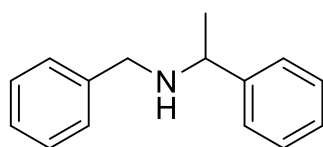
Pale yellow oil. Yield: 37.1 mg (0.18 mmol, 18 %), GC-FID: 65 %.

^{1}H NMR (400.3 MHz, CDCl$_3$, 298 K): δ = 7.19–7.37 (m, 10H, Ar), 3.79 (q, $^2J_{H,H}$ = 6.6 Hz, 1H, CH$_3$-C*H*), 3.61 (q, $J_{H,H}$ = 13.7 Hz 2H, CH-NH-C*H$_2$*), 1.63 (br s, 1H, CH-N*H*-CH$_2$), 1.35 (d, $^2J_{H,H}$ = 6.6 Hz, 3H, C*H$_3$*-CH); ^{13}C{^{1}H} NMR (100.6 MHz, CDCl$_3$, 298 K): δ = 145.7 (C$_q$), 140.8 (C$_q$), 128.6, 128.5, 128.3, 127.1, 127.0, 126.9 (aryl), 57.6 (CH), 51.8 (CH$_2$), 24.6 (CH$_3$). The NMR spectroscopic data are in accordance with the literature.[281]

HRMS (ESI) m/z calcd. for [C$_{15}$H$_{18}$N, M+H]$^+$: 212.1434; Found: 212.1434.

GC-FID Retention time (min): 9.706.

4.5.5.14 *N*-benzylhexan-1-amine (2m)
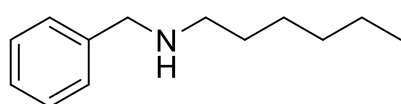
Pale yellow oil. Yield: 21.2 mg (0.11 mmol, 11 %), GC-FID: 81 %.

^{1}H NMR (600.3 MHz, CDCl$_3$, 298 K): δ = 7.29–7.35 (m, 4H, Ar), 7.21–7.28 (m, 1H, Ar), 3.79 (s, 2H, CH$_2$), 2.63 (t, *J*=7.15 Hz, 2H, CH$_2$), 1.47–1.33 (m, 2H, CH$_2$), 1. 25 –1.39 (br s partially overlapped by other signal (m), 7H, 3 CH$_2$, CH$_2$-N*H* –Ar), 0.86–0.90 (m, 3H, CH$_3$); ^{13}C{^{1}H} NMR (150.9 MHz, CDCl$_3$, 298 K): δ = 140.7 (C$_q$), 128.5, 128.2, 127.0 (aryl), 44.3, 49.7, 31.9, 30.2, 27.2, 22.8 (CH$_2$), 14.2 (CH$_3$). The NMR spectroscopic data are in accordance with the literature.[282]

HRMS (ESI) m/z calcd. for [C$_{13}$H$_{22}$N, M+H]$^+$: 192.1747; Found: 192.1745.

GC-FID Retention time (min): 8.717.

4.5.5.15 *N*-(4-methoxybenzyl)aniline (3a)
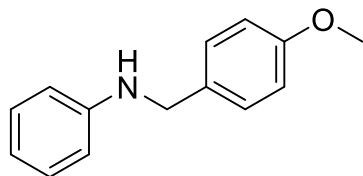
Orange oil. Yield: 105.5 mg (0.50 mmol, 50 %), GC-FID: 95 %.

^{1}H NMR (400.3 MHz, CDCl$_3$, 298 K): δ = 7.27–7.32 (m, 2H, Ar), 7.15–7.21 (m, 2H, Ar), 6.86–6.91 (m, 2H, Ar), 6.69–6.75 (m, 1H, Ar), 6.62–6.67 (m, 2H, Ar), 4.26 (s, 2H, Ar-C*H*$_2$-NH), 3.94 (br s, 1H, CH$_2$-N*H*-Ar), 3.81 (s, 3H, OCH$_3$); ^{13}C{^{1}H} NMR (100.6 MHz, CDCl$_3$, 298 K): δ = 159.0 (C$_q$), 148.4 (C$_q$), 131.6 (C$_q$), 129.4, 128.9, 117.6, 114.2, 113.0 (aryl), 55.5 (OCH$_3$), 48.0 (CH$_2$). The NMR spectroscopic data are in accordance with the literature.[192]

HRMS (ESI) m/z calcd. for [C$_{14}$H$_{16}$NO, M+H]$^+$: 214.1232; Found: 214.1227.

GC-FID Retention time (min): 11.900.

4.5.5.16 *N*-(4-bromobenzyl)aniline (3b)
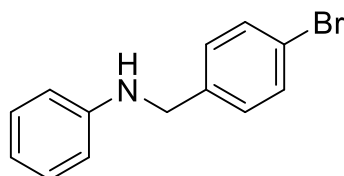
Dark orange oil. Yield: 99.0 mg (0.38 mmol, 38 %), GC-FID: 83 %.

^{1}H NMR (400.3 MHz, CDCl$_3$, 298 K): δ = 7.28–7.50 (m, 3H, Ar), 7.22–7.28 (m, 1H, Ar), 7.14–7.22 (m, 2H, Ar), 6.69–6.77 (m, 1H, Ar), 6.58–6.68 (m, 2H, Ar), 4.30 (br s, 2H, Ar-C*H*$_2$-NH), 4.05 (br s, 1H, CH$_2$-N*H*-Ar); ^{13}C{^{1}H} NMR (100.6 MHz, CDCl$_3$, 298 K): δ = 148.0 (C$_q$), 138.7 (C$_q$), 131.9, 129.4, 129.2, 121.1 (C$_q$), 118.0, 113.0 (aryl), 47.8 (CH$_2$). The NMR spectroscopic data are in accordance with the literature.[278]

HRMS (ESI) m/z calcd. for [C$_{13}$H$_{13}$BrN, M+H]$^+$: 262.0231; Found: 262.0222.

GC-FID Retention time (min): 11.091.

4.5.5.17 *N*-(4-chlorobenzyl)aniline (3c)
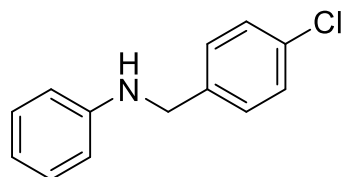
Orange oil. Yield: 76.1 mg (0.35 mmol, 35 %), GC-FID: 90 %.

^{1}H NMR (400.3 MHz, CDCl$_3$, 298 K): δ = 7.32 (br s, 4H, Ar), 7.15–7.21 (m, 2H, Ar), 6.71–6.77 (m, 1H, Ar), 6.60–6.65 (m, 2H, Ar), 4.32 (br s, 2H, Ar-C*H*$_2$-NH), 4.05 (br s, 1H, CH$_2$-N*H*-Ar);
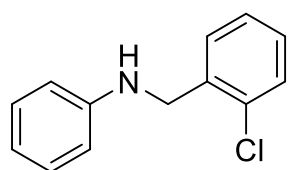
$^{13}C\{^1H\}$ NMR (100.6 MHz, CDCl$_3$, 298 K): δ = 148.0 (C$_q$), 138.2 (C$_q$), 133.0, 129.4, 128.9, 128.8 (C$_q$), 118.0, 113.0 (aryl), 47.8 (CH$_2$). The NMR spectroscopic data are in accordance with the literature.[192]

HRMS (ESI) m/z calcd. for [C$_{13}$H$_{13}$ClN, M+H]$^+$: 218.0736; Found: 218.0724.

GC-FID Retention time (min): 10.661.

4.5.5.18 *N*-(2-chlorobenzyl)aniline (3d)

Light orange oil. Yield: 133.3 mg (0.61 mmol, 61 %), GC-FID: 90 %.

^1H NMR (400.3 MHz, CDCl$_3$, 298 K): δ = 7.25–7.33 (m, 2H, Ar), 7.05–7.12 (m, 4H, Ar), 6.60–6.68 (m, 1H, Ar), 6.48–6.54 (m, 2H, Ar), 4.31 (s, 2H, Ar-C*H$_2$*-NH), 4.00 (s, br 1H, CH$_2$-N*H*-Ar); $^{13}C\{^1H\}$ NMR (100.6 MHz, CDCl$_3$, 298 K): δ = 147.8 (C$_q$), 136.8 (C$_q$), 133.3 (C$_q$), 129.6, 129.4, 129.1, 128.4, 127.0, 117.8, 113.0 (aryl), 45.9 (CH$_2$). The NMR spectroscopic data are in accordance with the literature.[278]

HRMS (ESI) m/z calcd. for [C$_{13}$H$_{13}$ClN, M+H]$^+$: 218.0736; Found: 218.0730.

GC-FID Retention time (min): 10.439.

4.5.5.19 *N*-(4-fluorobenzyl)aniline (3e)

Light brown oil. Yield: 81.4 mg (0.40 mmol, 40 %), GC-FID: 72 %.

^1H NMR (400.3 MHz, CDCl$_3$, 298 K): δ = 7.23–7.29 (m, 2H, Ar), 7.07–7.17 (m, 2H, Ar), 6.93–7.00 (m, 2H, Ar), 6.65–6.72 (m, 1H, Ar), 6.53–6.60 (m, 2H, Ar), 4.21 (s, 2H, Ar-C*H$_2$*-NH), 3.91 (br s, 1H, CH$_2$-N*H*-Ar); $^{13}C\{^1H\}$ NMR (100.6 MHz, CDCl$_3$, 298 K): δ = 162.1 (C$_q$, d, $^1J_{F,C}$ = 244.9 Hz), 148.1 (C$_q$), 135.2 (C$_q$, d, $^4J_{F,C}$ = 2.9 Hz), 129.4, 129.1 (d, $^3J_{F,C}$ = 8.1 Hz), 117.8, 115.5 (d, $^2J_{F,C}$ = 22.1 Hz), 113.0 (aryl), 47.6 (CH$_2$); ^{19}F NMR (659.0 MHz, CDCl$_3$, 298 K): –115.63 (m).

The NMR spectroscopic data are in accordance with the literature.[278]

HRMS (ESI) m/z calcd. for [C$_{13}$H$_{13}$FN, M+H]$^+$: 202.1032; Found: 202.1023.

GC-FID Retention time (min): 11.771.

4.5.5.20 *N*-(3-fluorobenzyl)aniline (3f)
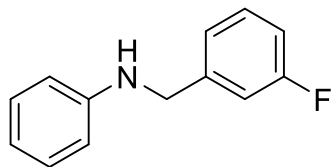
Dark brown oil. Yield: 71.3 mg (0.35 mmol, 35 %), GC-FID: 94 %.

^{1}H NMR (400.3 MHz, CDCl$_3$, 298 K): δ = 7.29–7.36 (m, 1H, Ar), 7.16–7.25 (m, 3H, Ar), 7.10–7.15 (m, 1H, Ar), 6.96–7.02 (m, 1H, Ar), 6.74–6.80 (m, 1H, Ar), 6.62–6.69 (m, 2H, Ar), 4.36 (s, 2H, Ar-C*H*$_2$-NH), 4.10 (br s, 1H, CH$_2$-N*H*-Ar); ^{13}C{^{1}H} NMR (100.6 MHz, CDCl$_3$, 298 K): δ = 163.3 (C$_q$, d, $^1J_{F,C}$ = 247.3 Hz), 148.0 (C$_q$), 142.5 (C$_q$, d, $^3J_{F,C}$ = 6.7 Hz), 130.2 (d, $^3J_{F,C}$ = 8.7 Hz), 129.4, 122.9 (d, $^4J_{F,C}$ = 2.9 Hz), 117.9, 114.3 (d, $^2J_{F,C}$ = 21.5 Hz), 114.1 (d, $^2J_{F,C}$ = 21.1 Hz), 113.0 (aryl), 47.9 (d, $^4J_{F,C}$ = 1.5 Hz, CH$_2$); ^{19}F NMR (659.0 MHz, CDCl$_3$, 298 K): –112.95 (m). The NMR spectroscopic data are in accordance with the literature.[283]

HRMS (ESI) m/z calcd. for [C$_{13}$H$_{13}$FN, M+H]$^+$: 202.1032; Found: 202.1029.

GC-FID Retention time (min): 10.622.

4.5.5.21 *N*-(2-fluorobenzyl)aniline (3g)
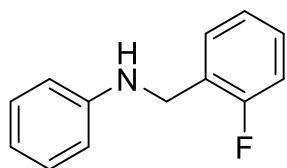
Yellow oil. Yield: 71.6 mg (0.36 mmol, 36 %), GC-FID: 65 %.

^{1}H NMR (400.3 MHz, CDCl$_3$, 298 K): δ = 7.30–7.36 (m, 1H, Ar), 7.16–7.23 (m, 1H, Ar), 7.10–7.16 (m, 2H, Ar), 6.98–7.07 (m, 2H, Ar), 6.66–6.72 (m, 1H, Ar), 6.57-6.62 (m, 2H, Ar), 4.35 (s, 2H, Ar-C*H*$_2$-NH), 3.98 (br s, 1H, CH$_2$-N*H*-Ar); ^{13}C{^{1}H} NMR (100.6 MHz, CDCl$_3$, 298 K): δ = 161.0 (C$_q$, d, $^1J_{F,C}$ = 245.7 Hz), 147.9 (C$_q$,), 129.5 (d, $^3J_{F,C}$ = 4.4 Hz), 129.4, 128.9 (d, $^3J_{F,C}$ = 8.2 Hz), 126.5 (C$_q$, d, $^2J_{F,C}$ = 14.7 Hz), 124.3 (d, $^4J_{F,C}$ = 3.7 Hz), 117.8, 115.4 (d, $^2J_{F,C}$ = 21.3 Hz), 113.0 (aryl), 41.9 (d, $^3J_{F,C}$ = 4.4 Hz, CH$_2$); ^{19}F NMR (659.0 MHz, CDCl$_3$, 298 K): –119.05 (m). The NMR spectroscopic data are in accordance with the literature.[278]

HRMS (ESI) m/z calcd. for [C$_{13}$H$_{13}$FN, M+H]$^+$: 202.1032; Found: 202.1027.

GC-FID Retention time (min): 9.592.

4.5.5.22 *N*-(4-methylbenzyl)aniline (3h)
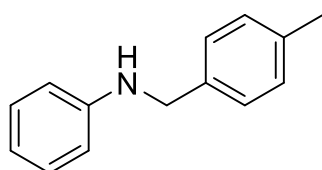
Orange oil. Yield: 88.1 mg (0.45 mmol, 45 %), GC-FID: 93 %.

^{1}H NMR (400.3 MHz, CDCl$_3$, 298 K): δ = 7.17–7.22 (m, 2H, Ar), 7.06–7.14 (m, 4H, Ar), 6.63–6.70 (m, 1H, Ar), 6.53–6.59 (m, 2H, Ar), 4.19 (s, 2H, Ar-C*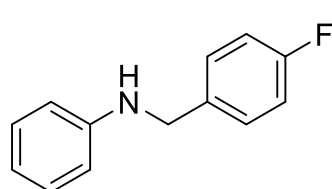H*$_2$-NH), 3.86 (br s, 1H, CH$_2$-N*H*-Ar), 2.29 (s, 3H, CH$_3$); ^{13}C{^{1}H} NMR (100.6 MHz, CDCl$_3$, 298 K): δ = 148.3 (C$_q$), 136.9 (C$_q$), 136.5 (C$_q$),

129.4, 129.3, 127.6, 117.5, 112.9 (aryl), 48.1 (CH_2), 21.1 (CH_3). The NMR spectroscopic data are in accordance with the literature.[192]

HRMS (ESI) m/z calcd. for [$C_{14}H_{16}N$, M+H]$^+$: 198.1283; Found: 198.1280.

GC-FID Retention time (min): 11.164.

4.5.5.23 *N*-(3-methylbenzyl)aniline (3i)
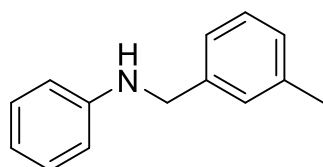
Yellow oil. Yield: 123.8 mg (0.63 mmol, 63 %), GC-FID: 88 %.

^{1}H NMR (400.3 MHz, CDCl$_3$, 298 K): δ = 7.04–7.17 (m, 5H, Ar), 6.98–7.02 (m, 1H, Ar), 6.61–6.67 (m, 1H, Ar), 6.49–6.55 (m, 2H, Ar), 4.15 (s, 2H, Ar-C*H*$_2$-NH), 3.82 (br s, 1H, CH$_2$-N*H*-Ar), 2.26 (s, 3H, CH$_3$); ^{13}C{^{1}H} NMR (100.6 MHz, CDCl$_3$, 298 K): δ = 148.3 (C_q), 139.4 (C_q), 138.2 (C_q), 129.3, 128.6, 128.3, 128.0, 124.6, 117.5, 112.9 (aryl), 48.3 (CH_2), 21.5 (CH_3). The NMR spectroscopic data are in accordance with the literature.[279]

HRMS (ESI) m/z calcd. for [$C_{14}H_{16}N$, M+H]$^+$: 198.1283; Found: 198.1278.

GC-FID Retention time (min): 11.087.

4.5.5.24 *N*-(2-methylbenzyl)aniline (3j)
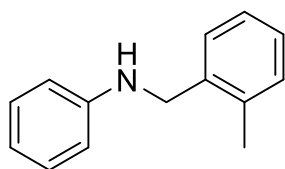
Orange oil. Yield: 84.4 mg (0.43 mmol, 43 %), GC-FID: 79 %.

^{1}H NMR (400.3 MHz, CDCl$_3$, 298 K): δ = 7.26–7.30 (m, 1H, Ar), 7.09–7.19 (m, 5H, Ar), 6.65–6.71 (m, 1H, Ar), 6.55–6.60 (m, 2H, Ar), 4.20 (s, 2H, Ar-C*H*$_2$-NH), 3.74 (br s, 1H, CH$_2$-N*H*-Ar), 2.32 (s, 3H, CH$_3$); ^{13}C{^{1}H} NMR (100.6 MHz, CDCl$_3$, 298 K): δ = 148.4 (C_q), 137.1 (C_q), 136.4 (C_q), 130.5, 129.4, 128.3, 127.5, 126.2, 117.5, 112.8 (aryl), 46.5 (CH_2), 19.0 (CH_3). The NMR spectroscopic data are in accordance with the literature.[278]

HRMS (ESI) m/z calcd. for [$C_{14}H_{16}N$, M+H]$^+$: 198.1283; Found: 198.1274.

GC-FID Retention time (min): 11.106.

4.5.5.25 *N*-(2-(piperidin-1-yl)ethyl)aniline (3k)
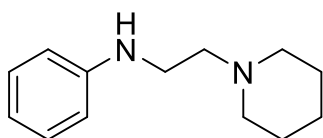
Yellow oil. Yield: 65.7 mg (0.32 mmol, 32 %), GC-FID: 32 %.

^{1}H NMR (400.3 MHz, CDCl$_3$, 298 K): δ = 7.16–7.23 (m, 2H, Ar), 6.68–6.74 (m, 1H, Ar), 6.62–6.68 (m, 2H, Ar), 4.34 (s, 1H, Ar-CH$_2$-N*H*), 3.17 (t, $^3J_{H,H}$ = 6.1 Hz, 2H, NH-CH$_2$-C*H*$_2$-Pip), 2.59 (t, $^3J_{H,H}$ = 6.1 Hz, 2H, NH-

C*H₂*-CH₂-Pip), 2.23–2.52 (m, 4H, 2 × C*H₂*), 1.53–1.66 (m, 4H, 2 × C*H₂*), 1.40–1.52 (m, 2H, C*H₂*); ^{13}C{^{1}H} NMR (100.6 MHz, CDCl₃, 298 K): δ = 148.8 (C$_q$), 129.3, 117.2, 113.0 (aryl), 57.6 (N-((CH₂)₂-(CH₂)₂)-CH₂), 54.5 (NH-CH₂-*CH₂*-N), 40.6 (NH-*CH₂*-CH₂-N), 26.1 (N-((CH₂)₂-(CH₂)₂)-*CH₂*), 24.6 (N-((CH₂)₂(CH₂)₂)-*CH₂*). The NMR spectroscopic data are in accordance with the literature.[284]

HRMS (ESI) m/z calcd. for [C₁₃H₂₁N₂, M+H]⁺: 205.1705; Found: 205.1701.

GC-FID Retention time (min): 9.879.

4.5.5.26 *N*-methylaniline (3l)

Dark yellow liquid. Yield: GC-FID: 16 %.

^{1}H NMR (400.3 MHz, CDCl₃, 298 K): δ = 7.17–7.23 (m, 2H, Ar), 6.69–6.74 (m, 1H, Ar), 6.60–6.65 (m, 2H, Ar), 3.87 (br s, 1H, N*H*), 2.84 (s, 3H, CH₃); ^{13}C{^{1}H} NMR (100.6 MHz, CDCl₃, 298 K): δ = 149.5 (C$_q$), 129.3, 117.4, 112.6 (aryl), 30.9 (CH₃). The NMR spectroscopic data are in accordance with the literature.[192]

HRMS (ESI) m/z calcd. for [C₇H₁₀N, M+H]⁺: 108.0813; Found: 108.0811.

GC-FID Retention time (min): 5.900.

4.5.5.27 *N*-ethylaniline (3m)
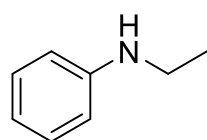
Dark yellow liquid. Yield: GC-FID: 82 %.

^{1}H NMR (400.3 MHz, CDCl₃, 298 K): δ = 7.32–7.41 (m, 2H, Ar), 6.87–6.92 (m, 1H, Ar), 6.77–6.82 (m, 2H, Ar), 3.75 (br s, 1H, N*H*), 3.33 (q, $^3J_{H,H}$ = 7.1 Hz, 2H, C*H₂*-CH₃), 1.43 (t, $^3J_{H,H}$ = 7.1 Hz, 3H, CH₂C*H₃*); ^{13}C{^{1}H} NMR (100.6 MHz, CDCl₃, 298 K): δ = 148.5 (C$_q$), 129.3, 117.3, 112.8 (aryl), 38.5 (CH₂), 14.9 (CH₃). The NMR spectroscopic data are in accordance with the literature.[192]

HRMS (ESI) m/z calcd. for [C₈H₁₂N, M+H]⁺: 122.0970; Found: 122.0960.

GC-FID Retention time (min): 6.359.

4.5.5.28 *N*-propylaniline (3n)
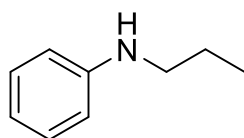
Orange oil. Yield: 6.6 mg (0.05 mmol, 5 %), GC-FID: 65 %.

^{1}H NMR (400.3 MHz, CDCl₃, 298 K): δ = 7.17–7.23 (m, 2H, Ar), 6.67–6.72 (m, 1H, Ar), 6.59–6.64 (m, 2H, Ar), 3.63 (br s, 1H, N*H*), 3.11 (t,

$^3J_{H,H}$ = 7.1 Hz, 2H, CH_2-CH$_2$-CH$_3$), 1.61–1.73 (m, 2H, CH$_2$-CH_2-CH$_3$), 1.03 (t, $^3J_{H,H}$ = 7.4 Hz, 3H, (CH$_2$)$_2$-CH_3); ^{13}C{^{1}H} NMR (100.6 MHz, CDCl$_3$, 298 K): δ = 148.7 (C$_q$), 129.3, 117.2, 112.8 (aryl), 45.9 (CH_2-CH$_2$-CH$_3$), 22.9 (CH$_2$-CH_2-CH$_3$), 11.8 ((CH$_2$)$_2$-CH_3). The NMR spectroscopic data are in accordance with the literature.[285]

HRMS (ESI) m/z calcd. for [C$_9$H$_{14}$N, M+H]$^+$: 136.1126; Found: 136.1119.

GC-FID Retention time (min): 6.997.

4.5.5.29 *N*-butylaniline (3o)

Orange oil. Yield: GC-FID: 72 %.
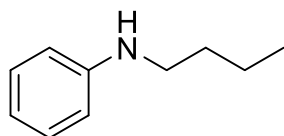
^{1}H NMR (400.3 MHz, CDCl$_3$, 298 K): δ = 7.15–7.21 (m, 2H, Ar), 6.67–6.72 (m, 1H, Ar), 6.59–6.64 (m, 2H, Ar), 3.59 (br s, 1H, NH), 3.12 (t, $^3J_{H,H}$ = 7.1 Hz, CH_2-(CH$_2$)$_2$-CH$_3$), 1.57–1.67 (m, 2H, CH$_2$-CH_2-CH$_2$-CH$_3$), 1.39–1.50 (m, 2H, (CH$_2$)$_2$-CH_2-CH$_3$), 0.97 (t, $^3J_{H,H}$ = 7.3 Hz, (CH$_2$)$_3$-CH_3); ^{13}C{^{1}H} NMR (100.6 MHz, CDCl$_3$, 298 K): δ = 148.7 (C$_q$), 129.4, 117.2, 112.8 (aryl), 43.8 (CH_2- (CH$_2$)$_2$-CH$_3$), 31.8 (CH$_2$-CH_2-CH$_2$-CH$_3$), 20.4 ((CH$_2$)$_2$-CH_2-CH$_3$), 14.0 ((CH$_2$)$_3$-CH_3). The NMR spectroscopic data are in accordance with the literature.[192]

HRMS (ESI) m/z calcd. for [C$_{10}$H$_{16}$N, M+H]$^+$: 150.1283; Found: 150.1274.

GC-FID Retention time (min): 7.630.

4.5.5.30 *N*-pentylaniline (3p)

Dark yellow oil. Yield: 10.3 mg (0.06 mmol, 6 %), GC-FID: 63 %.
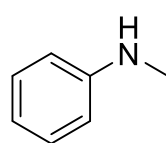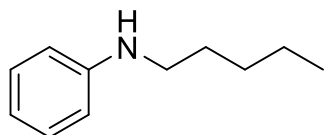
^{1}H NMR (400.3 MHz, CDCl$_3$, 298 K): δ = 7.15–7.23 (m, 2H, Ar), 6.67–6.73 (m, 1H, Ar), 6.60–6.65 (m, 2H, Ar), 3.60 (br s, 1H, NH), 3.12 (t, $^3J_{H,H}$ = 7.1 Hz, 2H, CH_2-(CH$_2$)$_3$-CH$_3$), 1.59–1.69 (m, 2H, CH$_2$-CH_2-(CH$_2$)$_2$-CH$_3$), 1.34–1.46 (m, 4H, (CH$_2$)$_2$-(CH_2)$_2$-CH$_3$), 0.94 (t, $^3J_{H,H}$ = 7.1 Hz, 3H, (CH$_2$)$_4$-CH_3); ^{13}C{^{1}H} NMR (100.6 MHz, CDCl$_3$, 298 K): δ = 148.7 (C$_q$), 129.3, 117.2, 112.8 (aryl), 44.1 (CH_2-(CH$_2$)$_3$-CH$_3$), 29.5 (CH$_2$-CH_2-(CH$_2$)$_2$-CH$_3$), 29.4 ((CH$_2$)$_2$-CH_2-CH$_2$-CH$_3$), 22.7 ((CH$_2$)$_3$-CH_2-CH$_3$), 14.2 ((CH$_2$)$_4$-CH_3). The NMR spectroscopic data are in accordance with the literature.[286]

HRMS (ESI) m/z calcd. for [C$_{11}$H$_{18}$N, M+H]$^+$: 164.1439; Found: 164.1432.

GC-FID Retention time (min): 8.206.

4.5.5.20 *N*-hexylaniline (3q)
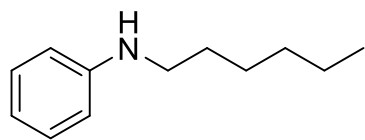
Orange oil. Yield: 53.7 mg (0.30 mmol, 30 %), GC-FID: 64 %.

^{1}H NMR (400.3 MHz, CDCl$_3$, 298 K): δ = 7.18–7.26 (m, 2H, Ar), 6.71–6.77 (m, 1H, Ar), 6.63–6.68 (m, 2H, Ar), 3.61 (br s, 1H, N*H*), 3.15 (t, $^3J_{H,H}$ = 7.2 Hz, 2H, C*H*$_2$- (CH$_2$)$_4$-C*H*$_3$), 1.62–1.71 (m, 2H, CH$_2$-C*H*$_2$-(CH$_2$)$_3$-CH$_3$), 1.33–1.51 (m, 6H, (CH$_2$)$_2$-(C*H*$_2$)$_3$-CH$_3$), 0.94–1.02 (m, 3H, (CH$_2$)$_5$-C*H*$_3$); ^{13}C{^{1}H} NMR (100.6 MHz, CDCl$_3$, 298 K): δ = 148.7 (C$_q$), 129.3, 117.2, 112.8 (aryl), 44.1 (*C*H$_2$- (CH$_2$)$_4$-CH$_3$), 31.8 (CH$_2$-*C*H$_2$-(CH$_2$)$_3$-CH$_3$), 29.7 ((CH$_2$)$_2$-*C*H$_2$-(CH$_2$)$_2$-CH$_3$), 27.0 ((CH$_2$)$_3$-*C*H$_2$-CH$_2$-CH$_3$), 22.7 ((CH$_2$)$_4$-*C*H$_2$-CH$_3$), 14.1 ((CH$_2$)$_5$-*C*H$_3$). The NMR spectroscopic data are in accordance with the literature.[192]

HRMS (ESI) m/z calcd. for [C$_{12}$H$_{20}$N, M+H]$^+$: 178.1596; Found: 178.1588.

GC-FID Retention time (min): 8.742.

4.5.5.20 *N*-(*iso*-propyl)aniline (3r)
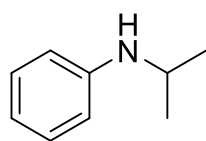
Brown oil. Yield: 100.3 mg (0.74 mmol, 74 %), GC-FID: 82 %.

^{1}H NMR (400.3 MHz, CDCl$_3$, 298 K): δ = 7.14–7.21 (m, 2H, Ar), 6.66–6.72 (m, 1H, Ar), 6.57–6.62 (m, 2H, Ar), 3.64 (sept, $^3J_{H,H}$ = 6.2 Hz, 1H, C*H*-(CH$_3$)$_2$), 3.44 (br s, 1H, CH-N*H*-Ar), 1.22 (d, $^3J_{H,H}$ = 6.2 Hz, 6H, CH-(C*H*$_3$)$_2$); ^{13}C{^{1}H} NMR (100.6 MHz, CDCl$_3$, 298 K): δ = 147.7 (C$_q$), 129.4, 117.1, 113.4 (aryl), 44.3 (*C*H-(CH$_3$)$_2$), 23.2 (CH-(*C*H$_3$)$_2$). The NMR spectroscopic data are in accordance with the literature.[285]

HRMS (ESI) m/z calcd. for [C$_9$H$_{14}$N, M+H]$^+$: 136.1126; Found: 136.1118.

GC-FID Retention time (min): 8.524.

4.5.5.20 *N*-(*sec*-butyl)aniline (3s)
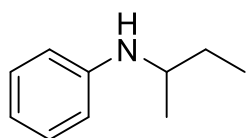
Orange oil. Yield: 82.4 mg (0.55 mmol, 55 %), GC-FID: 55 %.

^{1}H NMR (400.3 MHz, CDCl$_3$, 298 K): δ = 7.13–7.21 (m, 2H, Ar), 6.64–6.70 (m, 1H, Ar), 6.56–6.62 (m, 2H, Ar), 3.36–3.50 (m, 2H, CH-N*H*-Ar & CH$_3$-C*H*-CH$_2$-CH$_3$), 1.43–1.68 (m, 2H, CH$_3$-CH-C*H*$_2$-CH$_3$), 1.19 (d, $^3J_{H,H}$ = 6.5 Hz, 3H, C*H*$_3$-CH-CH$_2$-CH$_3$), 0.97 (t, $^3J_{H,H}$ = 7.5 Hz, 3H, CH$_3$-CH-CH$_2$-C*H*$_3$); ^{13}C{^{1}H} NMR (100.6 MHz, CDCl$_3$, 298 K): δ = 147.9 (C$_q$), 129.4, 116.9, 113.3 (aryl), 49.9 (CH$_3$-*C*H-CH$_2$-CH$_3$), 29.8 (CH$_3$-CH-*C*H$_2$-CH$_3$), 20.4 (*C*H$_3$-CH-CH$_2$-CH$_3$), 10.5 (CH$_3$-CH-CH$_2$-*C*H$_3$). The NMR spectroscopic data are in accordance with the literature.[287]

HRMS (ESI) m/z calcd. for [C$_{10}$H$_{16}$N, M+H]$^+$: 150.1283; Found: 150.1274.

GC-FID Retention time (min): 7.144.

4.5.5.20 *N*-(1-phenylethyl)aniline (3t)
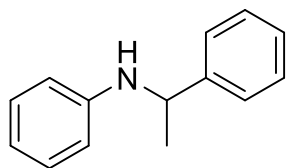
Brown oil. Yield: 51.5 mg (0.26 mmol, 26 %), GC-FID: 49 %.

^{1}H NMR (400.3 MHz, CDCl$_3$, 298 K): δ = 7.35–7.40 (m, 2H, Ar), 7.29–7.35 (m, 2H, Ar), 7.20–7.25 (m, 1H, Ar), 7.06–7.12 (m, 2H, Ar), 6.62–6.67 (m, 1H, Ar), 6.49–6.54 (m, 2H, Ar), 4.49 (q, $^3J_{H,H}$ = 6.7 Hz, 1H, CH$_3$-C*H*-Ar), 4.03 (br s, 1H, CH-N*H*-Ar), 1.52 (d, $^3J_{H,H}$ = 6.7 Hz, 3H, C*H*$_3$-CH-Ar); ^{13}C{^{1}H} NMR (100.6 MHz, CDCl$_3$, 298 K): δ = 147.4 (C$_q$), 145.4 (C$_q$), 129.2, 128.8, 127.0, 126.0, 117.4, 113.4 (aryl), 53.6 (CH$_3$-*C*H-Ar), 25.1 (*C*H$_3$-CH-Ar). The NMR spectroscopic data are in accordance with the literature.[286]

HRMS (ESI) m/z calcd. for [C$_{14}$H$_{16}$N, M+H]$^+$: 198.1283; Found: 198.1284.

GC-MS Retention time (min): 10.624

4.5.5.20 *N*-cyclohexylaniline (3u)
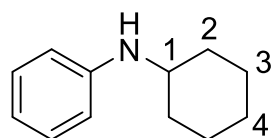
Orange oil. Yield: 45.2 mg (0.26 mmol, 26 %), GC-FID: 61 %.

^{1}H NMR (400.3 MHz, CDCl$_3$, 298 K): δ = 7.16–7.23 (m, 2H, Ar), 6.68–6.75 (m, 1H, Ar), 6.60–6.66 (m, 2H, Ar), 3.54 (br s, 1H, CH-N*H*-Ar), 3.25–3.36 (m, 1H, C*H*), 2.06–2.15 (m, 2H, 2 × C*H*$_{equatorial,2}$), 1.75–1.84 (m, 2H, 2 × C*H*$_{equatorial,3}$), 1.67–1.75 (m, 1H, C*H*$_{equatorial,4}$), 1.35–1.48 (m, 2H, 2 × C*H*$_{axial,3}$), 1.13–1.34 (m, 3H, 3 × C*H*$_{axial,2&4}$); ^{13}C{^{1}H} NMR (100.6 MHz, CDCl$_3$, 298 K): δ = 147.5 (C$_q$), 129.4, 116.9,

113.2 (aryl), 51.8 (*C*H-((CH$_2$)$_2$-(CH$_2$)$_2$)-CH$_2$), 33.6 (CH-((CH$_2$)$_2$-(CH$_2$)$_2$)-CH$_2$), 26.1 (CH-((CH$_2$)$_2$-(*C*H$_2$)$_2$)-CH$_2$), 25.1 (CH-((CH$_2$)$_2$-(CH$_2$)$_2$)-*C*H$_2$). The NMR spectroscopic data are in accordance with the literature.[287]

HRMS (ESI) m/z calcd. for [C$_{12}$H$_{18}$N, M+H]$^+$: 176.1439; Found: 176.1433.

GC-FID Retention time (min): 8.937.

4.5.5.20 *N*-(1-(naphthalen-1-yl)ethyl)-3-(3-(trifluoromethyl)phenyl)propan-1-amine (cinacalcet) (4)
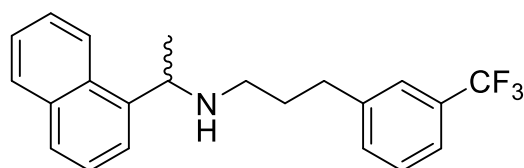
Orange oil. Yield: 36.6 mg (0.10 mmol, 10 %), GC-FID: 50 %.

^{1}H NMR (400.3 MHz, toluene-d_8, 298 K): δ = 8.13–8.18 (m, 1H, Ar), 7.62–7.68 (m, 2H, Ar), 7.53–7.58, (m, 1H, Ar), 7.19–7.36, (m, 5H, Ar), 6.87–6.93 (m, 2H, Ar), 3.80 (q, $^2J_{H,H}$ = 6.6 Hz, 1H, CH$_3$-C*H*), 4.36 (q, $J_{H,H}$ = 13.7 Hz, 2H, CH-NH-C*H$_2$*), 2.22–2.43 (m, 4H, NH-C*H$_2$*-CH$_2$-C*H$_2$*-Ar), 1.39–1.49 (m, 2H, NH-CH$_2$-C*H$_2$*-CH$_2$-Ar), 1.36 (br s, 1H, CH-N*H*-CH$_2$), 1.34 (d, $^2J_{H,H}$ = 6.5 Hz, 3H, C*H$_3$*-CH); ^{13}C{^{1}H} NMR (100.6 MHz, toluene-d_8, 298 K): δ = 143.8 (C$_q$), 141.9 (C$_q$), 134.8, 132.06, 132.02, 130.9 (q, $J_{C,F}$ = 31.5 Hz, CF$_3$), 129.4, 129.2, 127.6, 125.93, 125.86, 125.5, 123.5, 123.4, 122.8 (q, $J_{C,F}$ = 3.7 Hz, aryl), 54.7 (CH), 47.4, 33.5, 32.2 (CH$_2$), 23.9 (CH$_3$). The NMR spectroscopic data are in accordance with the literature.[288]

HRMS (ESI) m/z calcd. for [C$_{22}$H$_{23}$F$_3$N, M+H]$^+$: 358.1777; Found: 358.1778.

GC-FID Retention time (min): 12.430.

5 References

[1]   J. Leonard, A. J. Blacker, S. P. Marsden, M. F. Jones, K. R. Mulholland, R. Newton, *Org. Process Res. Dev.* **2015**, *19*, 1400-1410.

[2]   P. Anastas, N. Eghbali, *Chem. Soc. Rev.* **2010**, *39*, 301-312.

[3]   K. S. Hayes, *Applied Catalysis A: General* **2001**, *221*, 187-195.

[4]   R. A. Sheldon, *Chem Commun (Camb)* **2008**, 3352-3365.

[5]   P. T. Anastas, M. M. Kirchhoff, T. C. Williamson, *Applied Catalysis A: General* **2001**, *221*, 3-13.

[6]   P. F. Vogt, J. J. Gerulis, **2000**.

[7]   S. B. Markofsky, **2000**.

[8]   in *Organic Reactions*, pp. 267-306.

[9]   in *Organic Reactions*, pp. 337-449.

[10]   L. Bauer, O. Exner, *Angew. Chem., Int. Ed.* **1974**, *13*, 376-384.

[11]   in *Organic Reactions*, pp. 307-336.

[12]   P. Roose, K. Eller, E. Henkes, R. Rossbacher, H. Höke, **2015**, pp. 1-55.

[13]   S. Gabriel, *Ber. Dtsch. Chem. Ges.* **1887**, *20*, 2224-2236.

[14]   J. C. Sheehan, W. A. Bolhofer, *J. Am. Chem. Soc.* **1950**, *72*, 2786-2788.

[15]   J. Louie, J. F. Hartwig, *Tetrahedron Lett.* **1995**, *36*, 3609-3612.

[16]   A. S. Guram, R. A. Rennels, S. L. Buchwald, *Angew. Chem., Int. Ed.* **1995**, *34*, 1348-1350.

[17]   M. L. Louillat, F. W. Patureau, *Chem. Soc. Rev.* **2014**, *43*, 901-910.

[18]   M. M. Heravi, Z. Kheilkordi, V. Zadsirjan, M. Heydari, M. Malmir, *J. Organomet. Chem.* **2018**, *861*, 17-104.

[19]   B. Schlummer, U. Scholz, *Adv. Synth. Catal.* **2004**, *346*, 1599-1626.

[20]   P. Ruiz-Castillo, S. L. Buchwald, *Chem. Rev.* **2016**, *116*, 12564-12649.

[21]   M. L. Moore, **2011**, 301-330.

[22]   W. Eschweiler, *Ber. Dtsch. Chem. Ges.* **1905**, *38*, 880-882.

[23]   E. Podyacheva, O. I. Afanasyev, A. A. Tsygankov, M. Makarova, D. Chusov, *Synthesis* **2019**, *51*, 2667-2677.

[24]   O. I. Afanasyev, E. Kuchuk, D. L. Usanov, D. Chusov, *Chem. Rev.* **2019**, *119*, 11857-11911.

[25]   S. Gomez, J. A. Peters, T. Maschmeyer, *Adv. Synth. Catal.* **2002**, *344*, 1037-1057.

[26]   A. Corma, J. Navas, M. J. Sabater, *Chem. Rev.* **2018**, *118*, 1410-1459.

[27]   X. Ma, C. Su, Q. Xu, *Top. Curr. Chem.* **2016**, *374*, 27.

[28]   J. R. Ludwig, C. S. Schindler, *Chem* **2017**, *2*, 313-316.

[29]   W. F. McDonough, S. s. Sun, *Chem. Geol.* **1995**, *120*, 223-253.

[30]   M. Valko, H. Morris, M. Cronin, *Curr. Med. Chem.* **2005**, *12*, 1161-1208.

[31]   K. S. Egorova, V. P. Ananikov, *Organometallics* **2017**, *36*, 4071-4090.

[32]   K. S. Egorova, V. P. Ananikov, *Angew. Chem., Int. Ed.* **2016**, *55*, 12150-12162.

[33]   N. Deibl, K. Ament, R. Kempe, *J. Am. Chem. Soc.* **2015**, *137*, 12804-12807.

[34]   N. Deibl, R. Kempe, *Angew. Chem., Int. Ed.* **2017**, *56*, 1663-1666.

[35]   J. R. Khusnutdinova, D. Milstein, *Angew. Chem., Int. Ed.* **2015**, *54*, 12236-12273.

[36]   T. P. Goncalves, K. W. Huang, *J. Am. Chem. Soc.* **2017**, *139*, 13442-13449.

[37]   C. Gunanathan, D. Milstein, *Acc. Chem. Res.* **2011**, *44*, 588-602.

[38]   J. Maes, E. A. Mitchell, B. U. W. Maes, **2016**, pp. 192-202.

[39]   T. E. Müller, K. C. Hultzsch, M. Yus, F. Foubelo, M. Tada, *Chem. Rev.* **2008**, *108*, 3795-3892.

[40]   in *Organic Reactions*, pp. 1-554.

[41]   L. Huang, M. Arndt, K. Goossen, H. Heydt, L. J. Goossen, *Chem. Rev.* **2015**, *115*, 2596-2697.

[42]   in *Early Main Group Metal Catalysis*, pp. 59-91.

[43]   P. Colonna, S. Bezzenine-Lafollée, R. GIL, J. Hannedouche, *Adv. Synth. Catal.*, *n/a*.

[44]   K. C. Hultzsch, *Adv. Synth. Catal.* **2005**, *347*, 367-391.

[45]   N. Nishina, Y. Yamamoto, Top. Organomet. Chem., ed. V. P. Ananikov, M. Tanaka, Springer, Berlin, **2013**.

[46]   A. L. Reznichenko, A. J. Nawara-Hultzsch, K. C. Hultzsch, in *Stereoselective Formation of Amines* (Eds.: W. Li, X. Zhang), Springer Berlin Heidelberg, Berlin, Heidelberg, **2014**, pp. 191-260.

[47]   T. E. Müller, M. Beller, *Chem. Rev.* **1998**, *98*, 675-704.

[48]   S. Doye, in *Science of Synthesis, Vol. 40a*, Georg Thieme Verlag KG, Stuttgart, **2009**, pp. 241-304.

[49]   D. Steinborn, R. Taube, *Z. Chem.* **1986**, *26*, 349-359.

[50]   B. Schäfer, *Chem. unserer Zeit* **2013**, *47*, 174-182.

[51]   K. Komeyama, T. Morimoto, K. Takaki, *Angew. Chem., Int. Ed.* **2006**, *45*, 2938-2941.

[52]   S. Fleischer, S. Werkmeister, S. Zhou, K. Junge, M. Beller, *Chem. - Eur. J.* **2012**, *18*, 9005-9010.

[53]   E. Bernoud, P. Oulie, R. Guillot, M. Mellah, J. Hannedouche, *Angew. Chem., Int. Ed.* **2014**, *53*, 4930-4934.

[54]   C. B. Huehls, A. Lin, J. Yang, *Org. Lett.* **2014**, *16*, 3620-3623.

[55]   K. Burgess, M. J. Ohlmeyer, *Chem. Rev.* **1991**, *91*, 1179-1191.

[56]   F. Alonso, I. P. Beletskaya, M. Yus, *Chem. Rev.* **2004**, *104*, 3079-3159.

[57]   M. Beller, J. Seayad, A. Tillack, H. Jiao, *Angew. Chem., Int. Ed.* **2004**, *43*, 3368-3398.

5 References

[58]   K. D. Hesp, M. Stradiotto, *ChemCatChem* **2010**, *2*, 1192-1207.

[59]   M. Beller, C. Breindl, M. Eichberger, C. G. Hartung, J. Seayad, O. R. Thiel, A. Tillack, H. Trauthwein, *Synlett* **2002**, *2002*, 1579-1594.

[60]   A. Takemiya, J. F. Hartwig, *J. Am. Chem. Soc.* **2006**, *128*, 6042-6043.

[61]   A. M. Tondreau, C. C. Atienza, K. J. Weller, S. A. Nye, K. M. Lewis, J. G. Delis, P. J. Chirik, *Science* **2012**, *335*, 567-570.

[62]   A. E. Strom, J. F. Hartwig, *J. Org. Chem.* **2013**, *78*, 8909-8914.

[63]   S. M. Bronner, R. H. Grubbs, *Chem. Sci.* **2014**, *5*.

[64]   S. Zhu, S. L. Buchwald, *J. Am. Chem. Soc.* **2014**, *136*, 15913-15916.

[65]   J. Chen, B. Cheng, M. Cao, Z. Lu, *Angew. Chem., Int. Ed.* **2015**, *54*, 4661-4664.

[66]   W. Markownikoff, *Ann. Chem. Pharm.* **1870**, *153*, 228-259.

[67]   J. Haggin, *Chem. Eng. News* **1993**, *71*, 23-27.

[68]   J. Chatt, L. A. Duncanson, *J. Chem. Soc.* **1953**, 2939.

[69]   S. G. Davis, F. Scott, *J. Organomet. Chem.* **1980**, *188*, C41-C42.

[70]   S. G. Davies, M. L. H. Green, D. M. P. Mingos, *Tetrahedron* **1978**, *34*, 3047-3077.

[71]   M. Rosenblum, *Acc. Chem. Res.* **1974**, *7*, 122-128.

[72]   P. Lennon, M. Madhavarao, A. Rosan, M. Rosenblum, *J. Organomet. Chem.* **1976**, *108*, 93-109.

[73]   A. Rosan, M. Rosenblum, J. Tancrede, *J. Am. Chem. Soc.* **1973**, *95*, 3062-3064.

[74]   P. J. Lennon, A. Rosan, M. Rosenblum, J. Tancrede, P. Waterman, *J. Am. Chem. Soc.* **1980**, *102*, 7033-7038.

[75]   P. Lennon, A. M. Rosan, M. Rosenblum, *J. Am. Chem. Soc.* **1977**, *99*, 8426-8439.

[76]   D. L. Reger, E. C. Culbertson, *J. Am. Chem. Soc.* **1976**, *98*, 2789-2794.

[77]   P. K. Wong, M. Madhavarao, D. F. Marten, M. Rosenblum, *J. Am. Chem. Soc.* **1977**, *99*, 2823-2824.

[78]   S. R. Berryhill, M. Rosenblum, *J. Org. Chem.* **1980**, *45*, 1984-1986.

[79]   T. C. Flood, D. L. Miles, *J. Organomet. Chem.* **1977**, *127*, 33-44.

[80]   L. J. Dizikes, A. Wojcicki, *J. Am. Chem. Soc.* **1975**, *97*, 2540-2542.

[81]   E. A. K. Von Gustorf, *The organic chemistry of iron,* Elsevier, **2012**.

[82]   G. R. Stephenson, in *Science of Synthesis, Vol. Knowledge Updates 2014/1*, Thieme Verlagsgruppe, Stuttgart, New York, Delhi, Rio, **2014**, pp. 1-191.

[83]   E. Alberch, J. S. Ulicki, M. D. S. Asad, M. M. Hossain, *The Chemistry of Iron-Alkyl Complexes*, **2013**.

[84]   A. Zulys, M. Dochnahl, D. Hollmann, K. Lohnwitz, J. S. Herrmann, P. W. Roesky, S. Blechert, *Angew. Chem., Int. Ed.* **2005**, *44*, 7794-7798.

[85]   A. Mukherjee, T. K. Sen, P. K. Ghorai, P. P. Samuel, C. Schulzke, S. K. Mandal, *Chem. - Eur. J.* **2012**, *18*, 10530-10545.

[86] A. Mukherjee, T. K. Sen, P. K. Ghorai, S. K. Mandal, *Organometallics* **2013**, *32*, 7213-7224.

[87] J.-W. Pissarek, D. Schlesiger, P. W. Roesky, S. Blechert, *Adv. Synth. Catal.* **2009**, *351*, 2081-2085.

[88] R. M. Beesley, C. K. Ingold, J. F. Thorpe, *J. Chem. Soc., Trans.* **1915**, *107*, 1080-1106.

[89] B. L. Shaw, *J. Am. Chem. Soc.* **1975**, *97*, 3856-3857.

[90] S. M. Bachrach, *J. Org. Chem.* **2008**, *73*, 2466-2468.

[91] E. Bernoud, C. Lepori, M. Mellah, E. Schulz, J. Hannedouche, *Catal. Sci. Technol.* **2015**, *5*, 2017-2037.

[92] M. E. Jung, G. Piizzi, *Chem. Rev.* **2005**, *105*, 1735-1766.

[93] R. Blieck, J. Bahri, M. Taillefer, F. Monnier, *Org. Lett.* **2016**, *18*, 1482-1485.

[94] L. A. Perego, R. Blieck, A. Groué, F. Monnier, M. Taillefer, I. Ciofini, L. Grimaud, *ACS Catalysis* **2017**, *7*, 4253-4264.

[95] J. Michaux, V. Terrasson, S. Marque, J. Wehbe, D. Prim, J.-M. Campagne, *Eur. J. Org. Chem.* **2007**, *2007*, 2601-2603.

[96] X. Cheng, Y. Xia, H. Wei, B. Xu, C. Zhang, Y. Li, G. Qian, X. Zhang, K. Li, W. Li, *Eur. J. Org. Chem.* **2008**, *2008*, 1929-1936.

[97] M. S. Jung, W. S. Kim, Y. H. Shin, H. J. Jin, Y. S. Kim, E. J. Kang, *Org. Lett.* **2012**, *14*, 6262-6265.

[98] J. Gui, C. M. Pan, Y. Jin, T. Qin, J. C. Lo, B. J. Lee, S. H. Spergel, M. E. Mertzman, W. J. Pitts, T. E. La Cruz, M. A. Schmidt, N. Darvatkar, S. R. Natarajan, P. S. Baran, *Science* **2015**, *348*, 886-891.

[99] K. Zhu, M. P. Shaver, S. P. Thomas, *Chem. Sci.* **2016**, *7*, 3031-3035.

[100] M. Villa, A. Jacobi von Wangelin, *Angew. Chem., Int. Ed.* **2015**, *54*, 11906-11908.

[101] K. J. Gallagher, R. L. Webster, *Chem Commun (Camb)* **2014**, *50*, 12109-12111.

[102] M. Kamitani, M. Itazaki, C. Tamiya, H. Nakazawa, *J. Am. Chem. Soc.* **2012**, *134*, 11932-11935.

[103] W. Malisch, B. Klüpfel, D. Schumacher, M. Nieger, *J. Organomet. Chem.* **2002**, *661*, 95-110.

[104] M. Itazaki, S. Katsube, M. Kamitani, H. Nakazawa, *Chem Commun (Camb)* **2016**, *52*, 3163-3166.

[105] J. Hannedouche, C. Lepori, *Synthesis* **2016**, *49*, 1158-1167.

[106] T. C. T. Chang, B. M. Foxman, M. Rosenblum, C. Stockman, *J. Am. Chem. Soc.* **1981**, *103*, 7361-7362.

5 References

[107] A. Cutler, D. Ehntholt, W. P. Giering, P. Lennon, S. Raghu, A. Rosan, M. Rosenblum, J. Tancrede, D. Wells, *J. Am. Chem. Soc.* **1976**, *98*, 3495-3507.

[108] R. B. King, F. G. A. Stone, W. L. Jolly, G. Austin, W. Covey, D. Rabinovich, H. Steinberg, R. Tsugawa, *Inorg. Synth.* **1963**, *7*, 99-115.

[109] B. M. Mattson, W. A. G. Graham, *Inorg. Chem.* **1981**, *20*, 3186-3189.

[110] J.-S. Park, D.-H. Kim, J. Ko, S. H. Kim, S. Cho, C.-H. Lee, S. O. Kang, *Organometallics* **2001**, *20*, 4632-4640.

[111] C. A. Tolman, *Chem. Rev.* **1977**, *77*, 313-348.

[112] M. C. Nielsen, K. J. Bonney, F. Schoenebeck, *Angew. Chem., Int. Ed.* **2014**, *53*, 5903-5906.

[113] J. A. Timney, *Inorg. Chem.* **1979**, *18*, 2502-2506.

[114] W. S. Wadsworth, W. D. Emmons, *J. Am. Chem. Soc.* **1962**, *84*, 610-617.

[115] J. A. van Rijn, E. Gouré, M. A. Siegler, A. L. Spek, E. Drent, E. Bouwman, *J. Organomet. Chem.* **2011**, *696*, 1899-1903.

[116] S. El-Tarhuni, M. Ho, M. H. Kawser, S. Shi, M. W. Whiteley, *J. Organomet. Chem.* **2014**, *752*, 30-36.

[117] N. J. Coville, E. A. Darling, A. W. Hearn, P. Johnston, *J. Organomet. Chem.* **1987**, *328*, 375-385.

[118] H. S. Clayton, J. R. Moss, M. E. Dry, *J. Organomet. Chem.* **2003**, *688*, 181-191.

[119] *Organic Syntheses* **1987**, *65*, 42.

[120] J.-P. Barras, S. G. Davies, M. R. Metzler, A. J. Edwards, V. M. Humphreys, K. Prout, *J. Organomet. Chem.* **1993**, *461*, 157-165.

[121] R. B. King, A. Efraty, W. M. Douglas, *J. Organomet. Chem.* **1973**, *56*, 345-355.

[122] K. Jonas, P. Klusmann, R. Goddard, *Z. Naturforsch., B: Chem. Sci.* **1995**, *50*.

[123] T. V. Harris, J. W. Rathke, E. L. Muetterties, *J. Am. Chem. Soc.* **1978**, *100*, 6966-6977.

[124] A. Yukiko, H. Naoko, I. Toshiya, I. Ikuyo, M. Hitoshi, (NIPPON CATALYTIC CHEM IND), US6281389, **1999.**

[125] W. H. Knoth, *Inorg. Chem.* **1975**, *14*, 1566-1572.

[126] L. Cosslett, L. A. P. Kane-Maguire, *J. Organomet. Chem.* **1979**, *178*, C17-C19.

[127] S. Chapman, L. A. P. Kane-Maguire, *J. Chem. Soc., Dalton Trans.* **1995**, 2021-2026.

[128] T. S. Piper, G. Wilkinson, *J. Inorg. Nucl. Chem.* **1956**, *3*, 104-124.

[129] P. Zimmer, Y. Sun, W. R. Thiel, *J. Organomet. Chem.* **2014**, *774*, 12-18.

[130] A. Maercker, M. Passlack, *Chem. Ber.* **1982**, *115*, 540-577.

[131] D. G. Alway, K. W. Barnett, *Inorg. Chem.* **2002**, *17*, 2826-2831.

[132] B. F. Hallam, P. L. Pauson, *J. Chem. Soc.* **1956**, 3030.

[133] H.-j. Li, M. M. Turnbull, *J. Organomet. Chem.* **1991**, *419*, 245-249.

[134] W. N. Rogers, M. C. Baird, *J. Organomet. Chem.* **1979**, *182*, C65-C68.

[135] N. De Luca, A. Wojcicki, *J. Organomet. Chem.* **1980**, *193*, 359-378.

[136] T. Li, A. J. Lough, R. H. Morris, *Chem. - Eur. J.* **2007**, *13*, 3796-3803.

[137] F. G. Bordwell, N. R. Vanier, W. S. Matthews, J. B. Hendrickson, P. L. Skipper, *J. Am. Chem. Soc.* **1975**, *97*, 7160-7162.

[138] C. Xi, X. Yan, C. Lai, K.-i. Kanno, T. Takahashi, *Organometallics* **2008**, *27*, 3834-3839.

[139] G. R. Fulmer, A. J. M. Miller, N. H. Sherden, H. E. Gottlieb, A. Nudelman, B. M. Stoltz, J. E. Bercaw, K. I. Goldberg, *Organometallics* **2010**, *29*, 2176-2179.

[140] C. Elschenbroich, A. Salzer, *Organometallchemie,* B. G. Teubner, Stuttgart, **1988**.

[141] P. Eilbracht, L. Bärfacker, C. Buss, C. Hollmann, B. E. Kitsos-Rzychon, C. L. Kranemann, T. Rische, R. Roggenbuck, A. Schmidt, *Chem. Rev.* **1999**, *99*, 3329-3366.

[142] R. Franke, D. Selent, A. Borner, *Chem. Rev.* **2012**, *112*, 5675-5732.

[143] D. E. Fogg, E. N. dos Santos, *Coord. Chem. Rev.* **2004**, *248*, 2365-2379.

[144] C. Gunanathan, D. Milstein, *Science* **2013**, *341*, 1229712.

[145] B. Charles, R. Larsen, J. M. Martinelli, T. M. Raza, O. Thiel, (AMGEN INC.), WO 2009/002427, **2009.**

[146] M. Stradiotto, R. J. Lundgren, *Ligand Design in Metal Chemistry: Reactivity and Catalysis,* John Wiley & Sons, Ltd. , **2016**.

[147] B. M. Trost, M. C. Ryan, *Angew. Chem., Int. Ed.* **2017**, *56*, 2862-2879.

[148] J. M. O'Connor, C. P. Casey, *Chem. Rev.* **1987**, *87*, 307-318.

[149] B. L. Conley, M. K. Pennington-Boggio, E. Boz, T. J. Williams, *Chem. Rev.* **2010**, *110*, 2294-2312.

[150] Y. Shvo, D. Czarkie, Y. Rahamim, D. F. Chodosh, *J. Am. Chem. Soc.* **1986**, *108*, 7400-7402.

[151] H. J. Knölker, *J. Prakt. Chem./Chem.-Ztg.* **1996**, *338*, 190-192.

[152] A. Pagnoux-Ozherelyeva, N. Pannetier, M. D. Mbaye, S. Gaillard, J. L. Renaud, *Angew. Chem., Int. Ed.* **2012**, *51*, 4976-4980.

[153] I. Bauer, H. J. Knolker, *Chem. Rev.* **2015**, *115*, 3170-3387.

[154] S. Elangovan, S. Quintero-Duque, V. Dorcet, T. Roisnel, L. Norel, C. Darcel, J.-B. Sortais, *Organometallics* **2015**, *34*, 4521-4528.

[155] V. P. Ananikov, M. Tanaka, *Top. Organomet. Chem.* **2013**, *43*.

[156] M. H. S. A. Hamid, P. A. Slatford, J. M. J. Williams, *Adv. Synth. Catal.* **2007**, *349*, 1555-1575.

[157] Y. Watanabe, Y. Tsuji, Y. Ohsugi, *Tetrahedron Lett.* **1981**, *22*, 2667-2670.

5 References

[158] S.-I. Murahashi, K. Kondo, T. Hakata, *Tetrahedron Lett.* **1982**, *23*, 229-232.

[159] R. Grigg, T. R. B. Mitchell, S. Sutthivaiyakit, N. Tongpenyai, *J. Chem. Soc., Chem. Commun.* **1981**, 611.

[160] O. Doebner, W. v. Miller, *Ber. Dtsch. Chem. Ges.* **1881**, *14*, 2812-2817.

[161] Y. Tsuji, R. Takeuchi, H. Ogawa, Y. Watanabe, *Chem. Lett.* **1986**, *15*, 293-294.

[162] G. Guillena, J. R. D, M. Yus, *Chem. Rev.* **2010**, *110*, 1611-1641.

[163] D. Wang, D. Astruc, *Chem. Rev.* **2015**, *115*, 6621-6686.

[164] S. Michlik, R. Kempe, *Chem. - Eur. J.* **2010**, *16*, 13193-13198.

[165] V. R. Jumde, L. Gonsalvi, A. Guerriero, M. Peruzzini, M. Taddei, *Eur. J. Org. Chem.* **2015**, *2015*, 1829-1833.

[166] N. Kaloglu, I. Özdemir, N. Gürbüz, M. Achard, C. Bruneau, *Catal. Commun.* **2016**, *74*, 33-38.

[167] M. Wills, *Top. Curr. Chem.* **2016**, *374*, 14.

[168] T. Yan, B. L. Feringa, K. Barta, *Nat. Commun.* **2014**, *5*, 5602.

[169] A. Nerush, M. Vogt, U. Gellrich, G. Leitus, Y. Ben-David, D. Milstein, *J. Am. Chem. Soc.* **2016**, *138*, 6985-6997.

[170] J. O. Bauer, S. Chakraborty, D. Milstein, *ACS Catalysis* **2017**, *7*, 4462-4466.

[171] N. A. Espinosa-Jalapa, A. Kumar, G. Leitus, Y. Diskin-Posner, D. Milstein, *J. Am. Chem. Soc.* **2017**, *139*, 11722-11725.

[172] S. Chakraborty, U. K. Das, Y. Ben-David, D. Milstein, *J. Am. Chem. Soc.* **2017**, *139*, 11710-11713.

[173] N. A. Espinosa-Jalapa, A. Nerush, L. J. W. Shimon, G. Leitus, L. Avram, Y. Ben-David, D. Milstein, *Chem. - Eur. J.* **2017**, *23*, 5934-5938.

[174] A. Kumar, N. A. Espinosa-Jalapa, G. Leitus, Y. Diskin-Posner, L. Avram, D. Milstein, *Angew. Chem., Int. Ed.* **2017**, *56*, 14992-14996.

[175] U. K. Das, Y. Ben-David, Y. Diskin-Posner, D. Milstein, *Angew. Chem., Int. Ed.* **2018**, *57*, 2179-2182.

[176] P. Daw, A. Kumar, N. A. Espinosa-Jalapa, Y. Diskin-Posner, Y. Ben-David, D. Milstein, *ACS Catalysis* **2018**, *8*, 7734-7741.

[177] Y.-Q. Zou, S. Chakraborty, A. Nerush, D. Oren, Y. Diskin-Posner, Y. Ben-David, D. Milstein, *ACS Catalysis* **2018**, *8*, 8014-8019.

[178] A. Kumar, T. Janes, N. A. Espinosa-Jalapa, D. Milstein, *Angew. Chem., Int. Ed.* **2018**, *57*, 12076-12080.

[179] U. K. Das, Y. Ben-David, G. Leitus, Y. Diskin-Posner, D. Milstein, *ACS Catalysis* **2018**, *9*, 479-484.

[180] T. Zell, R. Langer, *ChemCatChem* **2018**, *10*, 1930-1940.

[181] M. E. van der Boom, D. Milstein, *Chem. Rev.* **2003**, *103*, 1759-1792.

[182]   E. Khaskin, M. A. Iron, L. J. Shimon, J. Zhang, D. Milstein, *J. Am. Chem. Soc.* **2010**, *132*, 8542-8543.

[183]   R. H. Crabtree, *Organometallics* **2011**, *30*, 17-19.

[184]   G. Koten, R. Gossage, *The Privileged Pincer-Metal Platform,* Springer International Publishing, Cham, **2015**.

[185]   F. Kallmeier, R. Kempe, *Angew. Chem., Int. Ed.* **2018**, *57*, 46-60.

[186]   T. Irrgang, R. Kempe, *Chem. Rev.* **2018**.

[187]   C. Gunanathan, Y. Ben-David, D. Milstein, *Science* **2007**, *317*, 790-792.

[188]   M. Bertoli, A. Choualeb, A. J. Lough, B. Moore, D. Spasyuk, D. G. Gusev, *Organometallics* **2011**, *30*, 3479-3482.

[189]   W. Kuriyama, T. Matsumoto, Y. Ino, O. Ogata, **2014.**

[190]   Y. Li, H. Li, H. Junge, M. Beller, *Chem Commun (Camb)* **2014**, *50*, 14991-14994.

[191]   A. Mukherjee, A. Nerush, G. Leitus, L. J. Shimon, Y. Ben David, N. A. Espinosa Jalapa, D. Milstein, *J. Am. Chem. Soc.* **2016**, *138*, 4298-4301.

[192]   S. Elangovan, J. Neumann, J. B. Sortais, K. Junge, C. Darcel, M. Beller, *Nat. Commun.* **2016**, *7*, 12641.

[193]   B. L. Small, M. Brookhart, A. M. A. Bennett, *J. Am. Chem. Soc.* **1998**, *120*, 4049-4050.

[194]   S. C. Bart, E. Lobkovsky, P. J. Chirik, *J. Am. Chem. Soc.* **2004**, *126*, 13794-13807.

[195]   S. K. Russell, E. Lobkovsky, P. J. Chirik, *J. Am. Chem. Soc.* **2011**, *133*, 8858-8861.

[196]   J. V. Obligacion, P. J. Chirik, *J. Am. Chem. Soc.* **2013**, *135*, 19107-19110.

[197]   S. P. Semproni, C. C. Hojilla Atienza, P. J. Chirik, *Chem. Sci.* **2014**, *5*, 1956.

[198]   S. P. Semproni, C. Milsmann, P. J. Chirik, *J. Am. Chem. Soc.* **2014**, *136*, 9211-9224.

[199]   P. J. Chirik, **2014**, pp. 189-212.

[200]   B. A. Schaefer, G. W. Margulieux, B. L. Small, P. J. Chirik, *Organometallics* **2015**, *34*, 1307-1320.

[201]   P. J. Chirik, *Acc. Chem. Res.* **2015**, *48*, 1687-1695.

[202]   J. V. Obligacion, J. M. Neely, A. N. Yazdani, I. Pappas, P. J. Chirik, *J. Am. Chem. Soc.* **2015**, *137*, 5855-5858.

[203]   V. A. Schmidt, J. M. Hoyt, G. W. Margulieux, P. J. Chirik, *J. Am. Chem. Soc.* **2015**, *137*, 7903-7914.

[204]   N. Deibl, R. Kempe, *J. Am. Chem. Soc.* **2016**, *138*, 10786-10789.

[205]   X. Yang, *ACS Catalysis* **2011**, *1*, 849-854.

[206]   M. Mastalir, M. Glatz, N. Gorgas, B. Stoger, E. Pittenauer, G. Allmaier, L. F. Veiros, K. Kirchner, *Chem. - Eur. J.* **2016**, *22*, 12316-12320.

[207]   G. Zhang, Z. Yin, S. Zheng, *Org. Lett.* **2016**, *18*, 300-303.

5 References

[208]   M. Vellakkaran, K. Singh, D. Banerjee, *ACS Catalysis* **2017**, *7*, 8152-8158.

[209]   K. Junge, V. Papa, M. Beller, *Chem. - Eur. J.* **2018**.

[210]   G. Zhang, B. L. Scott, S. K. Hanson, *Angew. Chem., Int. Ed.* **2012**, *51*, 12102-12106.

[211]   G. Zhang, S. K. Hanson, *Org. Lett.* **2013**, *15*, 650-653.

[212]   S. Rosler, J. Obenauf, R. Kempe, *J. Am. Chem. Soc.* **2015**, *137*, 7998-8001.

[213]   S. Rosler, M. Ertl, T. Irrgang, R. Kempe, *Angew. Chem., Int. Ed.* **2015**, *54*, 15046-15050.

[214]   M. Mastalir, G. Tomsu, E. Pittenauer, G. Allmaier, K. Kirchner, *Org. Lett.* **2016**, *18*, 3462-3465.

[215]   M. Mastalir, B. Stöger, E. Pittenauer, M. Puchberger, G. Allmaier, K. Kirchner, *Adv. Synth. Catal.* **2016**, *358*, 3824-3831.

[216]   E. Pedrajas, I. Sorribes, E. Guillamon, K. Junge, M. Beller, R. Llusar, *Chem. - Eur. J.* **2017**, *23*, 13205-13212.

[217]   J. Neumann, S. Elangovan, A. Spannenberg, K. Junge, M. Beller, *Chem. - Eur. J.* **2017**, *23*, 5410-5413.

[218]   A. Bruneau-Voisine, D. Wang, V. Dorcet, T. Roisnel, C. Darcel, J.-B. Sortais, *J. Catal.* **2017**, *347*, 57-62.

[219]   R. Fertig, T. Irrgang, F. Freitag, J. Zander, R. Kempe, *ACS Catalysis* **2018**, *8*, 8525-8530.

[220]   V. G. Landge, A. Mondal, V. Kumar, A. Nandakumar, E. Balaraman, *Org Biomol Chem* **2018**, *16*, 8175-8180.

[221]   M. Huang, Y. Li, Y. Li, J. Liu, S. Shu, Y. Liu, Z. Ke, *Chem Commun (Camb)* **2019**, *55*, 6213-6216.

[222]   B. G. Reed-Berendt, K. Polidano, L. C. Morrill, *Org Biomol Chem* **2019**, *17*, 1595-1607.

[223]   P. Chandra, T. Ghosh, N. Choudhary, A. Mohammad, S. M. Mobin, *Coord. Chem. Rev.* **2020**, *411*, 213241.

[224]   A. M. Tondreau, R. Michalczyk, J. M. Boncella, *Organometallics* **2017**, *36*, 4179-4183.

[225]   S. Fu, Z. Shao, Y. Wang, Q. Liu, *J. Am. Chem. Soc.* **2017**, *139*, 11941-11948.

[226]   F. Freitag, T. Irrgang, R. Kempe, *J. Am. Chem. Soc.* **2019**, *141*, 11677-11685.

[227]   P. Daw, A. Kumar, N. A. Espinosa-Jalapa, Y. Ben-David, D. Milstein, *J. Am. Chem. Soc.* **2019**, *141*, 12202-12206.

[228]   M. Garbe, K. Junge, M. Beller, *Eur. J. Org. Chem.* **2017**, 4344-4362.

[229]   Z. Liu, Z. Yang, X. Yu, H. Zhang, B. Yu, Y. Zhao, Z. Liu, *Adv. Synth. Catal.* **2017**, *359*, 4278-4283.

[230]   B. Zhao, Z. Han, K. Ding, *Angew. Chem., Int. Ed.* **2013**, *52*, 4744-4788.

[231]   H. Li, Y. Wang, Z. Lai, K.-W. Huang, *ACS Catalysis* **2017**, *7*, 4446-4450.

[232]   M.-H. Huang, J. Hu, K.-W. Huang, *J. Chin. Chem. Soc.* **2017**.

[233]   H. Li, B. Zheng, K.-W. Huang, *Coord. Chem. Rev.* **2015**, *293-294*, 116-138.

[234]   T. Chen, H. Li, S. Qu, B. Zheng, L. He, Z. Lai, Z.-X. Wang, K.-W. Huang, *Organometallics* **2014**, *33*, 4152-4155.

[235]   T. Chen, L.-P. He, D. Gong, L. Yang, X. Miao, J. Eppinger, K.-W. Huang, *Tetrahedron Lett.* **2012**, *53*, 4409-4412.

[236]   C. Hou, Z. Zhang, C. Zhao, Z. Ke, *Inorg. Chem.* **2016**, *55*, 6539-6551.

[237]   B. G. Reed-Berendt, L. C. Morrill, *J. Org. Chem.* **2019**, *84*, 3715-3724.

[238]   J. Sklyaruk, J. Borghs, O. El-Sepelgy, M. Rueping, *Angew. Chem., Int. Ed.* **2018**.

[239]   A. Brzozowska, L. M. Azofra, V. Zubar, I. Atodiresei, L. Cavallo, M. Rueping, O. El-Sepelgy, *ACS Catalysis* **2018**, *8*, 4103-4109.

[240]   C. Wang, B. Maity, L. Cavallo, M. Rueping, *Org. Lett.* **2018**, *20*, 3105-3108.

[241]   G. Zhang, T. Irrgang, T. Dietel, F. Kallmeier, R. Kempe, *Angew. Chem., Int. Ed.* **2018**, *57*, 9131-9135.

[242]   S. P. Midya, J. Pitchaimani, V. G. Landge, V. Madhu, E. Balaraman, *Catalysis Science & Technology* **2018**, *8*, 3469-3473.

[243]   A. M. Tondreau, J. M. Boncella, *Polyhedron* **2016**, *116*, 96-104.

[244]   B. de Bruin, E. Bill, E. Bothe, T. Weyhermüller, K. Wieghardt, *Inorg. Chem.* **2000**, *39*, 2936-2947.

[245]   P. J. Chirik, K. Wieghardt, *Science* **2010**, *327*, 794-795.

[246]   H. Li, T. P. Gonçalves, D. Lupp, K.-W. Huang, *ACS Catalysis* **2019**, *9*, 1619-1629.

[247]   B. E. Mann, R. A. Motterlini, D. A. Scapens, US 2010/0105770, **2010.**

[248]   M. H. Huang, T. P. Gonçalves, K. W. Huang, *J. Chin. Chem. Soc.* **2019**, *66*, 455-458.

[249]   M. K. Elmkaddem, C. Fischmeister, C. M. Thomas, J. L. Renaud, *Chem Commun (Camb)* **2010**, *46*, 925-927.

[250]   T. Norrby, A. Börje, L. Zhang, B. Åkermark, J. H. Wagenknecht, G. W. Francis, J. Szúnyog, B. Långström, *Acta Chem. Scand.* **1998**, *52*, 77-85.

[251]   K.-W. Huang, T. Chen, L. He, D. Gong, W. Jia, L. Yao, US 2012/0323007, **2012.**

[252]   A. J. Smith, E. D. Kalkman, Z. W. Gilbert, I. A. Tonks, *Organometallics* **2016**, *35*, 2429-2432.

[253]   J. Yin, B. Xiang, M. A. Huffman, C. E. Raab, I. W. Davies, *J. Org. Chem.* **2007**, *72*, 4554-4557.

[254]   J. Zhao, H. Chen, W. Li, X. Jia, X. Zhang, D. Gong, *Inorg. Chem. Commun.* **2018**, *57*, 4088-4097.

[255]   L. Homberg, A. Roller, K. C. Hultzsch, *Org. Lett.* **2019**, *21*, 3142-3147.

5 References

[256]   S. Elangovan, M. Garbe, H. Jiao, A. Spannenberg, K. Junge, M. Beller, *Angew. Chem., Int. Ed.* **2016**, *55*, 15364-15368.

[257]   D. Wei, A. Bruneau-Voisine, M. Dubois, S. Bastin, J. B. Sortais, *ChemCatChem* **2019**.

[258]   S. Vázquez, M. Barniol-Xicota, R. Leiva, C. Escolano, *Synthesis* **2016**, *48*, 783-803.

[259]   V. Papa, J. R. Cabrero-Antonino, E. Alberico, A. Spanneberg, K. Junge, H. Junge, M. Beller, *Chem. Sci.* **2017**, *8*, 3576-3585.

[260]   J. Das, D. Banerjee, *J. Org. Chem.* **2018**, *83*, 3378-3384.

[261]   Y. K. Jang, T. Kruckel, M. Rueping, O. El-Sepelgy, *Org. Lett.* **2018**, *20*, 7779-7783.

[262]   S. Chakraborty, P. Daw, Y. Ben David, D. Milstein, *ACS Catal* **2018**, *8*, 10300-10305.

[263]   X. Dai, F. Shi, *Org Biomol Chem* **2019**, *17*, 2044-2054.

[264]   F. Li, C. Sun, H. Shan, X. Zou, J. Xie, *ChemCatChem* **2013**, *5*, 1543-1552.

[265]   B. Sahoo, D. Formenti, C. Topf, S. Bachmann, M. Scalone, K. Junge, M. Beller, *ChemSusChem* **2017**.

[266]   G. Wienhofer, I. Sorribes, A. Boddien, F. Westerhaus, K. Junge, H. Junge, R. Llusar, M. Beller, *J. Am. Chem. Soc.* **2011**, *133*, 12875-12879.

[267]   Y. F. Chen, J. Chen, L. J. Lin, G. J. Chuang, *J. Org. Chem.* **2017**, *82*, 11626-11630.

[268]   K. Ganguli, S. Shee, D. Panja, S. Kundu, *Dalton Trans* **2019**, *48*, 7358-7366.

[269]   S. Weber, B. Stoger, K. Kirchner, *Org. Lett.* **2018**, *20*, 7212-7215.

[270]   S. Chakraborty, D. Milstein, *ACS Catalysis* **2017**, *7*, 3968-3972.

[271]   S. Chakraborty, G. Leitus, D. Milstein, *Angew. Chem., Int. Ed.* **2017**, *56*, 2074-2078.

[272]   H. Tang, X. Cheng, Z. Zhang, *Phosphorus, Sulfur Silicon Relat. Elem.* **2011**, *187*, 8-15.

[273]   C. Bolm, K. Weickhardt, M. Zehnder, T. Ranff, *Chem. Ber.* **1991**, *124*, 1173-1180.

[274]   Q. Chai, C. Song, Z. Sun, Y. Ma, C. Ma, Y. Dai, M. B. Andrus, *Tetrahedron Lett.* **2006**, *47*, 8611-8615.

[275]   O. El-Sepelgy, E. Matador, A. Brzozowska, M. Rueping, *ChemSusChem* **2019**, *12*, 3099-3102.

[276]   T. Liu, L. Wang, K. Wu, Z. Yu, *ACS Catalysis* **2018**, *8*, 7201-7207.

[277]   Y. Engel, A. Dahan, E. Rozenshine-Kemelmakher, M. Gozin, *J. Org. Chem.* **2007**, *72*, 2318-2328.

[278]   A. Zhdanko, M. E. Maier, *Angew. Chem., Int. Ed. Engl.* **2014**, *53*, 7760-7764.

[279]   E. Balaraman, S. Midya, A. Mondal, A. Begum, *Synthesis* **2017**, *49*, 3957-3961.

[280]   A. Adamczyk-Woźniak, I. Madura, A. H. Velders, A. Sporzyński, *Tetrahedron Lett.* **2010**, *51*, 6181-6185.

[281]   D. Hollmann, A. Tillack, D. Michalik, R. Jackstell, M. Beller, *Chem. - Asian. J.* **2007**, *2*, 403-410.

[282] G. B. Giovenzana, D. Imperio, A. Penoni, G. Palmisano, *Beilstein J. Org. Chem.* **2011**, *7*, 1095-1099.

[283] D. Wei, A. Bruneau-Voisine, D. A. Valyaev, N. Lugan, J. B. Sortais, *Chem. Commun.* **2018**, *54*, 4302-4305.

[284] K. Iseki, Y. Morita, T. Ishigaki, K. Kawamura, *Synthesis* **2007**, *2007*, 2517-2523.

[285] D. Hollmann, S. Bahn, A. Tillack, M. Beller, *Chem. Commun.* **2008**, 3199-3201.

[286] A. Kumar, S. Sharma, R. A. Maurya, *Adv. Synth. Catal.* **2010**, *352*, 2227-2232.

[287] T. J. Barker, E. R. Jarvo, *Angew. Chem., Int. Ed.* **2011**, *50*, 8325-8328.

[288] K. Geoghegan, S. Kelleher, P. Evans, *J. Org. Chem.* **2011**, *76*, 2187-2194.